Regulation of chromosome bi-orientation and sister chromatid disjunction during cell division

Rutger Cornelis Christiaan Hengeveld

ISBN: 9789462954373

Cover: Movie by Martijn J.M. Vromans, edited by Rutger C.C. Hengeveld: A U2OS cell stably expressing H2B-GFP imaged by video microscopy (stills are shown).
Printed by: Proefschriftmaken.nl, Uitgeverij BOXpress. 's-Hertogenbosch, The Netherlands

Regulation of chromosome bi-orientation and sister chromatid disjunction during cell division

Regulatie van chromosoom bi-oriëntatie en zuster-chromatide separatie tijdens de celdeling
(met een samenvatting in het Nederlands)

Proefschrift

ter verkrijging van de graad van doctor aan de Universiteit Utrecht op gezag van de rector magnificus, prof.dr. G.J. van der Zwaan, ingevolge het besluit van het college voor promoties in het openbaar te verdedigen op dinsdag 7 juni 2016 des middags te 2.30 uur

door

Rutger Cornelis Christiaan Hengeveld

geboren op 19 juli 1987 te Zwolle

Promotor: Prof. dr. S.M.A. Lens

Table of contents

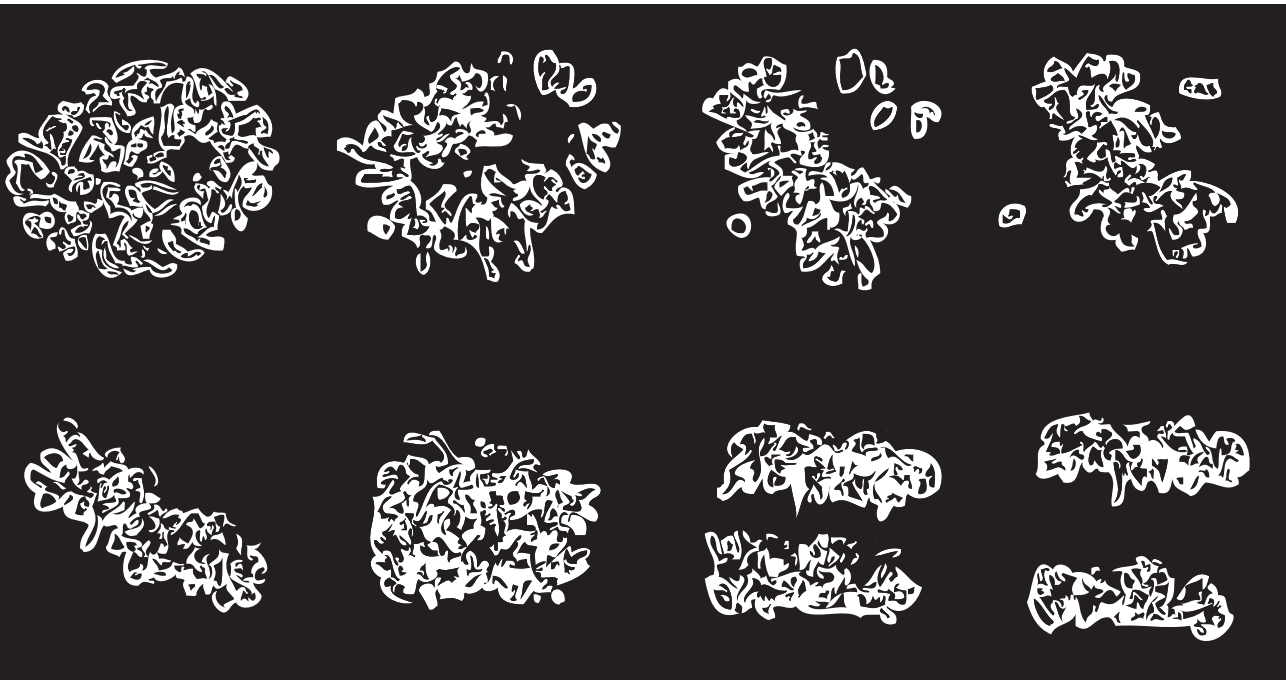

Chapter 1

General introduction

In part adapted from Van der Waal, Hengeveld *et al.*, Cell division control by the Chromosomal Passenger Complex, Experimental Cell Research, July 2012; 318, 1407-1420

Mitosis

Preface

Since the invention of the microscope and telescope in the late 1590's by Hans Lippershey and Sacharias Jansen, respectively, it became possible to magnify objects. Later in 1664 the physicist Robert Hooke looked through his own build microscope to dried cork and observed an ordered pattern composed of many tiny chambers, which he called 'cells'. Because Hooke's microscopes could only magnify 30X, he was not able to study these cells in detail. However, in the seventeenth century, Antoni van Leeuwenhoek improved the microscope lenses allowing impressive magnifications of up to 480X and the time of cellular microscopy was initiated. Much later, in 1874 the pioneer of mitotic research, Walther Flemming, visualized the different phases of mitosis and captured them in beautiful drawings using pencil and ink. Now, more than 140 years later, with the innovations in biochemistry, molecular biology and microscopy, mitosis is an extensively studied process and many molecular details have been and are still being revealed.

Mitosis: a general overview

The human genome consists of 23 chromosome pairs: 23 chromosomes originate from the sperm (paternal chromosomes) and 23 from the oocyte (maternal chromosomes). During DNA replication in S phase of the cell cycle all 46 chromosomes are duplicated, but the original chromosome and its copy remain linked until mitosis. In M phase (the cell cycle phase during which both nuclear division (mitosis), and cytoplasmic division (cytokinesis) takes place), the 46 pairs of chromosomes, now called sister chromatids, are separated and equally segregated to allow transmission of an exact copy of the genome to two newly formed daughter cells [1].

Mitosis is initiated by a sharp increase in the activity of the cyclin-dependent kinase 1 (CDK1) bound to cyclin B [2]. CDK1-cyclin B phosphorylates many substrates, such as proteins associated with the nuclear envelope, microtubules, or chromatin. This promotes dramatic changes in chromatin folding, drives the formation of essential mitotic structures, and CDK1-cyclin B activity levels orchestrates the different mitotic phases (Figure 1). The first phase of mitosis is **prophase** in which the sister chromatids start to condense and the nuclear envelope is broken down. Moreover, the in S phase duplicated centrosomes move to opposite poles of the cell and start nucleating microtubules to form the mitotic spindle [3]. The completion of nuclear envelope break down marks the onset of **prometaphase**, during which the sister chromatids are captured by microtubules of the mitotic spindle on a multi protein complex called the kinetochore [4]. In **metaphase**, all sister chromatids are attached to spindle microtubules and have congressed to the equator of the cell [5]. In this phase cyclin B and the separase-protease inhibitor, securin, are being degraded by the proteasome upon ubiquitination by the anaphase promoting complex/cyclosome (APC/C) [6]. The consequent reduction in CDK1 activity, and the activation of separase, drives the onset of **anaphase**, in which the sister chromatids are separated and pulled to opposite spindle poles by the depolymerizing microtubules. In **telophase**, the segregated chromosomes decondense and the nuclear envelope is reformed. Also, in late anaphase, the plasma membrane starts to ingress at the cell equator, marking the onset of **cytokinesis** during which two new daughter cells are formed [7].

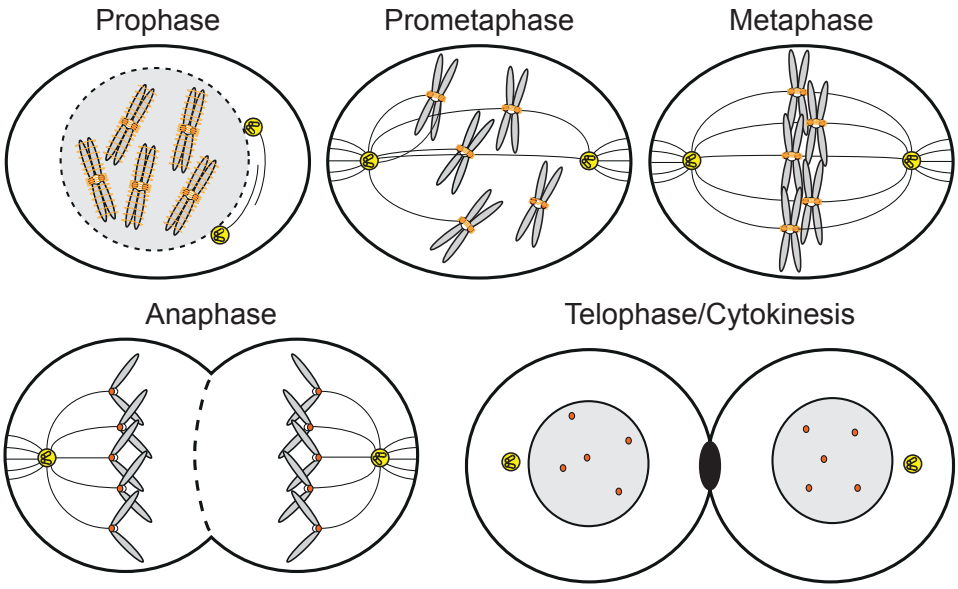

Figure 1| Mitosis
Schematic overview of the different stages of mitosis. DNA in grey, cohesin complex in orange, kinetochores in red and centrosomes in yellow.

Chromosomal instability

The challenge of mitosis is to faithfully segregate the duplicated chromosomes over two new daughter cells. Segregation errors occur at a very low frequency in healthy cells, yet cancer cells often display an increased rate of chromosome segregation errors during mitosis, referred to as chromosomal instability (CIN). CIN can be an indirect consequence of S phase problems such as replication stress and centrosome overduplication, or a direct consequence of an imperfect mitosis, due to cohesin defects, a weakened mitotic checkpoint, or defects in kinetochore-microtubule dynamics [8]. CIN gives rise to gains and losses of whole chromosomes and thereby aneuploidy (a karyotype that differs from diploid) as well as to structural chromosomal aberrations (genomic instability, GIN) [9-11]. The question whether CIN is a cause or consequence of cancer is being extensively investigated in various mouse models carrying mutations that impair faithful chromosome segregation. Although cancer appears not to be an obligatory outcome of CIN, evidence is accumulating that depending on the genetic background or tissue type it can contribute to cancer progression through loss of heterozygosity (LOH) of tumor suppressor genes [12]. To understand the cause of CIN in cancer cells, it is essential to comprehend how faithful chromosome segregation is normally ensured. The molecular requirements for faithful chromosome segregation during mitosis are discussed below.

Chromosome bi-orientation on the mitotic spindle

The prerequisite for error-free segregation of the duplicated chromosomes is chromosome bi-orientation, which means that the two kinetochores of the sister chromatids have to attach to microtubules emanating from opposite poles of the mitotic

spindle. This requires: **1)** formation of a bipolar mitotic spindle, **2)** regulation of sister chromatid cohesion, **3)** kinetochore assembly, which is on its turn is necessary for **4)** dynamic attachment of sister chromatids to the mitotic spindle, and **5)** signaling to the mitotic checkpoint. And finally, **6)** detection and correction of improper kinetochore microtubule attachments.

1) Formation of a bipolar mitotic spindle

In mammalian somatic cells, the in S phase duplicated centrosomes act as the major microtubule-organizing centers (MTOCs) to nucleate microtubules that form the mitotic spindle [13]. To form a bipolar spindle, the two centrosomes, which are in close proximity in G2 and early prophase, have to move to opposite poles of the cell [3]. This is mediated by the forces generated by the polymerizing microtubules and by microtubule-associated motor proteins. First, the plus-end directed microtubule motor protein EG5 (kinesin-5) is a kinesin containing two motor domains, that both interact with microtubules [14]. After binding to anti-parallel oriented microtubules it drives the sliding of these microtubules thereby pushing apart the inter-centrosomal microtubules and as a consequence the two centrosomes [15]. In addition a second plus-end-directed microtubule motor protein, KIF15/Hklp2 also contributes to bipolar spindle assembly by producing an outward force. KIF15 contains one motor domain at its N-terminus and is recruited to the mitotic spindle via its C-terminal leucine zipper domain, which can directly bind to the microtubule binding protein TPX2 [16, 17]. How KIF15 generates force in the spindle is unclear, as anti-parallel sliding has thus far not been demonstrated for this motor. Thirdly, the minus-end directed motor protein dynein contributes to centrosome separation in prophase by pulling on the astral microtubules emanating from the centrosomes while being tethered to the nuclear envelope [18]. Moreover, studies in *Drosophila* cells provided evidence that cortical localized dynein also contributes to centrosome separation during prophase [19, 20]. However, this has never been shown in human cells. On the other hand, microtubule-associated dynein generates a prominent inward force that opposes EG5 [21]. The current idea is that the balanced activities of these, plus and minus-end directed motor proteins are required for bipolar spindle assembly. Of note, centrosomes are not essential for the formation of (bipolar) mitotic spindles [22]. However, when centrosomes are present spindle formation is more efficient and spindle poles appear better focused during mitosis, which contributes to chromosome segregation fidelity [23, 24]. Finally, many cancer cells have more than 2 centrosomes, which can give rise to the formation of multipolar mitotic spindles and chromosome missegregation in anaphase.

2) Regulation of sister chromatid cohesion

During DNA replication in S phase the duplicated sister chromatid pairs become physically linked by the cohesin complex [25]. Moreover, as an indirect consequence of DNA replication the DNA strands intertwine (DNA catenation, discusses in **Chapter 4**). Both cohesion and DNA catenation keep the sister chromatids in close proximity, which is necessary for bi-orientation. However, at anaphase onset the cohesin complexes must be removed and DNA catenanes need to be resolved to allow sister chromatid separation. In mammalian cells cohesin removal occurs in two steps [26]. 1) In a phosphorylation dependent manner the bulk of cohesin is removed from the chromosomal arms during prophase by the action of wings apart-like protein homologue (WAPL) (prophase pathway). And 2) just before anaphase onset, the remaining cohesin at the centromere is cleaved by the cysteine protease separase (Figure 2a). Removal of cohesin also promotes the resolution of DNA catenanes (discussed in **Chapter 4** and

5) [27].

The cohesin complex, consisting of Structural Maintenance of Chromosome protein 1 and 2 (SMC1 and SMC3), the kleisin subunit RAD21 (sister chromatid cohesion protein 1 (Scc1) in yeast), stromal antigen 1 and 2 (SA 1 and 2; also known as STAG1/STAG2 and Scc3 in yeast) and its co-factors PDS5 (either PDS5A or B in vertebrates), sororin and WAPL, forms a ring-like structure that entraps the sister chromatids (Figure 2b) [28, 29]. In both SMC proteins two coiled coil domains connect a central hinge with a globular domain. Because each SMC protein folds back at its central hinge domain, the two globular domains at the N- and the C- termini are in close proximity forming a functional ATPase domain. The hinge domain of SMC1 dimerises with the hinge domain of SMC3, whereas RAD21/Scc1 bridges the ATPase domains of SMC1 and SMC3. SA2/Scc3 binds directly to RAD21/Scc1 and contributes to the recruitment of PDS5, sororin and WAPL. The loading of the cohesin complex takes place during telophase (G1) and is dependent on the loading factors Scc2 and Scc4 (NIPBL-MAU2 in human) [30-32]. Once loaded, opening of the SMC1/Scc1 hinge interface is thought to be required for DNA entrapment [33, 34]. Although, a recent *in vitro* study suggested that entrapment of DNA by the cohesin complex requires opening of the ring at the Smc3/Scc1 binding interface [35]. Not only DNA entrapment, but also release of the cohesin ring from the DNA requires opening of the cohesin complex at the Smc3/Scc1 binding interface, [34, 36, 37]. Turnover of the cohesin complex depends on WAPL, but during S phase the acetyltransferases ESCO1 and ESCO2 (Eco1 in yeast) acetylates SMC3, which results in the recruitment of sororin to the cohesin complex [38-42]. Sororin binds to PDS5 via its phenylalanine-glycine-phenylalanine (FGF) motif and prevents the binding of WAPL to cohesin [43]. In prophase sororin is phosphorylated by CDK1 and Aurora B resulting in its release from PDS5 [44, 45]. This allows WAPL to bind PDS5 via a similar FGF motif present in WAPL. The binding of WAPL to PDS5 leads to the removal of the cohesin complexes from chromosomal arms in prophase (Figure 2b). In addition, Polo-like kinase-1 (PLK1) phosphorylates SA2 to promote cohesin removal via a thus far unknown mechanism [46, 47].

At centromeres sororin and SA2 phosphorylation is counteracted by Shugoshin-1/Protein Phosphatase 2A (SGO1/PP2A) and in addition, SGO1 compete with WAPL for binding to SA2. (Figure 2b) [45, 48-54]. This establishes the protection of centromeric cohesion from WAPL and PLK1-dependent removal in prophase. The protection of centromeric cohesion not only ensures that sister chromatids remain connected until anaphase onset; it also resists the pulling forces of the kinetochore-bound depolymerizing microtubules. As such it allows the build-up of tension across sister-kinetochores upon bi-orientation. In addition, centromeric cohesion promotes the back-back orientation of sister-kinetochores facilitating their capture by microtubules from opposite spindle poles [55].

Interestingly, mutations in or deletions of STAG2 (encoding SA2) are found in a range of tumor types, and experimental disruption of STAG2 (its gene is located at the X-chromosome) leads to cohesion defects and aneuploidy [56-59]. However, because the cohesin complex also plays a role in gene transcription, DNA damage repair and processing of DNA replication intermediates [60], it is hard to assess whether the cohesion related mitotic defects are a cancer promoting.

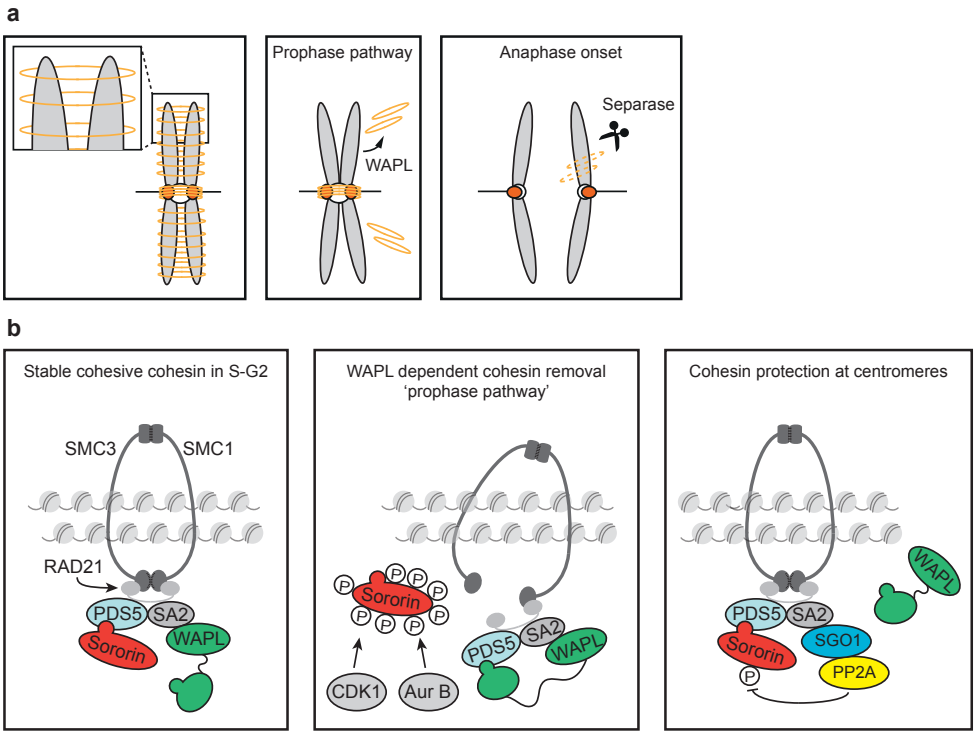

Figure 2| Cohesin removal

a) Cohesin removal during mitosis is a two-step process. In prophase the chromosomal arm-associated cohesin is removed by WAPL whereas centromeric cohesin is cleaved by separase just before anaphase onset. **b)** The DNA is entrapped by the cohesin complex during S-G2 phase. Sororin prevents WAPL dependent opening of the ring. During prophase, sororin is released from PDS5 by CDK1-cyclin B and Aurora B mediated phosphorylation, which promotes WAPL-dependent cohesin removal from the chromosomal arms. SGO1-PP2A at centromeres antagonizes prevents WAPL-dependent cohesin removal by counteracting sororin phosphorylation and by competing with WAPL for binding to SA2.

3) Assembly of the kinetochore

The kinetochore is a highly ordered structure consisting of three layers, the inner and outer-kinetochore, and the fibrous corona. The human kinetochore consists of more than 100 proteins and is assembled at the centromere, the constricted chromosome region where the sister chromatids remain linked until anaphase [61].

CENP-A: the basis of the kinetochore

Centromeric DNA consists of repeated arrays of 171 base pair sequences called α-satellite DNA repeats [62]. A 17 base pair sequence in the α-satellite DNA repeat, called the CENP-B box, facilitates the recruitment of centromere protein (CENP)-B to the centromere. CENP-B can bind directly to CENP-A and CENP-T and contributes to the recruitment of CENP-C to centromeres [63, 64]. However, the contribution of CENP-B to proper chromosome segregation is still controversial [65]. Moreover, the α-satellite DNA repeats are not essential for centromere specification [66]. Instead, centromeric DNA is packed into specific chromatin containing the centromere-specific histone H3 variant CENP-A, which is the key player for kinetochore assembly [67, 68]. CENP-A is incorporated at the centromeric region during telophase, the beginning of G1 phase. In human cells the Mis18 complex (Mis18α, Mis18β and M18BP1/KNL2) and the CENP-A chaperone HJURP are important factors for the loading of CENP-A in telophase [69-71].

Moreover, PLK1 promotes the localization the Mis18 complex and thereby initiation of CENP-A loading in telophase, while the assembly of the Mis18 complex is inhibited by CDK kinase activity in S phase, G2 phase and mitosis to prevent 'overloading' of CENP-A [72, 73]. The exact molecular mechanism by which these proteins facilitate CENP-A loading into the nucleosome remains to be established.

The inner and outer-kinetochore

The CENP-A containing nucleosomes recruit proteins of the constitutive centromere-associated network (CCAN) that consists of CENP-C, CENP-H, CENP-I, CENP-K-U, CENP-W and CENP-X. CENP-A and the CCAN form the inner kinetochore and function as a scaffold to build the outer-kinetochore [74]. The outer-kinetochore is involved in microtubule capture and mitotic checkpoint activation and is assembled in early mitosis via two subcomplexes. First, CENP-C binds directly to CENP-A containing nucleosomes and interacts with Nnf1, which is one of the four subunits of the Mis12 complex (the total Mis12 complex consists of Nnf1, Mis12, Dsn1/Mis13 and Nsl1) [75-80]. Nsl1 subsequently interacts with the HEC1 (highly expressed in cancer-1)/Ndc80 complex and KNL-1 (kinetochore nul-1)/Blinkin/CASC5 (Figure 3). The conserved HEC1/Ndc80 complex forms a rod-like structure, consisting of HEC1/Ndc80, Nuf2, Spc24 and Spc25. The C-termini of Spc24 and Spc25 bind to the Mis12 subunit Nls1 whereas the N-termini of Nuf2 and HEC1/Ndc80 bind directly to microtubules (Figure 3) [81]. Together, the Mis12 complex, the HEC1/Ndc80 complex and KNL1 form the microtubule attachment and mitotic checkpoint module of the kinetochore and is referred to as the KMN network [82, 83]. KNL1 also binds to Zwint, which is required for the recruitment of the Rod-Zwilch-Zw10 (RZZ) complex to the kinetochore [84, 85]. Together with KNL1, the RZZ complex is involved in the establishment and silencing of the mitotic checkpoint. Secondly, the CENP-T-W-S-X heterotetramer, which is also downstream of CENP-A, forms a nucleosome like structure that binds to DNA [86]. In turn, the C-termini of Spc24 and Spc25 bind directly to the long N-terminal tail of CENP-T and thereby facilitate the recruitment of the Ndc80 complex [87]. The function of the kinetochore in microtubule capture and activation of the mitotic checkpoint is discussed below.

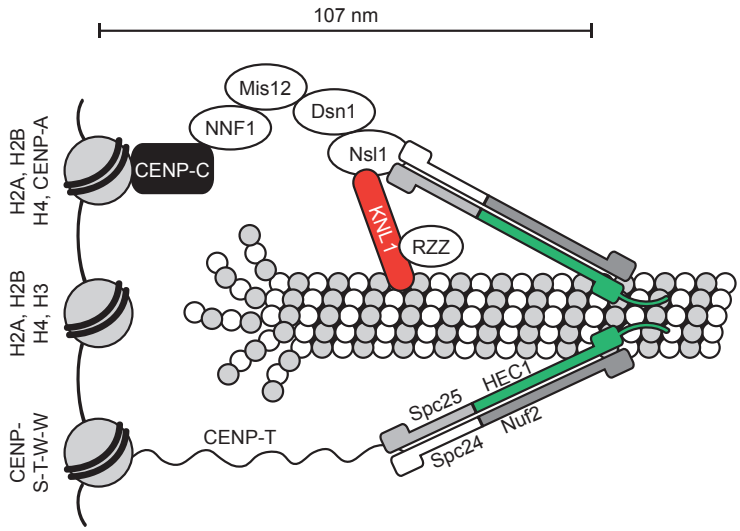

Figure 3l Kinetochore-microtubule attachment
Schematic representation of kinetochore protein complexes involved in microtubule binding. CENP-C is recruited to CENP-A containing nucleosomes and connects the KMN network (including the RZZ complex) to the centromere. CENP-T forms a nucleosome like heterotetramer with CENP-W-S-X to bind DNA and recruit the Ndc80 complex. In HeLa cells, the distance between CENP-A and the N-terminal globular domain of HEC1 is ~ 107nm when the kinetochore is under tension [88].

4) Function of the kinetochore: dynamic attachment of sister chromatids to the mitotic spindle

The main function of the kinetochore is to attach the sister chromatid to microtubules of the mitotic spindle. Electron microscopy studies showed that in human cells approximately 20 microtubules can bind per kinetochore [89]. In contrast to the budding yeast kinetochore that only binds one microtubule. Microtubules that are stably end-on attached to kinetochores are known as K-fibers. Microtubules emanating from the centrosomes polymerize (grow) and depolymerize (shrink), and this dynamic behavior helps in 'searching' for chromosomes [4, 90, 91] Furthermore, additional mechanisms are in place in a human cell that facilitate spindle assembly and accelerate the search and capture of kinetochores. A high concentration of Ran-GTP around the chromatin guides spindle assembly in the vicinity of chromosomes [92-95]. Secondly, microtubules can nucleate from existing microtubules through the recruitment of Augmin, and these additional microtubules are also thought to facilitate kinetochore capture [96].

Given the large surface area of the microtubule wall compared to the microtubule plus-end, the chances are high that sister chromatids become initially attached to the microtubule walls (lateral attachment) [5]. When a sister chromatid becomes laterally attached to en existing K-fiber, the kinetochore-bound plus-end directed motor protein CENP-E guides this chromosome to the equator [97, 98]. On the other hand, kinetochore-associated dynein can facilitate lateral attachments to astral microtubules and transport the chromosomes to the spindle poles using its minus-end-directed motor activity [99, 100]. The chromatin-associated kinesins, kinesin-4 (KIF4) and kinesin 10 (KID) create polar ejection forces, pushing the chromosome arms away form the centrosomes [101-103]. When chromosomes arrive at the spindle pole CENP-E takes over and laterally attaches the sister chromatid to existing K-fibers and facilitating chromosome congression to the equator. How CENP-E specifically guides chromosomes towards the equator of the cell and avoids movement along astral microtubules was recently revealed. CENP-E mediated chromosome congression is dependent on detyrosination of spindle microtubules [104]. Astral microtubules are tyrosinated and hence are not favored by CENP-E. Thus, CENP-E 'reads the tubulin code' to specifically transport chromosomes towards the equator of the mitotic spindle. Moreover, other recent studies showed that the outer-kinetochore, which includes CENP-E, can heavily expand when unattached [105, 106]. This is suggested to facilitate (lateral) microtubule capture.

To eventually bi-orient the chromosomes on the mitotic spindle the initial lateral kinetochore-microtubule attachments need to be converted into stable end-on attachments. This so-called end-on conversion requires the microtubule depolymerizing kinesin MCAK/KIF2C to release the laterally attached kinetochore from microtubules [107]. In addition, polar ejection forces generated by chromokinesins also contribute to the lateral to end-on conversion in *Drosophila* cells [108]. However the exact requirements for lateral to end-on conversion are not yet fully understood.

5) The mitotic checkpoint

Establishment of the mitotic checkpoint

The mitotic checkpoint provides time to achieve chromosome bi-orientation. Unattached kinetochores generate a signal that inhibits the E3 ubiquitin ligase APC/C-CDC20 (anaphase-promoting complex/cyclosome)(cell-division-cycle 20 homologue) and thereby prevents anaphase onset. On unattached kinetochores, the KMN network

serves as a platform for the recruitment and assembly of a diffusible inhibitory complex of the APC/C-CDC20 called the mitotic checkpoint complex (MCC) (Figure 4). The MCC is composed of MAD2 (mitotic arrest deficient 2), MAD3/BUBR1 (budding uninhibited by benzimidazole R1), BUB3 that binds CDC20 [6, 109, 110]. Upstream factors that promote MCC assembly are MPS1 (monopolar spindle 1) kinase, BUB1 kinase and MAD1, which are also recruited to the KMN network. Activation of the mitotic checkpoint requires kinetochore recruitment and activation of MPS1 and subsequent phosphorylation of its substrate KNL1 [111-115]. MPS1 mediated phosphorylation of multiple MELT and SHT motifs in KNL1 create a docking platform for BUB3/BUB1 dimers, which in turn facilitate the recruitment of BUBR1 (Figure 4) [116-120]. Essential for MCC assembly is the kinetochore recruitment of the MAD1/Closed-MAD2 (C-MAD2) tetramer. Although the exact mechanism of MAD1/C-MAD2 kinetochore recruitment is not fully understood in human cells, MPS1, BUB1, Mis12 and the RZZ complex all appear to be required [121-126]. Kinetochore-associated MAD1/C-MAD2 acts as a template to recruit inactive Open-MAD2 (O-MAD2) and mediates its conformational change into active C-MAD2 [127, 128]. Soluble C-MAD2 can bind to CDC20 leading to exposure of a BUBR1/BUB3 binding site to fully assemble the MCC [129]. The MCC prevents anaphase onset by binding to and inactivating the APC/C-CDC20 (Figure 4).

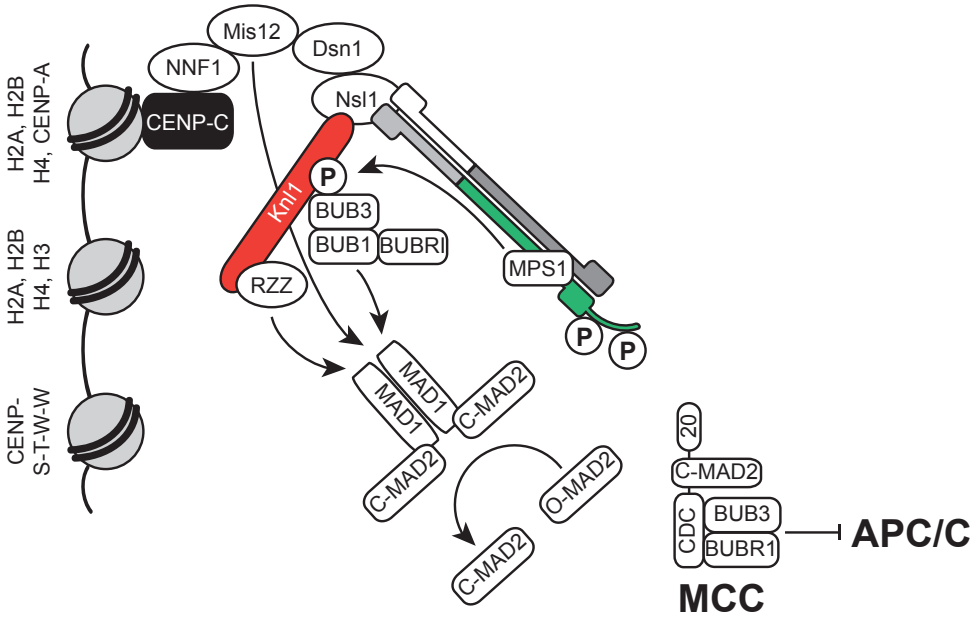

Figure 4| The mitotic checkpoint
The mitotic checkpoint is established at unattached kinetochores by the formation of a diffusible inhibitor of the APC/C-CDC20 called the MCC. The MCC consists of C-MAD2, MAD3/BUBR1, BUB3 and CDC20. MPS1, Mis12, BUB1 and the RZZ complex contribute to the recruitment of MAD1-/C-MAD2 to the kinetochore. MAD1/C-MAD2 mediates the conformational change of soluble inactive O-MAD2 into active C-MAD2, which can be incorporated into the MCC. MPS1 is recruited to HEC1, phosphorylates KNL1 to create a platform for the recruitment of BUB3, BUB1 and BUBR1 and indirectly for MAD1/C-MAD2.

Silencing of the mitotic checkpoint

Upon attachment of the final kinetochore, the mitotic checkpoint needs to be silenced to allow activation of the APC/C-CDC20 that targets cyclin B and securin for proteasomal degradation to inactivate CDK1 and promote separase-dependent cohesin cleavage, respectively checkpoint silencing is realized by stopping the formation of new MCC

and by MCC disassembly to liberate the APC/C from its inhibitor [129]. Microtubules and MPS1 compete for the same binding site at the kinetochore and upon microtubule attachment, MPS1 is displaced from kinetochores [130, 131]. In addition, RZZ and MAD1/MAD2 are actively removed from attached kinetochores by dynein-dependent transport along the K-fibers to the spindle poles [132]. Furthermore, Protein Phosphatase 1γ (PP1g) is recruited to KNL1 and dephosphorylates the MELT and probably SHT motifs in KNL1, which inhibits recruitment of the BUB proteins [133]. A number of proteins have been described to contribute to MCC disassembly. The CUE-domain containing protein, CUEDC2, binds to CDC20 and promotes the release of C-MAD2 from APC/C-CDC20 [134]. p31^{comet} directly binds to and removes C-MAD2 from the MCC [135-138]. In addition, the AAA-ATPase TRIP13 collaborates with p31 to inactivate the mitotic checkpoint by catalyzing the (C-MAD2 to O-MAD2) MAD2 conversion. Also CDC20 ubiquitination by UbcH10 and by the APC/C itself promotes disassembly of the MCC independent of CDC20 degradation [139, 140].

6) Detection and correction of improper kinetochore microtubule attachments
Although the abovementioned processes that facilitate search and capture of kinetochores contribute to bi-orientation, they do not fully prevent the formation of erroneous kinetochore-microtubule attachments, such as syntelic (both sister-kinetochores are attached by microtubules from the same spindle pole) and merotelic attachments (one sister-kinetochore is attached by microtubules from one spindle pole but the other sister-kinetochore is attached to microtubules emanating form both spindle poles) (Figure 5). These erroneous attachments are detected by the Chromosomal Passenger Complex (CPC), which detaches the incorrectly attached microtubules from kinetochores thereby creating a new chance to obtain bi-polar (amphitelic) attachments. This dynamic process of detachment and re-attachment facilitated by the CPC is called error-correction.

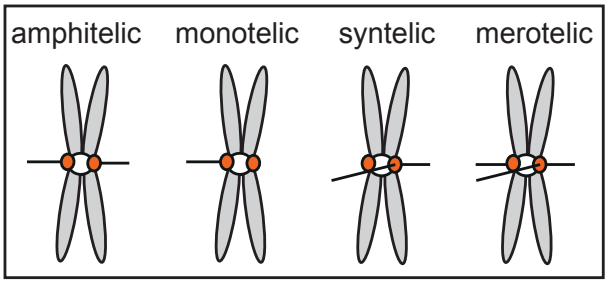

Figure 5l Kinetochore-microtubule attachment stadia
Schematic representation of correct bipolar (amphitelic) and incorrect (syntelic, merotelic) kinetochore-microtubule attachments.

The Chromosomal Passenger Complex

The CPC is a protein complex consisting of Aurora B kinase, INCENP, survivin and borealin (Figure 6/7). It ensures genomic stability by controlling multiple processes during both nuclear and cytoplasmic division [141]. The multifunctionality of the CPC is supported by its dynamic localization during cell division, allowing the enzymatic subunit of the complex, Aurora B, to encounter different substrates [142]. In early prophase it localizes on chromosomal arms, while it becomes confined to the inner centromere in late prophase, prometaphase and metaphase. Anaphase onset triggers the translocation of the CPC from centromeres to the interpolar overlapping microtubules of the central spindle, and the cell cortex, before the complex eventually concentrates at the midbody in telophase. Some of the functions of the CPC (Aurora B)

in early mitosis have been briefly mentioned above such as, cohesin removal from the chromosomal arms in prophase and the correction of non-bipolar chromosome-spindle attachments. Other functions include the regulation of chromosome structure, mitotic spindle formation, and regulation of the mitotic checkpoint. Moreover, in anaphase the CPC promotes the shortening of segregating chromosomes and it plays an essential role in cytokinesis and abscission [143]. Here I will focus on the functions of the CPC in chromosome bi-orientation and the mitotic checkpoint.

Error correction by the CPC

The CPC promotes chromosome bi-orientation by specifically destabilizing incorrect attachments thereby allowing the stabilization of bipolar attachments. Incorrectly attached kinetochore microtubules fail to generate tension across sister-kinetochores and Aurora B substrates at the outer-kinetochore, such as Dsn1/Mis13, KNL1 and HEC1/Ndc80 (all part of the KMN network) are within reach of Aurora B kinase localized at the inner centromere [82, 144-146]. The subsequent phosphorylation of the KMN network reduces its microtubule binding affinity thus facilitating the release of erroneously attached microtubules [82, 145, 146] (Figure 6). Importantly, when sister-kinetochores are attached by microtubules from opposite spindle poles, the tension generated across sister-kinetochores allows kinetochore-associated substrates to be pulled out of the sphere of influence of Aurora B. Moreover, Aurora B inhibits the recruitment of its counteracting phosphatase PP1γ by phosphorylation of the SILK-RVSF phosphatase-binding motif in KNL1. Upon tension, the SILK-RVSF phosphatase-binding motif is dephosphorylated by BUBR1-dependent PP2A-B56 allowing recruitment of PP1γ which, in turn promotes the stabilization of amphitelic kinetochore-microtubule attachments by dephosphorylation of the KMN network (Figure 6) [144, 147-149].

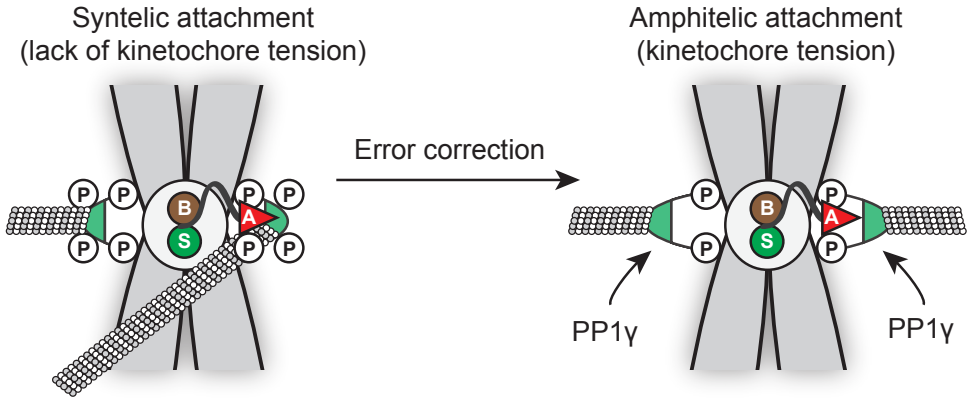

Figure 6l Error correction by the CPC

Schematic representation of the correction of syntelic kinetochore-microtubule attachment by the CPC. The CPC (S: survivin, B: borealin, A: Aurora B, connecting line: INCENP) phosphorylates outer-kinetochore (green) substrates to release incorrect attached microtubules from the kinetochore. When amphitelicaly attached, tension across the sister-kinetochores pulls substrates at the outer-kinetochore out of the sphere of influence of the CPC that localizes at the inner centromere. This results in recruitment of PP1g to the kinetochore, dephosphorylation of the outer-kinetochore substrates and stabilization of kinetochore-microtubule attachments.

Stabilization of bipolar end-on attachments is most likely further facilitated by the recruitment of Astrin/SPAG5/MAP126, Small Kinetochore-Associated Protein (SKAP/kinastrin/C15orf23), and the Ska complex consisting of Ska1, Ska2 and Ska3/Rama1/C13Orf3 to bi-oriented KTs, since depletion of these proteins disturbs the formation

of stable kinetochore-microtubule attachments [150-157]. Interestingly, kinetochore localization of Astrin, SKAP and the Ska complex depends on the KMN network, and is antagonized by Aurora B-dependent phosphorylation. Since Astrin and SKAP have not been reported as direct substrates of Aurora B, it is currently not known which Aurora B kinetochore-substrates need to be dephosphorylated in metaphase to facilitate the recruitment of Astrin and SKAP to bi-oriented kinetochores. Ska1 and Ska3 on the other hand, appear to be Aurora B substrates and phospho-mimicking mutants of these proteins fail to localize to metaphase kinetochores and fail to stabilize kinetochore-microtubule attachments. Although it has not been demonstrated whether non-phosphorylatable Ska1 and Ska3 mutants prematurely localize to unattached kinetochores, the work suggests that Ska1 and Ska3 have to be dephosphorylated in metaphase to allow their kinetochore recruitment [38]. Whether PP1Y is the responsible phosphatase involved in the kinetochore recruitment of Astrin, SKAP and the Ska complex is currently unknown.

Accumulation of the CPC at the inner centromere

Thus upon bi-orientation, tension is thought to spatially separate Aurora B from its outer-kinetochore substrates. Central to this model is the inner centromere localization of Aurora B. However, whether this localization is indeed essential for stable bi-orientation was recently debated and is investigated in **Chapter 2**. Within the CPC, the non-enzymatic subunits survivin and borealin, in complex with the N-terminus of INCENP, are essential to localize the complex to the inner centromere [158], and the site where the phosphorylations of two distinct histones (histone H3 phosphorylated by Haspin on T3 and histone H2A phosphorylated on T120 by BUB1) overlap, is thought to dictate the recruitment of the CPC to the inner centromere (Figure 7) [159-161]. This is mediated through direct interaction of the Baculoviaral IAP Repeat (BIR) domain in survivin with H3T3ph, while borealin interacts with Shugoshin-1 (SGO1) and Shugoshin-2 (SGO2), which on their turn bind to phosphorylated H2A [162]. In addition, the interaction between borealin and the Shugoshin proteins requires the phosphorylation of borealin by CDK1 [163], and this might explain why centromere accumulation of the CPC is first seen in late prophase. Since inhibition of Aurora B kinase activity reduces Aurora B localization to the inner centromere suggests positive feedback control [164]. Indeed, Aurora B phosphorylates Haspin on several residues leading to activation of Haspin, which in turn promotes the recruitment of the CPC [165]. How these phosphorylation events contribute to Haspin activation is still unclear. In contrast to direct activation of Haspin, Aurora B phosphorylates Repo-Man to antagonize targeting of the Repo-Man/PP2A/PP1g complex to the chromatin and thereby prevent premature H3-T3 dephosphorylation [166]. In addition, kinetochore recruitment of BUB1 and the subsequent phosphorylation of H2A also require Aurora B kinase activity [167, 168]. Thus Aurora B promotes its own centromere localization by enhancing Haspin kinase activity, preventing phosphatase recruitment and promoting the KT recruitment of BUB1.

Mitotic checkpoint control by the CPC

The CPC promotes establishment of the mitotic checkpoint

By generating unattached kinetochores during error-correction the CPC can indirectly activate the mitotic checkpoint (Figure 8). However, several lines of evidence have suggested that the CPC directly controls the mitotic checkpoint, independently from its role in destabilizing microtubules [169-171]. In particular, genetic experiments in fission

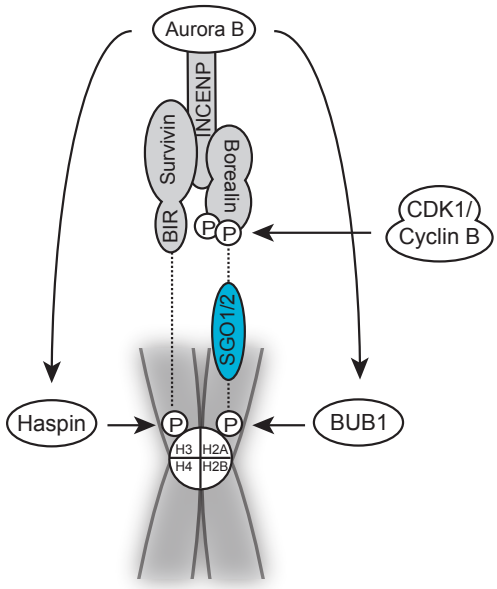

Figure 7l Regulation of centromere CPC localization
Inner centromere localization of the CPC is dependent on the direct binding of the BIR domain of survivin to histone H3 phosphorylated by Haspin and binding of borealin to SGO1 and SGO2, which in turn interact with histone H2A phosphorylated by BUB1. The interaction between borealin and the Shugoshin proteins is promoted by the phosphorylation of borealin by CDK1. Note that Aurora B itself regulates targeting of the CPC by controlling Haspin and potentially BUB1.

yeast and antibody injections in *Xenopus laevis* cells showed a clear requirement for Aurora B activity to sustain a mitotic checkpoint arrest even when kinetochores were unattached [172-174]. It was therefore proposed that incomplete inhibition of mammalian Aurora B by siRNA-mediated knock-down or by the various small molecule inhibitors was the reason for the inefficient checkpoint override in a high dose of nocodazole (a drug that depolymerizes microtubules and thus creates a situation where all kinetochores are unattached) in mammalian cells [109, 170]. Indeed, high concentrations of the Aurora B inhibitor Hesperadin rapidly silenced the mitotic checkpoint in nocodazole treated cells [175]. However, a combination of Aurora B knock-down and inhibition by ZM447439 did not reproduce this efficient checkpoint override [176], and neither did conditional knock-out of survivin or INCENP in chicken DT-40 cells [177, 178], suggesting that high Hesperadin concentrations may have additional off-target effects. More penetrant approaches to inhibit Aurora B activity, such as human cell knockouts expressing analog-sensitive Aurora B kinase [164], may be required to resolve whether human Aurora B is a central mitotic checkpoint component.

An alternative hypothesis is that the CPC could serve as an amplifier of the mitotic checkpoint signal in mammalian cells. Its activity would thus become essential to delay anaphase onset when only a few kinetochores are unattached and elicit less APC/C-CDC20- inhibitory signal (MCC), even though this activity would be largely redundant when all kinetochores can signal. Such an amplifier would be expected to become important again if the checkpoint signal is weakened even if all kinetochores remain unattached in nocodazole. Indeed, Aurora B inhibition was shown to efficiently override a nocodazole-induced mitotic arrest when BUB1, HEC1 or Nuf2 was (partially) knocked- down or when the checkpoint kinase MPS1 was partially inhibited [175, 176, 179]. Interestingly, when MPS1 was constitutively tethered to kinetochores, checkpoint silencing induced by HEC1 knock-down and Aurora B inhibition was rescued [176]. In line with this, at the onset of mitosis Aurora B is required for the kinetochore localization and activation of MPS1 as measured by the kinetochore recruitment of MAD2. This suggests that an Aurora B > HEC1 > MPS1 > MAD2 route serves to rapidly establish the

mitotic checkpoint when cells enter mitosis [175, 176]. Furthermore, Aurora B may also act more downstream in the mitotic checkpoint signaling cascade to maintain the APC/C inhibitory signal. This was revealed in cells in which MAD1 was constitutively targeted to kinetochores. This manipulation resulted in a metaphase arrest (with stably attached kinetochore microtubules) that depended on the binding of MAD2 to MAD1 and on active Aurora B [180]. How the CPC contributes to APC/C inhibition downstream of MAD1–MAD2 kinetochore localization remains to be determined. Lastly, initial experiments performed in *Xenopus laevis* egg extracts suggests that kinetochore expansion including mitotic checkpoint proteins is promoted by Aurora B phosphorylation and might contribute to mitotic checkpoint activity [106]. Taken together, in addition to its microtubule destabilizing activity that creates unattached kinetochores, the CPC also controls the mitotic checkpoint in a direct manner. This latter activity could serve to amplify the unattached kinetochore-derived signal thereby ensuring a robust checkpoint response when the number of unattached kinetochores is low.

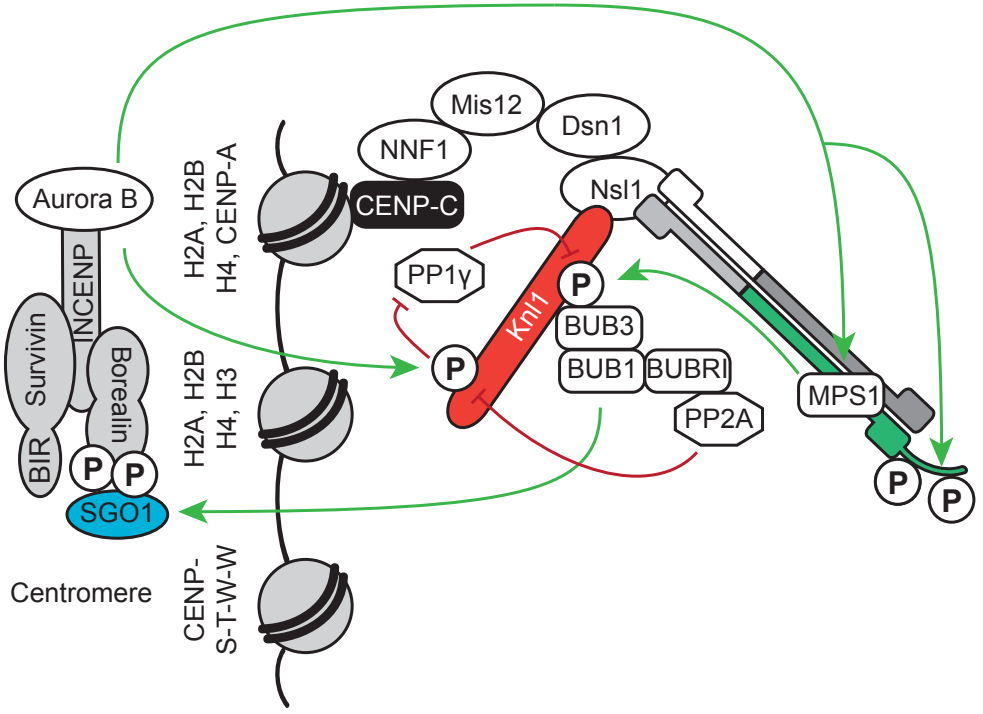

Figure 8l Feedback control between the CPC and the mitotic checkpoint
Schematic overview of the feedback loops between the CPC and the mitotic checkpoint.

Feedback between the mitotic checkpoint and CPC-dependent error correction

As described above, Aurora B activity is required for MPS1 recruitment to the outer-kinetochore component HEC1 [176]. In turn, MPS1 phosphorylates the MELT and SHT motifs in KNL1 to promote the recruitment of BUB3/BUB1/BUBR1 [119, 120]. When recruited to the kinetochore, BUB1 phosphorylates histone H2A, thereby creating a platform for Shugoshin-CPC recruitment to the inner centromere. This generates a positive feedback loop (CPC > MPS1 > BUB1 > SGO1 > CPC) between the error-correction machinery and the mitotic checkpoint (Figure 7/8). Depletion of BUBR1 results in increased phosphorylation of Aurora B substrates, suggesting that this checkpoint protein inhibits Aurora B activity [181]. Since Aurora B activity is required

for the kinetochore localization of BUBR1 [167, 182], Aurora B appears to recruit its own inhibitor. Indeed, BUBR1 contains a so-called KARD domain that recruits the phosphatase PP2A to the kinetochore [183-185]. BUBR1-PP2A counteracts Aurora B-dependent phosphorylation events including the phosphorylation of the SLIK-RVSF binding motif in KNL1 thereby facilitating the recruitment of PP1γ [133]. PP1γ in turn dephosphorylates the MELT and probably SHT motifs in KNL1, which will result in the delocalization of BUB3, BUB1 and BUBR1/PP2A and silencing of the mitotic checkpoint (Figure 8) [133]. However, in case of erroneous attachments, Aurora B will not only detach these microtubules but is also in reach of the SLIK-RVSF binding motif in KNL1 promoting the delocalization of PP1γ and restart of the feedback machinery until bi-orientation.

CPC function: Aurora B substrate phosphorylation in space and time

To carry out its various functions in the dividing cell, the enzymatic subunit of the CPC, Aurora B, needs to reach its substrates and be active at the right time and place to phosphorylate these substrates. Up to now, over 63 substrates of Aurora B have been identified (Table 1) and they at least in part explain how the CPC affects microtubule binding to the kinetochore (e.g. HEC1, Dsn1, KNL1, CENP-E, mDia3, MCAK, PLK1, Ska1, Ska3, Haspin, Repo-Man, sororin), promotes spindle assembly and spindle size (MCAK, KIF2a, KIF4a Katanin), facilitates checkpoint silencing (KNL1 and Zwint-1), mediates chromosome condensation in anaphase (Cnd2/Cap-H) and promotes cytokinesis and abscission (MLKP1, MgcRacGAP, Vimentin, Myosin Regulatory Light Chain 2, CHMP4C, Ataxin-10).

Table 1| Overview of the presently identified CPC substrates

Substrate	Organism	Phosphorylated Residue	Cellular localization	Method	Ref
CAP-H	*H. sapiens*	**S70**	Chromosome arms	*In Vivo*	[186]
Cnd2	*S. pombe*	**S5**IS41I**S52**	Chromosome arms	*In Vivo*	[186, 187]
Histone H1.4	*H. sapiens*	**S27**	Chromosome arms	*In Vivo*	[188]
Histone H3	*H. sapiens*	**S10**I**S28**	Chromosome arms	*In Vivo*	[189]
HMGN2	*H. sapiens*	**S25**I**S29**	Chromosome arms	*In Vivo*	[164]
MYBBP1A	*H. sapiens*	**S1303**	Chromosome arms	*In Vivo*	[190]
REC-8	*C. elegans*	T625	Chromosome arms	*In Vitro*	[191]
sororin	*H. Sapiens*	Multiple sites	Chromosome arms	*In Vivo*	[45, 164, 192]
YY1	*H. Sapiens*	**S184**	Chromosome arms	*In Vivo*	[193]
AURKB	*H. sapiens*	**T232**	Centromere/kinetochore	*In Vivo*	[194]
borealin	*H. sapiens*	S154IS165IS219IT275IT278	Centromere/kinetochore	*In Vitro*	[195, 196]
CENP-A	*H. sapiens*	**S7**	Centromere/kinetochore	*In Vivo*	[197]
CENP-E	*H. sapiens*	**T422**	Centromere/kinetochore	*In Vivo*	[148]
CENP-U	*H. sapiens*	S349IS350	Centromere/kinetochore	*In Vivo*	[198]
Dam1	*S. cerevisiae*	**S20**I**257**I**S265**	Centromere/kinetochore	*In Vivo*	[199]
DIA3	*H. sapiens*	T66I**S196**IS820IT882	Centromere/kinetochore	*In Vivo*	[200]
DSN1/MIS13	*H. sapiens*	**S100**I**S109**	Centromere/kinetochore	*In Vivo*	[146, 201]
Haspin	*H. sapiens*	Multiple sites	Centromere/kinetochore	*In Vivo*	[165]
INCENP	*H. sapiens*	T893IS894IS895	Centromere/kinetochore	*In Vivo*	[202]
KIF2A	*X. laevis*	**S132**	Centromere/kinetochore	*In Vitro*	[203]

KNL1/CASC5	*H. sapiens*	**S24**|**S60**	Centromere/kinetochore	*In Vivo*	[146, 147]
MCAK/KIF2C	*H. sapiens*	**S95**|S109|S111 |S115|S192	Centromere/kinetochore	*In Vivo*	[204]
MCAK/KIF2C	*X. laevis*	T95|S110|**S196**	Centromere/kinetochore	*In Vivo*	[205]
MEI-S332/SGO1	*D. melanogaster*	S124|S125|S126	Centromere/kinetochore	*In Vivo*	[206]
HEC1/NDC80	*H. sapiens*	S5|S15|S44|T49|S55|S69	Centromere/kinetochore	*In Vivo*	[145] [82]
PLK1	*D. melanogaster*	**T182**	Centromere/kinetochore	*In Vivo*	[207]
SGO2	*H. sapiens*	Multiple sites|**T537**	Centromere/kinetochore	*In Vivo*	[208]
SKA1	*H. sapiens*	T157|S242	Centromere/kinetochore	*In Vivo*	[38, 209]
SKA3	*H. sapiens*	S159	Centromere/kinetochore	*In Vivo*	[38, 210]
ZWINT-1	*H. sapiens*	S250|T251|S262	Centromere/kinetochore	*In Vivo*	[211]
Bim1p (EB1)	*S. cerevisiae*	S139|S148|S149|S165|S166|S176	Spindle	*In Vivo*	[212]
CKAP2/TMAP	*H. sapiens*	**S627**	Spindle/Chromosomes	*In Vivo*	[213]
KIF2A	*H. sapiens*	T97	Spindle	*In Vivo*	[214]
KIF4A	*H. sapiens*	**T799**|S801	Spindle	*In Vivo*	[215]
MKLP1 (isoform 1)	*H. sapiens*	**S911**	Spindle	*In Vivo*	[216]
MKLP1 (isoform 2)	*H. sapiens*	**S708**	Spindle	*In Vivo*	[217, 218]
MyoGEF	*H. Sapiens*	T544	Spindle	*In Vivo*	[219]
OP18/Stathmin	*X. laevis*	S16|S25|S39	Spindle	*In Vitro*	[220]
SHCBP1	*H. Sapiens*	**S634**	Spindle	*In Vitro*	[221]
Ataxin-10	*H. sapiens*	**S12**	Midbody	*In Vivo*	[222]
CHMP4C	*H. sapiens*	S210	Midbody	*In Vitro*	[223]
DESM	*H. sapiens*	**S12**|**T17**|**S60**	Midbody	*In Vivo*	[224]
EB3	*H. sapiens*	**S176**	Midbody	*In Vivo*	[225, 226]
GFAP	*H. sapiens*	**T7**|**S13**|**S38**	Midbody	*In Vitro*	[224]
HDAC5	*H. Sapiens*	**S278**	Midzone/Midbody	*In Vivo*	[227]
RACGAP1	*H. sapiens*	**S387**	Midbody	*In Vivo*	[228]
MRLC2	*H. sapiens*	**S20**	Midbody	*In Vitro*	[229, 230]
Nlp	*H. sapiens*	S185|S448|S585	Midbody	*In Vivo*	[231]
NPM1	*H. sapiens*	**S125**	Midbody	*In Vivo*	[232]
RASSF1A	*H. sapiens*	T202|**S203**	Midzone/Midbody	*In Vivo*	[233, 234]
SEPT-1	*H. sapiens*	S248|S307|S315	Midbody	*In Vitro*	[235]
survivin	*H. sapiens*	**T117**	Midbody	*In Vivo*	[236, 237]
Vimentin	*H. sapiens*	Multiple sites|**S72**	Midbody	*In Vivo*	[238]
Katanin	*X. laevis*	S131	Spindle poles	*In Vivo*	[239]
TLK-1	*C. elegans*	**S634**	Spindle poles	*In Vivo*	[240]
ATM	*H. sapiens*	**S1403**	Multiple locations	*In Vivo*	[241]
FHOD1	*H. sapiens*	Multiple sites	Other	*In Vivo*	[242]
HDAC4	*H. Sapiens*	**S265**	Other	*In Vivo*	[227]
HDAC9	*H. Sapiens*	**S242**	Other	*In Vivo*	[227]
KIBRA	*H. sapiens*	**S539**	Other	*In Vivo*	[243]
NSUN2	*H. sapiens*	S139	Other	*In Vivo*	[244]
P53	*H. sapiens*	S183|S269|T284	Other	*In Vivo*	[245]
Rb	*H. sapiens*	**S780**	Other	*In Vivo*	[246]

In addition, phosphoproteomic and chemical genetic screens (**Chapter 3**) revealed many more potential Aurora B substrates on expected cellular structures such as chromatin and kinetochores, but they also identified substrates involved in transcription, translation and DNA damage [164, 247-249]. This indicates that the CPC may fulfill many more functions also outside mitosis or that some of these proteins may have alternative functions during cell division.

Thesis outline

The research described in this thesis covers two processes required for proper chromosome segregation during mitosis. In **Chapter 2** and **3** we focus on the regulation of chromosome segregation by the CPC. In **Chapter 5** the role of Rif1 in the resolution of Ultra Fine DNA Bridges (UFBs) during anaphase is studied.

The importance of inner centromere localization of the CPC for chromosome bi-orientation
The CPC in promotes chromosome bi-orientation by destabilizing kinetochore-microtubule attachments that are not bipolar through phosphorylation of certain outer-kinetochore substrates, providing the sister chromatids with a new opportunity to interact with microtubules from opposite poles. When bipolar attachments have been acquired, tension pulls these kinetochore substrates out of the sphere of influence of the CPC resulting in dephosphorylation of kinetochore substrates and stabilization of these attachments. A prerequisite for this model is the inner centromere localization of the CPC because tension is thought to increase the distance between the inner centromere and outer-kinetochore. However, during the course of this research, work in budding yeast implied that (inner)centromere localization of the CPC is not essential for chromosome bi-orientation, thus challenging the 'spatial separation' model. In **Chapter 2** we analyzed whether inner centromere localization of the CPC is needed in mammals and show that it is an absolute requirement for stable bi-orientation through protection of centromeric cohesin via recruitment of SGO1. Our work suggests that the CPC and SGO1 are components of a feedback loop at the inner centromere that couples cohesion protection to tension sensing and mitotic checkpoint silencing.

Development of a chemical genetic approach for human Aurora B
To further study the function(s) of the CPC during mitosis, in collaboration with the lab of Kevan Shokat, we developed a chemical genetic approach to specifically inhibit Aurora B and to identify novel substrates of the kinase (**Chapter 3**). By mutating the gatekeeper residue in the ATP-binding pocket and by introduction of a second site suppressor mutation we were able to specifically inhibit Aurora B *in vitro* and in cells by PP1 inhibitors. Furthermore we could thiophosphorylate whole cell extracts and identify novel Aurora B substrates using mass spectrometry. We validate HMGN2 as a *bona fide* CPC substrate and suggest that its phosphorylation is required to release HMGN2 from nucleosomes during mitosis.

Rif1 promotes UFB resolution during anaphase
In **Chapter 3** we identify Rif1 as a potential Aurora B substrate. In the course of validating this substrate, we discovered it localized at UFBs in anaphase and decided to study (in collaboration with the lab of Marcel van Vugt) the role of Rif1 at UFBs first. Current

insights on formation and resolution of UFBs are reviewed in **Chapter 4**. In **Chapter 5** we show that Rif1 is recruited to UFBs independent of its known interaction partner 53BP1 but dependent on PICH. Absence of Rif1 leads to impaired UFB resolution and loss of genomic integrity.

Finally, in **Chapter 6**, the overall findings of this thesis are summarized and discussed in light of the current literature and provide suggestions for follow-up research.

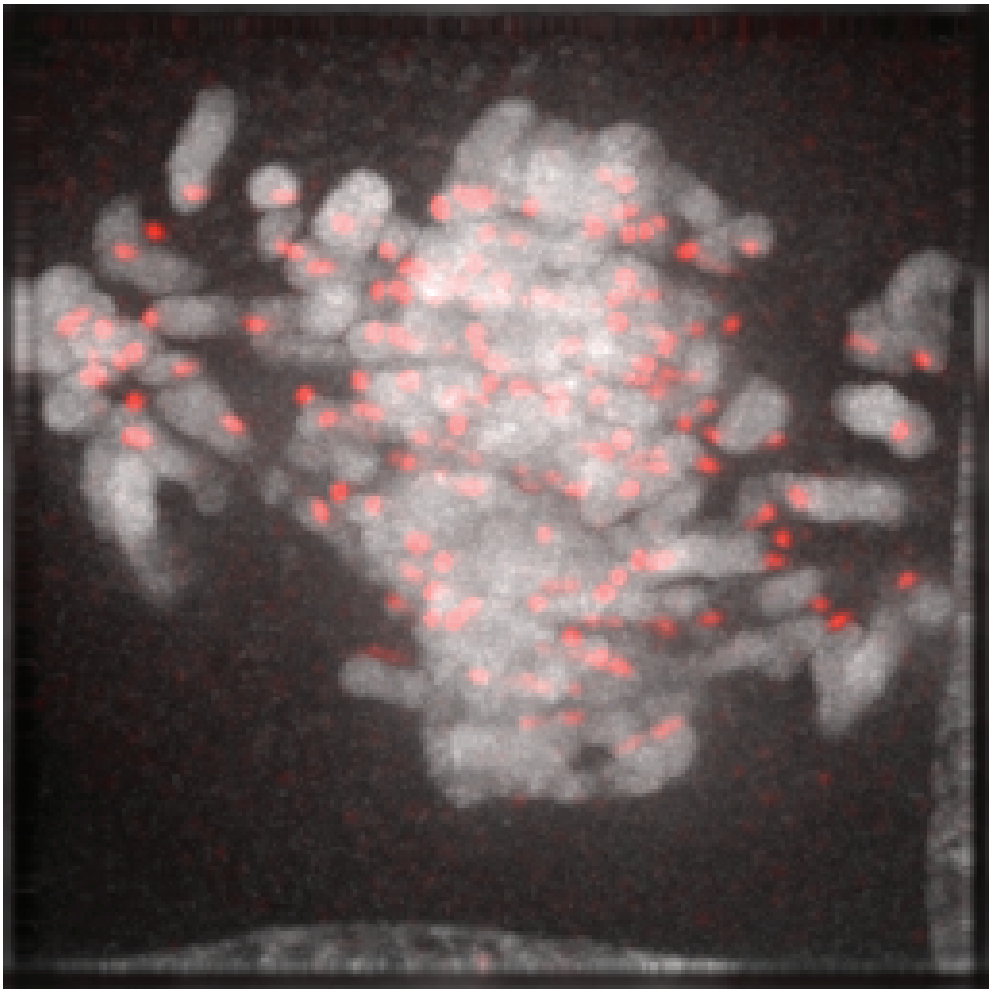

Chapter 2

Inner centromere localization of the CPC is required for cohesion protection and mitotic checkpoint silencing

Rutger C. C. Hengeveld[1], Martijn J.M. Vromans[1], Mathijs Vleugel[2], Michael A. Hadders[1], Susanne M.A. Lens[1]

From the [1]Department of Molecular Cancer Research, Center for Molecular Medicine, University Medical Center Utrecht, 3584 CG Utrecht, The Netherlands and [2]Hubrecht Institute, 3584 CT Utrecht, The Netherlands

Manuscript submitted

Abstract

Accurate transmission of the genome during cell division requires faithful segregation of the duplicated chromosomes. Proper chromosome segregation can only occur when all sister chromatids have become stably connected to microtubules from opposite poles of the mitotic spindle before anaphase onset. How this is accomplished remains incompletely understood. Here, we show that in human cells, chromosome bi-orientation requires inner centromere localization of the chromosomal passenger complex (CPC). We found that the CPC core provides inner centromere positioning cues for Shugoshin-1 (SGO1) to stabilize centromeric cohesion. Moreover, we demonstrate that CPC inner centromere localization is necessary to spatially separate Aurora B from its kinetochore substrate KNL1 and thereby for silencing of the mitotic checkpoint upon bi-orientation. We propose that the CPC and SGO1 are components of a feedback loop at the inner centromere that couples cohesion protection to tension sensing and mitotic checkpoint silencing.

Results and Discussion

Detachment of incorrect kinetochore-microtubule (KT-MT) connections is a consequence of Aurora B-mediated phosphorylation of outer-kinetochore substrates, including components of the KMN (KNL1, MIS12 and NDC80 complex) network, which directly interact with microtubules [82, 145]. Upon chromosome bi-orientation, tension across sister-kinetochores is thought to pull these outer-KT substrates out of the sphere of influence of Aurora B, resulting in the stabilization of bi-orientated attachments and anaphase onset [144, 204, 250]. Central to this 'spatial separation' model is the inner centromere localization of Aurora B. However, there is ongoing debate whether this confined localization of Aurora B is indeed essential for chromosome bi-orientation [251] [252]. Apart from its localization at the inner centromere, a small pool of active Aurora B at or near the kinetochore has been described in mammalian cells and suggested to control KT-MT stability [253]. Moreover, it was recently demonstrated that Aurora B localization to the inner centromere is not a prerequisite for faithful chromosome segregation in budding yeast [254], raising the question what function is executed by the inner centromere pool of Aurora B.

To study the function of inner centromere-localized Aurora B during mammalian mitosis, we made use of HeLa cell lines that ectopically expressed variants of the CPC scaffold protein INCENP from an inducible promoter, in conjunction with siRNA mediated knock-down of endogenous INCENP. The N-terminal inner centromere-targeting domain (CEN-box, amino acids 1-43) of INCENP, which interacts with the CPC members survivin and borealin [255], was either deleted (INCENPΔCEN) or replaced with different targeting moieties: Survivin (surv-INCENP), which re-localizes Aurora B to the inner centromere, or the centromere-targeting domain of CENP-B (CB-INCENP), which positions Aurora B at the (inner) kinetochore, away from the inner centromere (Figure 1a, b and Supplemental Figure S1a-e) [144, 256, 257].

Analysis of INCENPΔCEN expressing cells, confirmed that removal of the CEN-box disrupted the inner centromere localization of Aurora B, similar to Sli15-delta N-terminus (Sli15-dNT), its analog in *S. cerevisiae* (Figure 1b and Supplemental Figure S1b, c) [254, 257, 258]. Unlike Sli15-dNT, which supported chromosome bi-orientation in budding yeast, INCENPΔCEN did not rescue chromosome bi-orientation in human cells lacking endogenous INCENP. In fact, we found a strong correlation between the inner centromere localization of Aurora B and stable chromosome bi-orientation in human cells (Figure 1b-d). Close inspection of the misaligned chromosomes in cells with kinetochore-localized Aurora B (i.e. CB-INCENP-expressing cells) revealed the appearance of single sister chromatids. This was in marked contrast to cells lacking INCENP in which the misaligned chromosomes appeared as paired sister chromatids (Figure 1d, inset).

This suggested that CB-INCENP expressing cells experienced problems in maintaining sister chromatid cohesion upon bi-orientation, and we hypothesized that the inner centromere pool of Aurora B was needed to stabilize centromeric cohesion. Indeed, chromosome spreads of INCENP-depleted cells revealed that sister chromatids behaved as 'railroads' (Figure 2a), a phenotype seen in certain cohesinopathies, and explained by reduced centromeric cohesion, while retaining at least some cohesin on the chromosomal arms [259, 260]. The railroad phenotype was rescued by expression of WT-INCENP and surv-INCENP, but not by INCENP-ΔCEN (Figure 2a and Supplemental

Figure S2), in line with evidence that Aurora B kinase activity is required for cohesin removal from the chromosomal arms during prophase [261] [45, 262, 263], but at the same time also for protection of centromeric cohesin [208, 262]. However, in cells expressing CB-INCENP we also no longer observed railroad chromosomes but instead found a significant increase in cells with fully separated sister chromatids (Figure 2a, b). This suggested that kinetochore-localized Aurora B was insufficient in protecting centromeric cohesin. Moreover, it implied that localization of Aurora B or the other CPC members at the inner centromere is required to maintain centromeric cohesion upon chromosome bi-orientation.

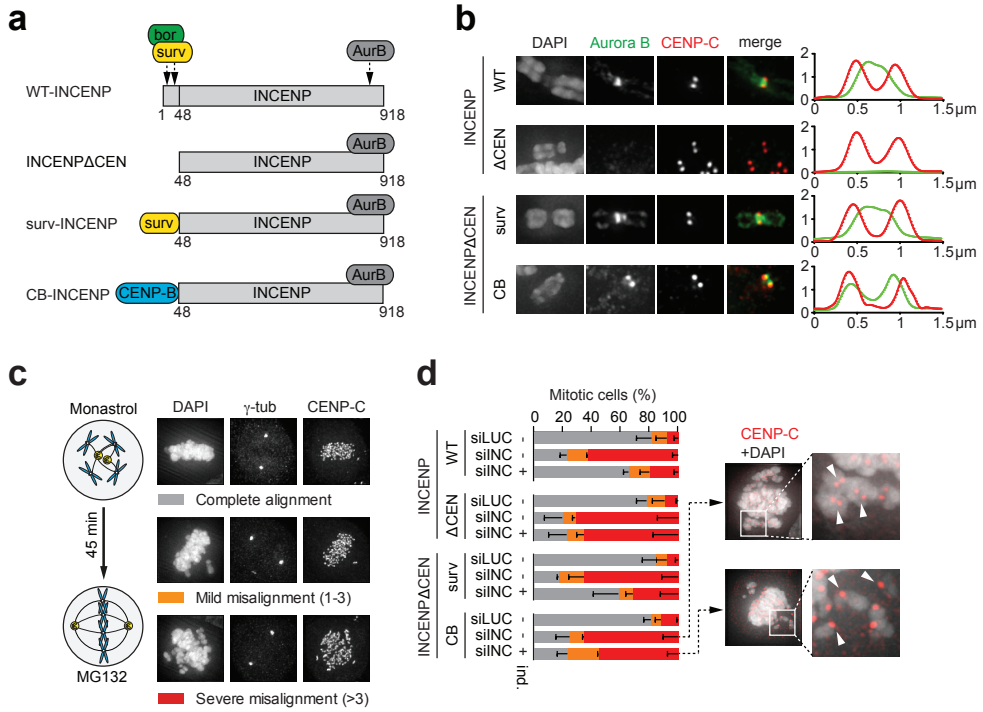

Figure 1l Inner centromere localization of the CPC is required for stable chromosome bi-orientation **a)** Scheme of human CPC (bor, borealin; surv, survivin; AurB, Aurora B) and of INCENPΔCEN (deletion of aa 1-48), survivin-INCENPΔCEN (surv-INCENP) and CENP-B-INCENPΔCEN (CB-INCENP). In all experiments HeLa Flp-In T-REx cells expressing the indicated mCherry-tagged INCENP variants were used. + ind. = expression induced by doxycyclin, - ind. = no induction of expression. **b)** IF of Aurora B and CENP-C on chromosome spreads of nocodazole treated cells. 1D line graphs of Aurora B (green) and CENP-C (red) are shown on the right. **c)** Scheme of the bi-orientation assay (i.e. release from a monastrol-induced mitotic arrest into medium containing MG132) and examples of the alignment categories. **d)** Cells were transfected with siRNAs for Luciferase (siLUC) or INCENP (siINC) and subjected to the bi-orientation assay and chromosome alignment was assessed (n=2 exp., ±100 cells/condition/exp., error bars are SEM). Representative images of two conditions, and enlargements of selected image regions are shown on the right. DNA is visualized using DAPI.

In support of this, we found that loss of the CPC from the inner centromere correlated with a loss of the cohesin protector SGO1 from this site in prometaphase cells. In INCENP knock-down or INCENPΔCEN expressing cells, SGO1 was absent from both the inner centromere and kinetochores (Figure 2c), in agreement with previous work [206, 262]. Inner centromere localization of SGO1 was restored by expression of WT-INCENP and surv-INCENP, but not upon expression of CB-INCENP (Figure 2d). In the latter SGO1 was predominantly found at kinetochores (Figure 2d), a SGO1 pool that

does not support centromeric cohesion [264-266]. Thus, CPC at the inner centromere appears to define spatial positioning cues for SGO1, thereby allowing it to maintain centromeric cohesion.

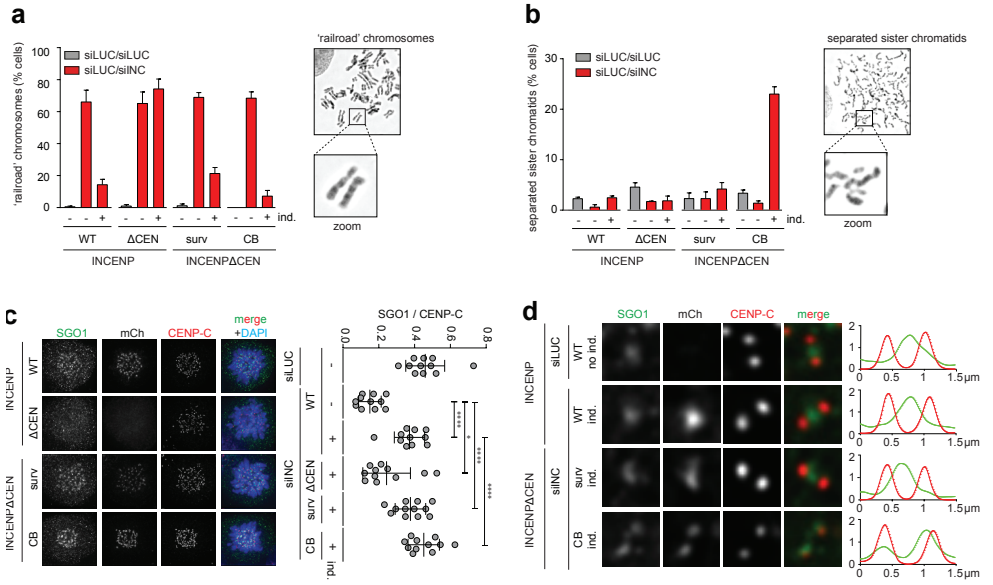

Figure 2l Inner centromere localization of the CPC is required for protection of centromeric cohesin a and b) Cells were transfected with the indicated siRNAs, synchronized as in Figure 1c, and treated with nocodazole for 15 min. after the 45 min. accumulation in MG132. Chromosome spreads were prepared and the percentage of cells in which all chromosomes appeared as "railroads" (a), or in which all sister chromatids were fully separated (b), was quantified (N=2 exp., ±200 cells/condition/exp., error bars are SEM). **c)** IF and quantification of fluorescence intensities (FI) of SGO1/CENP-C on centromeres and/or kinetochores in the depicted cell lines, transfected with the indicated siRNAs, and blocked in mitosis using STLC (1 exp. out of 2, ± 15 cells per condition, error bars are SD, ns=not significant; *P<0.05; ****P<0.0001; unpaired t test). DNA is visualized using DAPI. **d)** Representative sister-kinetochores with SGO1, mCherry and CENP-C and 1D line graphs of SGO1 (green) and CENP-C (red) of cells transfected with the indicated siRNAs, blocked in mitosis using STLC and expressing INCENP variants that rescued SGO1 centromere/kinetochore localization (c).

We then asked whether reduced centromeric cohesion was causing the bi-orientation defect in CB-INCENP-expressing cells (Figure 1d). To test this, we prevented cohesin removal by knockdown of the cohesin release factor WAPL or by overexpression of a sororin mutant (sororin-9A) that acts as a constitutive WAPL inhibitor (Figure 3a, b, f) [36, 37, 44, 53]. Indeed, retention of cohesin rescued chromosome alignment in CB-INCENP expressing cells (Figure 3c, f). Remarkably though, even with Aurora B at kinetochores (Figure 1b), bipolar, tension-generating, cold-stable end-on KT-MT attachments could be established when WAPL was depleted (Figure 3d and Supplemental Figure S3a, b). In line with this, the N-terminal tail of the Aurora B kinetochore substrate and microtubule binding protein HEC1/NDC80, was no longer phosphorylated (Figure 3e)[253]. This suggested that the bi-orientation defect observed upon Aurora B displacement in CB-INCENP expressing cells, is most likely a consequence of weakened centromeric cohesion that is unable to resist the opposing pulling forces originating from the attached KT-MT, a phenomenon known as cohesion fatigue [267].

We next considered two possibilities why centromeric cohesion was less robust in CB-INCENP expressing cells: Stable centromeric cohesion requires a pool of active Aurora B at the inner centromere, or it requires presence of the N-terminal CEN-box of INCENP,

missing in CB-INCENP. The latter possibility predicts that expression of the CEN-box would be sufficient to rescue chromosome alignment in CB-INCENP expressing cells. In fact, this prediction appeared to be true; re-introduction of the CEN-box in CB-INCENP expressing cells rescued chromosome alignment to a similar extent as expression of a sororin-9A mutant, which bypasses the requirement for SGO1-PP2A in maintaining centromeric cohesion (Figure 3f and Supplemental Figure S4a-d) [53]. Fusing an active form of Aurora B (Baronase [215]) onto the CEN-box, guided Baronase localization to the inner centromere but did not further improve chromosome bi-orientation, indicating that the CEN-box itself is critical in stabilizing centromeric cohesion (Figure 3f and Supplemental Figure S4a-d). To test whether this involved inner centromere localization of SGO1, we co-depleted endogenous INCENP and SGO1 in CB-INCENP expressing cells and re-introduced exogenous SGO1 or a fusion protein consisting of the CEN-box and SGO1 (CEN-SGO1)(Figure 3g and Supplemental Figure S4b). While exogenous SGO1 was capable of restoring chromosome bi-orientation in SGO1-depleted cells, it was incapable in INCENP and SGO1 double knock-down cells (Figure 3g). Similarly, expression of the CEN-box did not support chromosome alignment in CB-INCENP expressing cells in which both INCENP and SGO1 were depleted (Figure 3g). However, expression of a CEN-SGO1 fusion protein that localized to the inner centromere when CB-INCENP was expressed (Supplemental Figure S4b), significantly improved chromosome bi-orientation in INCENP/SGO1 double knock-down cells (Figure 3g). Importantly, a CEN-SGO1 N61I mutant that does not bind PP2A did not improve chromosome bi-orientation, highlighting the importance of PP2A in SGO1-dependent cohesion protection (Figure 3a, g)[50-52]. Taken together, our data suggest that the CEN-box in INCENP, either directly or through association with borealin and survivin, provides spatial cues for inner centromere positioning of SGO1, and is thereby needed to prevent precocious sister chromatid separation upon chromosome bi-orientation.

Our data further imply that Aurora B itself does not need to reside at the inner centromere to maintain centromeric cohesion or to allow the stabilization of correctly attached KT-MTs. We found that Aurora B localized at or near the kinetochore in CB-INCENP expressing cells, can correct erroneous KT-MT attachments (Figure 3c), and provide the necessary positive feedback for Haspin-induced H3T3 phosphorylation, and Bub1-mediated H2A-T120 phosphorylation, both of which are required for inner centromere recruitment of the CEN-box (Supplemental Figure S4b-d). This raised the question why Aurora B needs to be confined to the inner centromere.

Microtubules that are stably attached to kinetochores are expected to silence the mitotic checkpoint [268, 269]. However, we measured a significant metaphase delay in the CB-INCENP expressing cells in which we had knocked down WAPL (264. 5 ± 128.0 min vs. 51.8 ± 27.3 min in WAPL-depleted cells without CB-INCENP expression, Figure 4a and Supplemental Figure S5a-c). This suggested that despite stable bi-orientated attachments (Figure 3d and Supplemental Figure S3a), silencing of the mitotic checkpoint was impaired.

The kinetochore protein KNL1 is an important signaling hub for the mitotic checkpoint. It recruits several checkpoint proteins including, BUB1, BUB3, BUBR1 and MAD1, upon phosphorylation of its MELT motifs by Mps1 [270]. Phosphorylation of the KNL1 MELT motifs is antagonized by protein phosphatase 1 gamma (PP1γ), which is recruited to the N-terminal RVSF motif in KNL1 [133, 147]. Phosphorylation of this RVSF motif by Aurora B hampers PP1γ binding to KNL1 allowing optimal MELT phosphorylation and mitotic

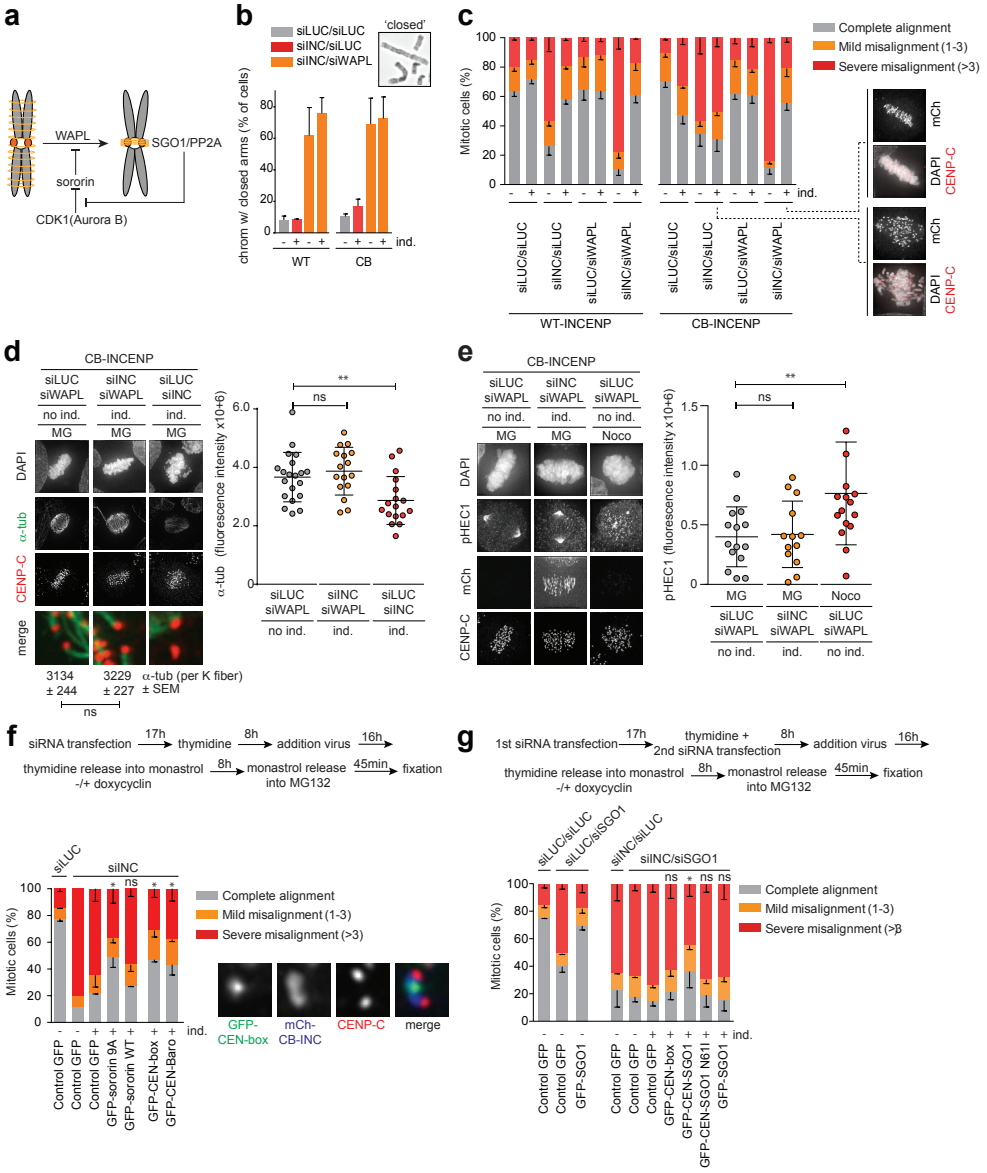

Figure 3l Cohesion maintenance rescues chromosome bi-orientation and promotes stable KT-MT attachments in CB-INCENP expressing cells

a) Scheme of the regulation of WAPL-dependent cohesin removal from chromosomal arms. **b)** Quantification of the % of cells with chromosomes with fully closed arms as a measure for efficiency of the siRNA-mediated WAPL knock-down (N=2 exp., ±200 cells/condition/exp., error bars are SEM). **c)** Cells were transfected with the indicated siRNAs and subjected to the bi-orientation assay (Figure 1c). Chromosome alignment was assessed (N=3 experiments, ±100 cells/condition/experiment, error bar is SEM). Representative images of two conditions are shown. **d)** IF for α-tubulin and CENP-C in cells transfected with the indicated siRNAs and subjected to the bi-orientation assay followed by ice-cold treatment. FI quantifications of spindle α-tubulin (1 out of 2 exp. N=16-20 cells/condition/exp, error bar is SD, ns=not significant; **P<0.01; unpaired t test). Numbers below images depict the mean FI of >17 individual K fibers. **e)** IF for phosho-HEC1 (Ser44, pHEC1), mCherry and CENP-C (1 out of 2 exp. N=15 cells/condition/exp., error bar is SD, ns=not significant; **P<0.01; unpaired t test). DNA is visualized using DAPI. **f and g)** Cells -/+ induction of CB-INCENP were subjected to the depicted experimental set-up (siSGO1 was co-transfected directly after thymidine addition (g)), and chromosome alignment was assessed (N=2 exp, ±100 cells/condition/exp., error bars are SEM, ns=not significant; *P<0.05; two-way ANOVA for % complete alignment compared to control GFP, +ind.).

checkpoint activity [133, 147]. We found that the phosphorylation status of the RVSF motif in KNL1 was enhanced on metaphase chromosomes of WAPL-depleted cells with Aurora B localized near kinetochores (Figure 4b). This correlated with enhanced MELT phosphorylation, increased kinetochore recruitment of BUB1, and low levels of MAD1 on all metaphase kinetochores (Figure 4c-e and Supplemental Figure S5d). This suggests that inner centromere localization of Aurora B is needed to spatially separate the kinase from its substrate KNL1, to promote mitotic checkpoint silencing upon chromosome bi-orientation. As mentioned, in contrast to KNL1, the N-terminal tail of HEC1 was no longer phosphorylated and KT-MT attachments were stable in CB-INCENP expressing, WAPL-depleted cells (Figure 3d, e and Supplemental Figure S3a). This suggests that spatial separation of Aurora B from its KT substrates may be a more relevant mechanism for mitotic checkpoint silencing than to allow the dephosphorylation of HEC1 and the stabilization of bi-orientated attachments.

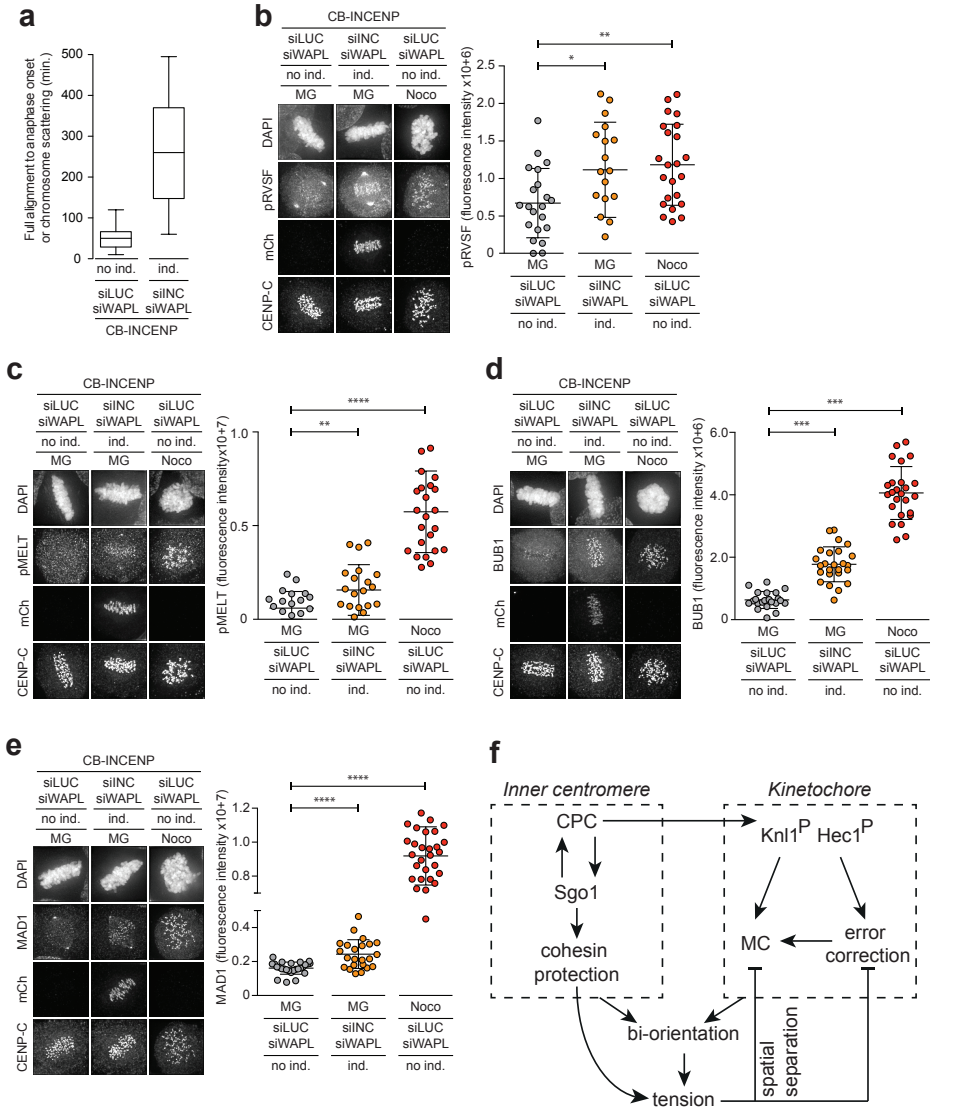

Figure 4| Spatial separation of Aurora B from KNL1 coordinates mitotic checkpoint silencing with bi-orientation
a) Time in metaphase for WAPL-and/or INCENP depleted cells +/- CB-INCENP (N=21-31 cells, see also Supplemental Figure S5). **b-e)** IF of mCherry, CENP- C and phospho-RVSF-KNL1 (pRVSF) (b), phospho-MELT-KNL1 (pMELT) (c), BUB1 (d) and MAD1 (e) in cells -/+ induction of CB-INCENP, transfected with indicated siRNAs and subjected to the bi-orientation assay. Quantifications of fluorescence intensities are shown on the right side of each panel (1 out of 2 exp. N= 15-25 cells/condition/exp, error bar is SD, *P<0.05; **P<0.01; ***P<0.001; ****P<0.0001; unpaired t test). **f)** Model for how the CPC regulates the inner centromere and kinetochore to allow the build-up of tension upon bi-orientation and to coordinate checkpoint silencing with bi-orientation.

Our work demonstrates that in human mitotic cells, inner centromere localization of the CPC is a prerequisite for stable chromosome bi-orientation for two main reasons (Figure 4f). First, it is required for inner centromere localization of SGO1 through the CEN-box of INCENP, and thereby for protection of centromeric cohesin from WAPL-mediated removal during prophase. Stable centromeric cohesion not only promotes tension across sister-kinetochores upon bi-orientation, but also prevents precocious sister chromatid separation when bipolar KT-MT attachments have been established. Second, we show that inner centromere confinement of the CPC is important to spatially separate Aurora B from KNL1 upon bi-orientation. This ensures that mitotic checkpoint silencing is coupled to chromosome bi-orientation.

Experimental Procedures

Cell lines and cell culture

HeLa Flp-In T-REx cells were cultured in Dulbecco's modified Eagle's medium (Sigma Aldrich) supplemented with 6% Tetracycline Screened HyClone Fetal Bovine Serum (GE Healthcare), 1 mM ultraglutamine (Lonza), 4 µg/ml Blasticidine S (Invitrogen) and streptomycin/penicillin (Sigma Aldrich). To generate stable cell lines, the pcDNA™5/FRT/TO plasmids encoding VSV-INCENP-mCherry, VSV-INCENPΔCEN-mCherry, VSV-survivin-INCENPΔCEN-mCherry and VSV-CB-INCENPΔCEN-mCherry (verified using sequencing by Macrogen) were co-transfected with pOG44 (Invitrogen) using the standard FuGENE 6 (Promega) transfection protocol. After transfection, cells were selected in medium supplemented with 200µg/ml Hygromycin B (Roche). To generate HeLa VSV-CB-INCENPΔCEN-mCherry cells stably expressing H2B-GFP, lentivirus was produced. HEK 293T cells were co-transfected with pWPT-H2B-GFP, pRSV, pMD2-G and pMDLG-I using the X-tremeGENE (Roche) transfection protocol. The transfected HEK 293T cells were cultured as described above without Blasticidine S. After 48 hours, viruses were harvested and the VSV-CB-INCENPΔCEN-mCherry expressing HeLa Flp-In T-REx cells were used as donor cells for viral transduction.

siRNA transfections and cell synchronization

The following siRNAs were used: siLUC (Luciferase GL2 duplex; Dharmacon/D-001100-01-20), siINCENP (Dharmacon/3'-UTR: GGCUUGGCCAGGUGUAUAU), siSGOL1 (Dharmacon/J-015475-12: GAUGACAGCUCCAGAAAUU) and siWAPL (Dharmacon/J-026287-10: GAGAGAUGUUUACGAGUUU). siRNAs were reverse transfected using HiPerFect (Qiagen) at 20nM for siLUC, siINCENP and siSGO1 and 40nM for siWAPL. Cells were seeded on 12 mm High Precision coverslips (Superior-Marienfeld GmbH & Co) in 24 wells plates. 16 hours after siRNA transfection, cells were synchronized in G1/S-phase by addition of 2.5µM thymidine (Sigma Aldrich). When SGO1 was co-depleted with INCENP, siINCENP was first reverse transfected

as described, and cells were subsequently forward transfected with siSGO1 directly after thymidine addition. After 24 hours, cells were released from the thymidine block into medium containing 20μM S-trityl-L-cysteine (STLC, Tocris), or 100μM monastrol (Sigma Aldrich). At the same time 1 μg/ml doxycycline (Sigma Aldrich) was added to induce protein expression. To assess the capacity to bi-orient chromosomes, monastrol was washed out 7 hours later and medium containing either 10μM MG132, or 0.83μM Nocodazole (Sigma Aldrich) (Calbiochem) was added for 45 minutes.

Antibodies and immunofluorescence

For immunofluorescence (IF) of γ-tubulin, cells were fixed for 5 min with 4% PFA (Sigma Aldrich), washed once with PBS and permeabilized with ice-cold methanol. After blocking in PBS containing 0.05% Tween 20 and 3% BSA, coverslips were incubated at room temperature with the following primary antibodies: mouse anti-γ-tubulin (1:500, Sigma Aldrich), rat anti-RFP (1:500, ChromoTek, to detect mCherry) and guinea pig anti-CENP-C (1:500, MBL, to visualize the kinetochores). For IF of Aurora B, SGO1, pDSN1, pRVSF-KNL1, pMELT-KNL1, MAD1, BUB1, pH3T3 and pH2A-T120, a brief pre-extraction with 100mM Pipes pH 6.8, 10mM EGTA pH 8, 1mM $MgCl_2$, 0.2% Triton X-100 (PEM/T) was performed followed by addition of an equal volume of 4% PFA. After 5 min., the mixture was removed and 4% PFA was added for 5 minutes. After washing once with PBS, the coverslips were blocked as described above and subsequently incubated with mouse anti-Aurora B (1:1000, BD Transduction Laboratories) or mouse anti-SGOL1 (1:1000, Abnova), rabbit anti-pDSN1-S109 (1:2000), rabbit anti-pRVSF-KNL1-S60 (1:1000, kind gifts of Iain Cheeseman, [146]), rabbit anti-pMELT-KNL1-T601 (1:2000, kind gift of Geert Kops), mouse anti-MAD1 (Merck Millipore), rabbit anti-BUB1 (1:1000, Abcam), rabbit anti-pH3T3 (1:2000, Upstate) and rabbit anti-pH2A-T120 (1:2000, Active Motif). Anti-MAD1 was incubated overnight at 4^0C, whereas all other antibodies were incubated at room temperature for 2 hours. Affinity-purified phospho-specific antibody recognizing KNL1-pMELT-T601 was generated by injection of rabbit with KLH-coupled MDLpTESHTSNLGSQC peptide and affinity purification of bleed-out serum (GenScript). For the cold-stable microtubule assay, cells were incubated with ice-cold medium for 5 min. Then the cells were pre-extracted with PEM/T as described above and mouse anti-α-tubulin (1:10.000, Sigma Aldrich) was used as primary antibody. Goat anti-mouse IgG-Alexa 488, goat anti-rabbit IgG-Alexa 488, goat anti-rat IgG-Alexa 568 and goat anti-guinea pig IgG-alexa 647 were used as secondary antibodies (1:500, Invitrogen). DNA was stained with 1 μg/ml 4',6-diamidino-2-phenylindole (DAPI, Sigma) for 2 min. The coverslips were washed once with PBS, dipped in 100% ethanol, dried and mounted onto glass slides using ProLong Antifade Gold (ThermoFisher) mounting media. The coverslips were imaged on a DeltaVision with a CoolSNAP HQ2 camera and a 100X objective. All image quantifications were performed using ImageJ with a macro that automatically select the kinetochores, these selection were enlarged with 3 pixels, the region of interest (ROI) was then measured in all channels. For background subtraction, a selected area surrounding the DAPI signal was selected, this area was enlarged with 4 px (ROI-A) and with 6 px (ROI-B). Then ROI-A was subtracted from ROI-B, this selected region created the background ROI. For quantification of α-tubulin fluorescence intensity per individual K-fiber, an ROI was selected surrounding part of the MT extending 1μm from the kinetochore. Statistical analyses were done in GraphPad Prism (methods and P-values and are indicated in figure legends).

Chromosome spreads

Cells were synchronized as described for the bi-orientation assay. Forty five minutes

after the release from monastrol into 10μM MG132, nocodazole was added to a final concentration of 0.83μM and incubated for 15 min. Cells were swollen by gradually increasing the concentration of Hank's Balanced Salt Solution (HBSS, Invitrogen) for 35 min. in 5% CO_2 at 37°C and cells were fixed by gradually increasing the concentration of MeOH/Acetic acid (3:1 ratio) at room temperature. When chromosome spreads were combined with IF for Aurora B, cells were released from a thymidine block into medium containing 0.83μM nocodazole and they were allowed to swell in 55mM KCl_2 for 15 min in 5% CO_2 at 37°C. The cells were subsequently centrifuged onto coverslips in a 24 wells plate at 4400 rcf for 1 minute, permeabilized using PEM/T, and fixed with 4% PFA as described above.

Live cell imaging
The HeLa cell line stably co-expressing VSV-CB-INCENPΔCEN-mCherry and H2B-GFP was transfected with the indicated siRNAs and seeded into 8-well chamber slides (Ibidi) and live cell imaging was started 5h after thymidine release. Alternatively, cells were released into Leibovitz's medium (Gibco) containing monastrol with or without doxycycline. Live cell imaging was started 7h after monastrol addition and cells were released from the monastrol block in the course of the imaging experiment into medium containing MG132. Live cell imaging was performed using a DeltaVision microscope equipped with a CoolSNAP HQ2 camera and a 60X objective. All image quantifications were performed using ImageJ.

SDS-PAGE and Westernblotting
Cell lines were seeded into 6 wells plates and synchronised and released from a thymidine block into medium supplemented with 20μM STLC. Seven hours later cells were harvested and washed with PBS once followed by lysis in Laemmli buffer. SDS-PAGE and western blotting were performed using the standard Bio-Rad protocols. The nitrocellulose membranes were blocked in TBS/0.1% Tween 20 (TBST) containing 4% milk for 30 minutes and incubated with the following primary antibodies: rat anti-RFP (1:500, ChromoTek, to detect mCherry), mouse anti-α-tubulin (1:10000, Sigma) or rabbit anti-GFP (custom made). After washing in TBST, the membranes were incubated in HRP-conjugated secondary antibodies goat anti-rat (1:2000, Santa Cruz) or goat anti-mouse (1:2500, Dako) in TBST-4% milk ECL (Advansta) was used as substrate of HRP and chemiluminescence was measured using an Amersham Imager 600.

BacMam virus production and transduction
pACEBac1-CMV encoding GFP-CENP-B (aa 1-498 of CENP-B), VSV-CEN-box-GFP (aa 1-63 of INCENP), VSV-CEN-Baronase-GFP (Baronase according to [215]), VSV-SGO1-GFP, VSV-CEN-Sgo1 WT/N61I-GFP and sororin WT/9A-GFP (sororin WT/9A manufactured by IDT) were transformed into EmBacY cells to generate recombinant bacmids that were subsequently transfected for the production of viruses as described in van der Horst *et al.* [142]. For optimal viral transduction and protein expression the HeLa cell lines were cultured in RPMI (Sigma) medium containing supplements as described above. The cells were synchronized as described for the bi-orientation assay, and viral transduction was performed 24 h prior to fixation.

Acknowledgements

We thank Prof. Dr. G. Kops and Dr. Vader for valuable input, the Kops and Lens lab members for their feedback, and I. Cheeseman, and G. Kops for their generous gifts of reagents. This work was supported by The Netherlands Organization of Scientific Research (NWO-Vici 91812610 to S.M.A.L; and NWO-Veni 91610036 to M.A.H)

Supplemental information

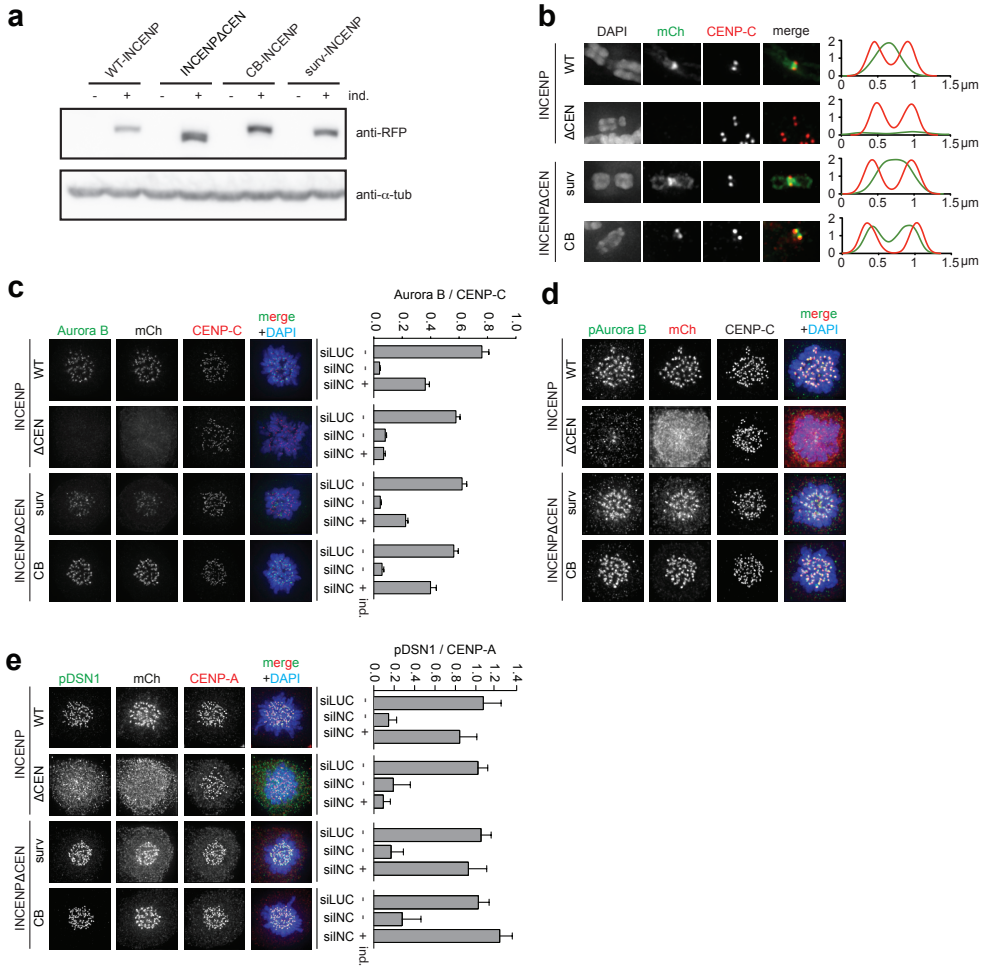

Figure S1l Expression, localization and functionality of INCENP variants used in this study
a) Western blot showing the expression levels of the indicated INCENP variants in HeLa Flp-In T-REx cells -/+ induction (ind.) by doxycyclin for 8 hrs. **b)** IF of mCherry and CENP-C on chromosome spreads of nocodazole treated HeLa Flp-In T-REx cells expressing the indicated mCherry-tagged INCENP variants and transfected with siINCENP. 1D line graphs of mCherry (green) and CENP-C (red) are shown on the right. Of note, although surv-INCENP and Aurora B accumulate at the inner centromere in surv-INCENP-expressing prometaphase cells, we also observed some localization of surv-INCENP and Aurora B over the chromosomal arms. Since survivin directly interacts with pH3T3 [160, 161] and we frequently detected pH3T3 along the chromosomal arms, this most likely explains the additional arm localization. **c)** IF of Aurora B, mCherry and CENP-C in cells +/- induction of the indicated mCherry-tagged INCENP variants, transfected with the indicated siRNAs and blocked in mitosis with STLC. Quantification of the fluorescence intensities of Aurora B/CENP-C is shown on the right (1 exp. out of 2, ±15 cells/condition/exp., error bars are SD). **d)** IF of phospho-Aurora B (T232, pAurora B), mCherry and CENP-C. **e)** IF of phospho-DSN1 (pDSN1), mCherry and CENP-C in cells transfected with the indicated siRNAs and treated with STLC. Quantification of the fluorescence intensities of pDSN1/CENP-A is shown on the right (1 exp. out of 2, ±15 cells/condition/exp., error bars are SD).

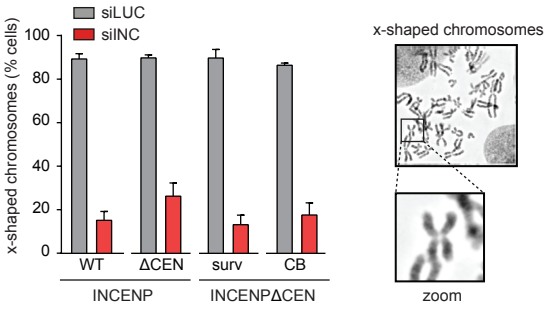

Figure S2l The CPC is required for centromeric cohesion

HeLa Flp-In T-REx cells expressing the indicated INCENP variants, were transfected with the indicated siRNAs, synchronized as in Figure. 1c, and treated with nocodazole for 15 min. after the 45 min. accumulation in MG132. Chromosome spreads were prepared and the percentage of cells with X-shaped chromosomes was quantified (N=2 exp., ±200 cells/condition/exp., error bars are SEM). Representative images of chromosome spread are shown.

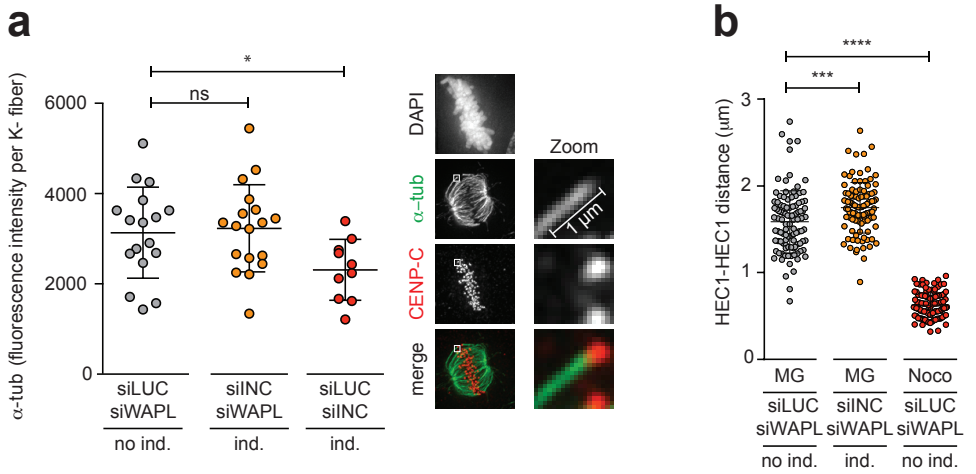

Figure S3l Establishment of tension-generating, cold-stable KT-MT attachments in cells with kinetochore-localized Aurora B

a) IF for α-tubulin and CENP-C in cells transfected with the indicated siRNAs and subjected to the bi-orientation assay (Figure 1c) followed by ice-cold treatment. Quantification of α-tubulin fluorescence intensity of individual K-fiber regions extending 1μm from the kinetochore. Example of a K-fiber region is shown on the right (1 representative exp., 10-18 K fibers/condition, error bar is SD, ns=not significant; *P<0.05; unpaired t test). **b)** HEC1-HEC1 distances measured for >100 kinetochore pairs of ±10 cells per condition (1 representative exp. out of 2; ***P<0.001, ****P<0.0001 ; unpaired t test).

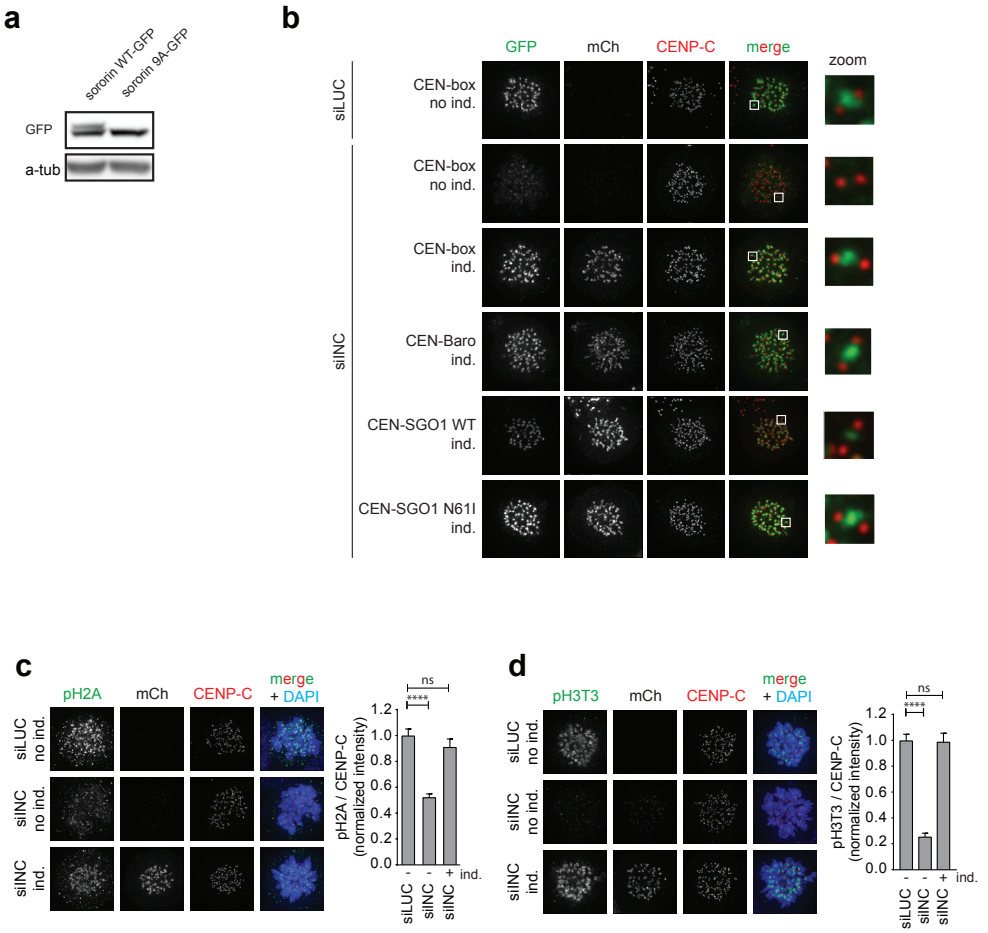

Figure S4l Expression of CB-INCENP restores phosphorylation of H3-T3 and H2A-T120 in INCENP knock-down cells which is required to localize exogenously expressed GFP-CEN-box

a) Detection of expression of sororin proteins by Western blotting after viral transduction into CB-INCENP expressing HeLa Flp-In T-REx cells. Blots were probed with anti-GFP. **b)** IF of GFP (to visualize the GFP-tagged CEN-box, CEN-Baronase, or CEN-box SGO1 fusion proteins), mCherry and CENP-C in HeLa Flp-In T-REx cells -/+ induction CB-INCENP-mCherry and subjected to the experimental set-up as depicted in Figure. 3f and g but fixed when in STLC. Enlargements of selected image regions are shown on the right. **c and d)** IF of mCherry, CENP-C and phospho-H2A (T120, pH2A) (c) and phospho-H3T3 (pH3T3) (d), in HeLa Flp-In T-REx cells +/- induction of CB-INCENP, transfected with the indicated siRNAs and blocked in mitosis with STLC. Quantifications of the relative fluorescence intensities (+/-SEM) of pH2A/CENP-C (c) and of pH3T3/CENP-C (d) are shown on the right (one representative exp. out of 2, ±15 cells/condition/exp.). Of note, in contrast to Klein et al. [271], in our hands GFP-tagged CEN-box did not localize to the inner centromere in INCENP-depleted cells, most likely because of the lack of pH3T3 and pH2A. Phosphorylation of these histones is mediated by Haspin and Bub1, respectively, and both kinases require Aurora B activity for their activation, respectively kinetochore localization [160-163, 165, 182]. In the presence of endogenous INCENP or of CB-INCENP, GFP-CEN-box does localize to the inner centromere, and this correlates with the presence of the pH3T3 and pH2A.

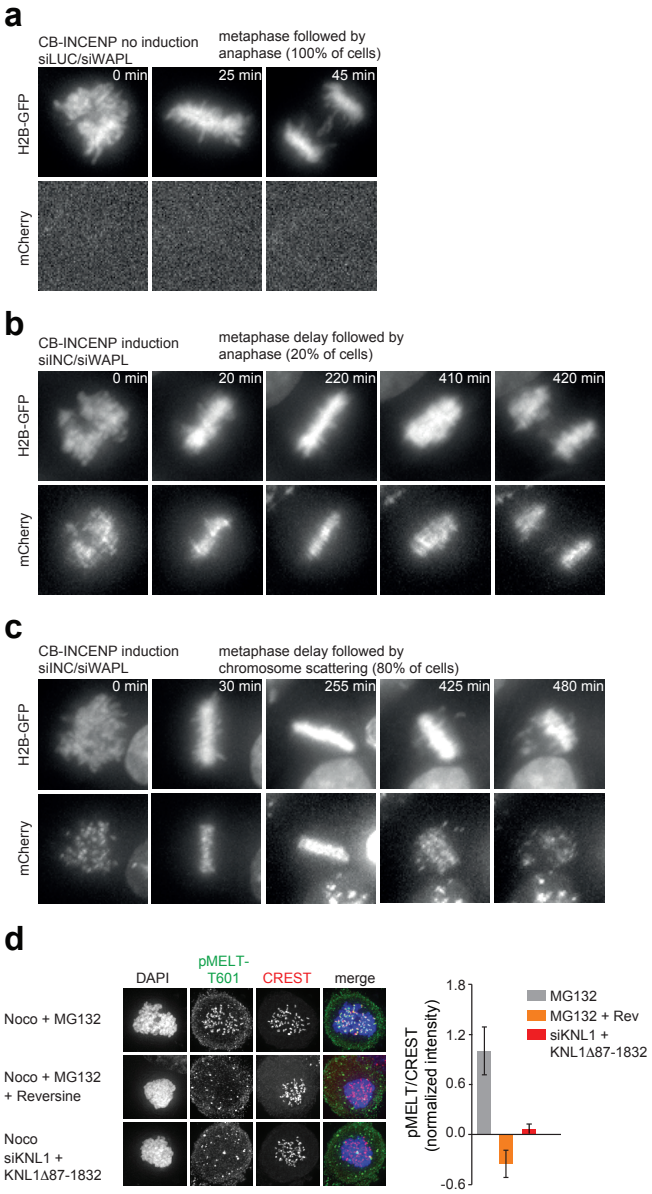

Figure S5l Metaphase delay in WAPL-depleted cells when Aurora B is localized at kinetochores
a-c) HeLa Flp-In T-REx cells -/+ induction of CB-INCENP-mCherry and stably expressing H2B-GFP were transfected with indicated siRNAs, released from a thymidine block and imaged "live" by video microscopy. Stills of one representative cell for each condition and category are shown. T=0 is the first frame after NEB, the following image represents the first frame in which all chromosomes were aligned at the metaphase plate. Time from complete alignment to anaphase or chromosome scattering was calculated and is presented in Figure 4a. Of note, after a 264.5 ± 28.0 min delay, ±20% of the CB-INCENP expressing cells went into anaphase, whilst 80% of the cells showed signs of chromosome scattering, i.e. cohesion fatigue, and remained in mitosis. This suggests that an overall increase in cohesin might not fully compensate for defective centromeric cohesion. **d)** Validation of the KNL1-pMELT1-T601 antibody. The indicated phospho-specific antibody was used to stain HeLa cells that were blocked in mitosis using nocodazole and treated with the MPS1 inhibitor reversine (plus MG132 to prevent mitotic exit). In addition, cells in which endogenous KNL1 was knocked-down by siRNA and replaced by exogenously expressed KNL1 lacking aa 87-1832 was included in the analysis.

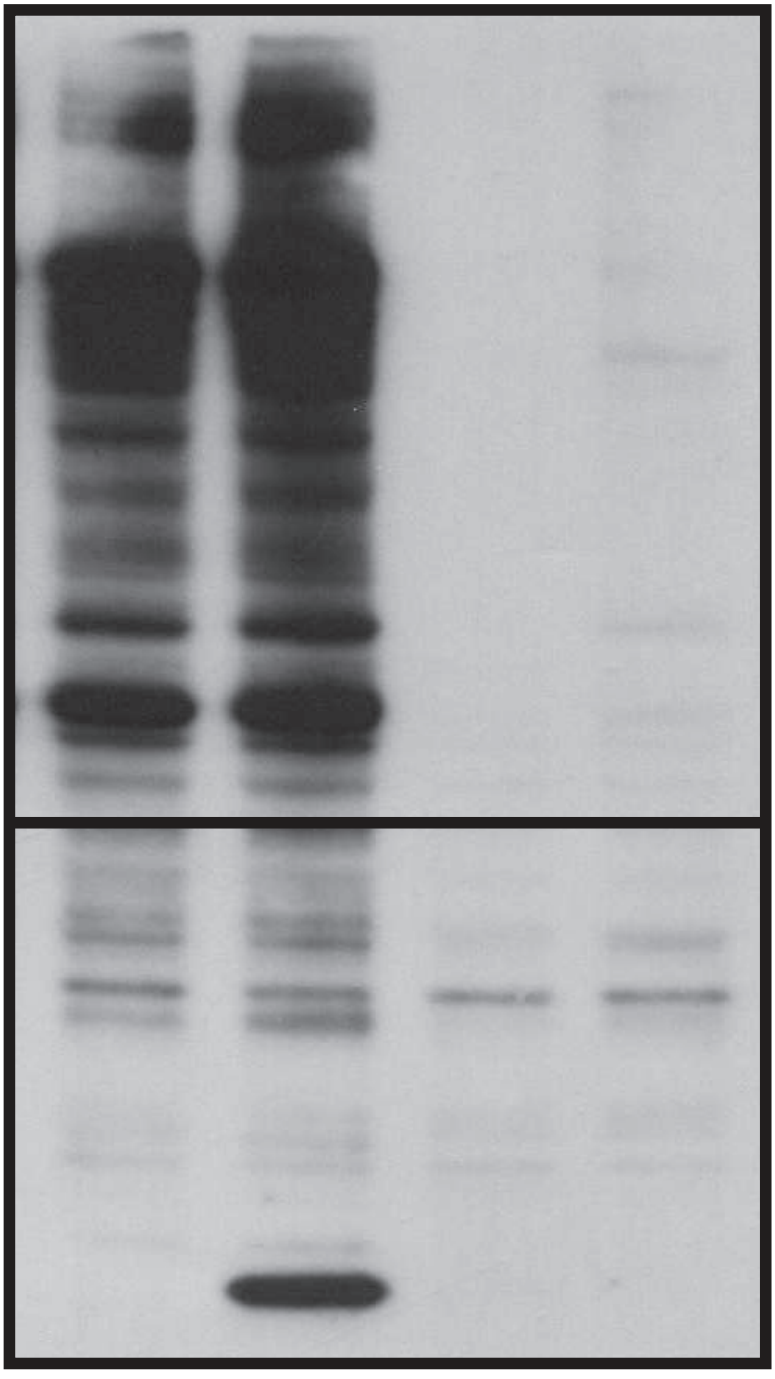

Chapter 3

Development of a chemical genetic approach for human Aurora B kinase identifies novel substrates of the chromosomal passenger complex

Rutger C. C. Hengeveld‡[1], Nicholas T. Hertz‡[2,5], Martijn J. M. Vromans[1], Chao Zhang[4], Alma L. Burlingame[3], Kevan M. Shokat[2], Susanne M.A. Lens[1]

From the [1]Department of Medical Oncology, University Medical Center, 3584 CG Utrecht, The Netherlands, the [2]Howard Hughes Medical Institute and the Department of Cellular and Molecular Pharmacology, University of California, San Francisco, California 94158, the [3]Department of Pharmaceutical Chemistry, University of California, San Francisco, California 94158, [4]Department of Chemistry, University of Southern California, California 90089, and the [5]Program in Chemistry and Chemical Biology, University of California, San Francisco, California 90089
‡These authors contributed equally

Adapted from Molecular & Cellular Proteomics, January 2012; 11:10.1074, 47-59

Abbreviations

as	analog sensitive
APC/C	Anaphase Promoting Complex/Cyclosome
CPC	Chromosomal Passenger Complex
6-Bn-ATPγS	N^6-Benzyl-ATPγS
3BrB-PP1	(1-(*tert*-butyl)-3-(3-bromobenzyl)-PP1
23-DMB	(1-(*tert*-butyl)-3-(2,3-dimethylbenzyl)-PP1
EGFP	Enhanced Green Fluorescent Protein
ETD	Electron-transfer dissociation
6-Fu-ATPγS	N^6-Furfuryl-ATPγS
GST	Glutathione S-transferase
HCD	Higher-energy C-trap dissociation
HMGN	High mobility group nucleosome-binding domain-containing protein
INCENP	Inner CENtromere Protein
3MB –PP1	1-(*tert*-butyl)-3-(3-methylbenzyl)-PP1
2MB-PP1	1-(*tert*-butyl)-3-(2-methylbenzyl)-PP1
NA-PP1	1-(1,1-dimethylethyl)-3-(1-naphthalenyl)-PP1
NM-PP1	1-(1,1-dimethylethyl)-3-(1-naphthalenylmethyl)-PP1
6-PhEt-ATPγS	N^6-Phenylethyl-ATPγS
PP1	1H-pyrazolo[3,4-d]pyrimidin-4-amine
SLIP	Site location in peptide
UPLC	Ultra Performance Liquid Chromatography
Vsv	vesicular stomatitis virus
XIC	Extracted ion chromatogram

Abstract

To understand how the Chromosomal Passenger Complex (CPC) ensures chromosomal stability, it is crucial to identify its substrates and to find ways to specifically inhibit the enzymatic core of the complex, Aurora B. We therefore developed a chemical genetic approach to selectively inhibit human Aurora B. By mutating the gatekeeper residue L154 in the kinase active site, the ATP binding pocket was enlarged but kinase function was severely disrupted. A unique second-site suppressor mutation was identified that rescued kinase activity in the L154 mutant and allowed the accommodation of bulky N^6-substituted adenine analogs. Using this analog-sensitive Aurora B kinase we found that retention of the CPC at the centromere depends on Aurora B kinase activity. Furthermore, analog-sensitive Aurora B was able to use bulky ATPγS analogs and could thiophosphorylate multiple proteins in cell extracts. Utilizing an unbiased approach for kinase substrate mapping we identified several novel substrates of Aurora B, including the nucleosomal-binding protein HMGN2. We confirmed that HMGN2 is bona-fide Aurora B substrate *in vivo* and show that its dynamic association to chromatin is controlled by Aurora B.

Introduction

Faithful chromosome segregation requires that the duplicated sister chromatids bi-orient on the mitotic spindle, and that anaphase onset does not start before this is accomplished for all chromosomes. The Chromosomal Passenger Complex is essential for this as it specifically destabilizes incorrectly attached spindle microtubules from the kinetochores of the chromosomes and acts on the mitotic checkpoint that inhibits the APC/C until all chromosomes have acquired the correct bipolar attachments [272]. In addition, this complex is important for cytoplasmic division and may have additional functions outside mitosis, such as DNA damage repair in G2 [273] and the epigenetic silencing of gene expression [274]. While it is accepted that the CPC is essential for proper cell division, its potential functions outside mitosis are only beginning to be uncovered. To reveal new *in vivo* functions of the CPC and to understand how this complex is capable of fulfilling all these different functions it is important to specifically and completely inhibit the enzymatic core of the complex (Aurora B) without affecting the stability of the other CPC subunits (INCENP, borealin, survivin).

Current approaches to inhibit Aurora B (siRNA and small molecule inhibitors) are important research tools but they do suffer from variations in the level of protein knockdown or kinase inhibition [275]. In particular, the presence of two other Aurora kinases (A and C) with a high degree of homology to Aurora B, makes it particularly challenging to identify small molecules that selectively inhibit Aurora B [276]. Due to the high level of active site homology, finding an inhibitor concentration that completely inhibits the kinase of interest in cells without affecting any other kinase is nearly impossible. Hence, using the current approaches to target Aurora B makes it difficult to unequivocally resolve the *in vivo* functions of the CPC and may complicate the assignment of true Aurora B substrates. We have therefore developed a chemical-genetic system that allows specific Aurora B inhibition and direct substrate identification.

Chemical genetics refers to a strategy where a kinase is genetically engineered to render it capable of utilizing non-natural ATP analogs to be preferentially utilized as substrates and additionally to be sensitive to unique inhibition by cell permeable ATP analogs [277, 278]. This so-called analogue-sensitive kinase harbors a specific mutation in the ATP-binding pocket that changes a bulky amino acid (i.e. methionine, leucine, phenylalanine or threonine) into a small amino-acid (glycine or alanine). Mutation of this 'gate-keeper' residue enlarges the ATP-binding pocket allowing it to accommodate bulky side-chains of ATP analogs and making it susceptible to cell-permeable derivatives of the Src inhibitor PP1 (PP1 inhibitors) [279]. Approximately 30% of kinases lose their catalytic activity after mutation of the gate-keeper residue, but functionality can be restored by introduction of one or more second-site suppressor mutations [280]. Catalytic activity is critical when attempting to map direct kinase substrates in an unbiased manner [281].

Human Aurora B turned out to be one of the kinases that did not tolerate mutation of the gate-keeper residue (L154) and for which mutation of the predicted second-sites failed to restore functionality. We here describe the identification of a unique second-site suppressor mutation that restored activity of the Aurora B gatekeeper mutants and that made the kinase susceptible to inhibition by PP1 analogs. Using these analog-sensitive Aurora B mutants we demonstrate that retention of the CPC at the centromere depends on Aurora B kinase activity. We also show that the activated Aurora B is capable of using bulky ATPγS analogs to thiophosphorylate multiple proteins in complex cell extracts,

including a number of known Aurora B substrates. As this approach is not biased with respect to known consensus sites or for particular functional categories of putative substrates, it is particularly useful for identifying novel direct substrates. Indeed, we found a number of potential novel Aurora B phosphorylation sites on previously reported substrates, as well as novel substrates of the kinase including the nucleosomal-binding protein HMGN2.

Results

Human Aurora B does not tolerate mutation of the Leucine 154 gatekeeper

Generation of an analog-sensitive kinase requires engineering of the ATP-binding pocket by mutation of a bulky amino acid (the so-called 'gate-keeper') into a small amino-acid (glycine or alanine), to accommodate bulky side-chains of ATP analogs and making it susceptible to cell-permeable derivatives of the Src inhibitor PP1 (PP1 inhibitors) [278, 279]. The gatekeeper of human Aurora B is leucine-154 (Figure 1a) [282] and this hydrophobic residue was mutated into the smaller alanine or glycine residues to alter the shape of the ATP-binding pocket. Recombinant Aurora B^{wt} readily phosphorylated Ser10 of Histone H3 *in vitro*, but both Aurora B gatekeeper mutants failed to do so, similar to a known kinase-dead Aurora B^{K106R} mutant (Figure 1b). In cells, Aurora B resides in a complex with INCENP, borealin and survivin (the chromosomal passenger complex, CPC) and the binding of Aurora B to the COOH-terminal IN-box of INCENP is required for full Aurora B kinase activity [202, 283, 284]. To test if the gate-keeper mutants were active when in complex with the other CPC members, flag-tagged Aurora B^{L154A} and Aurora B^{L154G} mutants were expressed in U2OS cells, immunoprecipitated from mitotic cell extracts, and the protein complexes were subjected to *in vitro* kinase reactions. Also under these conditions only wild-type Aurora B displayed kinase activity while the kinase-dead and gatekeeper mutants were inactive (Figure 1d). Thus, mutation of the L154 gatekeeper residue is not tolerated in human Aurora B.

Identification of a unique second-site suppressor mutation for the human Aurora B gatekeeper mutants

Approximately 30% of kinases do not tolerate gatekeeper mutations, and we showed that Aurora B falls within this group. For several intolerant kinases second-site suppressor mutations were identified that could rescue kinase activity [280]. For the yeast homologues of Aurora B (Ipl1 in *S. cerevisiae* and Ark1 in *S. pombe*) such a second site suppressor mutation was identified [285, 286] and we therefore expected to find the second site suppressor residue for human Aurora B via amino acid sequence alignment. In the *Ipl1-as*, and *Ark1-as* mutants, respectively T244 and S229, were changed into glycine or alanine [285, 286]. Surprisingly, mammalian Aurora B and Aurora A already carry an alanine at that position (Figure 1a), indicating that mammalian Aurora's require a different second-site suppressor mutation. Recently four Aurora B mutations were identified in cell lines with acquired resistance for the small molecule Aurora B inhibitor ZM447439 [287]. Three of these mutations were located in the catalytic active site, while the fourth, H250Y, was in close proximity of the activation loop and strongly enhanced the Aurora B kinase activity [287] (and Figure 1b). Interestingly, multiple sequence alignment showed that Ipl1 had a tyrosine residue at this position (Figure 1a). To test if the H250Y mutation could rescue kinase activity of the Aurora B gatekeeper mutants, we engineered the Aurora $B^{L154A/H250Y}$ and Aurora $B^{L154G/H250Y}$ double

mutants by site-directed mutagenesis. FLAG-tagged mutant proteins were expressed in U2OS cells, immunoprecipitated from mitotic cell extracts and kinase activity of the protein complexes against Histone H3 was tested *in vitro*. Strikingly, the Aurora $B^{L154A/H250Y}$ mutant phosphorylated Histone H3 similar to wild-type Aurora B, but unlike Aurora B^{wt}, its activity was inhibited by the bulky PP1 analog NA-PP1 (Figure 1d, f). The Aurora $B^{L154G/H250Y}$ mutant displayed lower kinase activity than the Aurora $B^{L154A/H250Y}$ mutant, but its activity was further inhibited by NA-PP1 (Figure 1d, f). This shows that the H250Y mutation acts as a second site suppressor and rescues the kinase activity of the Aurora B gatekeeper mutants (Figure 1f). Of note, both mutants needed an intact CPC (or at least INCENP) to be active, since bacterially expressed recombinant Aurora B mutants were not active (data not shown). Importantly, we found exactly the same results for mouse Aurora B where loss of kinase activity due to mutation of the L159 gatekeeper residue into alanine was rescued by mutation of H255 into tyrosine (Figure 1e).

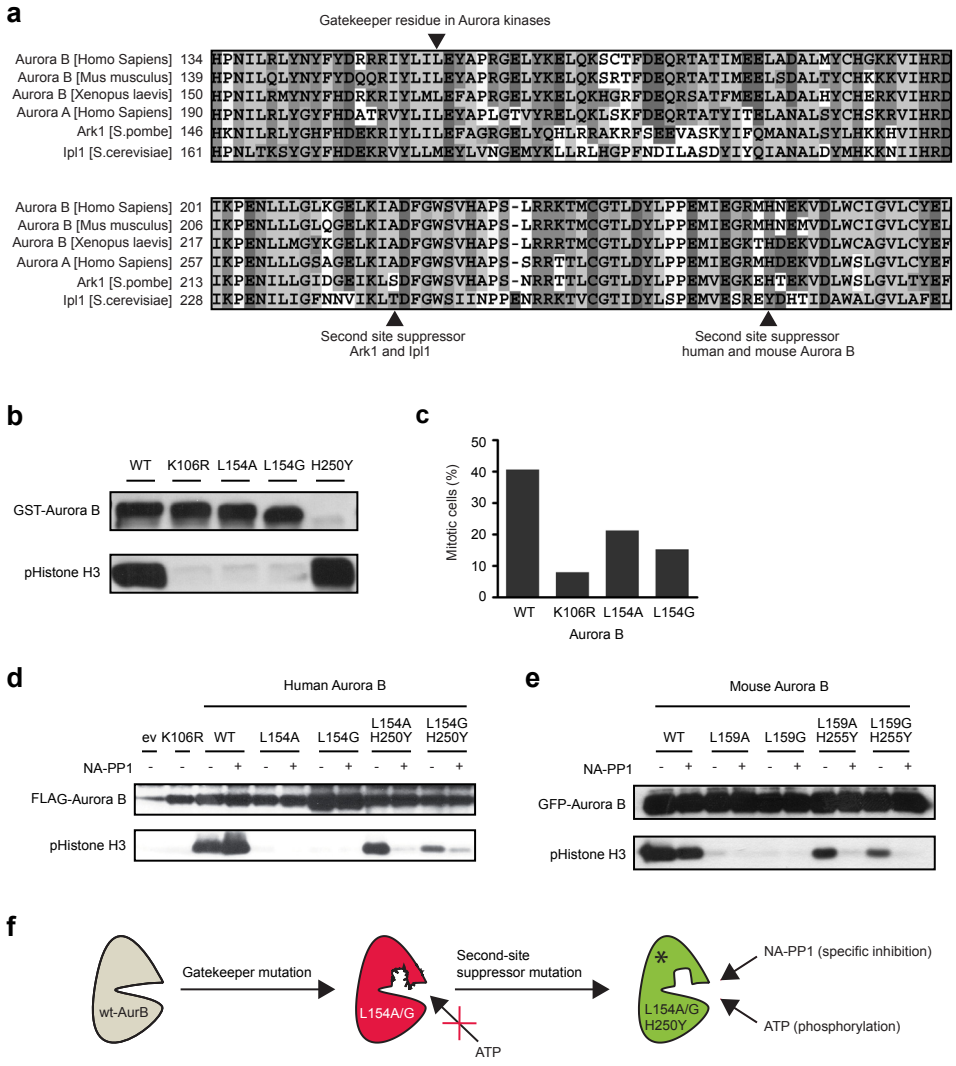

Figure 1l The H250Y mutation rescues kinase activity of Aurora B gatekeeper mutants
a) Multiple sequence alignment of the Aurora kinases in different species. The gatekeeper residue and the second site suppressor mutation found in Ark1 and Ipl1 as well as the newly identified second site suppressor mutation for human and mouse Aurora B are indicated. **b)** *In vitro* kinase assay with the indicated recombinant GST-tagged Aurora B proteins and recombinant Histone H3 as substrate. Since one master mix of kinase reaction buffer plus Histone H3 was used, each reaction was supplemented with the same amount of substrate. Phosphorylation of Histone H3 was detected with an antibody specific for phosphoserine 10. Note that even a small amount of Aurora B^{H250Y} results in massive phosphorylation of Histone H3. **c)** Mitotic index of paclitaxel treated U2OS cells transfected with cDNAs encoding the indicated Aurora B mutants. All three mutants are dominant-negative over the endogenous kinase and therefore reduce the mitotic delay induced by paclitaxel. **d, e)** FLAG-tagged human Aurora B mutants (d) and GFP-tagged mouse Aurora B mutants (e) were immunoprecipitated from mitotic U2OS cells. Kinase reactions were performed in the presence of ATP and with or without NA-PP1 (2 μM). Histone H3 was used as substrate. **f)** The H250Y mutation rescues kinase activity of Aurora B gatekeeper mutants. The double mutants are inhibited by NA-PP1.

Analog-sensitive Aurora B mutants are inhibited by low concentrations of NA-PP1 in cells

To study the function of Aurora $B^{L154A/H250Y}$ and Aurora $B^{L154G/H250Y}$ in cells, we analyzed the behavior of Aurora $B^{L154A/H250Y}$ and Aurora $B^{L154G/H250Y}$ expressing U2OS cells in paclitaxel. Paclitaxel is a microtubule-stabilizing drug that induces a mitotic delay due to the activity of the mitotic checkpoint [288]. Inhibition of Aurora B in paclitaxel-treated cells compromises the mitotic checkpoint and cells exit mitosis [167, 182]. The mitotic index of cells treated with paclitaxel was therefore used as a measure of Aurora B kinase function. Aurora B^{wt} expressing cells were arrested in mitosis after exposure to paclitaxel and addition of 2 μM NA-PP1 did not affect this mitotic arrest (Figure 1c, Figure 2a, b). As expected the mitotic index of Aurora B^{K106R} expressing cells was reduced to <5% (Figure 1c, 2a), confirming that this kinase-dead mutant is dominant negative and that reduced Aurora B activity overrides the mitotic checkpoint when microtubules are stabilized by paclitaxel [167, 289, 290]. Interestingly, while overexpression of the inactive Aurora B^{L154A} and Aurora B^{L154G} single mutants perturbed the response to paclitaxel (Figure 1c), Aurora $B^{L154A/H250Y}$ expressing cells reached a mitotic index of approx. 40%, similar to Aurora B^{wt} expressing cells (Figure 2a). However, addition of NA-PP1 to the Aurora $B^{L154A/H250Y}$ expressing cells resulted in a dramatic reduction in the mitotic index, indicating that Aurora $B^{L154A/H250Y}$ only acts in a dominant-negative fashion when inhibited by NA-PP1 (Figure 2a). In line with its reduced activity (Figure 1d), cells expressing Aurora $B^{L154G/H250Y}$ displayed a reduced mitotic index in paclitaxel (± 25%) compared to Aurora B^{wt} and Aurora $B^{L154A/H250Y}$ expressing cells. Addition of NA-PP1 further reduced the mitotic index, showing that Aurora $B^{L154G/H250Y}$ was also sensitive to NA-PP1 (Figure 2a, b). To test which PP1 inhibitor analog was the most potent inhibitor of Aurora B-as kinases, we tested six different PP1 inhibitors (NA-PP1, NM-PP1, 3MB-PP1, 3BrB-PP1, 2MB-PP1 and 23-DMB) against Aurora $B^{L154A/H250Y}$ and Aurora $B^{L154G/H250Y}$ expressing cells and determined the mitotic index after paclitaxel treatment (Figure 2a, Supplemental Figure S1). All of these inhibitors inhibited the Aurora B-as mutants at a concentration of 2 μM, but titration of NA-PP1, NM-PP1 and 23-DMB showed that both Aurora B-as mutants were most sensitive to NA-PP1 (Supplemental Figure S1). Further titration of this compound demonstrated that 0.06 μM of NA-PP1 was sufficient to compromise the response to paclitaxel because of efficient Aurora B kinase inhibition (Figure 2b).

Aurora B kinase activity is required to retain CPC localization at the centromere

To further prove that the Aurora $B^{L154A/H250Y}$ and Aurora $B^{L154G/H250Y}$ analog-sensitive mutants behave as Aurora B^{wt} in the absence of cell permeable ATP analogs, we analyzed their localization in mitosis. As expected, GFP-tagged Aurora B^{wt} co-localized with endogenous survivin to centromeres in prometaphase (Figure 3), and

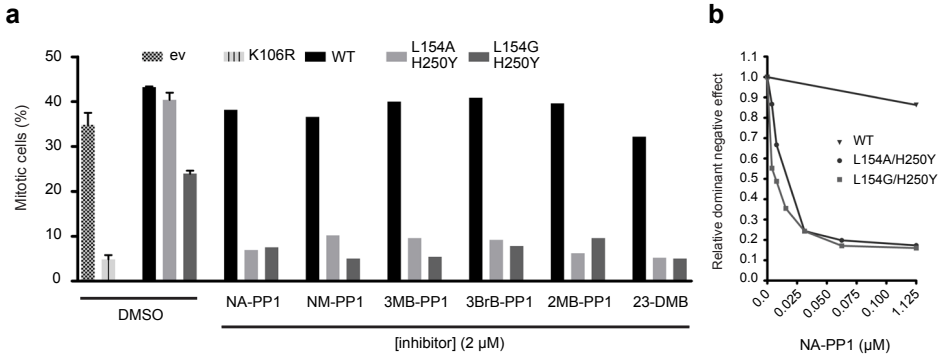

Figure 2l The analog-sensitive Aurora B mutants are inhibited by PP1 analogs in cells
a) U2OS cells expressing the indicated proteins were released from a thymidine induced G1/S block into medium containing paclitaxel plus or minus the indicated PP1 analogs. Seventeen hours after release, the mitotic index was determined by propidium iodide/MPM2 monoclonal antibody labeling and FACS analysis. **b)** Similar as in a) but now different concentrations of NA-PP1 were added to the cells. For each transfected cell population the mitotic index without PP1 inhibitor was set to 100% and the relative reduction in mitotic index in the presence of PP1 inhibitor determined.

to the central spindle in anaphase (not shown) [272]. Addition of NA-PP1 did not affect this centromeric localization. The Aurora B^{K106R} kinase-dead mutant failed to localize properly to centromeres and was displaced over the chromosomal arms (Figure 3). This also resulted in the displacement of endogenous survivin (Figure 3). This atypical localization of Aurora B^{k106R} was seen before, only after heavy overexpression of the kinase-dead protein [167]. Interestingly, when we overexpressed GFP-tagged Aurora $B^{L154A/H250Y}$ it localized normally to centromeres together with survivin (Figure 3). Yet, when we inhibited its kinase activity with NA-PP1, both exogenous Aurora B and endogenous survivin displaced from the centromeres to the chromosomal arms (Figure 3), indicating that Aurora kinase activity is required for centromeric localization of CPC proteins (Aurora B and survivin) in mitosis [165]. In line with this, the Aurora $B^{L154G/H250Y}$ mutant that is slightly less active than the L154A/H250Y mutant was partially displaced from the centromeres in the absence of NA-PP1 and completely displaced when NA-PP1 was present (Figure 3). Based on this we conclude that centromeric retention of survivin and Aurora B, requires Aurora B kinase activity.

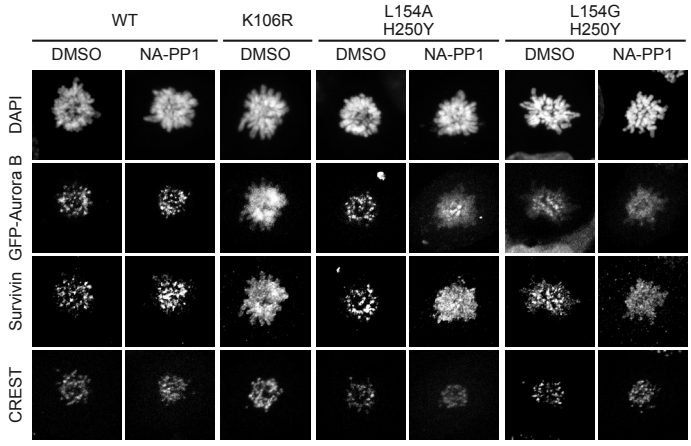

Figure 3l Localization of the analog-sensitive Aurora B mutants
U2OS cells expressing the indicating GFP-tagged proteins were fixed 14 hours after release from a thymidine induced G1/S block into the Eg5 inhibitor S-Trityl-L-cysteine with or without NA-PP1 (2 μM). Centromeres were detected with human CREST antiserum and endogenous survivin with anti-survivin pAb. DNA was counterstained with DAPI. Note the displacement over the chromosomal arms when kinase activity is inhibited by NA-PP1.

Analog-sensitive Aurora B mutant can thiophosphorylate multiple proteins in cell extracts

To selectively label and isolate Aurora B substrates from cell extracts one has to use bulky ATPγS analogs to thiophosphorylate target proteins. However, to achieve this it is crucial to obtain sufficient amounts of active recombinant kinase that can utilize these bulky ATPγS analogs. We therefore isolated recombinant Aurora B in complex with His-INCENP from insect (Sf9) cells and tested if this recombinant protein complex phosphorylated Histone H3 *in vitro*. Similar to our previous results with the immunoprecipitated proteins (Figure 1d), we found that the recombinant INCENP/Aurora B^{wt} and INCENP/Aurora $B^{L154A/H250Y}$ protein complexes readily phosphorylated Histone H3 *in vitro* while phosphorylation by INCENP/Aurora $B^{L154G/H250Y}$ was reduced (Figure 4a). Again, NA-PP1 only inhibited the recombinant analog-sensitive Aurora B mutants and not Aurora B^{wt}.

Remarkably, though, when we tested three different bulky ATPγS analogs, we found that INCENP/Aurora $B^{L154G/H250Y}$, but not INCENP/Aurora $B^{L154A/H250Y}$ and INCENP/Aurora B^{wt} efficiently thiophosphorylated Histone H3 in the presence of all three bulky ATPγS analogs (Figure 4b). Since INCENP/Aurora B^{wt} showed some reactivity with N^6-Bn-ATPγS, and thiophosphorylation of Histone H3 by INCENP/Aurora $B^{L154G/H250Y}$ was more efficient with N^6-Fu-ATPγS than with N^6-PhEt-ATPγS (Figure 4b), we choose N^6-Fu-ATPγS to perform a kinase reaction in a whole cell extract prepared from mitotic HeLa cells. As shown in Figure 4c, INCENP/Aurora $B^{L154G/H250Y}$ could still thiophosphorylate recombinant Histone H3 in the presence of 50 µg of total cell extract and more importantly, we detected multiple thiophosphorylated proteins in the extract in which recombinant His-INCENP/ Aurora $B^{L154G/H250Y}$ was present that were not present in the negative control indicating these proteins were thiophosphorylated by INCENP/Aurora $B^{L154G/H250Y}$.

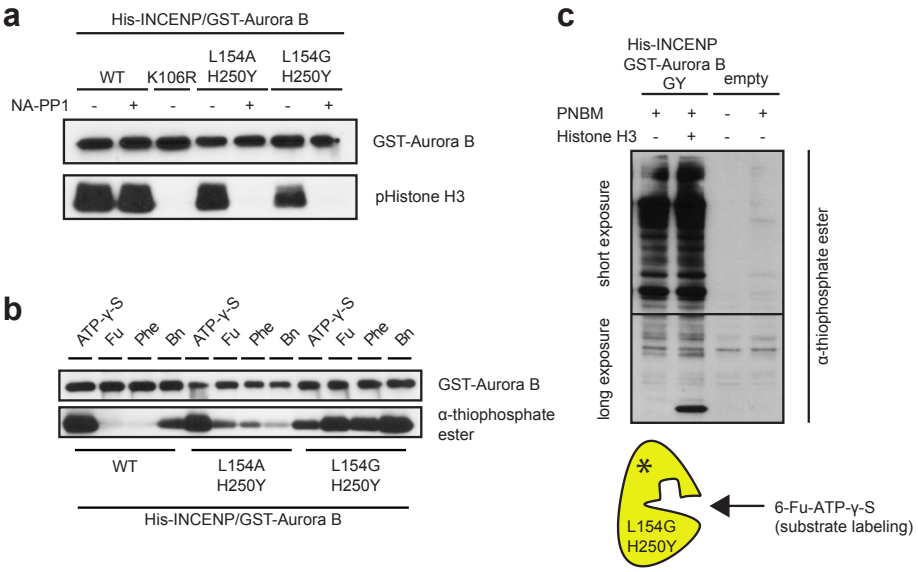

Figure 4| The Aurora B analog-sensitive mutant thiophosphorylates multiple proteins in cell extracts
a) *In vitro* kinase assay with recombinant His-INCENP/GST-tagged Aurora B, co-purified from SF9 cells, in the presence of ATP and with or without NA-PP1 (2 μM). Histone H3 was used as a substrate. **b)** *In vitro* kinase assay with recombinant His-INCENP/GST-tagged Aurora B (wt or analog-sensitive mutants) in the presence of ATPγS, N^6-Furfuryl-ATPγS (Fu), N^6-Phenylethyl-ATPγS (Phe) or N^6-Benzyl-ATPγS (Bn). Thiophosphorylated Histone H3 was detected with a thiophosphate ester epitope-specific antibody [291]. **c)** *In vitro* kinase assay with His-INCENP/GST-Aurora $B^{L154G/H250Y}$ in the presence of N^6-Furfuryl-ATPγS. Fifty microgram of a mitotic HeLa cell lysate was used as input and Histone H3 was spiked into this lysate to serve as positive control. For the lower part of the blot (containing proteins with MW 15-50 kD) a longer exposure is shown.

Identification of Aurora substrates and their phosphorylation sites in cell extracts
Next, we performed two independent kinase reactions with 4 μg recombinant His-INCENP/Aurora $B^{L154G/H250Y}$ complex and 4 mg of mitotic cell extract, or with 4 mg of mitotic cell extract without addition of the recombinant protein complex (negative control) (Figure 5a). Thiophosphorylated peptides were isolated according to the covalent capture-and-release methodology, described by Blethrow *et al.* [281] and Hertz *et al.* [292], and peptides were analyzed by mass spectrometry. The phosphopeptides were then compared between the samples, and only peptides that were never identified in the negative control samples but were present with INCENP/Aurora $B^{L154A/H250Y}$ were predicted to be putative Aurora B substrates (Figure 5a). In total 114 phosphorylated peptides were identified in the plus His-INCENP/Aurora $B^{L154G/H250Y}$ samples, revealing 92 unique phosphosites in a total of 58 proteins (Table 1, Supplemental Table S1). When we only considered the phosphosites with a SLIP score threshold of 6, or singly present in the peptide [293] (n= 70, Table 1, Supplemental Table S1), we found in 57 of the 70 phosphosites (81%) an arginine (R) at position -2, in line with the previously predicted Aurora consensus motif [K/R]-X-[S/T][I/L/V] [294] (where X represents any residue) and in line with a recent peptide-library screen by Alexander *et al.* [295] (Table 1, Supplemental Table S2). Similar to that work we also found a preference for hydrophobic residues in the +1 (36/57 sites) or +2 position (14/57 sites)(Table 1, Supplemental Table S2). Moreover, in line with the published finding that a proline (P) at position +1 is not tolerated by Aurora kinases [295], we did not find peptides with an R at -2 and a P at +1. In the 13 non R-X-[S/T] sites we found in 2 cases an arginine (R) or a lysine (K) at -1, and in 3 cases an R at -3, in each case combined with an hydrophobic residue in position +1 or +2, a situation that may also be considered as Aurora-specific [247]. For 5 out of the 8 remaining non R-X-[S/T] sites, an adjacent R-X-[S/T] motif was not present in the purified peptide, and these could thus represent novel unexpected Aurora sites (Supplemental Table S2). Yet, given the fact that one of these sites is a validated Cdk1 site in INCENP (T59) [296, 297], we deem this possibility unlikely.

Importantly, while T232 of Aurora B was most likely missed due to the nearby cysteine (C235) that can form a thioether linkage with the iodoacetyl-agarose beads and is therefore not liberated by oxidation-promoted hydrolysis [281], within the R-X-[S/T] group we found back a number of known Aurora B substrates and sites, such as INCENP S893; S894 [202, 284], Myb-binding protein 1A/MYBBP1A S1303 [190]; Vimentin/VIM S73 [238] (Supplemental Table S2). Moreover, we here confirm that the novel site in INCENP (S72) is indeed an Aurora site. A recombinant protein of the N-terminus of INCENP (aa 1-80) was generated and used as substrate in an *in vitro* kinase reaction with the recombinant INCENP/Aurora B^{wt} complex. Indeed, INCENP 1-80 was readily phosphorylated *in vitro*, but its phosphorylation was significantly reduced when S72 was mutated into alanine (Figure 6a). Overall, the thiophosphate-labeling approach revealed candidate Aurora B substrates involved in a wide range of cellular functions such as chromosome segregation, cytokinesis, and spindle formation, chromatin remodeling,

DNA repair, the DNA damage response, mRNA processing, and transcription and translation (Figure 5b). Moreover, we identified at least 20 potential Aurora B substrates that were not found in a recent screen that combined quantitative phosphoproteomics with Aurora kinase inhibition using small molecules [247](Table 2).

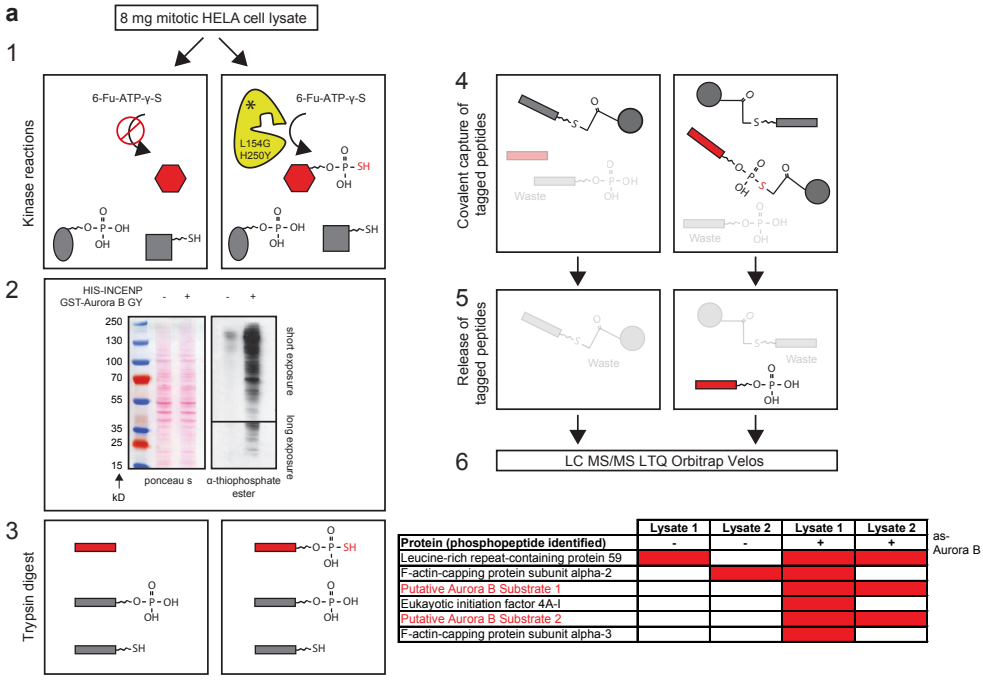

Protein (phosphopeptide identified)	Lysate 1 -	Lysate 2 -	Lysate 1 +	Lysate 2 +
Leucine-rich repeat-containing protein 59				
F-actin-capping protein subunit alpha-2				
Putative Aurora B Substrate 1				
Eukayotic initiation factor 4A-I				
Putative Aurora B Substrate 2				
F-actin-capping protein subunit alpha-3				

as-Aurora B

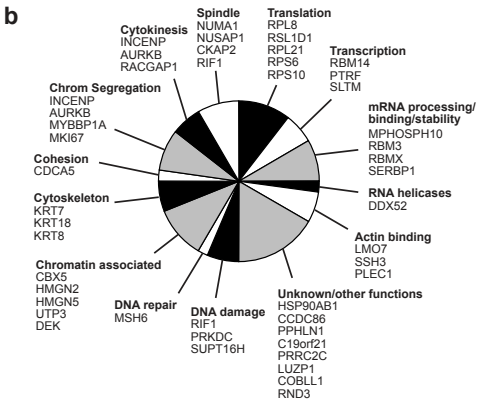

Figure 5l Identification of putative Aurora B substrates by covalent capture and release of thiolabeled peptides

a) Set-up of Aurora B substrate screen using the covalent capture-and-release method. **1l** A kinase reaction performed with His-INCENP/GST-Aurora $B^{L154G/H250Y}$ and N^6-furfuryl-ATPgS results in specific substrate tagging with a thiophosphate group. **2l** Western blot control **3l** The protein mixture containing tagged substrates is digested to peptides. **4l** Thiol-containing peptides react with iodoacetyl-agarose to form covalent bonds. Unbound peptides are washed away. **5l** Only thiophosphopeptides are eluated by oxidation-promoted hydrolysis of the sulfur–phosphorus bond. The thiophosphoryl sulfur atom is replaced with oxygen in this step. **6l** Mixtures are analyzed by mass spectrometry. **b)** Potential Aurora B substrates containing the R-X-[S/T] consensus motif (including ambiguous sites). Substrates were only listed if thiophosphorylated peptides were found in two independent experiments.

TABLE I
Overview of the 92 thiophosphorylated sites found in all 114 peptides (peptides were found in one or two experiments) corresponding to 58 proteins

	Number of phosphosites	Site	
		SLIP score of ≥6 or singly present in peptide	Ambiguous
Total	92	70	22
R*X*(S/T)Φ	43	36	7
R*X*(S/T)*X*Φ	18	14	4
R*X*(S/T)*XX*	7	7	0
Non-R*X*(S/T)	24	13	11

TABLE II
Aurora B substrates unique to this screen
The criteria for inclusion include phosphopeptide(s) found in two independent experiments, RX(S/T) motif, E-score ≤ 10E-4, SLIP score ≥ 6, and substrate not found by Kettenbach *et al.* (30).

Name	Full name	Phosphosite	Site found in other phosphoproteome database? (www.phosphosite.org)	Reported function
DEK	DEK	Thr-67	No	Chromatin associated
UTP3	Something about silencing protein 10	Ser-462	No	Chromatin associated
HMGN2	Non-histone chromosomal protein HMG-17	Ser-29	Yes	Chromatin associated
HMGN5	High mobility group nucleosome-binding domain-containing protein 5	Ser-20, Ser-24	Yes	Chromatin associated
KRT8	Keratin, type II cytoskeletal 8	Thr-6, Ser-34	No/Yes	Cytoskeleton
KRT7	Keratin, type II cytoskeletal 7	Ser-27	No	Cytoskeleton
RIF1	Telomere-associated protein RIF1	Ser-2205	Yes	Spindle/DNA damage
PRKDC	DNA-dependent protein kinase catalytic subunit	Ser-511	Yes	DNA damage
RPS10	40 S ribosomal protein S10	Thr-118	No	Translation
RPL21	60 S ribosomal protein L21	Ser-104	Yes	Translation
RPL8	60 S ribosomal protein L8	Ser-130	No	Translation
PTRF	Polymerase I and transcript release factor	Ser-300	Yes	Transcription
SSH3	Protein phosphatase Slingshot homolog 3	Ser-37	Yes	Actin binding
RACGAP1	Rac GTPase-activating protein 1	Thr-249	Yes	Cytokinesis
MPHOSPH10	M phase phosphoprotein 10	Thr-332	No	mRNA processing
HSP90AB1	Heat shock protein HSP 90-β	Ser-452	Yes	Unknown
COBLL1	Cordon-bleu protein-like 1	Ser-955	No	Unknown
PPHLN1	Periphilin-1	Ser-110	Yes	Unknown
PRRC2C/BAT2D1	BAT2 domain-containing protein 1	Ser-1013	No	Unknown
C19orf21	Uncharacterized protein C19orf21	Ser-348	No	Unknown

HMGN2 is a mitotic substrate of Aurora B

To further validate our approach we next asked if the high mobility group nucleosomal binding protein 2 (HMGN2) we identified as a potential Aurora B substrate (Table 2, Figure 5b) could be validated as a *bona fide in vivo* substrate of the kinase. Since HMGN2 is highly phosphorylated in mitosis [298], we tested if Aurora B kinase activity was responsible for its mitotic phosphorylation. Mitotic HeLa cells were treated with two different small molecule inhibitors (Hesperadin and ZM447439) both shown to inhibit Aurora B significantly better than Aurora A [167, 182], and GFP-tagged HMGN2 was immunoprecipitated from these extracts. The mitotic phosphorylation of S25/S29 in HMGN2 was clearly inhibited by Hesperadin and ZM447439, as was the phosphorylation of His-

tone H3 at Ser10, a well-known substrate of Aurora B (Figure 6b). Interestingly, HMGN2 binds to chromatin in interphase, but the protein dissociates from chromatin when cells enter mitosis. (Supplemental Figure S2) and [298]. Both S25 and S29 lie within the nucleosomal binding domain (NBD) of HMGN2 and an HMGN2 S25E;S29E mutant no longer binds to nucleosomes *in vitro* [299]. We therefore tested if the mitotic dissociation of HMGN2 was mediated by Aurora B. Indeed when we let cells enter into mitosis in the presence of Hesperadin or ZM447439, we observed a dramatic increase in the number of mitotic cells with enhanced chromosomal localization of HMGN2 (Figure 6c, d, Supplemental Figure S2). In line with this, HMGN2 appears to re-associate with chromatin in anaphase when Aurora B translocates from the centromeres to the central spindle (Supplemental Figure S2). We have thus identified HMGN2 as a novel mitotic target of Aurora B whose dynamic chromatin association is under control of the kinase.

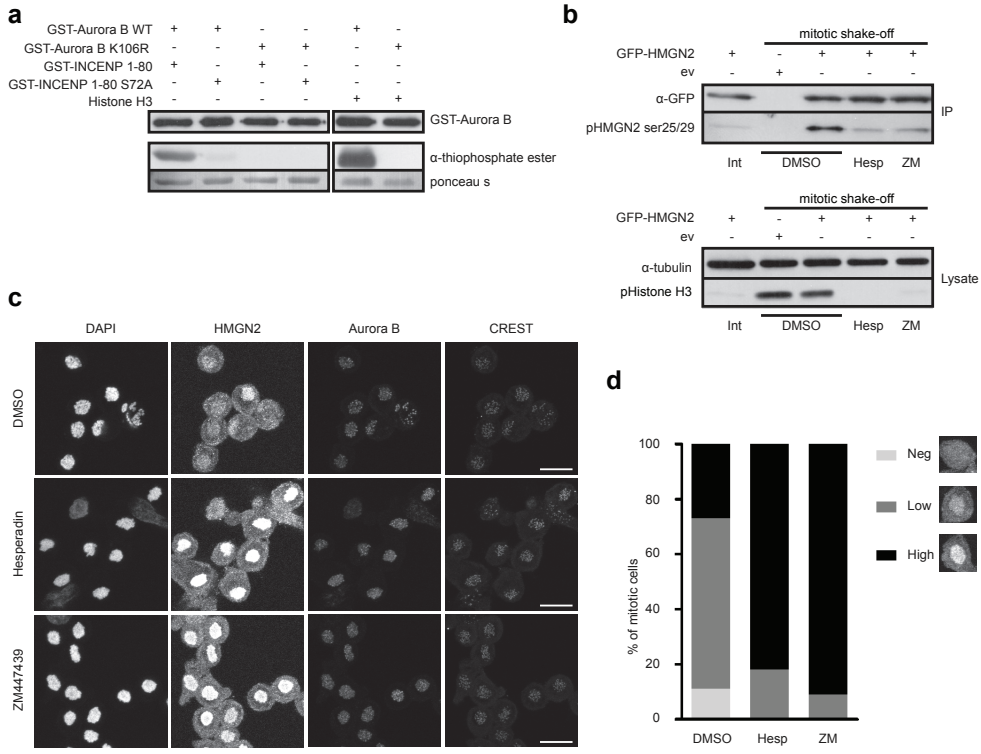

Figure 6l Validation of potential novel Aurora B phosphorylation sites and substrate
a) *In vitro* kinase assay with recombinant His-INCENP/GST-tagged Aurora B (wild-type and kinase-dead), in the presence of ATPγS. Recombinant GST-INCENP 1-80, GST-INCENP 1-80S72A or Histone H3 was added as substrate. **b)** U2OS cells were transfected with either empty GFP vector (ev) or a plasmid encoding GFP-HMGN2. Mitotic cells were collected by mitotic shake-off, and the remaining adherent cells were used as interphase cell input. The overexpressed proteins were immunoprecipitated from the interphase or mitotic cell lysates with an anti-GFP antibody. The precipitated proteins were separated by SDS-PAGE and western blots were probed with an antibody specific for phosphorylated Ser25/S29 in HMGN2 (middle panel) and subsequently reprobed with an anti-GFP antibody (upper panel). Western blots of whole cell extracts were probed with an antibody specific for phosphorylated Histone H3 (Ser10, lower panel). **c, d)** U2OS cells were released into nocodazole in the presence or absence of the indicated Aurora B inhibitors. HMGN2, Aurora B and centromeres (CREST) were visualized with specific antibodies. Images of fields of mitotic cells were captured by a Zeiss LSM microscope (c) and the fraction of mitotic cells with no, lo or high levels of HMGN2 on mitotic chromosomes was quantified (d). For each condition > 100 cells were counted. Scale bar = 20 micrometer.

Discussion

We successfully generated an important new research tool for the functional analysis of human Aurora B, a kinase essential for genomic stability. In contrast to a recent study that identified L138V in Aurora B as a second site-suppressor mutation based on modeling using the published crystal structure of Aurora A bound to ADP [300], the here described H250Y mutation that restored activity of the Aurora B gatekeeper mutants (L154A/G) was found by combining orthologous Aurora sequence alignment and reported information on Aurora B mutations that enhanced kinase activity [301]. This could thus be considered as an alternative strategy to find second-site suppressor mutations for kinases intolerant to gatekeeper mutations.

The unique analog-sensitive mutant of Aurora B is functional in cells and inhibited by low concentrations of the PP1 analog NA-PP1, opening up the possibility to stably replace endogenous Aurora B kinase for this mutant and generate cell lines in which Aurora B can be selectively inhibited. Moreover, the Aurora $B^{L154G/H250Y}$ double mutant is capable of using bulky ATP analogs to thiophosphorylate proteins in cell extracts. This resulted in the isolation of multiple unique phosphopeptides of which 71% corresponded to either a R-X-[S/T]-Φ or a R-X-[S/T]-X-Φ motif (where Φ stands for an hydrophobic residue).

Thus far we identified only highly abundant proteins present in a non-fractionated cell extract as potential Aurora B substrates, but we expect to find more (less abundant) Aurora B substrates when using fractionated cell extracts, enriched for certain subcellular compartments, as input for the kinase reactions [281]. Based on the recent screen by Kettenbach *et al.* [247], that combined quantitative phosphoproteomics with Aurora kinase inhibition using small molecules, our candidates represent only a small portion of the Aurora B substrates. However, the use of chemical inhibitors may affect multiple downstream pathways and non-specific pathways due to off-target kinase inhibition, while our screen will identify only direct Aurora B substrates. Both screens may thus be nicely complementary in finding relevant Aurora B targets. Indeed, we identified at least 20 potential Aurora B substrates that were not uncovered by the Kettenbach screen [247] (Table 2). Importantly, we found RACGAP1, which is a validated substrate of Aurora B [228, 238] and for HMGN2 we demonstrated in this study that it is a novel mitotic target of Aurora B. Moreover, 22 of the 40 recovered R-X-[S/T] Aurora phosphosites were also found in other phosphoproteomic data sets (www.phosphosite.org) [302], indicating that the majority of these sites are also phosphorylated *in vivo*.

Advantages of the chemical genetic approach are that only direct targets of the kinase are labeled, and that we can use different functionally relevant subcellular fractions as input, such as purified chromosome fractions and isolated midbodies, to enable more comprehensive coverage of less abundant Aurora substrates. Yet the challenge will be to verify if the identified sites are also *in vivo* phosphorylated and to establish if the sites are indeed specific for Aurora B. Since the recombinant kinase is no longer confined to its normal cellular locations and Aurora B and A tend to phosphorylate overlapping peptide sequences [295], it is expected that both Aurora B and A substrates will be found. Indeed, 5 out of the 17 phospho-sites that overlapped with the screen by Kettenbach *et al.* [247], were clustered as Aurora A specific sites in that study, while 8 out of 17 were clustered as Aurora B specific and 4 out of 20 as Aurora ambiguous (the latter meaning that the site is mostly likely phosphorylated by both Aurora A and B). Thus, combining the advantages of different substrate screens together with functional

validation experiments, will built a complete picture of the physiologically relevant Aurora B substrates.

To prove that the *in vitro* thiophosphate-labeling approach could indeed identify novel *in vivo* Aurora B substrates, we selected HMGN2 as a candidate for further validation. HMGN2 belongs to a group of non-histone chromosomal proteins (HMGN1-5) that bind to nucleosomes and modulate the structure and function of chromatin. HMGN2 reduces the compaction of chromatin fibers most likely to facilitate gene expression [303], and promotes repair of UV-induced DNA lesions [304]. HMGN2 is highly phosphorylated in mitosis and this phosphorylation coincides with the dissociation of the protein from mitotic chromosomes [298]. We showed that Aurora B kinase is responsible for its mitotic phosphorylation and dissociation from chromosomes. Interestingly, the Aurora B phosphorylation sites (S25 and S29) lie within the RRSARLSA core of the nucleosomal binding domain (NBD) that is conserved between all the members of this protein family [303], and we therefore predict that all HMGN proteins will be Aurora B targets. Indeed, S20 and S24 of HMGN5 were also identified as potential Aurora sites in our screen (Table 1, Supplemental Table S1, Figure 5b), and similar to HMGN2 also HMGN5 dissociates from mitotic chromosomes [305]. Currently, we do not know why the HMGN proteins have to dissociate from chromatin when cells enter mitosis. Since they reduce chromatin compaction, their mitotic dissociation might contribute to full chromatin condensation in mitosis promoting proper chromosome segregation in anaphase.

In conclusion, we have generated a powerful new tool to inhibit Aurora B kinase activity and to identify downstream targets of the kinase. The fact that we uncovered candidate substrates involved in a wide-range of cellular functions could indicate that Aurora B may have multiple functions outside mitosis, or that the putative substrates have additional functions during cell division.

Experimental Procedures

Mutagenesis and cloning

Aurora B^{L154A} and Aurora B^{L154G} were generated by site-directed mutagenesis (QuikChange, Agilent Technologies Wilmington DE, USA) using the following primers: fwd-GGAGGATCTACTTGATTGCAGAGTATGCCCCCCGCGC and rev: CCGCGGGGGGCATACTCTGCAATCAAGTCGATCCTCC for L154A, and fwd: GGAGGATCTACTTGATTGGAGAGTATGCCCCCCGCGG and rev: CCGCGGGGGGCATACTCTCCAATCAAGTAGATCCTCC for L154G, and flag-Aurora B^{wt} (pCR3, Invitrogen by Life Technologies, Paisley, UK) and GST-Aurora B^{wt} (pGEX-4T-1, GE Healthcare, Hoevelaken, The Netherlands) as templates. Aurora $B^{L154A/H250Y}$ and Aurora $B^{L154G/H250Y}$ were generated from the flag-Aurora B^{L154A} (pCR3), flag-Aurora B^{L154G} (pCR3, Invitrogen), plasmids by mutagenesis PCR using fwd: GATTGAGGGGCGCATGTACAATGAGAAGGTGGATC and rev: GATCCACCTTCTCATTGTACATGCGCCCCTCAATC as primers. The Aurora $B^{L154A/H250Y}$ and Aurora $B^{L154G/H250Y}$ PCR products were digested with EcoRI and ligated into the EGFP-C2 (Clonetech, Mountain View CA, USA), pCR3-vsv [289], pGEX-4T-1 and pFastBac (Invitrogen) vectors, to introduce N-terminal GFP, VSV or GST tags, respectively or for expression in Sf9 insect cells. Full length HMGN2 was generated by PCR using the following primers fwd- ATTGAATTCCCCAAGAGAAAGGCTGAAG and

rev-ATTCTCGAGGGGCCCTCACTTGGCATCTCCAGC. The PCR product was ligated into the pJET1.2/blunt cloning vector (Fermentas by Thermo Scientific, St. Leon-Rot, Germany). The vector was digested with EcoRI and ApaI and HMGN2 was ligated into EGFP-C2. All constructs were verified by DNA sequencing.

Cell culture and transfection

U2OS (human osteosarcoma cell line) and HeLa (human cervical cancer cell line) cells were cultured in Dulbecco's modified Eagle's medium (DMEM, Invitrogen) supplemented with 6% fetal calf serum (Invitrogen), 1 mM ultraglutamine (Lonza, Cologne, Germany) and streptomycin/penicillin (Invitrogen). Cell lines were maintained in 5% CO_2 at 37°C. All cDNA transfections were performed using the standard calcium phosphate transfection protocol.

Purification of recombinant proteins

The Aurora B/pGEX-4T-1 vectors were introduced into BL21 bacteria and the transformants were plated on LB-agar plates containing ampicillin and chloramphenicol (both from Sigma-Aldrich, St Louis MO, USA). Protein expression was induced for four hours at 30°C by addition of 1mM IPTG (Isopropyl β-D-thiogalactopyranoside, Sigma-Aldrich). After induction, bacteria pellets were lysed in lysis buffer containing 10 mM EGTA, 10 mM EDTA, 0.1% Tween-20, 250 mM NaCl, 5 mM DTT, 0.325 mg/ml lysozym and protease inhibitors (Complete™, Roche Diagnostics, Almere, The Netherlands). Cells were sonicated and centrifuged at 38,724 rcf for 30 min. at 4°C. Supernatants were coupled to Glutathione-Sepharose 4B beads (Amersham Biosciences, Roosendaal, The Netherlands) and proteins were eluted in buffer containing 50 mM Tris (pH 8.0), 20 mM reduced glutathione and 75 mM KCl. The GST-Aurora B/His-INCENP complexes were purified from baculovirus infected SF9 cells. Protein expression was induced for four days at 27°C. SF9 were pelleted and lysed in buffer containing: 50 mM Tris (pH 8.0), 400 mM NaCl, 1.0% NP-40, 0.5% sodium deoxycholate, 20 mM glycerol-2-phosphate, 0.3 mM $NaVO_3$, 1µg/ml Leupeptin , 1µg/ml Pepstatin, 1µg/ml Aprotinin and 1 mM PMSF (all from Sigma-Aldrich). Cells were sonicated and centrifuged at 15,870 rcf for 20 min at 4°C. Supernatants were coupled to Ni-NTA agarose beads (Qiagen, Venlo, The Netherlands) and washed twice in buffer containing 100 mM Na_2HPO_4, 100 mM NaH_2PO_4, 300 mM NaCl, 10% Glycerol and 20mM imidazole. Protein complexes were eluted in buffer containing 250 mM imidazole.

Immunoprecipitation and *in vitro* kinase reactions

U2OS cells were transiently transfected with FLAG- or GFP- tagged cDNA constructs. Cells were treated with nocodazole (250 µg/ml) for 18 hrs. and mitotic cells were collected by shake-off. Mitotic cells were lysed as described previously [271] and cleared lysates were added to Prot A/G beads coupled to anti-GFP or anti-FLAG (M2, Sigma-Aldrich). Immunoprecipitated or recombinant kinases were included into a 25 µl reaction containing kinase buffer (10 mM $MgCl_2$, 25 mM Hepes (pH 7.5), 25 mM β-Glycerophosphate, 0.5 mM DTT and 0.5 mM Vanadate) and 0.2 mg/ml Histone H3 (Roche Diagnostics), 100 µM ATP with or without 2 µM NA-PP1 (Calbiochem/ Merck Chemicals, Darmstadt, Germany). For thiophosphorylation assays different concentrations of ATPγS or bulky ATPγS analogs (Biolog, Hayward CA, USA) were used. After 30 min at 30°C, reactions were stopped by the addition of 25 µl 2x sample buffer. Thiophosphorylated samples were subsequently incubated with 2.5 mM p-nitrobenzyl mesylate (PNBM, Epitomics, Burlingame CA, USA). This thiol-specific alkylating agent generates a bio-orthogonal tiophosphate ester that is recognized by a thiophosphate

ester-specific antibody (Epitomics) [291].

Western Blotting
Protein samples were separated by SDS-PAGE and transferred to nitrocellulose membranes by standard procedures. Membranes were blocked with 4% milk in Tris-buffered saline containing 1% Tween-20 (TBST) prior to incubation with the following primary antibodies in 4% milk-TBST: Mouse anti-GST (GE Healthcare), rabbit anti-phospho-Ser10 Histone H3 (Upstate Biotechnology, Charlottesville VA, USA), mouse anti-FLAG (Campro Scientific, Berlin, Germany), rabbit anti-GFP (gift of The Netherlands Cancer Institute), mouse anti-Aurora B (BD Biosciences, Breda, The Netherlands), mouse anti-VSV (Sigma-Aldrich), rabbit anti-thiophosphate ester (Epitomics), or anti-phospho Ser25/29 HMGN2 (Acris Antibodies, Herford, Germany). After extensive washing in TBST, blots were incubated with horseradish peroxidase (HRP)-conjugated goat anti-mouse or goat anti-rabbit antibodies (DAKO, Glostrup, Denmark) in 4% milk-TBST. Immunocomplexes were visualized using the ECL chemiluminescence detection kit from Amersham (GE Healthcare).

FACS
Cells were cultured and transfected as describe above. Thymidine (250 µM, Sigma) was added to block the cells in G1/S phase. Cells were released in medium containing: 1 µM pacilitaxel (Sigma-Aldrich) plus DMSO or different concentrations of PP1 analogs. After 18 hours, cells were harvested and fixed in 70% ethanol. Cells were washed 2 times in PBS/0.05% Tween-20 and incubated with mouse anti-MPM2 (Upstate Biotechnology) as primary antibody and goat anti-mouse Cy5 (Jackson ImmunoResearch, West Grove PA, USA) as secondary antibody. Cells were subsequently incubated with staining solution containing propidium iodide and RNase and analyzed by flow cytometry (BD FACSCalibur, BD Sciences).

Immunofluorescence microscopy
The cells were cultured on coverslips and transfected as describe above. After a thymidine block, cells were released in medium containing 20 µM STLC (S-trityl-l-cysteine, Sigma-Aldrich) plus either DMSO or 2 µM NA-PP1 for 14 hrs. Coverslips were fixed in 4% PFA, followed by ice-cold methanol. After blocking in Dulbecco's PBS plus 3% BSA, coverslips were incubated overnight at 4°C with the following antibodies: Human anti-CREST (Cortex Biochem, San Leandro CA, USA), mouse anti-Aurora B (BD Biosciences) and rabbit anti-Survivin (R&D Systems, Abingdon, Oxon, UK) For secondary antibodies goat anti-human Alexa-647, goat anti-mouse Alexa-488 and goat anti-rabbit Alexa-568 (all from Molecular Probes by Life Technologies, Paisley, UK) were used, and DNA was stained with 1 µg/ml DAPI. Images were acquired with a Zeiss LSM 510 Meta confocal microscope with 63X 1.4 N.A. objective. Images were analyzed with Image J. For HMGN2 immunofluorescence a brief PEM/Triton 0.2% pre-extraction was performed prior to fixation with 4% PFA, and rabbit anti-HMGN2 pAb (Acris Antibodies) was used as primary antibody.

Isolation of thiophosphorylated peptides
Covalent capture of thiophosphorylated substrate proteins was preformed essentially as described [292] except for the following modifications. The labeled HeLa cell lysates were denatured by adding 60% by volume solid urea, 1 M tris(2-carboxyethyl)phosphine (TCEP) to 10 mM and incubating at 55°C for 1 hour. Proteins were then digested by diluting the urea to 2 M by addition of 100 mM NH_4HCO_3 (pH 8), adding additional

TCEP to 10 mM final, 0.5 M EDTA to 1 mM, and trypsin (Promega, Madison WI, USA) 1:20 by weight. The labeled lysates were digested for 16 hours at 37°C, acidified to 0.5% trifluoro acetic acid (TFA), and desalted by using a Sep-Pak C18 column (Waters, Milford MA, USA) eluting into 1 ml 50% acetonitrile 0.1%TFA. The desalted peptides were dried by using a speed vacuum to 40 µl. The pH of the peptides was adjusted by adding 40 µl of 200 mM HEPES (pH 7.0), 75 µl acetonitrile and brought to pH 7.0 by addition of 10% NaOH. The peptide solution was then added to 100 µl iodoacetyl beads (Pierce, Rockford IL, USA) pre-equilibriated with 200 mM HEPES (pH 7.0) and incubated with end-over-end rotation at room temperature in the dark for 16 hours. The beads were then added to small disposable columns, washed with H_2O, 5 M NaCl, 50% acetonitrile, 5% formic acid, and 10 mM DTT, followed by elution with 100 µl and 200 µl (300 µl total) 1 mg/mL oxone (Sigma-Aldrich), desalted and concentrated on a 10 µl ZipTip (Millipore, Billerica MA, USA) eluting into 60 µl total volume. The resulting phosphopeptides were concentrated to 10 µl and analyzed by LC MS/MS.

Mass Spectrometry

The phosphopeptides resulting from oxidation promoted hydrolysis and concentration on a ZipTip were concentrated to 10 µl and separated using a 2-50% acetonitrile gradient on a NanoAcquity (Waters) reversed phase 75 micron capillary UPLC column on-line to an LTQ Velos Orbitrap mass spectrometer (Thermo-Fisher, Waltham MA, USA) by both ETD and HCD analysis. Peak lists were generated by using PAVA software (UCSF Release 2011) and searched by batch-tag on Protein Prospector software (UCSF Version 5.3.1) for phosphopeptides with the following conditions: Database: SwissProt.2011.07.06 (20,237 protein entries, 3,618677 enzyme fragments) Taxonomy: Homo sapiens, Precursor charge range: 2,3,4, monoisotopic masses. Parent mass tolerance, 20 ppm. Fragment mass tolerance (20 ppm for HCD, 0.5 Da for ETD). Digest, Trypsin. Non-specific, 0 termini. Max missed cleavages, 2. Constant mods, 0. Expectation calc method, Linear tail fit. Variable mods, Acetyl (protein N-Term), Acetyl+Oxidation (protein N-Term M) Gln->pyro-Glu (N-term Q) Met-loss (Protein N-term M) Met-loss+Acetyl (Protein N-term M) Oxidation (M) Phospho (S/T). After search, we utilized search compare with the parameters as follows: Min score protein 22, Min score peptide 15, Max E value protein 0.01, Max E value peptide 0.05, DB peptide, variable mods, protein mods, SLIP Threshold 6 [293]. Phosphosites where the SLIP score is below 6 are reported as ambiguous. Phosphosites that were identified in at least 2 experiments in the plus INCENP/Aurora $B^{L154G/H250Y}$ samples (at least 2 biological replicates were performed per sample) and not in the negative controls (by XIC) were reported as putative Aurora B substrates.

Viewing Annotated Spectra of Results

Accompanying this document as supplemental information are two zipped peak list files and one results file (tab-delimited text files). These files allow all of the search results to be freely viewed using a spectral viewer; e.g. MS-Viewer (part of the public Protein Prospector website). This software is already on the public website found at this address: http://prospector.ucsf.edu/prospector/cgi-bin/msform.cgi?form=msviewer. The results can be viewed by uploading peak list and results files accompanying this document. Alternatively, the results can be accessed using the links below (where we have already uploaded the results and set up the display parameters).

Aurora B-as_ETD:
http://prospector2.ucsf.edu/prospector/cgi-bin/mssearch.cgi?report_title=MS-Viewer&search_key=fddk75hfbx&search_name=msviewer

Aurora B-as_HCD:
http://prospector2.ucsf.edu/prospector/cgi-bin/mssearch.cgi?report_title=MS-Viewer&search_key=kcwtffdeo6&search_name=msviewer

Acknowledgements

Mass spectrometry was made possible by NIH grants NCRR RR015804 and NCRR RR001614 and Howard Hughes Medical Institute. S.M.A.L, R.C.C.H, M.J.M.V are supported by grants from the Dutch Cancer Society (UU 2009-4311) and the Netherlands Organization for Scientific Research (Vidi 917.66.332). N.T.H was supported by a predoctoral fellowship from Genentech and a Rapid Response Innovation Award from the MJFF. N.T.H and K.M.S are supported by NIH grant R01EB001987 and The Howard Hughes Medical Institute. We thank Prof. R. H. Medema for critical reading of the manuscript.

Supplemental information

Supplemental Table S1| Overview of all peptides isolated from the two mitotic HeLa extracts independently thiophosphorylated by INCENP/Aurora B$^{L154G/H250Y}$

Protein	Site	SLIP Score	Peptide	Peptide score	Expect Score
INCENP	S72	Phospho@72=66	RIS(Phospho)YVQDENRDPIR	36,6	1,60E-11
INCENP	S909	Phospho@909=12	VPS(Phospho)SLAYSLK	33,9	1,80E-08
INCENP	S893; S894	Phospho@894=11;Phospho@892I893	RTS(Phospho)S(Phospho)AVWNSPPLQGAR	37,8	1,60E-10
INCENP	T59	Phospho@59=16	EFSKEPELM(Oxidation)PKT(Phospho)PSQK	28,9	8,20E-10
INCENP	S518	Phospho@518=51	SVM(Oxidation)KS(Phospho)FIKR	28,4	1,20E-09
INCENP	S518	Phospho@518=49	SVM(Oxidation)KS(Phospho)FIK	30,1	2,40E-09
INCENP	S909	Phospho@909=11	VPS(Phospho)SLAYSLKK	39,3	6,30E-09
INCENP	S893	892I893I894	TS(Phospho)SAVWNSPPLQGAR	35,9	4,90E-09
INCENP	S894; S899	Phospho@899=38;Phospho@892I893I894	TSS(Phospho)AVWNS(Phospho)PPLQGAR	35,9	4,90E-09
INCENP	S72	Phospho@72=27	IS(Phospho)YVQDENRDPIRR	20,9	1,00E-05
INCENP	T494	Phospho@494=31	VVRPLRT(Phospho)FLHTVQR	10,6	8,10E-04
INCENP	S446	Phospho@446=6	TDQADGPREPPQS(Phospho)ARR	10,1	0,0032
INCENP	S893; S899	892I893I894	TS(Phospho)SAVWNS(Phospho)PPLQGAR	35,9	4,90E-09
AURKB	S7; T16	Phospho@7=24;Phospho@16=46	ENS(Phospho)YPWPYGRQT(Phospho)APSGLSTLPQR	46	5,00E-16
AURKB	T16	Phospho@16=40	ENSYPWPYGRQT(Phospho)APSGLSTLPQR	52,2	8,20E-16
AURKB	T16	Phospho@16=35	QT(Phospho)APSGLSTLPQR	44,5	2,70E-13
AURKB	T16	Phospho@16=38	Q(Gln->pyro-Glu)T(Phospho)APSGLSTLPQR	44	8,90E-12
AURKB	S19	Phospho@19I22	QTAPS(Phospho)GLSTLPQR	26,9	1,00E-07
NUMA1	S1969	Phospho@1969=95;Oxidation@1970	RAS(Phospho)M(Oxidation)QPIQIAEGTGITTR	38,6	2,40E-11
NUMA1	S1792IS1800IT1804	Phospho@1792I1800I1804	SQAPLESSLDS(Phospho)LGDVFLDSGRKTR	30,4	2,40E-11
NUMA1	T1811	Phospho@1811=18;Oxidation@1819	RRT(Phospho)TQIINITM(Oxidation)TK	24,4	1,10E-08
NUMA1	T1811IT1812	Phospho@1811;Phospho@1812;Oxidation@1819	RRT(Phospho)T(Phospho)QIINITM(Oxidation)TK	24,5	3,70E-10
NUMA1	S2047IT2055	Phospho@2047=10;Oxidation@2048;Phospho@2055=48	RQS(Phospho)M(Oxidation)AFSILNT(Phospho)PK	30,1	2,10E-08
NUMA1	S2047	Phospho@2047=35;Oxidation@2048	RQS(Phospho)M(Oxidation)AFSILNTPK	28,6	4,00E-09
HNRNPA1	S337IS338	Phospho@337I338	S(Phospho)SGPYGGGGQYFAKPR	71,4	2,60E-19
HNRNPA1	S337IS338	Phospho@337I338	GGNFGGRS(Phospho)SGPYGGGGQYFAKPR	49,8	1,40E-12
HIST1H2BJ	S79IY84	Phospho@79;Phospho@84	IAGEAS(Phospho)RLAHY(Phospho)NKR	20	2,00E-06
LMO7	S116	Phospho@116I117	INRLS(Phospho)TPIAGLDNINVFLK	43,1	2,50E-12
LMO7	S1197	Phospho@1197=9	RRS(Phospho)QFFEQGSSDSVVPDLPVPTISAPSR	45,7	1,30E-11
LMO7	S1197IS1204IS1205IS1207	Phospho@1197I1204I1205I1207	RRSQFFEQGSS(Phospho)DSVVPDLPVPTISAPSR	39,6	2,50E-11
LMO7	S751	Phospho@751=11	RKS(Phospho)YTSDLQK	32,4	4,50E-08
LMO7	S751	Phospho@751=18	S(Phospho)YTSDLQK	22,5	1,00E-06
LMO7	S300	Phospho@300	RIS(Phospho)AVEPK	21,8	5,80E-06
LMO7	S1197	Phospho@1197I1204I1205I1207	S(Phospho)QFFEQGSSDSVVPDLPVPTISAPSR	19,4	8,80E-06
SERBP1	S203IS203	Phospho@202I203	SS(Phospho)FSHYSGLK	33	2,50E-10
SERBP1	S199IS203IS203	Phospho@199I202I203	HSGS(Phospho)DRSSFSHYSGLK	21,6	9,10E-08
SERBP1	S203IS205	Phospho@203I205	HSGSDRSS(Phospho)FSHYSGLK	11,4	0,0025
SERBP1	S202	Phospho@202I203I205	S(Phospho)SFSHYSGLKHEDKR	16,9	4,80E-05
DDX3X	S82	Phospho@82=10	GKS(Phospho)SFFSDR	23,1	3,10E-09
DDX3X	S594	Phospho@594=13	SSRFS(Phospho)GGFGAR	38,1	9,90E-09
DDX3X	S605	Phospho@605=12	DYRQS(Phospho)SGASSSSFSSSR	20,8	7,20E-05
DDX3X	S594	Phospho@594	FS(Phospho)GGFGAR	21,1	9,90E-06
CBX5	S92	Phospho@92=36	KS(Phospho)NFSNSADDIK	30,9	1,40E-10
CBX5	S92	Phospho@92=28	RKS(Phospho)NFSNSADDIK	50,5	6,10E-07
CBX5	S92	Phospho@92=20	S(Phospho)NFSNSADDIK	29,9	9,80E-08
HSP90AB1	S452	Phospho@452	RLS(Phospho)ELLR	27,3	1,80E-04
HSP90AB1	S452	Phospho@452	RRLS(Phospho)ELLR	10	0,01
HSP90AB1	S255	Phospho@255=16	IEDVGS(Phospho)DEEDDSGKDKK	26,1	0,0078
MYBBP1A	S1303	Phospho@1303	ARLS(Phospho)LVIR	30,8	1,40E-05
MYBBP1A	S1303	Phospho@1303	LS(Phospho)LVIR	27,4	3,50E-05
MYBBP1A	S1303	Phospho@1303	KARLS(Phospho)LVIR	23,5	6,20E-04
HMGN2	S29	Phospho@29=28	LS(Phospho)AKPAPPKPEPKPK	21,5	1,80E-09
HMGN2	S29	Phospho@29=25	SARLS(Phospho)AKPAPPKPEPKPK	31,4	4,20E-05
HMGN2	S25	Phospho@25I29	S(Phospho)ARLSAKPAPPKPEPKPK	25,6	1,40E-12
MKI67	S538	Phospho@538=49;Oxidation@541	S(Phospho)LVM(Oxidation)HTPPVLK	21	2,00E-06
MKI67	S374	Phospho@374	RES(Phospho)VNLGK	31,1	8,60E-07
MKI67	S538	Phospho@538=33;Oxidation@541	RKS(Phospho)LVM(Oxidation)HTPPVLK	39,8	3,10E-04
NAGK	S76	Phospho@76=24	SLGLSLS(Phospho)GGDQEDAGR	61,5	1,20E-16
MPHOSPH10	T332	Phospho@332=88	RVT(Phospho)FALPDDAETEDTGVLNVKK	50,4	2,60E-16
RBM14	S618	Phospho@618=16	RLS(Phospho)ESQLSFR	39,2	7,40E-08
RBM14	S649	Phospho@649=18	YS(Phospho)GSYNDYLR	30,9	2,80E-08
RPL8	S130	Phospho@130=9	AS(Phospho)GNYATVISHNPETK	30,7	4,50E-07
RPL8	S130	Phospho@130=13	AS(Phospho)GNYATVISHNPETKK	24,6	0,0046
KRT7	S27	Phospho@27=8	LS(Phospho)SARPGGLGSSSLYGLGASRPR	13,3	2,50E-06
KRT7	S27	Phospho@27=8	GAQVRLS(Phospho)SARPGGLGSSSLYGLGASRPr	41	2,60E-05
HMGN5	S20; S24	Phospho@20=61;Phospho@24=61	S(Phospho)ARLS(Phospho)AM(Oxidation)LVPVTPEVKPK	28,6	1,10E-08
HMGN5	S20	Oxidation@26;Phospho@20I24	S(Phospho)ARLSAM(Oxidation)LVPVTPEVKPK	22,4	1,50E-06
HMGN5	S24	Phospho@24=18;Oxidation@26	SARLS(Phospho)AM(Oxidation)LVPVTPEVKPK	33,5	1,40E-05

RSL1D1	T312	Phospho@312=16	KT(Phospho)ASVLSKDDVAPESGDTTVK	56,6	7,50E-13
RDBP	S131	Phospho@131=51	S(Phospho)LYESFVSSSDR	31,6	4,60E-14
PTRF	S300	Phospho@300=23	S(Phospho)FTPDHVVYAR	50,5	3,00E-11
KRT18	T8IS7	Phospho@7I8	ST(Phospho)FSTNYR	21,4	4,20E-07
KRT18	S7IT8	Phospho@7I8	S(Phospho)TFSTNYR	32,2	3,00E-06
NUSAP1	S240	Phospho@240=37	GRLS(Phospho)VASTPISQR	40,6	4,50E-11
CCDC86	S255	Phospho@255;Oxidation@257	RFS(Phospho)QM(Oxidation)LQDKPLR	35,6	4,90E-10
PPHLN1	S110	Phospho@110=34	S(Phospho)FYSSHYAR	30,6	2,20E-08
PPHLN1	S110	Phospho@110=38	RKS(Phospho)FYSSHYAR	17,3	1,80E-05
CKAP2	T39	Phospho@39	RKT(Phospho)LFAYK	36,5	4,10E-08
MSH6	S5	Phospho@5=10	M(Met-loss+Acetyl)SRQS(Phospho)TLYSFFPK	32	3,30E-05
KRT8	S34	Phospho@34=9	IS(Phospho)SSSFSR	31	6,50E-06
KRT8	T6	Phospho@6=21	M(Met-loss+Acetyl)SIRVT(Phospho)QK	22,2	4,90E-05
RACGAP1	T249	Phospho@249=14	RKT(Phospho)GTLQPWNSDSTLNSR	55,1	6,80E-13
CDCA5	S83	Phospho@83	IS(Phospho)FFLEKENEPPGR	27,9	2,50E-09
CDCA5	S83	Phospho@83	IS(Phospho)FFLEK	28,9	5,60E-04
C19orf21	S348	Phospho@348=50	GRPS(Phospho)LYVQR	43,5	4,60E-07
PRRC2C (BAT2D1)	S1013	Phospho@1013	S(Phospho)GPIKKPVLR	30,2	2,70E-08
SSH3	S37	Phospho@37	RQS(Phospho)FAVLR	26,1	5,10E-07
UTP3	S462	Phospho@462=26	KEEQRYS(Phospho)GELSGIR	32,4	8,20E-09
RIF1	S2205	Phospho@2205=69	RVS(Phospho)FADPIYQAGLADDIDRR	26,1	1,20E-09
PRKDC	S511	Phospho@511=38	GPESESEDHRAS(Phospho)GEVR	34	1,30E-04
PLEC1	T2886	Phospho@2886	RLT(Phospho)VNEAVK	31,1	6,10E-08
RBM3	S147	Phospho@147=23	NQGGYDRYS(Phospho)GGNYR	10,7	1,70E-05
ZC3H11A	S758	Phospho@758=11	RLS(Phospho)SASTGKPPLSVEDDFEK	40,4	4,70E-07
SLTM	T855	Phospho@855	DERRT(Phospho)VIIHDRPDITHPR	31,2	0,0019
SUPT16H	T494	Phospho@494	RLT(Phospho)EQKGEQQIQK	45,8	1,70E-05
AHNAK	T158	Phospho@158=32	RVT(Phospho)AYTVDVTGR	33,2	2,30E-07
DHX8	S1214	Phospho@1214	YEEPNAWRIS(Phospho)R	39,3	4,90E-07
LUZP1	S877IS878	Phospho@877I878	S(Phospho)SIIIKPSDPVER	22,8	2,30E-08
RBMX	S326	Phospho@326=18	DGYGGSRDS(Phospho)YSSSR	28,3	4,00E-07
RBMX	S189	Phospho@189=8	GRDS(Phospho)YGGPPR	16,1	0,037
COBLL1	S955	Phospho@952=23	RVS(Phospho)GHYVTSAAAK	22,2	3,40E-05
DEK	T67	Phospho@67=35;Oxidation@68	LT(Phospho)M(Oxidation)QVSSLQR	31,2	1,80E-06
SH2D4A	S261	Phospho@261	RLS(Phospho)LGAQK	20,6	3,30E-04
VIM	S72IS73	Phospho@72I73	LRSS(Phospho)VPGVR	18,6	2,90E-06
VIM	S47IT48IS49	Phospho@47I48I49	TYSLGSALRPS(Phospho)TSR	11,5	0,0013
DDX52	S22	Phospho@22	RFS(Phospho)ADAAR	24	9,80E-06
DDA1	S33	Phospho@33=14	ASNRRPS(Phospho)VYLPTR	31,2	2,20E-04
RPL21	S104	Phospho@104=15	SRDS(Phospho)FLKR	27	5,70E-05
ARHGAP21	S130	Phospho@130	VNGES(Phospho)VIGK	23,9	3,40E-05
RND3	S218IS222	Oxidation@220;Phospho@218I222	RIS(Phospho)HM(Oxidation)PSRPELSAVATDLRK	27	0,0091
RND3	S218IS222	Oxidation@220;Phospho@218I222	RISHM(Oxidation)PS(Phospho)RPELSAVATDLRK	26,1	0,0089
SF3B5	Y5IT6	Met-loss+Acetyl@1;Phospho@5I6	M(Met-loss+Acetyl)TDRYT(Phospho)IHSQLEHLQSK	27,5	1,90E-04
RPS6	S235IS236	Phospho@235I236	RLS(Phospho)SLR	23,5	2,50E-04
RPS10	T118	Phospho@118	GLEGERPARLT(Phospho)R	20	9,50E-06

Supplemental Table S2| Comparison of peptides isolated from the thiophosphorylated mitotic HeLa extracts to other phosphoproteomic data sets. Full references for the different phospho-screens can be found on www.phosphosite.org.

Protein	Site	Peptide	RX[S/T]	position hydrophobic residue	Kettenbach, 2011 (N or A, B, Ambig)	phosphosite.org. (Y/N)
INCENP	S72	RIS(Phospho)YVQDENRDPIR	Y	plus 2	B	Y
INCENP	S909 (RVPS)	VPS(Phospho)SLAYSLK	N	plus 2	N	N
INCENP	S893; S894 (TSS motif)	RTS(Phospho)S(Phospho)AVWNSPPLQGAR	Y;N	plus 2, plus 1	B; B	Y
INCENP	T59	EFSKEPELM(Oxidation)PKT(Phospho)PSQK	N	plus 1	N	N
INCENP	S518	SVM(Oxidation)KS(Phospho)FIKR	N	plus 1	N	N
INCENP	S518	SVM(Oxidation)KS(Phospho)FIK	N	plus 1	N	N
INCENP	S909	VPS(Phospho)SLAYSLKK	N	plus 2	N	N
INCENP	S893	TS(Phospho)SAVWNSPPLQGAR	Y	plus 2	B	Y
INCENP	S894; S899	TSS(Phospho)AVWNS(Phospho)PPLQGAR	N;N	plus 1; plus 1	B; N	Y
INCENP	S72	IS(Phospho)YVQDENRDPIRR	Y	plus 2	B	Y
INCENP	T494	VVRPLRT(Phospho)FLHTVQR	N	plus 1	N	N
INCENP	S446	TDQADGPREPPQS(Phospho)ARR	N	plus 1	N	Y
INCENP	S893; S899	TS(Phospho)SAVWNS(Phospho)PPLQGAR	Y;N	plus 2; plus 1	B; N	Y
AURKB	S7; T16 (KENS)	ENS(Phospho)YPWPYGRQT(Phospho)APSGLSTLPQR	N;Y	plus 2; plus 1	N; N	Y
AURKB	T16	ENSYPWPYGRQT(Phospho)APSGLSTLPQR	Y	plus 1	N	N
AURKB	T16	QT(Phospho)APSGLSTLPQR	Y	plus 1	N	N
AURKB	T16	Q(Gln->pyro-Glu)T(Phospho)APSGLSTLPQR	Y	plus 1	N	N
AURKB	S19	QTAPS(Phospho)GLSTLPQR	N	plus 1	N	N
NUMA1	S1969	RAS(Phospho)M(Oxidation)QPIQIAEGTGITTR	Y	plus 1	A	Y
NUMA1	S1792	SQAPLESSLDS(Phospho)LGDVFLDSGRKTR	N	plus 1	N	Y
NUMA1	T1811	RRT(Phospho)TQIINITM(Oxidation)TK	Y	plus 3	A	Y
NUMA1	T1811; T1812	RRT(Phospho)T(Phospho)QIINITM(Oxidation)TK	Y;Y	plus 3; plus 2	A	Y
NUMA1	S2047; T2055	RQS(Phospho)M(Oxidation)AFSILNT(Phospho)PK	Y;N	plus 1; plus 1	A; N	Y
NUMA1	S2047	RQS(Phospho)M(Oxidation)AFSILNTPK	Y	plus 1	A	N
HNRNPA1	S337	S(Phospho)SGPYGGGGQYFAKPR	N	plus 2	N	Y
HNRNPA1	S337	GGNFGGRS(Phospho)SGPYGGGGQYFAKPR	N	plus 2	N	Y
HIST1H2BJ	S79; Y84	IAGEAS(Phospho)RLAHY(Phospho)NKR	N;N	plus 2	N	N
LMO7	S116	INRLS(Phospho)TPIAGLDNINVFLK	Y	plus 2	Ambig	N
LMO7	S1197	RRS(Phospho)QFFEQGSSDSVVPDLPVPTISAPSR	Y	plus 2	Ambig	Y
LMO7	S1205	RRSQFFEQGSS(Phospho)DSVVPDLPVPTISAPSR	N	plus 3	N	N
LMO7	S751	RKS(Phospho)YTSDLQK	Y	plus 5	N	Y
LMO7	S751	S(Phospho)YTSDLQK	Y	plus 5	N	Y
LMO7	S300	RIS(Phospho)AVEPK	Y	plus 1	N	Y
LMO7	S1197	S(Phospho)QFFEQGSSDSVVPDLPVPTISAPSR	Y	plus 2	Ambig	Y
SERBP1	S203	SS(Phospho)FSHYSGLK	Y	plus 1	N	Y
SERBP1	S199	HSGS(Phospho)DRSSFSHYSGLK	N	plus 5	N	N
SERBP1	S203	HSGSDRSS(Phospho)FSHYSGLK	Y	plus 1	N	Y
SERBP1	S202	S(Phospho)SFSHYSGLKHEDKR	N	plus 2	N	Y
DDX3X	S82	GKS(Phospho)SFFSDR	N	plus 2	N	Y
DDX3X	S594	SSRFS(Phospho)GGFGAR	Y	plus 1	B	Y
DDX3X	S605	DYRQS(Phospho)SGASSSSFSSSR	Y	plus 2	N	Y
DDX3X	S594	FS(Phospho)GGFGAR	Y	plus 1	B	Y
CBX5	S92	KS(Phospho)NFSNSADDIK	Y	plus 2	B	Y
CBX5	S92	RKS(Phospho)NFSNSADDIK	Y	plus 2	B	Y
CBX5	S92	S(Phospho)NFSNSADDIK	Y	plus 2	B	Y
HSP90AB1	S452	RLS(Phospho)ELLR	Y	plus 2	N	Y
HSP90AB1	S452	RRLS(Phospho)ELLR	Y	plus 2	N	Y
HSP90AB1	S255	IEDVGS(Phospho)DEEDDSGKDKK	N	plus 7	N	Y
MYBBP1A	S1303	ARLS(Phospho)LVIR	Y	plus 1	B	Y
MYBBP1A	S1303	LS(Phospho)LVIR	Y	plus 1	B	Y
MYBBP1A	S1303	KARLS(Phospho)LVIR	Y	plus 1	B	Y
HMGN2	S29	LS(Phospho)AKPAPPKPEPKPK	Y	plus 1	N	Y
HMGN2	S29	SARLS(Phospho)AKPAPPKPEPKPK	Y	plus 1	N	Y
HMGN2	S25 (QRRSARL)	S(Phospho)ARLSAKPAPPKPEPKPK	Y	plus 1	N	Y
MKI67	S538	S(Phospho)LVM(Oxidation)HTPPVLK	Y	plus 1	B	Y
MKI67	S374	RES(Phospho)VNLGK	Y	plus 1	B	Y
MKI67	S538	RKS(Phospho)LVM(Oxidation)HTPPVLK	Y	plus 1	B	Y
NAGK	S76	SLGLSLS(Phospho)GGDQEDAGR	N	plus 1	N	Y
MPHOSPH10	T332	RVT(Phospho)FALPDDAETEDTGVLNVKK	Y	plus 1	N	N
RBM14	S618	RLS(Phospho)ESQLSFR	Y	plus 4	Ambig	Y
RBM14	S649 (ARYSG)	YS(Phospho)GSYNDYLR	Y	plus 1	N	Y
RPL8	S130 (RAS)	AS(Phospho)GNYATVISHNPETK	Y	plus 1	N	N
RPL8	S130 (RAS)	AS(Phospho)GNYATVISHNPETKK	Y	plus 1	N	N
KRT7	S27	LS(Phospho)SARPGGLGSSSLYGLGASRPR	Y	plus 2	N	N
KRT7	S27	GAQVRLS(Phospho)SARPGGLGSSSLYGLGASRPr	Y	plus 2	N	N
HMGN5	S20; S24	S(Phospho)ARLS(Phospho)AM(Oxidation)LVPVTPEVKPK	Y;Y	plus 1, plus 1	N	Y
HMGN5	S20	S(Phospho)ARLSAM(Oxidation)LVPVTPEVKPK	Y	plus 1	N	Y
HMGN5	S24	SARLS(Phospho)AM(Oxidation)LVPVTPEVKPK	Y	plus 1	N	Y
RSL1D1	T312 (RKT)	KT(Phospho)ASVLSKDDVAPESGDTTVK	Y	plus 1	N (T375; S361)	N
RDBP	S131 (RKS)	S(Phospho)LYESFVSSSDR	Y	plus 1	N (S49: S249)	Y
PTRF	S300 (RKS)	S(Phospho)FTPDHVVYAR	Y	plus 1	N	Y
KRT18	T8 (TRST)	ST(Phospho)FSTNYR	Y	plus 1	N	Y
KRT18	S7 (TRST)	S(Phospho)TFSTNYR	N	plus 2	N	Y
NUSAP1	S240	GRLS(Phospho)VASTPISQR	Y	plus 1	B	Y
CCDC86	S255	RFS(Phospho)QM(Oxidation)LQDKPLR	Y	plus 2	Ambig	Y
PPHLN1	S110	S(Phospho)FYSSHYAR	Y	plus 1	N	Y
PPHLN1	S110	RKS(Phospho)FYSSHYAR	Y	plus 1	N	Y

CKAP2	T39	RKT(Phospho)LFAYK	Y	plus 1	N (S327)	N
MSH6	S5	M(Met-loss+Acetyl)SRQS(Phospho)TLYSFFPK	Y	plus 2	N (S79)	N
KRT8	S34 (RIS)	IS(Phospho)SSSFSR	Y	plus 4	N	Y
KRT8	T6	M(Met-loss+Acetyl)SIRVT(Phospho)QK	Y	plus 6	N	N
RACGAP1	T249	RKT(Phospho)GTLQPWNSDSTLNSR	Y	plus 1	N	Y
CDCA5	S83 (RISFF)	IS(Phospho)FFLEKENEPPGR	Y	plus 1	A	Y
CDCA5	S83 (RISFF)	IS(Phospho)FFLEK	Y	plus 1	A	Y
C19orf21	S348	GRPS(Phospho)LYVQR	Y	plus 1	N	N
PRRC2C (BAT2D1)	S1013 (RRS)	S(Phospho)GPIKKPVLR	Y	plus 1	N	N
SSH3	S37	RQS(Phospho)FAVLR	Y	plus 1	N	Y
UTP3	S462	KEEQRYS(Phospho)GELSGIR	Y	plus 1	N	N
RIF1	S2205	RVS(Phospho)FADPIYQAGLADDIDRR	Y	plus 1	N	Y
PRKDC	S511	GPESESEDHRAS(Phospho)GEVR	Y	plus 1	N	Y
PLEC1	T2886	RLT(Phospho)VNEAVK	Y	plus 1	N (other sites)	Y
RBM3	S147	NQGGYDRYS(Phospho)GGNYR	Y	plus 1	B	Y
ZC3H11A	S758	RLS(Phospho)SASTGKPPLSVEDDFEK	Y	plus 2	Ambig	Y
SLTM	T855	DERRT(Phospho)VIIHDRPDITHPR	Y	plus 1	N	N
SUPT16H	T494	RLT(Phospho)EQKGEQQIQK	Y	plus 4	N (S267, S508)	N
AHNAK	T158	RVT(Phospho)AYTVDVTGR	Y	plus 1	N (S3320)	N
DHX8	S1214	YEEPNAWRIS(Phospho)R	Y	plus 2	N	N
LUZP1	S877 (VSRSSII)	S(Phospho)SIIIKPSDPVER	N	plus 2	N (S573, T702, S956)	N
RBMX	S326	DGYGGSRDS(Phospho)YSSSR	Y	plus 8	A	Y
RBMX	S189	GRDS(Phospho)YGGPPR	Y	plus 2	N	Y
COBLL1	S955	RVS(Phospho)GHYVTSAAAK	Y	plus 1	N	N
DEK	T67 (RLT)	LT(Phospho)M(Oxidation)QVSSLQR	Y	plus 1	N	N
SH2D4A	S261 (KRLS)	RLS(Phospho)LGAQK	Y	plus 1	N	Y
VIM	S73	LRSS(Phospho)VPGVR	Y	plus 1	N	Y
VIM	S47	TYSLGSALRPS(Phospho)TSR	Y	plus 1	N	Y
DDX52	S22	RFS(Phospho)ADAAR	Y	plus 1	N	N
DDA1	S33	ASNRRPS(Phospho)VYLPTR	Y	plus 1	N	Y
RPL21	S104	SRDS(Phospho)FLKR	Y	plus 1	N	Y
ARHGAP21	S130	VNGES(Phospho)VIGK	N	plus 1	N	N
RND3	S218	RIS(Phospho)HM(Oxidation)PSRPELSAVATDLRK	Y	plus 2	N	N
RND3	S222	RISHM(Oxidation)PS(Phospho)RPELSAVATDLRK	N	plus 2	N	N
SF3B5	T6	M(Met-loss+Acetyl)TDRYT(Phospho)IHSQLEHLQSK	Y	plus 1	N	N
RPS6	S235	RLS(Phospho)SLR	Y	plus 2	N	Y
RPS10	T118	GLEGERPARLT(Phospho)R	Y	plus 2	N	N

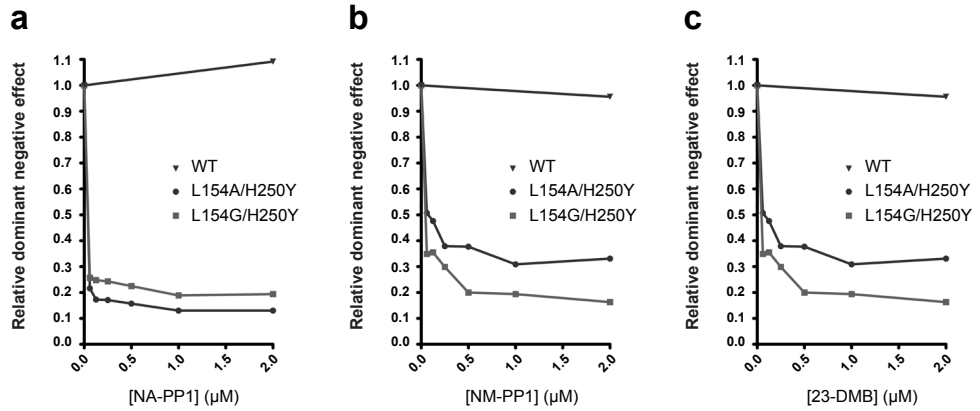

Supplemental Figure S1l Titration of PP1 inhibitors

a-c) U2OS cells expressing the indicated proteins were released from a G1/S block into medium containing paclitaxel plus or minus different concentrations of NA-PP1 (a), NM-PP1 (b) or 23-DMB (c). Eighteen hours after release, the mitotic index was determined by propidium iodide/MPM2 monoclonal antibody labeling and FACS analysis. For each transfected cell population the mitotic index without PP1 inhibitor was set to 100% and the relative reduction in mitotic index in the presence of PP1 inhibitor determined.

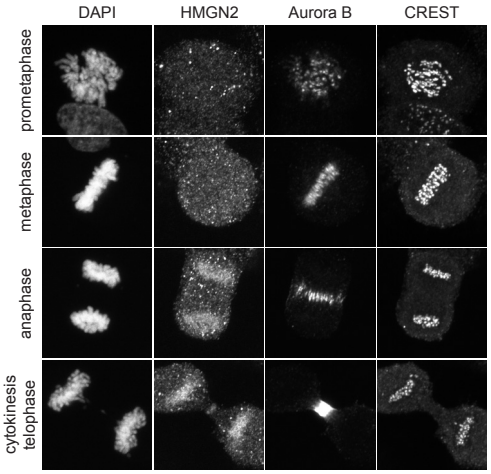

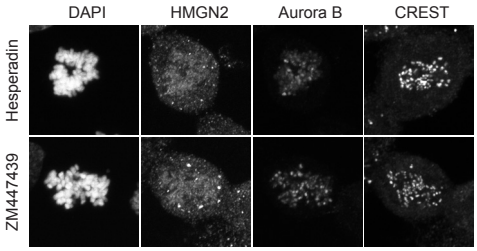

Supplemental Figure S2l Localization of HMGN2 in mitosis and post-mitosis

Asynchronously growing U2OS cells were fixed and HMGN2, Aurora B and centromeres (CREST) were visualized with specific antibodies. Cells in different stages of cell division were imaged. Note that HMGN2 is visible on chromatin in anaphase when Aurora B has translocated to the central spindle.

Chapter 4

The formation and resolution of ultrafine DNA bridges in anaphase

Introduction

During the cell cycle the entire genome is duplicated in S phase and equally divided over two new daughter cells during M phase. To maintain genomic integrity the DNA must be precisely and timely replicated, and repaired when damaged. Whereas DNA replication is normally completed by the end of S phase, DNA catenanes that arise during S phase are subsequently decatenated in mitosis. Moreover, centromeric DNA catenanes can persist until early anaphase and form UltraFine DNA Bridges (UFBs) that require active resolution by Topoisomerase IIα (TOPOIIα) (Figure 1a) [306]. Improper resolution of centromeric UFBs can interfere with chromosome disjunction and segregation during mitosis (Figure 1b). Additionally, when DNA replication is hampered, incompletely replicated DNA loci arise at so-called Common Fragile Sites (CFSs) [307]. These under-replicated CFSs are also actively processed during mitosis, and if this does not happen properly or timely, CFSs can give rise to the formation of UFBs, chromosome segregation defects and loss of genomic integrity (Figure 1c). The current knowledge on the formation and resolution of UFBs are discussed in this chapter.

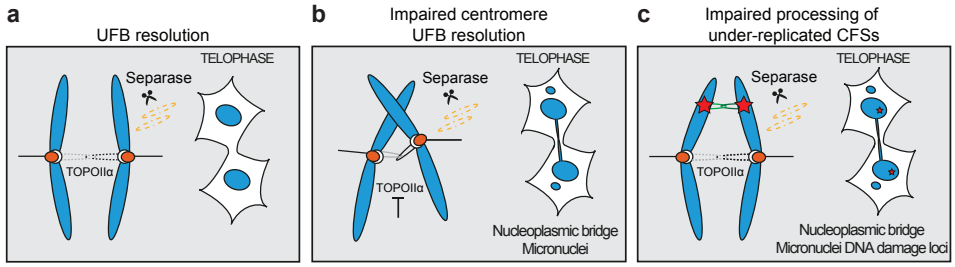

Figure 1l The resolution of ultrafine DNA bridges in anaphase
Schematic overview of UFB resolution emanating from centromeres and CFS. **a)** Centromeric DNA catenanes persist until the cohesin complexes (orange) are cleaved by separase. The DNA catenanes become visible as UFBs (light and dark grey lines) during anaphase, which are resolved through the action of TOPOIIα. This results in proper segregation of the sister chromatids during anaphase/telophase. **b)** Reduction of TOPOIIα activity during anaphase results in impaired centromere UFB resolution, which gives rise to nucleoplasmic bridges and micronuclei in telophase. **c)** Under-replicated CFSs that are not processed during (pro)metaphase (red stars) give rise to the formation UFBs during anaphase and nucleoplasmic bridges, micronuclei and DNA damage loci in telophase.

Resolution of DNA catenanes during mitosis

DNA catenation, the intertwining of fully replicated sister DNA strands, occurs when two converging replication forks meet, and is a normal consequence of DNA replication. Although catenanes can involve both double stranded (ds) and single stranded (ss) DNA, here we only discuss the formation and resolution of dsDNA catenanes. Together with cohesin, which entraps the sister chromatids into a ring-like structure (Chapter 1), DNA catenanes contribute to sister chromatid linkage, which is a prerequisite for chromosome bi-orientation in mitosis [308]. However, timely removal of cohesin and resolution of DNA catenanes is required for proper sister chromatid disjunction during anaphase. Similar to cohesin, DNA catenanes are resolved in two steps. In early mitosis, the cohesin complexes at the chromosomal arms are disassociated by the cohesin release factor WAPL. Subsequently, DNA decatenation of the chromosomal arms takes place through the action of TOPOIIα [27, 308]. TOPOIIα cuts one double stranded DNA helix, passes the other DNA helix through the break and subsequently religates the break [309].

Cohesin removal and DNA decatenation are performed in a sequential order because the cohesin complex is thought to 'shield' DNA catenanes from TOPOIIα dependent removal [27, 308, 310]. In line with this idea, the centromeric cohesin protector SGO1/PP2A that antagonizes WAPL activity at centromeres (chapter 1) also prevents DNA decatenation at these sites [48-52]. The second step of cohesin removal occurs at the end of metaphase when the mitotic checkpoint is silenced and separase becomes active and cleaves the centromeric cohesin complexes. This provides TOPOIIα accessibility to DNA catenanes at the centromeres allowing their decatenation in early anaphase [311].

DNA catenanes and centromeric UFBs

As mentioned above, centromeric DNA catenanes remain unresolved until anaphase onset, and at the metaphase to anaphase transition they are visible as UFBs [311]. UFBs are DNA bridges that are free from nucleosomes and cannot be visualized by DNA fluorescent dyes such as 4',6 -diamino-2-phenylindole (DAPI), which binds to the minor groove of the DNA helix. An explanation for this could be that the conformation of the UFBs differs from the conventional DNA helix structure and that therefore the minor groove of DNA is loosing its affinity for DAPI. The presence of DNA in UFBs was shown by incorporation of Bromodeoxyuridine (BrdU) in UFBs [312, 313], and by the disappearance of UFBs upon DNAase treatment [311]. Because of the difficulty to visualize UFBs with conventional DNA dyes, at the moment UFBs are visualized by immunofluorescence (IF) of proteins that are recruited to these structures. The protein that identified the UFBs and is currently used as a 'UFB marker' is Plk1-Interacting Checkpoint Helicase (PICH), a member of the DNA-dependent SNF2 ATPase family [311]. As its name suggests, PICH was identified in a screen for PLK1-polo box binding proteins. The interaction of PICH with Plk1 was subsequently shown to facilitate the recruitment of PICH to kinetochores, although the function of PICH at these sites has remained unclear [311, 314]. Next to PICH localization at kinetochores, PICH was visible as thin threads that connected the separating sister-centromeres in anaphase (i.e. UFBs) [311]. Whether this localization of PICH requires Plk1 binding or activity is not clear. PICH-positive UFBs are readily detectable during early anaphase, but their numbers rapidly decrease when anaphase progresses, suggesting an active resolution mechanism. Indeed, the resolution of PICH-positive UFBs is impaired after inhibition of TOPOIIα, which indicates that PICH-coated UFBs are DNA catenanes [311].

Interestingly, the recruitment of PICH to UFBs seems to depend on the forces generated by the depolymerizing microtubules of the mitotic spindle. This was initially based on the observation that PICH-positive UFBs disappeared upon treatment with paclitaxel, a drug that stabilizes microtubules [311]. Further support for this hypothesis came from a recent *in vitro* study using recombinant proteins, microfluidics and optical tweezers [315]. This study showed that PICH is not a DNA helicase, but a DNA translocase that can directly bind to DNA. Interestingly, PICH recruitment to the DNA appeared to be more efficient when mechanical tension was applied on the DNA strands. This implies that sister chromatid separation in early anaphase might stretch the UFBs to promote the recruitment of PICH.

The discovery of PICH was the starting point of the identification of additional UFB binding proteins, including members of the BTRR complex, Replication Protein 70 (RPA70),

Fanconi Anemia Complementation Group M (FANCM) and Rif1 (chapter 5), and PICH appeared to be an upstream recruitment factor for the BTRR complex members and Rap1-Interacting Factor 1 Homolog (Rif1) [312, 316, 317]. The BTRR complex consists of the Bloom's Syndrome RecQ-like DNA helicase (BLM), topoisomerase IIIα (TOPO IIIα) and RecQ-Mediated Genome Instability 1 and 2 (RMI1 and RMI2) [318]. Studies in cell lines derived from patients with Bloom's syndrome in which BLM is mutated, as well as siRNA-mediated knock-down of BLM in cancer cell lines demonstrated a prominent role for BLM in UFB resolution [312, 316]. BLM and PICH were suggested to clear UFBs from histones, thereby providing accessibility for topoisomerases and probably additional DNA repair enzymes that facilitate optimal UFB resolution [316]. Whether this requires the helicase activity of BLM or the other members of the BTRR complex is currently unclear. In addition, PICH was recently shown to stimulate the catalytic activity of TOPOIIα *in vitro*, which could support timely resolution of UFBs during anaphase [319]. Clearly, further *in vitro* and cellular studies are needed to exactly understand how PICH and the BTRR complex resolve UFBs. Moreover, the localization of additional UFB binding proteins such as FANCM and RPA70 implies that UFB resolution is more complicated than initially thought because both FANCM and RPA70 are recruited to UFBs during later stages of anaphase or even telophase, when PICH and BLM are no longer visible [317, 320]. In line with this, FANCM and RPA70 rarely colocalize with PICH or BLM, although, their recruitment to UFBs appears to depend on BLM (discussed in Chapter 6)[317, 320].

UFBs from under-replicated CFSs

As mentioned earlier, DNA catenanes are not the only source of UFBs during anaphase. Replication stress, either physiologically or chemically induced by low concentrations of the Polymerase α, δ and ε inhibitor aphidicolin (APH) can lead to the formation of non-centromeric PICH and BLM-positive UFBs that bridge CFSs [321]. CFSs are DNA regions that are intrinsically difficult to replicate, and therefore prone to form under-replicated DNA loci when replication fork progression is hampered (a situation referred to as replication stress) [307]. CFSs are prone to break and frequently affected in cancer, which could be due to oncogene-induced replication stress that may reduce the presence of active replication origins, induce unscheduled replication initiation or promote defective replication fork progression [322]. There are several potential obstacles that could stall the replication forks during DNA replication at CFSs. For example the presence of DNA sequences like CGG- and AT-rich repeats are able to form single stranded DNA secondary structures in the leading strand, such as guanine rich G-quadruplexes and hairpin structures [307]. Another cause of the fragility of CFSs is the interference of DNA replication by active transcription of large genes located at CFSs [323]. In addition, the rare presence of replication origins in CFSs forces the replication machinery to travel over long distances, making the CFSs more sensitive for replication stress [324-326].

Under-replicated CFSs do not signal to the DNA damage checkpoint and cells with these DNA 'lesions' proceed from S phase, to G2 into mitosis where they are expressed as 'gaps' on mitotic chromosomes and where processing of these under-replicated regions takes place (discussed below) [321, 327]. The first proteins described to specifically associate with CFSs were the Fanconi Anaemia (FA) proteins FANCD2 and FANCI [321,

327]. Thus far 15 genes have been identified in FA patients and eight of these FA genes (FANCA, FANCB, FANCC, FANCE, FANCF, FANCG, FANCL and FANCM) form a FA core complex that functions as an ubiquitin ligase that ubiquitinates FANCD2 and FANCI [328]. Ubiquitination of these two FA proteins facilitates their recruitment to chromatin seen as foci at under-replicated CFSs in S and G2 phase [321]. In addition, FANCD2 and FANCI localize at the extremities of UFBs induced after APH-induced replication stress, and these proteins are therefore often used as markers for CFS-derived UFBs. Whether and how FANCD2 and FANCI contribute to the processing of under-replicated CFSs remains unclear, because proteins that are involved in the processing of under-replicated CFSs are recruited independently of FANCD2 and FANCI (discussed below). Another study suggested a role for FANCC in the resolution of CFSs associated UFBs, because loss of FANCC resulted in an increase in the number of PICH-positive UFBs, whereas the number of BLM positive UFBs remained unchanged. This suggested that the loading of BLM, but not PICH, to CFS-associated UFBs required FANCC [327]. However, in cells that lack FANCC, ubiquitination and localization of FANCD2 and FANCI is also blocked, making it difficult to determine how and why these UFBs arise.

Interestingly, cells deficient for FANCA, -D1, -G, -I and –M show an elevation of BLM-positive UFBs, even in the absence of chemically induced replication stress [320]. Since these FA-proteins play a role in DNA repair during S phase, their absence most likely causes replication stress and indirectly results in an elevation of CFS-associated UFBs during anaphase. Thus whether these FA-proteins contribute to UFB resolution during anaphase remains to be determined. Also, whether UFBs derived from CFSs differ from centromeric UFBs in terms of DNA structure and protein recruitment is not fully understood (discussed in Chapter 6).

Processing of under-replicated DNA at CFSs before anaphase onset

Even in cells that experience replication stress, the frequency of CFS-derived UFBs is very low, because under-replicated DNA at CFSs is being actively processed in mitosis prior to anaphase [307]. The Rosselli and Hickson labs showed that the endonuclease complexes XPF-ERCC1 (Xeroderma Pigmentosum, Complementation Group F/ Excision Repair Cross-Complementation 1) and MUS81-EME1 (MUS81 Structure-Specific Endonuclease Subunit/Essential Meiotic Structure-Specific Endonuclease 1) are recruited to under-replicated CFSs during mitosis, independently of the FANC core protein FANCC, but dependent on the recently identified FA-protein SLX4 (FANCP), a nuclease scaffold protein [329, 330]. Interestingly, APH-induced CFS ‘expression’ (i.e. the small gaps observed in one of the two mitotic sisters chromatids), was abrogated in the absence of the XPF-ERCC1 and MUS81-EME1 endonucleases, suggesting that these endonucleases contribute to the processing of under-replicated CFSs before anaphase onset [329, 330]. Knock-down of XPF-ERCC1 and/or MUS81-EME1 in combination with APH-induced replication stress resulted in a strong elevation of PICH and BLM-positive CFS-associated UFBs in anaphase [329, 330], and this suggested that the resolution of CFS-derived UFBs during anaphase most likely serves as a backup system to resolve under-replicated DNA. Interestingly, APH-induced replication stress was recently shown to activate POLD3-associated DNA polymerase δ-dependent (POLD3) DNA synthesis at under-replicated CFSs in mitosis [331]. DNA synthesis at these sites required the recruitment of the endonucleases, suggesting that the DNA replication ‘lesions’ were

first cleaved to allow proper DNA synthesis by POLD3. Why under-replicated CFSs are not processed during S phase where all the high fidelity polymerases are ready to repair these lesions remains an open question. DNA synthesis at under-replicated CFSs appears to require the condensin complex and removal of cohesin, but exactly how this contributes to DNA synthesis during mitosis remains to be established [331]. Maybe the condensin complex directly recruits the SLX4-associated endonucleases to under-replicated CFSs, whereas the cohesin complex must first be removed to provide access for these factors. Additionally, the changes in chromatin morphology induced by chromosome condensation may contribute to the 'exposure' of the under-replicated CFSs and thereby promote the recruitment of processing factors.

UFB formation at telomeres

Telomeres are regions at the ends of each chromosome consisting of repetitive double stranded and single stranded TTAGGG DNA sequences. The so-called shelterin complex (consisting of TRF1, TRF2, POT1, RAP1, TIN2 and TPP1) is recruited to the telomeres to allow the formation of a t-loop, serving as a chromosome cap to prevent access of proteins involved in DNA damage signaling and repair [332]. Due to the guanine rich DNA sequences that are prone to form G-quadruplexes and the shelterin components that may block the road for DNA replication, the telomere is difficult to replicate and can be regarded as CFS. In line with this idea, APH-induced DNA replication stress also leads to telomere-associated PICH-positive UFB formation during anaphase [333]. In addition, UFB formation is elevated in the absence of TRF (Telomeric Repeat Binding Factor) 1. Interestingly, TOPOIIα binds to telomeres in a TRF1-dependent manner and inhibition of TOPOIIα results in telomeric fragility (i.e. elevation of sister chromatid end-to-end fusions and multitelomeric chromosomes [334]). However, whether TOPO IIα inhibition increases the number of telomere- associated UFBs remains to be established. A recent study showed that elevated levels of TRF2 result in the formation of telomere-UFBs, extensive telomeric shortening and end-to-end fusions [335]. And finally, the telomere-localized protein ZFP (Zinc Finger Protein) 365 was found to protect telomeres from the DNA damage response and to prevent UFB formation on CFSs and telomeres [336]. Thus proper expression levels of components of the shelterin complex are essential to maintain telomere integrity and are required to prevent telomere-UFB expression during anaphase. However, whether defective processing of telomere UFBs can in fact cause telomere fragility and genomic instability is not clear. Moreover, how the shelterin complex and ZFP365 contribute to the processing of telomeric CFSs is also unclear.

Consequences of failed processing of under-replicated DNA and UFB resolution

Bloom's syndrome and Fanconi anemia are rare genetic disorders in which DNA replication and DNA repair pathways are defective, which leads to loss of genomic integrity. Bloom's syndrome and Fanconi anemia patients have short life expectancy, elevated cancer predisposition and growth retardation [337, 338]. Next to the general replication defects observed in Bloom's syndrome and Fanconi anemia patient-derived cell lines, an increase in both centromeric- and CFS-induced UFBs is commonly

observed which could contribute to the observed genomic instability [312, 316, 320, 321, 327]. For instance, defects in centromere-associated UFB resolution might lead to chromosome segregation defects during anaphase and give rise to aneuploidy [311, 312, 316, 317, 319]. Alternatively, missegregating chromosomes might be the cause of the increased frequency of micronuclei observed in cell lines derived from these patients. And chromosomes in micronuclei are more prone to undergo chromothripsis [339].

The second and third source of UFBs, from CFSs and telomeres respectively, are more likely to cause DNA damage and genomic instability [321, 327, 329-331]. UFBs that are formed upon replication stress recruit FANCD2/FANCI and the DNA damage marker γH2AX to their extremities [321, 327]. Moreover, APH-induced replication stress gives rise to a symmetrical pattern of 53BP1 (Tumor Protein P53-Binding Protein 1) nuclear bodies (53BP1 NBs) in newly formed daughter cells in G1 phase and the number of these 53BP1 NBs strongly increases when replication stress is combined with knock-down of XPF-ERCC1, MUS81-EME1, POLD3, PICH or BLM [317, 329-331, 340, 341]. This suggests that inefficient resolution of under-replicated DNA and impaired UFB resolution may cause DNA damage that persists in G1 phase. The exact physiological role of these 53BP1 NBs is not fully understood. Given the known function of 53BP1 in regulating the choice between non-homologous end joining (NHEJ) and homologous recombination [342-345], 53BP1 might mark the DNA lesions in these nuclear bodies to be repaired via NHEJ in G1 phase. Alternatively, since this manner of repair is rather inaccurate it has also been suggested that 53BP1 NBs might protect the DNA lesions and promote their repair by replicative polymerases during S phase [307]. Moreover, whether the DNA repair machinery can cope with a vast increase in the number of 53BP1 NBs remains an open question. In general, it is far from clear whether and how impaired UFB resolution contributes to genomic instability or cancer. This is mainly due to the fact that many of the proteins found on UFBs and thought the play a role in their resolution, also play essential roles in DNA replication and DNA repair. Answering these questions requires sophisticated knock-in approaches that allow specific perturbation of the endogenous genes during anaphase, and to introduce mutations that specifically disrupt their function in UFB resolution.

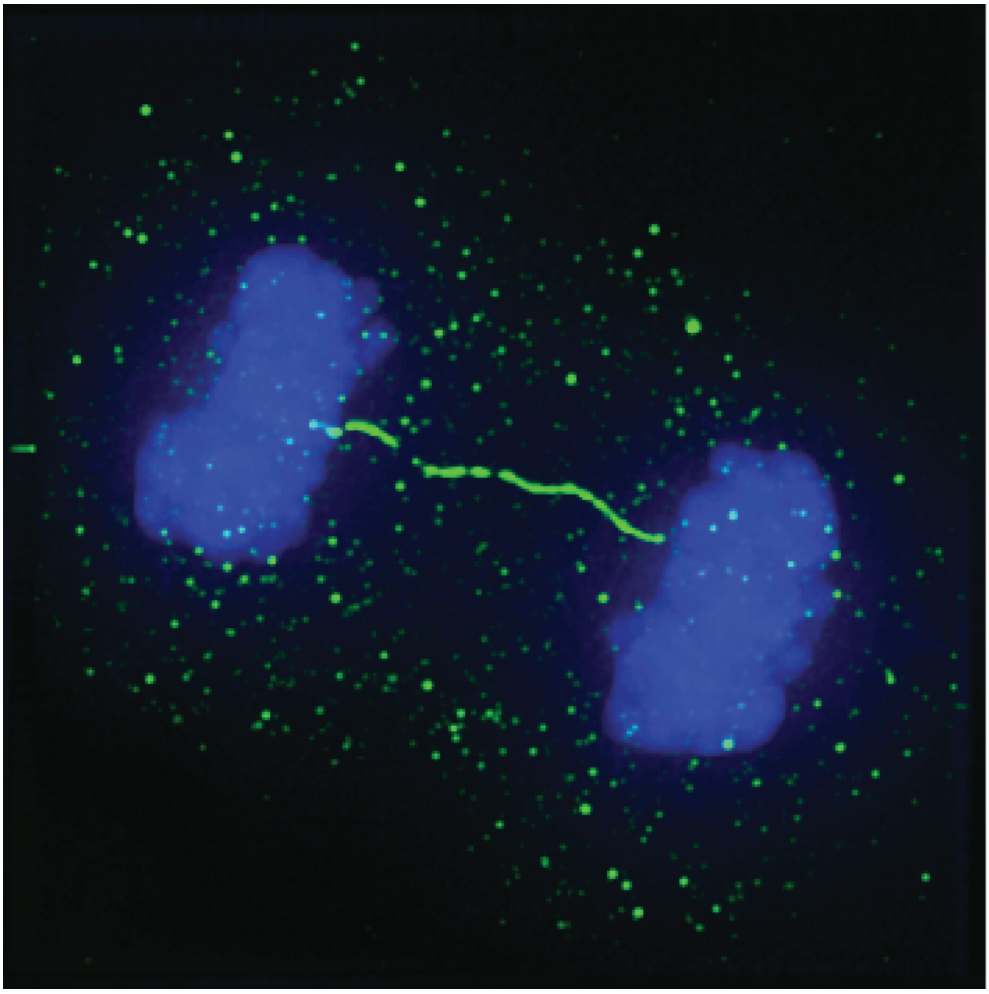

Chapter 5

Rif1 is required for resolution of ultrafine DNA bridges in anaphase to ensure genomic stability

Rutger C.C. Hengeveld[1,3], H. Rudolf de Boer[2,3], Pepijn M. Schoonen[2], Elisabeth G.E. de Vries[2], Susanne M.A. Lens[1,4,] and Marcel A.T.M. van Vugt[2,4]

From the [1]Department of Molecular Cancer Research, University Medical Center Utrecht, Universiteitsweg 100, 3584 CG Utrecht, the Netherlands and [2]Department of Medical Oncology, University Medical Center Groningen, University of Groningen, Hanzeplein 1, 9723 GZ Groningen, the Netherlands
[3]Co-first author
[4]Co-senior author

Adapted from Developmental Cell, August 2015; 34, 466-474

Abstract

Sister chromatid disjunction in anaphase requires the resolution of DNA catenanes by topoisomerase II together with Plk1-interacting checkpoint helicase (PICH) and Bloom's helicase (BLM). We here identify Rif1 as a factor involved in the resolution of DNA catenanes that are visible as ultrafine DNA bridges (UFBs) in anaphase to which PICH and BLM localize. Rif1, which during interphase functions downstream of 53BP1 in DNA repair, is recruited to UFBs in a PICH-dependent fashion, but independently of 53BP1 or BLM. Similar to PICH and BLM, Rif1 promotes the resolution of UFBs: its depletion increases the frequency of nucleoplasmic bridges and RPA70-positive UFBs in late anaphase. Moreover, in the absence of Rif1, PICH, or BLM, more nuclear bodies with damaged DNA arise in ensuing G1 cells, when chromosome decatenation is impaired. Our data reveal a thus far unrecognized function for Rif1 in the resolution of UFBs during anaphase to protect genomic integrity.

Introduction

Proper chromosome segregation in mitosis requires that chromosomes correctly attach to microtubules of the mitotic spindle. Upon silencing of the mitotic checkpoint, the cohesin complexes that hold sister chromatids together are cleaved by separase, allowing sister chromatid separation in anaphase [346]. Besides linkage by cohesin, sister chromatids are also physically connected by DNA catenanes [307].

Sister chromatid catenation is a direct and physiological consequence of DNA replication in S phase [347]. DNA catenanes require topoisomerase II activity for their resolution [348], a process that at chromosome arms is completed prior to metaphase [349]. However, at centromeric regions, catenanes persist until anaphase and are visible as ultrafine DNA bridges (UFBs) [308, 312, 350]. Alternatively, UFBs can also arise between common fragile sites (CFSs) at chromosome arms after induction of replication stress in the previous S phase [321]. UFBs differ from canonical bulky chromatin bridges in that they are devoid of histones and cannot be stained with conventional DNA dyes. Their presence can thus far only be demonstrated by immunofluorescence (IF) staining of proteins that bind to these DNA bridges, such as PICH, BLM, and Replication Protein A 70 (RPA70) [350]. UFB resolution must be completed by the end of anaphase to ensure sister chromatid disjunction [308, 312, 316, 350, 351]. Exactly how UFBs are resolved, the factors required for UFB resolution, and the consequences of defective UFB resolution for genome integrity are not completely understood.

PICH, a DNA translocase from the Swi/SNF family, and BLM, a RecQ family helicase, are thought to act in conjunction with topoisomerases (IIa and III) to resolve UFBs [308, 311-313]. Here, we present Rif1 as an UFB binding protein. Originally identified as an interactor of the telomere-binding protein Rap1 in budding yeast [352], Rif1 was recently shown to function in DNA break repair downstream of ATM and 53BP1 [342, 343, 345, 353-355] and in controlling replication timing in situations of stress [356-359]. We demonstrate that Rif1 plays a thus far unrecognized role in protecting the genome from damage through resolution of UFBs during anaphase.

Results

Rif1 localizes to UFBs during anaphase

The cellular response to DNA damage is rewired during mitosis [360]. While DNA double-strand breaks (DSBs) are normally detected in mitosis, downstream effectors, including 53BP1, are no longer recruited, most likely to prevent unwanted telomere fusions [361, 362]. In analogy to 53BP1, we found that Rif1 cannot be recruited to DNA DSBs during mitosis in untransformed RPE-1 cells (Figure 1a, 1b) and in MCF-7 and HeLa cells (Supplemental Figure S1a, b). However, we noticed that in anaphase, Rif1 localized to thread-like structures that bridged segregating chromosomes, irrespective of earlier inflicted DNA damage (Figure 1d). Although previous work suggested that Rif1 co-localizes with midzone microtubules [355], cold-induced depolymerization of midzone microtubules did not significantly affect Rif1 localization during anaphase, indicating that the majority of these thread-like structures does not reflect microtubules (Supplemental Figure S1c, d).

Rif1-positive thread-like structures were present in high numbers at anaphase onset,

but progressively disappeared upon sister chromatid segregation (Figure 1d, e). This localization pattern of Rif1 resembles that of PICH and BLM, which localize to UFBs in early anaphase [311, 312]. In non-transformed and non-stressed cells, UFBs are mainly caused by catenated centromeric DNA that requires topoisomerase activity for its decatenation during anaphase [313]. Since Rif1-positive threads appeared between centromeres in unperturbed RPE-1 cells (Figure 1d), it suggested that these UFBs reflected persistent DNA catenanes, rather than under-replicated fragile sites at chromosome arms that arise as a consequence of replication stress and that can be distinguished from centromeric UFBs by the presence of FANCD2 foci [321, 350]. To investigate this, RPE-1 cells were released from a G2 arrest imposed by the Cdk1 inhibitor RO-3306 (Figure 1c). At 15 min after the release, cells were treated with a low concentration of the topoisomerase II inhibitor ICRF-193 to delay decatenation at anaphase onset (Figure 1c) [313].

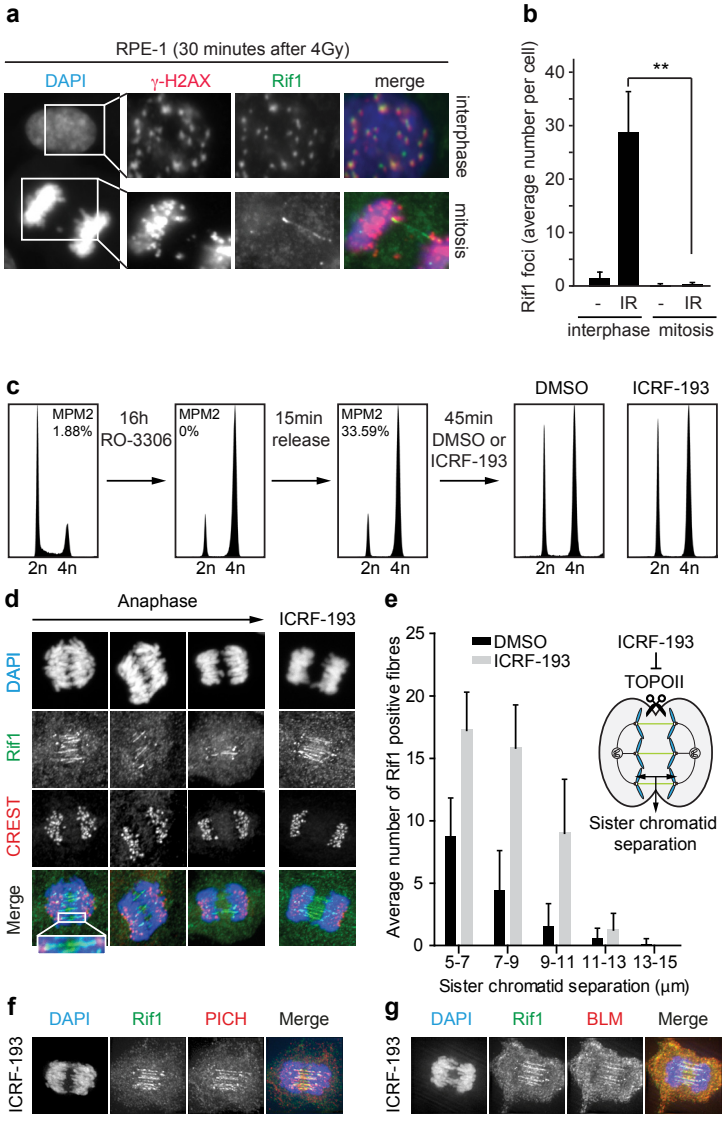

Figure 1l Rif1 is localized to DNA DSBs during interphase and to UFBs in anaphase

a) Representative images of Rif1 and γ-H2AX during interphase and anaphase in non-transformed RPE-1 cells, 30 min after 4 Gy irradiation. **b)** Quantification of average numbers of Rif1 foci per cell, with or without 5 Gy irradiation (IR) in RPE-1 cells (n = 3). The error bars indicate SD (n > 25 cells/condition) (**p < 0.01 and unpaired Student's t test). **c)** Synchronization protocol: RPE-1 cells were arrested in G2 phase using the reversible Cdk1 inhibitor RO-3306. The washout of RO-3306 allowed synchronous mitotic entry. At 15 min later, the cells were treated with ICRF-193 (160 nM). **d and e)** RPE-1 cells were treated as in (c) and subsequently stained with Rif1 and CREST antibodies and DAPI. The DMSO-treated or ICRF-193-treated anaphase cells were categorized based on the distance between chromosome packs. The number of Rif1-positive bridges per anaphase was scored. The error bars indicate SD (n > 25 cells/condition). **f and g)** RPE-1 cells were treated as in (c) and cells were stained for Rif1 and PICH (g) or Rif1 and BLM (g). See also Supplemental Figure S1.

This resulted in a significant increase in the number of Rif1-positive threads during early anaphase (Figures 1d, e). Moreover, these Rif1-positive threads were not flanked by FANCD2-positive foci (Supplemental Figure S1e), suggesting that in both unperturbed and ICRF-193-treated cells, Rif1 is indeed predominantly recruited to UFBs that reflect DNA catenanes. To further confirm that Rif1 associates with UFBs, we analyzed its co-localization with PICH and BLM. Indeed, Rif1 showed overlapping localization at anaphase bridges with both PICH and BLM (Figure 1f, g). The specificity of Rif1 localization at UFBs was verified by short interfering (si)RNA-mediated Rif1 depletion (Figure 2c-e) and by using GFP-tagged Rif1 (Supplemental Figure S1e, f). Finally, although the centromeric UFBs we detected in unperturbed and ICRF-193-treated cells reflected catenated DNA, when we induced replication stress by treatment with aphidicolin (APH), we observed occasional UFBs that connected FANCD2 foci. Also to these UFBs Rif1 was recruited, suggesting that Rif1 is a common component of UFBs, irrespective of their origin (Supplemental Figure S1e).

Rif1 recruitment to UFBs occurs independently of 53BP1, ATM, and BLM but requires PICH

We next investigated the molecular requirements for Rif1 localization to UFBs. In mitosis, the recruitment of 53BP1, and hence Rif1, to DSBs is suppressed by Cdk1-dependent phosphorylation of 53BP1 and RNF8 [362] (Figure 1a and Supplemental Figure S1a, b). Interestingly, depletion of 53BP1 did not affect Rif1 localization at UFBs in anaphase (Figure 2a and Supplemental Figure S2a, g), while it did perturb Rif1 recruitment to irradiation-induced foci (IRIF) in interphase (Supplemental Figure S2b, c). In fact, Rif1 recruitment to UFBs was independent of ATM signaling altogether, as ATM inhibition did not prevent Rif1 recruitment to PICH-positive UFBs (Figure 2b and Supplemental Figure S2d–S2f, h).

Rif1 was previously shown to reside in a complex with BLM during S phase and its recruitment to stalled replication forks was delayed in BLM-deficient cells [363]. BLM was therefore considered a likely candidate to mediate localization of Rif1 to UFBs. However, when we delayed UFB resolution by ICRF-193 treatment at anaphase onset, we found that Rif1 normally localized to UFBs in BLM-depleted cells (Figure 2c, e and Supplemental Figure S2i, j). In contrast, when we depleted PICH, Rif1 recruitment to UFBs was completely blocked (Figure 2d, e and Supplemental Figure S2i, k). Neither the localization of PICH nor BLM depended on the presence of Rif1 (Figure 2c-e and Supplemental Figure S2j, k). This demonstrates that BLM and Rif1 localize to UFBs independently of each other. However, Rif1 requires the presence of PICH to localize to UFBs, similar to the requirement of PICH for BLM recruitment to UFBs.

To investigate whether Rif1 and PICH are part of the same protein complex, we transfected GFP-Rif1 and FLAG-PICH into HEK293T cells and performed co-immunoprecipitation experiments. Precipitation of GFP-Rif1 pulled down FLAG-tagged PICH in HEK293T cells (Supplemental Figure S2l), showing that Rif1 and PICH can form a complex in cells. This interaction depended on the N- and C-terminal tetratricopeptide repeat (TPR) domains of PICH, since deletion of either the N-terminal 76 amino acids or C-terminal 160 amino acids spanning these domains partially affected the interaction with Rif1, whereas deletion of both the N- and C-termini (PICH 76-1090) fully abrogated the interaction between Rif1 and PICH (Supplemental Figure S2l). Of note, we were unable to detect endogenous Rif1 by western blot after PICH immunoprecipitation in either interphase or anaphase cells, suggesting that only a small fraction of Rif1 is associated with PICH.

Deletion of the PICH TPR domains impaired kinetochore localization of PICH in mitosis, but did not affect PICH localization to UFBs in anaphase (Supplemental Figure S2m). Surprisingly, however, PICH 76-1090 was still able to restore Rif1 localization to UFBs in PICH-depleted cells, suggesting that PICH does not recruit Rif1 to UFBs through direct or indirect protein interaction (Supplemental Figure S2m).

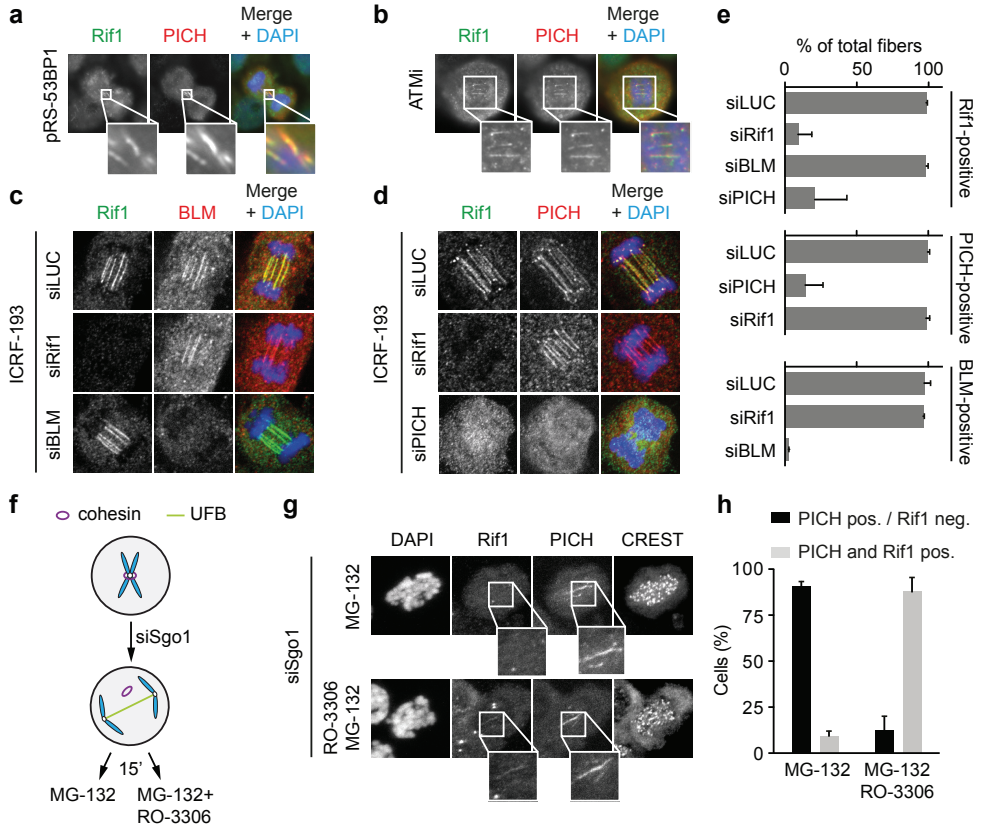

Figure 2l Rif1 localization to UFBs is Independent of ATM, 53BP1, and BLM, requires PICH, and is blocked by Cdk1 activity

a and b) MCF-7 cells were stably depleted of 53BP1 (a) or treated with ATM inhibitor KU-55933 (b) and co-immunostained for PICH and Rif1. **c and d)** RPE-1 cells were transfected with the indicated siRNAs (siRNA#1 was used for Rif1), treated as in Figure 1c, and fixed and immunostained for Rif1 and BLM (c) or for Rif1 and PICH (d). **e)** Quantification of (c) and (d). The number of cells with Rif1-, PICH-, or BLM-positive bridges positive is depicted. The error bars indicate SD (n = 3 experiments and >50 cells/condition). **f)** Schematic representation of SGO1-mediated cohesin protection at centromeres and of the experimental setup. **g)** RPE-1 cells were depleted of SGO1 and treated with or without RO-3306. In both of the conditions, MG-132 was added to prevent mitotic exit. The cells were fixed and stained for Rif1, PICH, and CREST. **h)** Quantification of (g). The percentages of mitotic cells with PICH-positive/Rif1-negative bridges (black) versus cells with PICH-positive/Rif1-positive (gray) are depicted. The error bars indicate SD (n = 3 experiments with at least 50 cells/condition). See also Supplemental Figure S2.

Rif1 recruitment to UFBs is suppressed by Cdk1 activity before anaphase

Before anaphase, cohesin is thought to shield centromeric DNA from topoisomerase II-mediated decatenation [364-366]. In line with this notion, premature removal of centromeric cohesin in (pro)metaphase after depletion of the cohesin protector Shugoshin1 (SGO1), resulted in the visualization of PICH-positive UFBs in prometaphase cells (Figure 2f, h) [311]. Remarkably, these UFBs did not contain Rif1 (Figure 2g, 2),

suggesting the recruitment of Rif1 to UFBs is somehow prevented before anaphase. Since cyclin B-Cdk1 activity is high until anaphase onset, we hypothesized that Cdk1 could prevent the recruitment of Rif1 to UFBs in (pro)metaphase. Indeed, after chemical Cdk1 inhibition, Rif1 was recruited to PICH-positive UFBs in SGO1-depleted prometaphase cells (Figure 2g, h). From these data it can be inferred that Rif1 recruitment to UFBs, and most likely centromeric UFB resolution altogether, is inhibited by Cdk1 and as such restricted to anaphase.

Rif1 is required for timely UFB resolution

PICH and BLM are thought to promote UFB resolution during anaphase and absence of these proteins leads to an increased frequency of histone-containing anaphase bridges [311, 312, 316, 340]. To understand the relevance of Rif1 at UFBs in anaphase, we depleted Rif1 with two independent siRNAs in H2B-YFP expressing HeLa cells and monitored chromosome behavior using time-lapse microscopy. Whereas chromatin bridges were observed in approximately 10% of anaphases in control-depleted cells, ~30% of Rif1-depleted cells showed thin chromatin bridges during anaphase (Figure 3a, 3b and Supplemental Movie S1, S2). Although sometimes hard to detect with H2B-YFP, these DNA bridges appeared to persist during telophase, given the presence of cytokinetic bridges (Figure 3a). Importantly, comparable increases of nucleoplasmic bridges were observed after PICH or BLM depletion (Figure 3b and Supplemental Movie S3, S4), suggesting that PICH, BLM, and Rif1 act together in resolving these DNA bridges.

To further characterize the DNA bridges that persisted in Rif1-depleted cells, we analyzed the presence of the single-stranded (ss)DNA-binding protein RPA70, which was previously shown to be recruited to UFBs [350, 351]. Overall, depletion of Rif1 increased the frequency of cells with persistent RPA70-positive bridges in late anaphase (Figure 3c, d). In marked contrast, we failed to detect RPA70-positive UFBs in late anaphases of BLM-depleted cells (Figure 3d), despite the persistence of nucleoplasmic bridges (Figure 3b). This implies that BLM is (in)directly required for RPA70 recruitment to UFBs.

Because RPA70-positive UFBs have been described in cancer cell lines in which replication stress was induced [367], we tested whether the increased frequency of RPA70-positive UFBs after Rif1 depletion in otherwise unchallenged HeLa cells was an indirect consequence of stalled DNA replication. We therefore analyzed DNA replication in single DNA fibers after sequential CldU and IdU incorporation (Supplemental Figure S3a). Whereas treatment with hydroxyurea (HU) clearly blocked ongoing replication, depletion of Rif1, PICH, or BLM did not significantly alter replication progression (Supplemental Figure S3a, b). Although indirect effects cannot be fully excluded, we deemed it more likely that the increased frequency of RPA70-positive UFBs in Rif1-depleted cells were not caused by replication stress. To assess whether RPA70 recruitment to UFBs in Rif1-depleted cells could thus be a consequence of impaired UFB resolution in anaphase, we inhibited topoisomerase IIα activity at anaphase onset to delay DNA decatenation (Figure 1c). Strikingly, this resulted in a dramatic increase in the appearance of RPA70-positive UFBs in anaphase (Figure 3e, f). In contrast to the decrease in PICH-positive threads upon anaphase progression, RPA70 recruitment to UFBs initially increased upon chromosome segregation, reaching a maximum when separating sister chromatid packs attained a distance of ~10 mm (Figure 3f). At later stages of anaphase, RPA70 disappeared along with the resolution of PICH-positive

fibers. Interestingly, also under these conditions, we were unable to detect RPA70 on UFBs when BLM was depleted (Figure 3e). Taken together, these data demonstrate that RPA70 is recruited to UFBs in a BLM-dependent manner when DNA decatenation is delayed and that Rif1 is required for timely resolution of these UFBs.

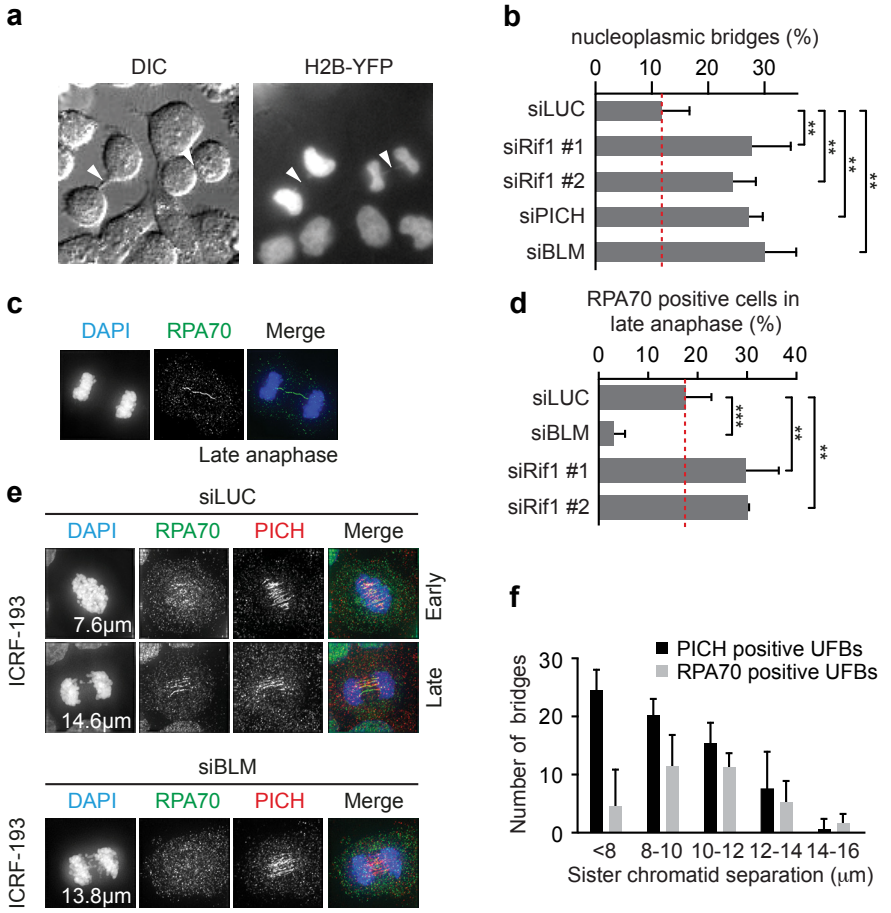

Figure 3l Rif1 is required for proper sister chromatid disjunction
a) HeLa cells stably expressing YFP-H2B were transfected with Rif1 siRNAs. After a thymidine release, the cells were analyzed by live cell video microscopy. The representative DIC and YFP stills of Movie S2 are shown. The arrowheads indicate nucleoplasmic bridges. **b)** HeLa-YFP-H2B cells were transfected with the indicated siRNAs and anaphases were quantified for nucleoplasmic bridges using live cell video microscopy (for examples, see Movies S1, S2, S3, and S4). The error bars indicate SD (n = 3 experiments, 30 cells/condition, **p < 0.01, and unpaired Student's t test). **c)** RPA70 is recruited to persistent UFBs. The HeLa cells were released from a RO-3306-inflicted G2 arrest and fixed 45 min later. The cells were stained for RPA70. The representative late anaphase cell is shown. **d)** Cells were transfected with indicated siRNAs and treated as in (c). The anaphase cells were scored for the presence of RPA70 positive bridges. There were >100 cells/condition that were analyzed (**p < 0.01 and ***p < 0.001) (unpaired Student's t test). **e)** HeLa cells were transfected with indicated siRNAs and treated as in Figure 1c. The cells were fixed and stained for PICH and RPA70. The representative early and late anaphases are depicted. **f)** HeLa cells treated as in (e). The anaphase cells were categorized based on the distance between chromosome packs and the numbers of PICH and RPA70-positive bridges per anaphase were scored. The error bars indicate SD (n > 25 cells/ condition). See also Supplemental Figure S3.

Rif1 depletion increases the frequency of micronuclei formation

We next assessed whether impaired UFB resolution due to loss of Rif1 could have consequences for genomic integrity. Since knockdown of PICH and BLM was associated with micronuclei formation [316], we tested whether Rif1 inactivation would also give rise to micronuclei. In our hands, transient knockdown of Rif1, BLM, or PICH in either RPE-1 or HeLa cells only induced a minor increase in micronuclei formation, compared to control cells. We therefore analyzed RIF1, BLM, and ERCC6L (encoding PICH) knockout cells obtained through CRISPR/Cas9-mediated gene editing of HAP1 cells [368] (Figure 4a). Prolonged inactivation of RIF1 significantly increased the frequency of HAP1 cells with micronuclei to a similar extent as ERCC6L or BLM gene mutation (Figure 4b).

Impaired UFB resolution gives rise to nuclear bodies with damaged DNA in G1

Unresolved late-stage replication intermediates lead to the formation of nuclear bodies in ensuing G1 cells. These nuclear bodies consist of Mdc1 and 53BP1 among others and shield sites of damaged DNA in nuclear compartments until recombination-mediated repair is available in the following S/G2 phase [340, 341]. Currently, it is unclear whether these nuclear bodies can in fact originate from unresolved UFBs.

We therefore tested whether delayed UFB resolution per se, without prior DNA replication defects, gives rise to nuclear bodies in G1. To delay UFB resolution, we again used a low concentration of ICRF-193. To reassure that this treatment does not cause significant replication defects, especially when combined with Rif1, PICH, or BLM depletion, we analyzed replication dynamics in MCF-7 cells using three independent assays. First, global replication analysis by flow cytometry was used to show that low dose ICRF1-193 treatment did not notably alter Edu incorporation, even when Rif1, BLM, or PICH were depleted (Supplemental Figure S4a, b). Second, mitotic cells were analyzed immediately after a 15-min pulse of EdU to demonstrate that ICRF-193 treatment of control-depleted or Rif1-depeted cells did not result in any EdU incorporation in mitotic cells (Supplemental Figure S4c, d). This indicated that active replication in these cells has finished well before mitotic entry [351]. Third, DNA replication speed measured at single DNA fiber resolution was also not significantly affected by the low dose of ICRF-193 that we used to increase the number of UFBs (Figure 4c, d). Importantly, depletion of neither Rif1, BLM, nor PICH caused a decrease in replication speed in ICRF-193-treated cells (Figure 4c, d).

Having established that a low dose of ICRF-193 in combination with knockdown of Rif1, BLM, or PICH did not notably delay replication progression, we used MCF-7 cell lines, stably expressing GFP-Mdc1 or GFP-53BP1, in combination with cyclin A staining to discriminate S/G2 cells from G1 cells to assess whether impaired DNA decatenation would result in nuclear body formation in G1 (Supplemental Figure S4e, f). Treatment with ICRF-193 alone resulted in the formation of Mdc1-GFP and GFP-53BP1 nuclear bodies in G1 phase (Supplemental Figure S4e, f) and also resulted in nuclear bodies consisting of endogenous 53BP1 (Figure 4e). Importantly, we found that depletion of Rif1, PICH, or BLM significantly increased the number of these 53BP1 nuclear bodies in ICRF-193-treated cells (Figure 4e, f). Of note, the increase in 53BP1 nuclear bodies after Rif1 depletion was comparable to the increase in PICH or BLM-depleted cells. Since PICH was not previously reported to play a role during S phase, and even localizes to the cytoplasm during interphase [311], our data suggest that the observed nuclear 53BP1 bodies are due to an inability to resolve UFBs by a pathway comprising PICH, BLM, and Rif1. To further strengthen this notion, we co-depleted PICH with Rif1 or PICH

with BLM (Supplemental Figure S4g). This did not lead to the formation of additional 53BP1 nuclear bodies compared to PICH-depleted cells (Figure 4g), supporting our findings that the localization of both Rif1 and BLM to UFBs is dependent on PICH (Figure 2) and strengthening the model that Rif1, PICH, and BLM function in a similar pathway to resolve DNA catenanes during anaphase to ensure genomic integrity (Figure 4H).

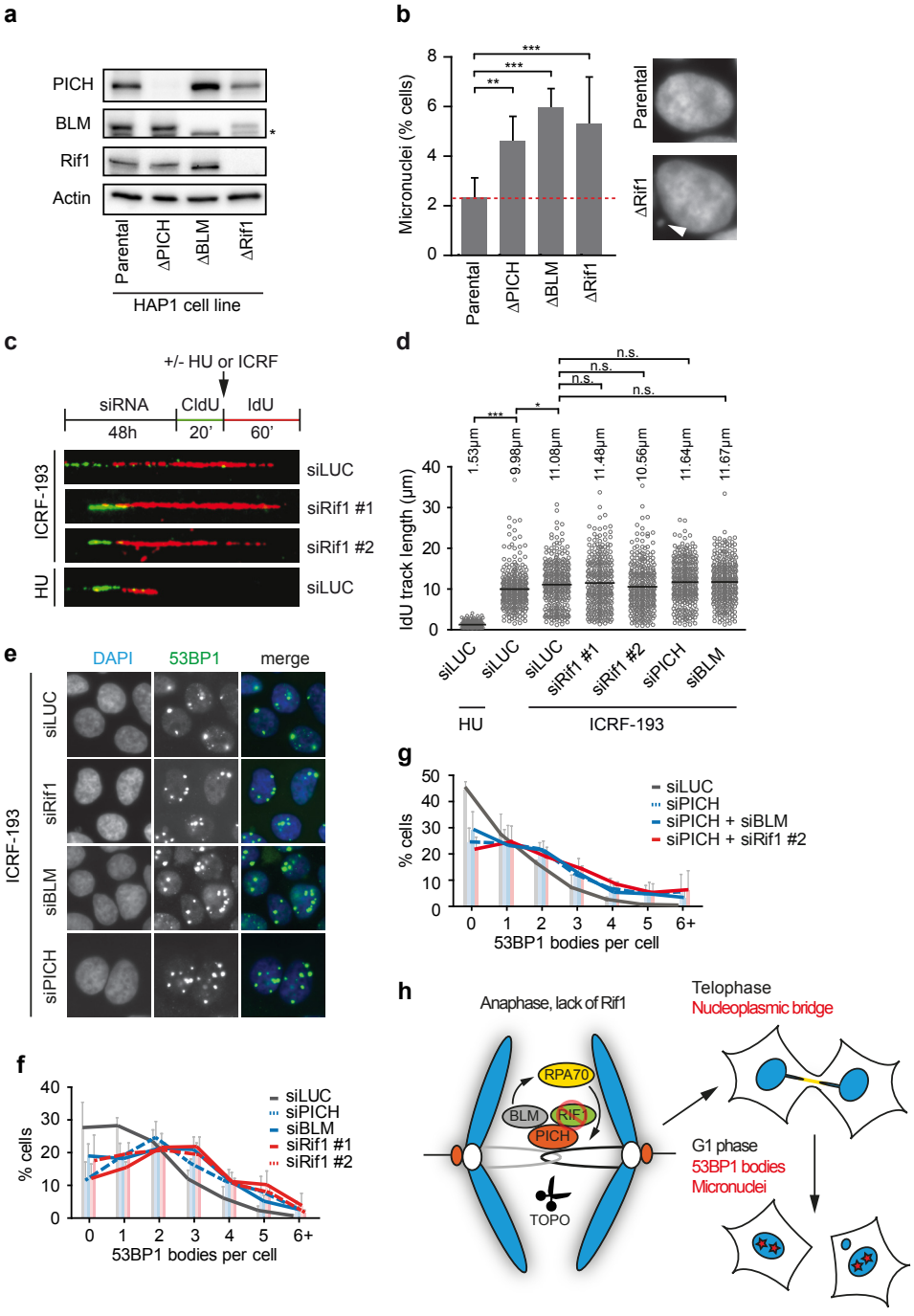

Figure 4l Impaired UFB resolution increases frequency of micronuclei and 53BP1 nuclear body formation
a) PICH, BLM, Rif1, and actin levels in the parental or indicated HAP1 knockout cell lines determined by immunoblotting, (*) aspecific band. **b)** Parental HAP1 cells or HAP1 cell lines harboring frame shift mutations in RIF1, BLM, or ERCC6L were analyzed for micronuclei (arrow in image). The mean ± SD of three experiments (>1,000 cells/condition in each experiment) (**p < 0.01, ***p < 0.001, and unpaired Student's t test). **c and d)** MCF-7 cells were transfected with indicated siRNAs and labeled with CldU and IdU, according to the indicated scheme. Where indicated, cells were treated with ICRF-193 during IdU incubation or with HU as a positive control. The DNA was spread into single fibers and IdU track length was determined for 300 fibers per condition. The representative fibers are shown in (c) and actual and average fiber lengths are plotted in (d) (*p < 0.05, ***p < 0.001, n.s. = not significant, and unpaired Student's t test). **e–g)** MCF-7 cells were transfected with indicated siRNAs and treated for 24 hr with ICRF-193. At 48 hr after transfection, the cells were fixed and stained for 53BP1. The nuclear 53BP1 bodies per cell were scored. The percentages are mean ± SD of three experiments with >400 cells per condition. The representative images of 53BP1 bodies in siRNA transfected MCF-7 cells are shown in (e). **h)** During anaphase, Rif1 and BLM are recruited to UFBs in a PICH-dependent fashion. In the absence of Rif1, UFB resolution is impaired. This gives rise to nucleoplasmic bridges in anaphase/telophase and to micronuclei and nuclear bodies with damaged DNA in G1. See also Supplemental Figure S4.

Discussion

We here uncovered a role for Rif1 in UFB resolution in anaphase. During interphase, Rif1 functions downstream of 53BP1 in controlling DNA DSB repair choice [342, 345, 353, 369] [343] and timing of DNA replication [356-359]. We here show that the recruitment of Rif1 to UFBs in anaphase is 53BP1 independent. Interestingly, while the cellular response to DNA damage is re-wired during the cell cycle, and mitosis specifically [360], also the here described role for Rif1 at UFBs appears to be subject to cell-cycle regulation. In line with Cdk1-mediated inactivation of the 53BP1-Rif1 signaling axis during mitosis [362], also Rif1 recruitment to UFBs is inhibited by Cdk1 activity. These data point at a generic role for Cdk1 in suppressing the cellular response to DNA lesions during mitosis, both in response to DNA DSBs as well as unresolved DNA catenanes.

Rif1 is recruited to UFBs in anaphase together with the BLM DNA helicase. Besides DNA helicase activity, also topoisomerase activity and regulatory factors including TopBP1 and RMI1 are recruited to UFBs [312, 351]. This complex resembles the BLM-Topoisomerase IIIa-RMI1-RMI2 (BTRR) complex that is recruited to resolve recombination intermediates and promote stalled replication recovery during S phase [370]. Our data show that the recruitment of BLM to UFBs in anaphase differs from recruitment of BLM to replication intermediates during S phase. Whereas during S phase, Rif1 appears to be the DNA binding interface mediating BLM recruitment [363], BLM recruitment to UFBs is independent of Rif1, but depends on PICH. These differential requirements may be necessitated by the fundamentally different chromatin state during anaphase, with elevated levels of tension and the absence of histones [315]. Although PICH and Rif1 can be found in the same protein complex, this interaction does not appear to be required for the PICH-dependent loading of Rif1 on UFBs, implying an alternative mode of Rif1 UFB recruitment regulation. Since PICH functions as DNA translocase [315], it suggests a DNA remodeling role for PICH at UFBs. We propose this may enhance the accessibility of DNA for Rif1, without PICH directly recruiting Rif1.

We found that the ssDNA-binding protein RPA70 was recruited to UFBs, especially when UFB resolution was delayed by topoisomerase II inhibition and the localization of RPA70 to UFBs was completely dependent on the presence of BLM. RPA70 recruitment to UFBs most likely reflects ssDNA generation, given that RPA70 only binds ssDNA efficiently [371]. As such, RPA70 recruitment may reflect BLM DNA helicase activity, with Rif1 having an inhibitory effect on BLM activity at UFBs. This idea is in line with a

previously reported genetic interaction between Rif1 and BLM, in which Rif1 inhibits BLM function [343]. This latter observation, however, was made in the context of eroded telomere processing and it is unclear whether BLM and Rif1 interact similarly at UFBs. Since RPA70 showed preferential recruitment to longer UFBs when compared to optimal PICH recruitment, we cannot formally exclude the possibility that DNA under high tension may adopt alternative confirmations in which bases are exposed that allow interaction with RPA70 [315]. Clearly, future studies are required to uncover how Rif1, BLM, and PICH act at the molecular level to resolve UFBs.

Finally, we demonstrated that impaired UFB resolution gives rise to nuclear bodies with damaged DNA in G1. The inability to properly resolve DNA catenanes or other late-stage replication intermediates that lead to UFBs in anaphase could thus lead to accumulation of genomic lesions and may as such contribute to tumorigenesis.

Experimental Procedures

Synchronization and treatment of cell lines

Human cervical cancer HeLa cells were cultured in a 1:1 mixture of DMEM (Gibco) and Ham's F12 (Gibco) medium, supplemented with penicillin (100 units/ml), streptomycin (100 µg/ml) (Gibco) and 10% fetal calf serum (FCS, Bodinco BV). MCF-7 human breast cancer cells were cultured in RPMI-1640 (Gibco) medium supplemented with penicillin (100 units/ml), streptomycin (100 µg/ml) and 10% FCS. Human retinal pigment epithelium (RPE-1) cells and human embryonic kidney (HEK) 293T cells were cultured in DMEM medium supplemented with penicillin (100 units/ml), streptomycin (100 µg/ml) and 10% FCS. HAP1 cells were obtained from Haplogen GmbH (Vienna, Austria) and maintained in IMDM medium (Gibco), supplemented with penicillin (100 units/ml), streptomycin (100 µg/ml) (Gibco) and 10% FCS. CRISRP/Cas9-mediated gene targeting was used to generate ΔRif1 (Guide RNA sequence: ACTCAGCTCCGAGTTTTGAC, caused a 7-bp deletion in exon 4, creating a frameshift), ΔERCC6L (Guide RNA sequence: GGGCTCAAGGCCTCGGCTTC, caused a 2 bp deletion in exon 1, creating a frameshift) and ΔBLM (Guide RNA sequence: AGATTTCTTGCAGACTCCGA, caused a 5 bp deletion in exon 3, creating a frameshift). HeLa and RPE-1 cells were blocked in G2 phase using RO-3306 (5 µM and 7.5 µM respectively, Calbiochem) for 18 hr. At 15 min after release from the RO-3306 block, ICRF-193 was added (160 nM, Sigma). Where indicated, cells were gamma-irradiated using CIS Bio international/IBL 637 irradiator, equipped with a $Cesium^{137}$ source (dose rate: 0.01083 Gy/s), or treated with 10µM ATM inhibitor KU-55933 (Axon Medchem, Groningen, the Netherlands), 0.15, 0.2 or 2µM Aphidicolin (Sigma Aldrich), 2.5 µM thymidine, 2 or 5mM hydroxyurea (Sigma Aldrich), or 5µM MG132 (Sigma Aldrich).

RNA interference

MCF-7, HeLa, or RPE-1 cells were transfected at 30%-60% confluency with the following siRNA's targeting Rif1: 5'-GACUCACAUUUCCAGUCAA-3' (Rif1#1, Dharmacon), and 5'- CCAGUGUACUUGGGCAUAUUUCUUU-3' (HSS124069, Rif1#2, Life Technology). For BLM depletion we used either 5'-ACAGGGAAUUCUAUGAAGGAGUUAA-3' (HSS101023, Life Technology) or 5'-GGAGCACAUCUGUAAAUUA-3' (Dharmacon). For PICH depletion we used 5'-UGUACACAUGUGAUCUGUCUGUUAA-3' (HSS147788, Life Technology) or 5'- AGGCCAGACUUAAUGAAAA-3' (Dharmacon). For SGOL1 depletion we used 5'- GAUGACAGCUCCAGAAAUU-3' (Dharmacon). siRNA targeting

Luciferase (GL2 duplex, Dharmacon) was used as a control. Prior to siRNA transfection, culture media were exchanged to OptiMEM (Gibco) without FCS or antibiotics, and subsequently cells were transfected using Oligofectamine reagent (Invitrogen) or HiPerFect reagent (Qiagen) according to manufacturer's recommendations.

Plasmids and transfections

For retroviral short-hairpin RNA (shRNA) delivery, MCF-7 or HeLa cells were retrovirally infected with VSV-G pseudotyped viruses containing control pRetrosuper (scrambled: 5- TTCTCCGAACGGTGCACGT-3') or pRetrosuper-53BP1 (53BP1-targeting sequence: 5'- GAACGAGGAGACGGTAATA-3') as described previously [372]. In short, HEK293T cells were transfected with indicated pRetrosuper plasmids along with pMDG and pMDG/p in a (3:2:1) ratio. Twenty-four hours after transfection, medium was replaced. Subsequently, virus-containing medium was collected, filtered using a 0.45 µm PVDF syringe filter (Millipore) and used for three consecutive 12 hour periods to infected target cells. At 24 hours after the last infection, cells were selected with 2µg/ml puromycin. For expression of GFP-Rif1, the pDEST pcDNA5/FRT/TO-eGFP plasmid containing human Rif1 was kindly provided by Dr. Daniel Durocher (University of Toronto, Canada) [345]. Full length human PICH and indicated fragments were generated by PCR on a human cDNA library and ligated into the pCR3 vector (Invitrogen), containing an N-terminal FLAG tag or into pcDNA5/FRT/TO (Invitrogen), containing an N-terminal AcGFP-tag. HeLa FLP-In cells (Life Technologies) were transfected with pcDNA5/FRT/TO containing eGFP-Rif1, AcGFP- PICH or AcGFP-PICH 76-1090 along with pOG44, encoding the Flp-recombinase, (Invitrogen) using Xtreme Gene 9 DNA Transfection Reagent (Roche). At 48 hours after transfection, cells with successful integration were selected with 400µg/ml hygromycin (Invitrogen) and expanded as polyclonal cell lines. GFP-Rif1 expression was induced for 48 hours with 2µg/ml doxycycline (Sigma), and GFP-Rif1-positive cells were FACS-sorted and expanded as monoclonal cell lines for further use.

Antibodies

BLM pAb (#ab2179) and FANCD2 mAb (#ab108928) were from Abcam. PICH mAb (H00054821, Abnova, Figure 2A, B). Rif1 pAb (A300-568A, Bethyl Laboratories). FLAG mAb (F425) was from Sigma. Phospho-Thr68-Chk2 pAb (2197), phospho-Ser139-H2AX pAb (9718) and RPA70 pAb (2267) were from Cell Signaling. 53BP1 pAb (sc22760), BLM pAb (sc1611), CDK4 pAb (sc-260-g) and Chk2 pAb (sc56297) and GFP mAb (sc9996) were from Santa Cruz. Phospho-Ser139-H2AX (05-636), PICH mAb (142-26-3) and MPM2 mAb (05-368) were from Millipore and mouse anti-Actin was from MP Biomedicals (#69100). CREST pAb (cs-1058) was from Cortex Biochem. For immunoblotting, HRP-conjugated secondary antibodies (DAKO P044801; P026002) were used in combination with enhanced chemiluminescence (ECL) using Lumi-Light (Roche). Membranes were visualized using a ChemiDoc in combination with Quantity One 4.5.0 software (Bio-Rad). Alexa-488, Alexa-568, and Alexa- 647-conjugated secondary antibodies (Invitrogen A11008; A11001; A21134; A21235; A21244) were used for immunofluorescence microscopy and flow cytometry.

Immunoprecipitation

HEK293T cells were cultured to ~50% confluency and were transfected with 4 µg FLAG-PICH or indicated deletion mutants in combination with 1 µg GFP-Rif1 or 0.2 µg GFP-encoding cDNA using a standard calcium phosphate protocol. After 16 hours, medium was replaced and after another 24 hours cells were harvested in lysis buffer (50 mM Tris–HCl pH 7.7; 150 mM NaCl; 0.5% (v/v) Nonidet P-40 (Sigma)), supplemented with

protease inhibitor cocktail (Roche). After sonication, GFP-Rif1 was immunoprecipitated using GFP-Trap beads (ChromoTek). After extensive washing, GFP-Rif1 and FLAG-PICH were analyzed by SDS-Page and immunoblotting.

Immunofluorescence and flow cytometry

HeLa, MCF-7, HAP1 or RPE-1 cells were grown on glass cover slips for at least 48 hours to a maximum confluence of 80%. Cells were then fixed with 3.7% formaldehyde (Sigma) or paraformaldehyde (Sigma) in phosphate-buffered saline (PBS) for 5 minutes. Cells were permeabilized for 5 minutes in 0.1% Triton-X100 (Sigma) in PBS or PBS containing 0.5% NP40 (Sigma). Cells were subsequently blocked in PBS containing 0.05% Tween-20 (Sigma) and 2.5% bovine serum albumin (BSA; GE Healthcare). Cells were incubated with primary antibodies in PBS/Tween-20/BSA for 16 hours, followed by extensive washing and incubation with secondary antibodies. Subsequently, cells were incubated with Hoechst 33342 (Sigma) or 500 ng/mL DAPI (Sigma) before mounting slides with Kaiser's glycerol/gelatine (Sigma) or with ProLong Gold antifade reagent (Life Technologies). Micronuclei analysis in HAP1 cell lines was performed in three independent experiments, with at least 1,000 cells analyzed per experiment per cell line. In order to visualize DNA replication, cells were incubated with 5-Ethynyl-2´-deoxyuridine (EdU, final concentration 10mM) for 30 minutes. Cells were subsequently harvested by trypsinization and fixed in 70% ice-cold ethanol for flow cytometry analysis, or alternatively in 3.7% formaldehyde for microscopy. Incorporated Edu was subsequently labeled with Alexa-488 using click chemistry by incubating in staining buffer (100mM Tris pH8.5, 1mM $CuSO_4$, 100mM L- ascorbic acid), supplemented with 10mM Alexa-488-azide (Invitrogen, A10266) for 30 minutes at room temperature in the dark. Cells were subsequently counterstained with propidium Iodide (50µg/ml) / RNAse (100µg/ml) for flow cytometry or with DAPI for microscopy analysis. The Mann-Witney U test (95% confidence intervals) was performed for statistical analysis. For flow cytometry, at least 5,000 events were analyzed per sample on a FACS-Calibur (Becton Dickinson) using Cell Quest software (Becton Dickinson).

Microscopy

Immunofluorescence microscopy was done with a Leica DM-6000 microscope, equipped with a DFC360FX camera, a CTR6000 Xenon light source, 63X objective, and LAS-AF Software (Leica). Alternatively, a DeltaVision Elite microscope, equipped with a CoolSNAP HQ2 camera and 100X objective was used to analyze HeLa cells, expressing YFP-tagged Histone-H2B. Live cell IF microscopy was done using a Zeiss Axiovert 200M microscope, equipped with a 40X objective.

DNA fiber analysis

To assess replication dynamics HeLa cells were pulse-labeled with CIdU (25µM) for 20 minutes. Next, cells were washed with medium and incubated with hydroxyurea (HU, 2mM) for 4 hours. Subsequently, cells were washed with media and pulse-labeled with IdU (250µM) for 1 hour. Cells were harvested using trypsine and lysed on microscopy slides in lysis buffer (0.5% sodium dodecyl sulfate (SDS), 200mM Tris (pH 7.4), 50mM EDTA). DNA fibers were spread by tilting the slide and were subsequently air–dried and fixed in methanol/acetic acid (3:1) for 10 minutes. Fixed DNA spreads were stored for 24 hours at 4°C before the immuno-labeling spreads were treated with 2.5M HCl for 1.5 hours. CIdU was detected by staining with rat anti-BrdU (1:1000, AbD Serotec) for 1 hour and IdU was detected with mouse anti-BrdU (1:500, Becton Dickinson) for 1 hour and further incubated with AlexaFluor 488-conjugated anti-rat IgG (1:500) and AlexaFluor

647-conjugated anti- mouse IgG (1:500) for 1.5 hours. Images were acquired on a Leica DM-6000RXA fluorescence microscope, equipped with Leica Application Suite software. The lengths of CIdU and IdU tracks were measured using ImageJ software. An unpaired Student's t-test (95% confidence intervals) was used for statistical analysis.

DNA replication and nuclear body formation
At 48 hr after siRNA transfection, MCF-7 cells were incubated with Edu (10 μM), CldU (25 μM), or IdU (250 μM), and fixed in 70% ethanol for flow cytometry, in formaldehyde (3.7%) for microscopy, or processed for single DNA fiber analysis. At least 300 fibers were analyzed per condition. Nuclear body formation was assessed in MCF-7 cells expressing Mdc1-GFP or GFP-53BP1 or through staining of formaldehyde-fixed cells for endogenous 53BP1.

Statistical analysis
Data are shown as mean ± SD where indicated. An unpaired Student's t test or Mann-Whitney U test was performed using GraphPad statistical analysis and p values % 0.05 were considered significant.

Acknowledgements

We thank Dr. A. Duursma for valuable comments on the manuscript and members of the S.M.A.L., Kops, and M.A.T.M.v.V. laboratories for helpful discussions. This work is financially supported by grants from the Netherlands Organization for Scientific Research (NWO-VICI 91812610 to S.M.A.L. and NWO-VIDI 91713334 to M.A.T.M.v.V.), the Dutch Cancer Society (UU2009-4311 to S.M.A.L. and RUG2011-5093 to M.A.T.M.v.V.), and the European Research Council (ERC-Advanced Grant ERC-2011-293-445 to E.G.E.d.V.).

Supplemental information

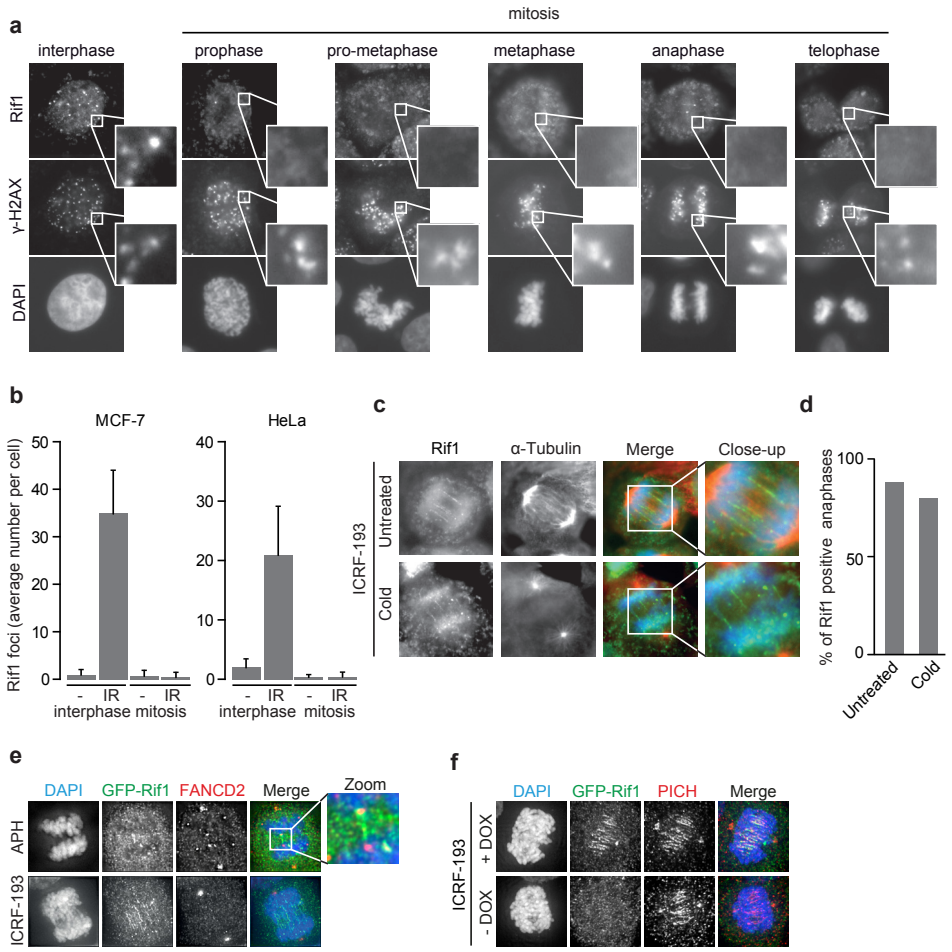

Figure S1, related to Figure 1l Cell cycle-dependent localization of Rif1 to IRIF
a) Rif1 localizes to irradiation-induced foci (IRIF) during interphase, but not in mitosis. Representative images of Rif1 and γ-H2AX localization to IRIF in MCF-7 cells during interphase or the various stages of mitosis at 30 minutes after irradiation with 5 Gy. **b)** Quantification of average numbers and standard deviations of Rif1 foci from a representative experiment in MCF-7 cells before irradiation (interphase n=50, mitosis n=69) or after 5 Gy irradiation (interphase n=48, mitosis n=61) and in HeLa cells before irradiation (interphase n=31, mitosis n=40) or after 5 Gy irradation (interphase n=25, mitosis n=47). **c)** Rif1 recruitment to anaphase bridges is independent of microtubules. MCF-7 cells were treated with ICRF-193 (160nM) to induce Rif1-positive anaphase bridges. At 1 hour after ICRF-193 treatment, cells were treated with a cold-shock to destabilize central spindle microtubules, fixed and stained for α- Tubulin and Rif1. **d)** Quantification of results from panel c. Anaphase cells from untreated (n=42) or cold treated (n=30) conditions were analyzed for the presence of Rif1-positive threads. **e)** HeLa with stable inducible expression of GFP-Rif1 were treated with doxycycline (DOX) for 24 hours and treated with ICRF-193 (160nM) or Aphidicolin (APH, 150nM). After one hour of ICRF-193 treatment or 24 hours of APH treatment, cells were fixed and stained for FANCD2 and DAPI. **f)** HeLa cells stably expressing inducible GFP-Rif1 were treated with doxycycline for 24 hours and subsequently stained for PICH and DAPI.

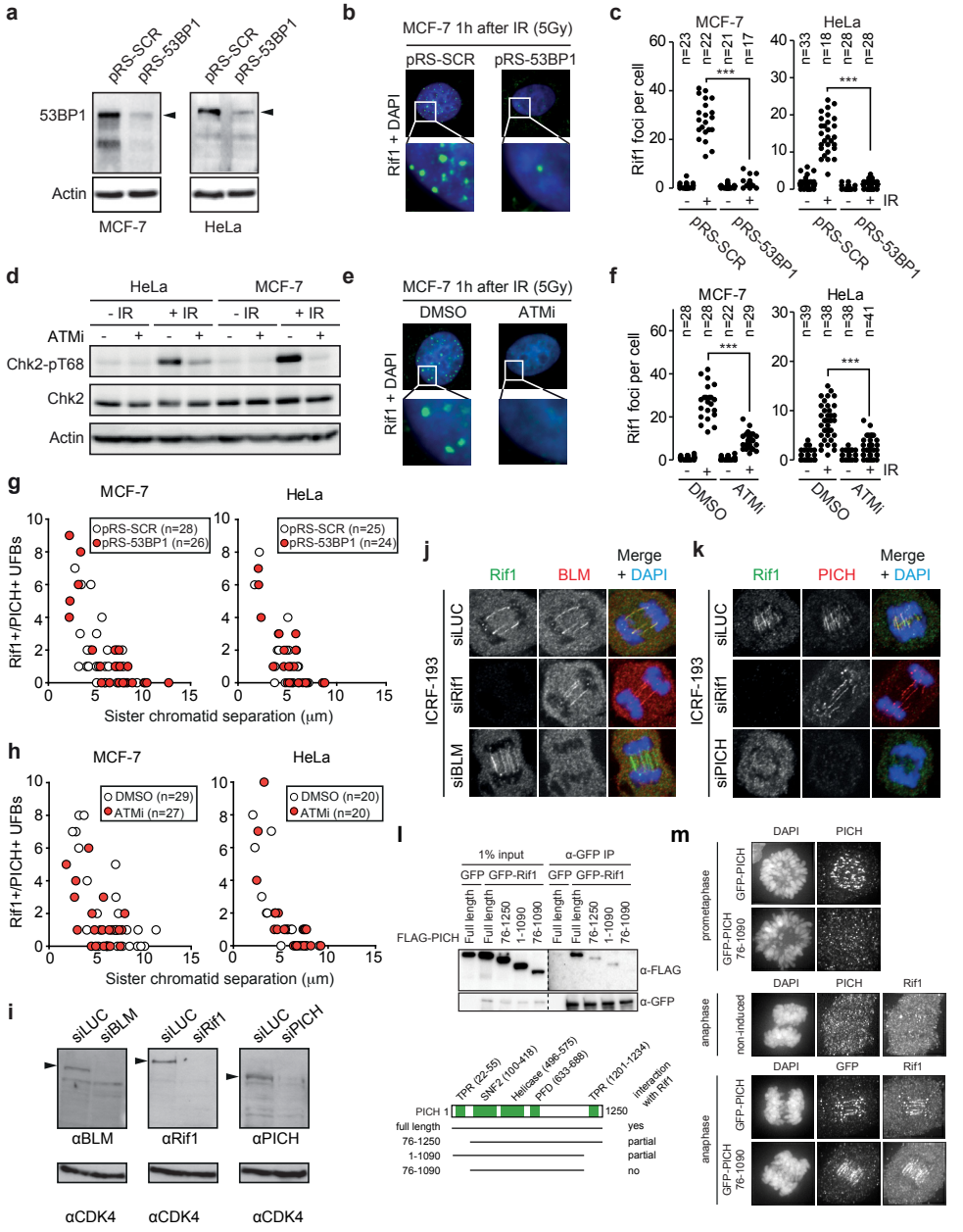

Figure S2, related to Figure 2l Rif1 recruitment to anaphase bridges is independent of 53BP1 and ATM, but dependent of PICH a) HeLa and MCF-7 cells were stably infected with retroviral short hairpins targeting 53BP1 or scrambled sequence (pRS-53BP1, pRS-SCR). Levels of 53BP1 were assessed by immunoblotting. **b)** IR- induced Rif1 foci formation in interphase cells is 53BP1-dependent. MCF-7 cells expressing pRS-SCR or pRS-53BP1 were fixed at 1 hour after irradiation with 5 Gy. Cells were stained for Rif1 and nuclei were stained with DAPI. **c)** MCF-7 cells and HeLa cells were treated as for panel b). Rif1 foci per interphase cell in HeLa or MCF-7 cells from one representative experiment are plotted. Numbers of analyzed cells per condition are indicated in the graph. *** p<0.001 (unpaired Student's t-test). **d)** ATM inhibition using KU-55933 prevents Chk2 phosphorylation. One hour prior to irradiation (5 Gy) HeLa and MCF-7 cells were treated with KU-55933. Chk2 phosphorylation at Thr-68 was assessed by immunoblotting. **e)** IR-induced Rif1 foci formation in interphase

cells depends on ATM activity. MCF-7 cells were treated with KU-55933 at 1 hour prior to irradiation (5 Gy), and fixed 1 hour after irradiation. Cells were stained for Rif1 and nuclei were stained with DAPI. **f)** Quantification of numbers of Rif1 foci per cell in HeLa or MCF-7 cells as shown in e). Rif1 foci per interphase cell in HeLa or MCF-7 cells are indicated from one representative experiment. The number of analyzed cells per condition is indicated in the graph. ***p<0.001 (unpaired Student's t-test). **g)** Rif1 localizes to PICH- positive UFBs independent of 53BP1. MCF-7 cells and HeLa cells infected with pRS-SCR or pRS-53BP1 were co-immunostained for PICH and Rif1. Distance between sister chromatids (μm) was measured and plotted against the number of Rif1/PICH-positive UFBs. Numbers of analyzed cells per condition are indicated in the legend of the graph. **h)** Rif1 localization to PICH-positive UFBs is independent of ATM. MCF-7 and HeLa cells were treated with KU-55933 and cells were co-immunostained for PICH and Rif1 and analyzed as shown in g. Numbers of analyzed cells per condition are indicated in the legend of the graph. **i)** RPE-1 cells were transfected with indicated siRNA and levels of Rif1, PICH, BLM and Cdk4 were assessed by immunoblotting at 48 hours after transfection. **j, k)** HeLa cells were transfected with indicated siRNAs and treated as in Figure 1c. Cells were fixed and stained for Rif1 and PICH (j), or were stained for Rif1 and BLM (k) in combination with DAPI. **l)** GFP-Rif1 was immunoprecipitated from HEK293T cells expressing full length FLAG-PICH or indicated deletion mutants. Input samples (1%) and immunoprecipitations were immunoblotted for Rif1 and FLAG. Domain organization of PICH is indicated in the lower panel (TPR: tetratricopeptide repeats; SNF2: sucrose non-fermenting-family domain; PFD: PICH family domain). **m)** HeLa cells stably expressing doxycycline-inducible GFP-tagged PICH or GFP-tagged PICH 76-1090 were transfected with PICH siRNA. Cells were processed to visualize PICH and Rif1 or GFP and Rif1. Note that PICH-Rif1 protein complex formation (shown in l) is not required for PICH-dependent recruitment of Rif1 to UFBs.

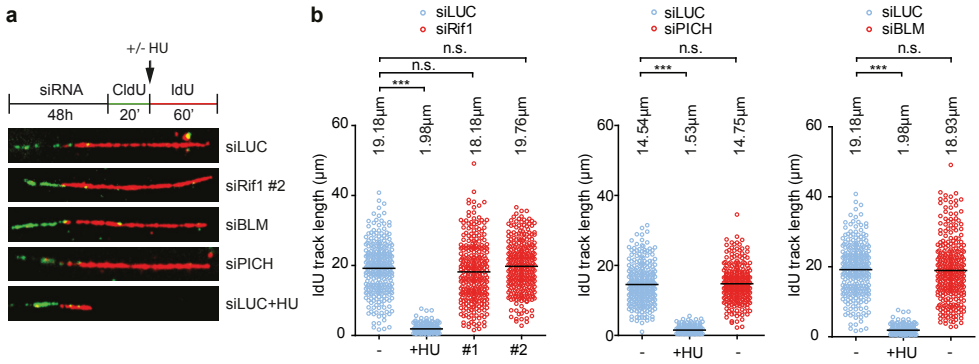

Figure S3, related to Figure 3l Depletion of PICH, Rif1 or BLM does not result in DNA replication delay
a) MCF-7 cells were transfected with the indicated siRNAs and labeled with IdU and CldU according to the indicated time scheme. Where indicated, cells were treated with hydroxyurea (HU, 5mM) during CldU incubation. DNA was spread into single fibers and representative images of IdU/CldU tracks are shown. **b)** CldU track length was determined of at least 300 fibers per condition. Fiber length is indicated in μm. n.s = not significant; *** p<0.001 (unpaired two-sided Student's t-test).

Figure S4, related to Figure 4l DNA replication in ICRF-193-treated cells with or without Rif1, PICH or BLM
a, b) MCF-7 cells were transfected with indicated siRNAs and treated with aphidicolin (APH) or ICRF- 193 for 24h incubation. 48 hours after transfection, cells were incubated with EdU for 15 minutes and subsequently fixed. EdU was conjugated to azide-Alexa488 and DNA was stained with propidium iodide, combined with RNAse treatment, and cells were subsequently analyzed by flow cytometry. **b)** Quantification of Edu-Alexa488 signal in at least 5,000 cells per condition from panel a. **c)** Cells were treated as in panel a and EdU incorporation was analyzed by fluorescent microscopy. Edu was conjugated to azide-Alexa488 and DNA was stained with DAPI. Representative images of mitotic and interphase cells are indicated. **d)** Quantification of Edu-Alexa488 signal in mitotic and interphase cells from panel c. At least 120 cells were quantified per condition. n.s. = not significant; * p<0.05; *** p<0.001 (Mann-Whitney U test). **e, f)** MCF-7 cells stably expressing Mdc1-GFP (e) or 53BP1-GFP (f) were treated with or without ICRF-193 for 24 hours. Cells were subsequently fixed and stained with anti-cyclin A and DAPI. Representative images of Mdc1-GFP nuclear bodies (e) and 53BP1-GFP nuclear bodies (f) in cyclin A-negative cells are shown. Below microscopy images, quantifications of Mdc1- GFP and 53BP1-GFP bodies per cell are plotted in relation to cyclin A status. **g)** MCF-7 cells were transfected with indicated siRNAs and levels of Rif1, PICH, BLM and Actin were assessed by immunoblotting at 48 hours after transfection.

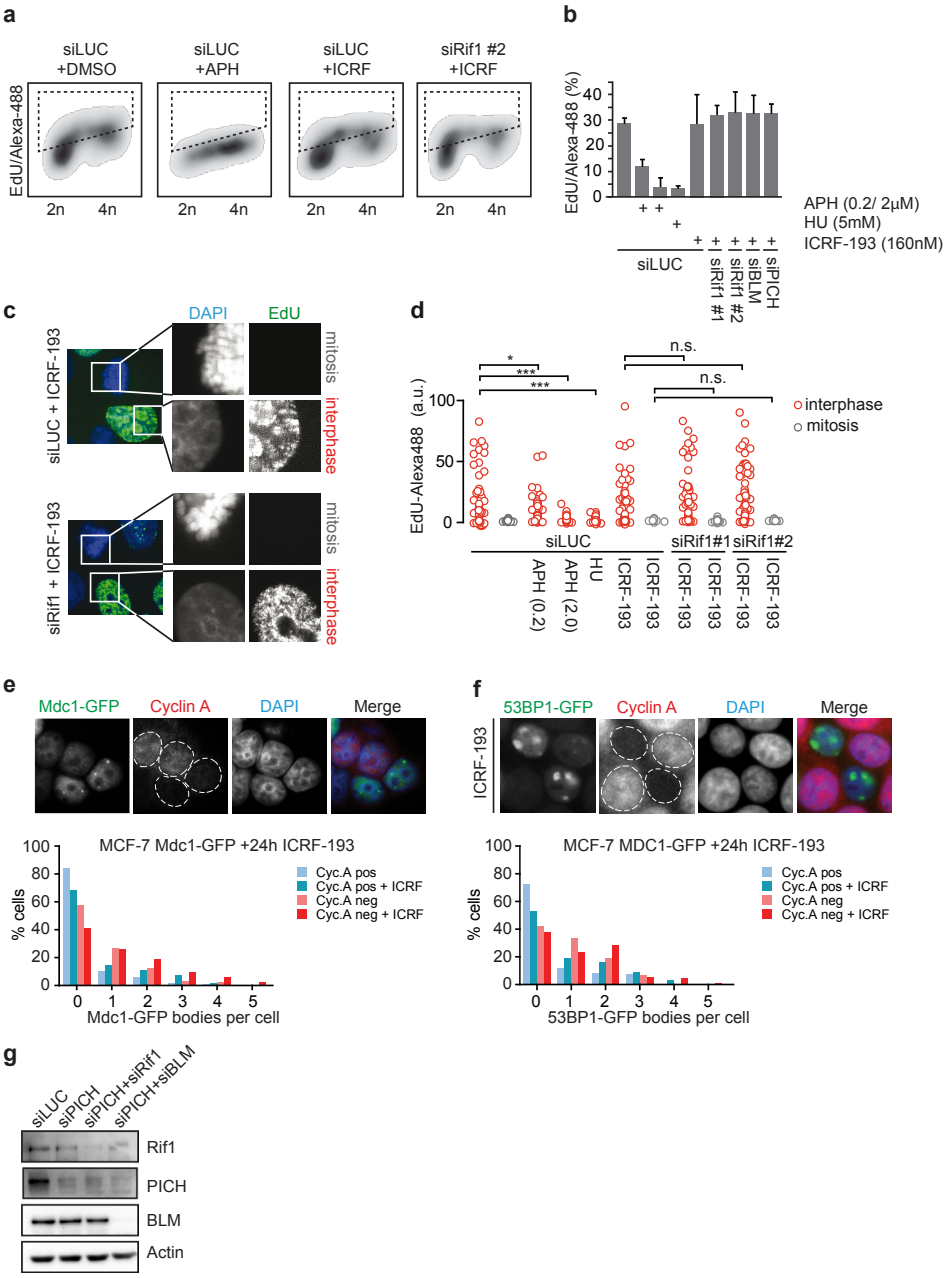
a
siLUC +DMSO
siLUC +APH
siLUC +ICRF
siRif1 #2 +ICRF
EdU/Alexa-488
2n
4n
b
EdU/Alexa-488 (%)
APH (0.2/ 2μM)
HU (5mM)
ICRF-193 (160nM)
siLUC
siRif1 #1
siRif1 #2
siBLM
siPICH
c
DAPI
EdU
siLUC + ICRF-193
siRif1 + ICRF-193
mitosis
interphase
d
EdU-Alexa488 (a.u.)
interphase
mitosis
n.s.
siLUC
siRif1#1
siRif1#2
APH (0.2)
APH (2.0)
HU
ICRF-193
e
Mdc1-GFP
Cyclin A
DAPI
Merge
MCF-7 Mdc1-GFP +24h ICRF-193
Cyc.A pos
Cyc.A pos + ICRF
Cyc.A neg
Cyc.A neg + ICRF
% cells
Mdc1-GFP bodies per cell
f
53BP1-GFP
ICRF-193
MCF-7 MDC1-GFP +24h ICRF-193
53BP1-GFP bodies per cell
g
siLUC
siPICH
siPICH+siRif1
siPICH+siBLM
Rif1
PICH
BLM
Actin

Chapter 6

Summary and Discussion

Summary

Maintenance of a stable genome requires accurate DNA replication during S phase and error-free chromosome segregation during cell division. To allow proper chromosome segregation it is essential that the duplicated chromosomes (sister chromatids) remain linked in early mitosis and become attached to microtubules that emanate from opposite spindle poles, a process referred as chromosome bi-orientation [373]. Time to accomplish bi-orientation is provided by the mitotic checkpoint, which senses the attachment status of kinetochores. Kinetochores are large multi-subunit protein complexes that assemble at the centromeric regions of chromosomes and mediate chromosome attachment to the mitotic spindle. The mitotic checkpoint prevents anaphase onset until all sister chromatids have established end-on attachments with microtubules of the mitotic spindle [270]. The highly conserved Chromosomal Passenger Complex (CPC) (consisting of Aurora B, Inner CENtromere Protein (INCENP), survivin and borealin) is indispensable for chromosome bi-orientation and proper functioning of the mitotic checkpoint [374], and one of the aims of this thesis was to understand how this protein complex controls chromosome bi-orientation and faithful segregation of the sister chromatids. The enzymatic core of the complex, Aurora B kinase, is a member of the Aurora family of serine/threonine kinases, which includes Aurora A and Aurora C in addition to Aurora B [375]. Aurora B requires the other CPC members for its activation (INCENP C-terminus) [202, 283, 284] and localization (INCENP N-terminus that interacts with borealin and survivin) [255, 271, 376], and they most likely also guide substrate specificity. In prometaphase and metaphase the CPC localizes at the inner centromeric region of the chromosomes (i.e. the region between the two sister-kinetochores)(Figure 1) and this was crucial to its role in promoting chromosome bi-orientation [144, 146, 204, 250]. However this view was challenged by work in budding yeast from Campbell and Desai [254]. In Chapter 2 we therefore investigated the importance of inner centromere localization of the CPC for chromosome bi-orientation in human cells. Furthermore, since the function of the CPC is dictated by the substrates that are phosphorylated by Aurora B, we developed a chemical genetic approach for this kinase to identify novel substrates of the CPC (Chapter 3). One of these substrates, Rif1, caught our attention because its localization appeared to overlap with Aurora B in anaphase. However, in the course of studying Rif1 we revealed a thus far unrecognized function for this protein in maintaining genomic integrity through the resolution of Ultrafine-Fine DNA Bridges (UFBs) in anaphase, independent of Aurora B (Chapter 5). Here the results presented in this thesis are further discussed and directions for future research suggested.

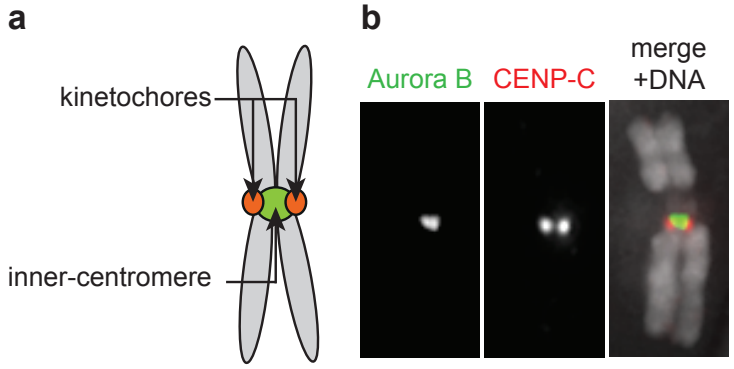

Figure 1l Centromere and kinetochores
a) Schematic representation of sister chromatids (grey), inner centromere (green) and kinetochores (red). **b)** Immunofluorescence, of Aurora B, CENP-C (red) and DAPI (DNA, gray) on a chromosome spread of a nocodazole treated HeLa cell. It shows the inner centromere localization of Aurora B in between the two kinetochores represented by CENP-C.

Inner centromere localization of the CPC is essential for chromosome bi-orientation in human cells

In Chapter 2 we investigated the importance of inner centromere localization of the CPC for chromosome segregation in human cells. We used a set-up in HeLa cells in which we knocked-down the endogenous CPC scaffold protein INCENP and replaced the endogenous protein by exogenously expressed INCENP variants. Deletion of the first 48 amino acids of INCENP (INCENP-ΔCEN) disrupts INCENP binding to survivin and borealin and the CPC can therefore not localize to the inner centromere [258]. Inner centromere localization was restored by either expressing wt-INCENP or a fusion protein consisting of survivin and INCENP-ΔCEN. While survivin contributes to inner centromere localization through a direct interaction with phosphorylated histone H3-T3 [159-161], it can also interact with borealin (independent of the CEN-box of INCENP) [257], which in turn can bind to phosphorylated histone H2A-T120, via a Shugoshin (SGO) intermediate [162, 163, 255]. We assume that the survivin-borealin interaction contributes the inner centromere localization of the survivin-INCENP fusion protein. Finally, expression of a CENP-B-INCENPΔCEN (CB-INCENP) fusion protein allowed us to position endogenous Aurora B away from the inner centromere and to cluster it closer to the kinetochore [144]. Using this knock-down/add-back approach we revealed that stable chromosome bi-orientation required the inner centromere localization of the CPC to protect centromeric cohesin. In early mitosis the bulk of cohesin is removed from the chromosomal arms by WAPL, but centromeric cohesin is protected from this removal through the localization of the cohesin protector SGO1 in complex with the protein phosphatase PP2A [377]. WAPL promotes cohesin removal when CDK1 and Aurora B phosphorylate its inhibitor sororin, and this phosphorylation is counteracted by SGO1-PP2A [44, 45, 53, 54]. Centromeric cohesin, protected by SGO1-PP2A, thus holds sister chromatids together until the metaphase to anaphase transition (Figure 2A), and not surprisingly siRNA mediated knock-down of SGO1 causes precocious sister chromatid separation in prometaphase [48, 49]. We found that weakened centromeric cohesin correlated with the absence of SGO1 from the inner centromere. Particularly, the observation that expression of CB-INCENP induced kinetochore localization of SGO1 as well as precocious sister chromatid separation upon attempted chromosome bi-orientation, suggested that proper protection of centromeric cohesin required the precise, inner centromere positioning of SGO1 (Figure 2B). This was further corroborated by experiments in which we forced inner centromere localization of exogenous SGO1 in CB-INCENP expressing cells and found that this improved chromosome bi-orientation. Moreover, combined with the finding that expression of a small N-terminal INCENP fragment (amino acids 1-63, also called CEN-box) could also improve chromosome bi-orientation in CB-INCENP expression cells, we inferred that the N-terminus of INCENP (which is absent in the CB-INCENP fusion protein) somehow provided spatial cues to position SGO1 at the inner centromere (Figure 2C).

How does the CPC regulate SGO1-dependent centromeric cohesin protection?

The localization of SGO1 to the kinetochore and inner centromere involves multiple (direct) protein interactions. First, a conserved C-terminal basic domain in SGO1 directly interacts with histone H2A that is phosphorylated by BUB1 on T120 [162, 163] and this interaction appears required for the kinetochore localization of SGO1 [378]. Second, SGO1 directly interacts with cohesin and this interaction involves the phosphorylation

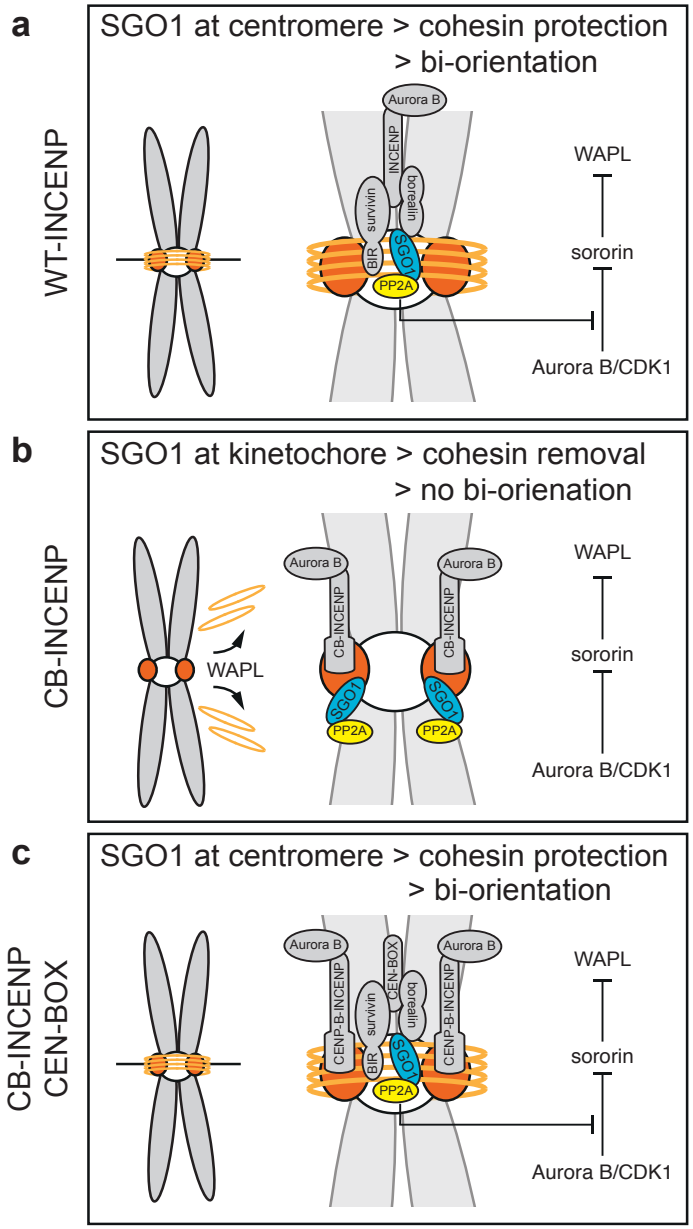

Figure 2l Inner centromere localization of the CPC is required for stable chromosome bi-orientation and protection of centromeric cohesin

a) Inner centromere localization of the CPC is required for the positioning of SGO1-PP2A at the inner centromere to protect centromeric cohesin and allow bi-orientation. Centromeric SGO1-PP2A counteracts mainly CDK1 and maybe Aurora B-mediated phosphorylation of sororin to keep sororin in a configuration to inhibit WAPL-dependent cohesin removal. **b)** Positioning of Aurora B away from the inner centromere by CB-INCENP delocalizes SGO1-PP2A from the inner centromere to the kinetochore. This allows sororin phosphorylation and WAPL activation. WAPL removes centromeric cohesin, which leads to impaired bi-orientation. **c)** The recruitment of the CEN-box of INCENP (and indirectly survivin and borealin) repositions SGO1-PP2A to the centromere in CB-INCENP expressing cells. This restores centromeric cohesin protection and chromosome bi-orientation.

of SGO1 at T346 by CDK1 [53, 265]. A SGO1 mutant rendered insensitive to CDK1-dependent phosphorylation (SGO1-T346A) did not localize to the inner centromere, but predominantly localized at kinetochores, and did not protect centromeric cohesin [265]. This suggested that the SGO1-cohesin interaction is needed for inner centromere localization of SGO1 and centromeric cohesin protection. In addition, heterochromatin protein 1 alpha (HP1α) has been suggested to promote the recruitment of SGO1 and the CPC to the inner centromere [266]. The chromoshadow domain (CSD) of HP1α binds to PxVxI/L motifs in SGO1, INCENP and borealin, whereas the chromodomain of HP1α recognizes tri-methylated histone H3K9 (H3K9me3) [379]. During mitosis the bulk of HP1α is removed from the chromatin by Aurora B-mediated phosphorylation of histone H3 on S10, because this interferes with the binding of the HP1α chromodomain to histone H3K9me3 [380, 381]. Yet despite this phosphorylation, HP1α remains present at centromeres during mitosis and this was suggested to contribute to the inner centromere localization of SGO1 and the CPC and to enable protection of centromeric cohesin [266, 382]. Moreover, Tanno *et al.* [266] showed a correlation between reduced levels of centromeric HP1α, SGO1 and CPC and chromosomal instability (CIN) in cancer cell lines. Remarkably, restoring the centromere levels of HP1α and SGO1 through expression of SUV39H, the methyltransferase that trimethylates histone H3K9, suppressed CIN in a number of CIN+ cell lines [266]. While this implies an important role for HP1α in localizing SGO1 to the inner centromere and as such for the protection of centromeric cohesin, these data stand in marked contrast to work from the lab of Hongtou Yu showing that a SGO1 mutant, defective in HP1α binding, localized normally to the inner centromere during mitosis and more importantly, rescued loss of centromeric cohesin in SGO1 knock-down cells [379]. Moreover, they demonstrated that the centromeric pool of HP1α was dependent on the PxVxI/L motif of INCENP. INCENP depletion or expression of an INCENP-ΔHP1 mutant completely abolished HP1α recruitment to the inner centromere [379]. Interestingly, since both INCENP and SGO1 bind to HP1α CSD domain via their respective PxVxI/L motifs, it is highly unlikely that the HP1α bound to INCENP can also bind SGO1 [379]. This implies that the inner centromere localization of SGO1 would be dependent on cohesin as well as on a pool of HP1α that binds to histone H3K9Me3 [266]. How the latter is possible given the high Aurora B-dependent histone H3 S10 phosphorylation at this location remains to be resolved. How does the CPC feed into the inner centromere recruitment of SGO1? For one, Aurora B kinase activity is required for SGO1 localization as inhibition of Aurora B activity or knock-down of INCENP causes the loss of SGO1 from the inner centromere/kinetochores and its dispersal over the chromosomal arms [168, 262] (Chapter 2). This is most likely explained by the loss of BUB1 from kinetochores and the consequent reduction in phosphorylation of histone H2A at T120 near the kinetochore [167, 168]. In line with this, expression of CB-INCENP in INCENP depleted cells rescued histone H2A phosphorylation and kinetochore localization of SGO1, but not its inner centromere localization. Although we have not yet formally demonstrated that SGO1 is recruited to the inner centromere when we express the INCENP N-terminus in the context of CB-INCENP, we deem it very likely that it will, given its positive effect on chromosome bi-orientation. Future studies are required to reveal how the CEN-box of INCENP contributes to the positioning of SGO1 at the inner centromere. An obvious hypothesis is that the reported direct interaction between borealin and SGO1 contributes to this [163], and it would therefore be interesting to express a CEN-box mutant defective in borealin binding [255]. However, a complicating factor is that SGO1 in turn contributes to the inner centromere localization of the CPC, and such a mutant might affect the localization of the CEN-box. Alternatively, since cohesin binding appears to be required

for inner centromere localization and cohesin protection by SGO1 [265], and a recent study suggested that SGO1 is first loaded on the kinetochore an then transferred to cohesin at the inner centromere by RNA polymerase II dependent transcription, the CEN-box of INCENP might contribute to this transfer [378].

Finally, our results also clarify why budding yeast does not require (inner) centromere localization of the CPC for chromosome bi-orientation [254]. The prophase pathway does not exist in budding yeast and hence Sgo1 is not required for the (centromeric) cohesin protection during budding yeast mitosis [383]. In line with this, centromeric CPC only fulfils a non-essential role in maintenance of cohesin in budding yeast because the Sli15-ΔNT mutant (the budding yeast analogue of INCENP-ΔCEN) was synthetically lethal with mutants of Mcm21 and Ctf19, subunits of the Ctf19 kinetochore complex which provide a non-essential function in centromeric cohesion, and with deletion of Ctf18, a non-essential mutant affecting cohesin establishment [254, 384, 385].

Does spatial separation of Aurora B from its kinetochore substrates explain tension-dependent stabilization of bi-orientated attachments?

The CPC promotes chromosome bi-orientation through specific destabilization of incorrectly attached kinetochores-microtubules (i.e. syntelic and merotelic attachments), a process referred to as error correction. However, bipolar or amphitelic attachments are stabilized and this translates into the question how the CPC discriminates between incorrectly (tension-less) and correct (tension-generating) kinetochore-microtubule attachments [251]. An answer was provided by the so-called “spatial separation” model: Upon bi-orientation, tension across the sister-kinetochores would spatially separate Aurora B at the inner centromere from its substrates at the outer-kinetochore [144, 146]. Indeed, displacing Aurora B from the inner centromere towards the kinetochore through expression of a CB-INCENP fusion protein, allowed detachment of incorrectly attached microtubules but failed to stabilize bipolar attachments [144]. However, in Chapter 2 we found that amphitelic attachments could be stabilized and the N-terminal tail of HEC1 dephosphorylated, in CB-INCENP expressing cells when cohesin removal was prevented by depletion of WAPL. This could mean that the main effect of displacing Aurora B from the inner centromere is loss of centromeric cohesin rather than continued phosphorylation of kinetochore substrates upon bi-orientation, as initially thought [144]. Through maintaining centromeric cohesin, inner centromere localized CPC would promote the build-up of tension upon bi-orientation, and tension in turn might directly stabilize attachments. This is not without precedent as Akiyoshi *et al.* [386] demonstrated that tension itself enhances the stability of kinetochore-microtubule interactions *in vitro*, using purified yeast kinetochore particles and a laser trap to apply mechanical tension. Still, purified kinetochores containing Aurora B phosphomimetic mutations in the N-terminal tail of Ndc80 (the yeast homolog of HEC1) resisted less tension compared to wild-type Ndc80-containing kinetochores, suggesting that tension may contribute to the stabilization of correct kinetochore-microtubule attachments both directly, and indirectly via an effect on Aurora B-dependent phosphorylation events [386, 387]. In case of the latter, kinetochore tension might somehow directly affect the kinetochore localization and activity of kinases and phosphatases or contribute to spatial separation of Aurora B from its outer-kinetochore substrates. It could very well be that despite the closer proximity of Aurora B to the kinetochore in the CB-INCENP

expressing cells, due to the presence of cohesin, sufficient tension may accumulate to pull the HEC1 N-terminal tail out of reach from Aurora B [88]. If true then WAPL depletion is expected to no longer rescue bi-orientation when Aurora B is placed even closer to the (outer) kinetochore. In this scenario, not single sister chromatids (due to cohesin loss) but paired sister chromatids may fall out of the metaphase plate as amphitelic attachments would be destabilized. We tried this by expressing Mis12-INCENP [144], but were unsuccessful due to the low expression levels of this fusion protein.

Another alternative for how tension could stabilize attachments is that kinetochore tension modifies the internal configuration of the kinetochore in such a way that it reduces the susceptibility of kinetochore substrates, including the N-terminal tail of HEC1, for Aurora B mediated phosphorylation [254]. This could be tested by acute recruitment of an active Aurora B/INCENP fusion protein [284] to the outer kinetochore at the moment that kinetochores are fully attached and under tension. This can be achieved using rapamycin-induced chemical dimerization of an outer FKBP-tagged-kinetochore protein and active FRB-tagged-Baronase [388]. A GFP-tagged protein that specifically localizes to unattached kinetochore such as GFP-MAD1 could be used as readout for the attachment status. If tension would indeed reduce the susceptibility of substrates for Aurora B-mediated phosphorylation, the kinetochores would remain attached to microtubules even when active Aurora B is recruited to the kinetochore when all sister chromatids are bi-polar attached.

Inner centromere localization of the CPC is required for mitotic checkpoint silencing

Unattached kinetochores signal to the mitotic checkpoint by producing an APC/C inhibitor, the MCC [6]. Upon attachment of the final kinetochore, the checkpoint is silenced and anaphase proceeds [389]. It has for long be a debate whether the mitotic checkpoint responds to the attachment status of kinetochore or to tension. Recent experiments in HeLa cells expressing a non-phosphorylatable HEC1 tail mutant that increased its affinity for microtubules, demonstrated that cells could silence the mitotic checkpoint in the absence of tension [268, 269]. This suggested that mere kinetochore-microtubule attachment suffices to silence the checkpoint. We were therefore surprised that the WAPL-depleted CB-INCENP expressing cells were dramatically delayed in metaphase as their kinetochores were stably, end-on attached to microtubules (Chapter 2).

The CPC promotes establishment of the mitotic checkpoint at the onset of mitosis by initiating the recruitment of MPS1 to HEC1 at the kinetochore [114, 176]. Subsequent MPS1-dependent phosphorylation of the KNL1 MELT and SHT motifs facilitates the kinetochore recruitment of additional checkpoint proteins including BUB1, BUB3, BUBR1, MAD1, MAD2 and CDC20, which all contribute to MCC assembly [116-120]. In addition, Aurora B antagonizes PP1γ recruitment to KNL1 by phosphorylation of its SILK-RVSF phosphatase-binding motif, and this ensures that the MELT/SHT motifs in KNL1 are not dephosphorylated [133, 147]. Silencing of the mitotic checkpoint is associated with the reversal of these phosphorylation events [133]. This is in part accomplished by microtubule-dependent removal of MPS1 from the kinetochore [130, 131]. Upon attachment, microtubules outcompete MPS1 for binding to the Calponin Homology

domain in HEC1 [130, 131]. In addition, PP2A bound to BUBR1 dephosphorylates the RVSF motif in KNL1 thereby allowing PP1γ recruitment, which in turn dephosphorylates the KNL1 MELT (and probably SHT) motifs [133]. We found that Aurora B-dependent phosphorylation of the RVSF phosphatase-binding motif in KNL was increased at bi-orientated sister chromatids in CB-INCENP expressing cells in which cohesin removal was prevented by depletion of WAPL. Since Aurora B is in closer proximity of KNL1 in the CB-INCENP expressing cells, it suggests that KNL1 needs to be spatially separated from Aurora B to allow its dephosphorylation and recruitment of PP1γ. Although, we did not provide direct evidence for reduced PP1γ recruitment, we did show a small but significant increase in the phosphorylation of KNL1-MELT and elevated kinetochore recruitment of BUB1 and MAD1. We did not yet determine the kinetochore levels of MPS1 at the fully aligned chromosomes in the WAPL-depleted CB-INCENP expressing cells. Since the phosphatase-binding motif in KNL1 was shown to be required for optimal microtubule-dependent delocalization of MPS1 [130] it could be that in the above-described conditions, some MPS1 might still be present on the attached kinetochores. It is important to mention that after a long (±264 min) metaphase delay, in 20% of the cells, the checkpoint was eventually silenced and cells entered anaphase. Recent studies demonstrated that the checkpoint has different “strengths” depending the number of unattached kinetochores that elicit the checkpoint signal [390, 391]. Although we found an increase in MAD1 levels at all the aligned chromosomes in comparison to control metaphases, these MAD1 levels were reduced compared to cells in which all kinetochores were unattached (nocodazole condition), most likely explaining why the checkpoint is “weaker” than in for instance nocodazole treated cells.

Our data suggest that kinetochore-microtubule attachments are not sufficient to silence the checkpoint when Aurora B is still in reach of KNL1. We propose that under normal conditions (i.e. when Aurora B is localized at the inner centromere), tension across kinetochores promotes the separation of KNL1 from Aurora B. This would ensure that checkpoint silencing occurs after chromosome bi-orientation and implies that efficient checkpoint silencing requires tension.

Analog sensitive Aurora B can be specifically inhibited by analog sensitive kinase inhibitors

Timely inhibition of the CPC is essential to dissect the various functions of the CPC during different stages of cell division. This cannot be accomplished by siRNA mediated knock-down approaches of the CPC subunits but requires highly specific, fast-acting cell-permeable inhibitors of the enzymatic subunit of the complex, Aurora B. Although at least 4 different small molecule inhibitors (ZM447439, Hesperadin, AZD1152-HQPA and GSK1070916) of Aurora B exist, their efficiency and specificity varies [392]. Moreover, in the presence of the highly similar Aurora A and C kinases it is rather difficult to identify Aurora B specific small molecule inhibitors [392]. Therefore we generated an analog-sensitive Aurora B mutant to specifically inhibit Aurora B and to identify potential novel substrates of the kinase (Chapter 3). The first step in generating an analog sensitive mutant kinase is to identify the so-called gatekeeper residue, which is a bulky amino acid (i.e. methionine, leucine, phenylalanine, or threonine) in the kinase active site that makes direct contact with the N6 group of ATP [277, 278]. This residue can be mutated into a smaller amino acid such as alanine or glycine to create an enlarged

ATP-binding pocked. The mutated kinase, termed an analog-sensitive (as) kinase, is accessible and can be specifically inhibited by reversible cell-permeable bulky ATP analogs [279]. Aurora B turned out to be one of the kinases that did not tolerate mutation of its gatekeeper residue (Leu-154) into either alanine or glycine [280, 282]. Therefore we needed to identify a second site suppressor mutation that restored kinase activity of the Aurora-B^{L154A} and Aurora-B^{L154G} mutants. In line with human Aurora B, also the yeast homologs of Aurora B (Ipl1 in *Saccharomyces cerevisiae* and Ark1 in *Schizosaccharomyces pombe*) do not tolerate mutation of the gatekeeper residue and a second site suppressor mutation was identified [285, 286]. However, according to multiple sequence alignments mammalian Aurora B already carries the optimal residue at that position. In addition, for several kinases that did not tolerate mutation of its gatekeeper residue, second-site suppressor mutations were identified [280]. Several second site suppressor mutations were found in the conserved kinase domains and led to a predication model for rescuing kinase activity of intolerant kinases [280]. Unfortunately, none of the predictions could be applied to Aurora B and we needed an alternative. In a study of Girdler *et al.* [287] Aurora B mutants were identified that caused resistance to the Aurora B kinase inhibitor ZM447439. One of these mutations, H250Y, which is in close proximity of the activation loop of Aurora B, rendered the kinase hyperactive and we hypothesized that this mutation might function as a second site suppressor mutation for our gatekeeper mutants. Multiple sequence alignment demonstrated that Ipl1 has a tyrosine residue at this position. Aurora-B$^{L154A/H250Y}$ appeared as active as wild-type Aurora B when immunoprecipitated from mitotic cells. More importantly, the bulky ATP analog NA.PP1 could specifically inhibit this mutant. Overexpressed Aurora B$^{L154A/H250Y}$ localized similar as overexpressed wild-type Aurora B to the inner centromere. However, unlike wild-type Aurora B, it behaved in a dominant negative fashion in the presence of low concentrations of NA.PP1. Aurora$^{L154G/H250Y}$ appeared only partially active but could utilize bulky ATP analogs to phosphorylate substrates. Although our studies suggest that the analog-sensitive mutants (in particular Aurora B$^{L154A/H250Y}$) behave as wild-type Aurora B, we cannot be 100% sure that kinase function is fully restored and that these mutations do not affect for instance substrate specificity. Since the functional assays were performed in the presence of endogenous Aurora B, Aurora B$^{L154A/H250Y}$ and Aurora B$^{L154G/H250Y}$ should be expressed in an Aurora B knock-down or knock-out background to establish whether these mutants can complement for the loss of endogenous Aurora B. If they can, it would be interesting to introduce these mutations into the endogenous Aurora B locus using CRISPR (Clustered Regularly Interspaced Short Palindromic Repeats)/Cas9 genome editing [393]. This would provide us with cell lines in which we might efficiently and specifically inhibit Aurora B.

Thiophosphorylation of proteins in whole cell extracts using analog sensitive Aurora B

The Aurora B$^{L154G/H250Y}$ mutant kinase could use bulky N6-alkylated ATPγS analogs to thiophosphorylate substrates in cell extracts (Chapter 3). Since wild-type kinases cannot utilize these bulky ATPγS analogs, this can be used as a unique tool to specifically label and identify substrates [281]. We co-purified recombinant His-tagged INCENP with GST-tagged Aurora B$^{L154G/H250Y}$ from *Spodoptera frugiperda* (SF9) cells to thiophosphorylate proteins in HeLa mitotic cell extracts. By covalent capture and release of thiophosphorylated peptides followed by mass spectrometry we identified

58 novel Aurora B substrates. We found that 71% of the identified phosphopeptides harbored an Aurora B phosphorylation consensus sequence, which indicated that the *in vitro* labeling was reliable and suggested that Aurora $B^{L154G/H250Y}$ did not lose substrate specificity. However, because, Aurora A, B and C tend to phosphorylate overlapping peptide consensus sequences, it might be that Aurora $B^{L154G/H250Y}$ also phosphorylate substrates of the other Aurora kinases *in vitro*.

To our surprise, we did not identify well-characterized Aurora B kinetochore substrates, such as HEC1. Since the kinase reactions were performed in complex cell lysates and because recombinant INCENP/Aurora $B^{L154G/H250Y}$ is not localized, this could influence the efficiency and specificity of substrate phosphorylation. Labeling of mitotic chromatin-enriched fractions could be an alternative method to identify less abundant Aurora B kinetochore substrates. Alternatively, a more sophisticated and complex way would be to thiophosphorylate Aurora B substrates in cells in which the L154G/H250Y mutations are introduced into the endogenous Aurora B locus and the bulky ATPγS analogs are offered by mild permeabilization of the plasma membrane [394]. Finally, since we labeled mitotic cell extracts, we also considered the possibility that relevant substrates were already phosphorylated by endogenous Aurora B and that this could interfere with the *in vitro* thiophosphorylation reaction by Aurora $B^{L154G/H250Y}$. We therefore performed experiments in which cells were treated with an Aurora B kinase inhibitor prior to cell lyses to allow dephosphorylation of substrates. However, despite extensive dialysis of the cell extract to remove the inhibitor, *in vitro* labeling reactions were much less efficient, suggesting that we were unable to get rid of the kinase inhibitor. To circumvent the use of an inhibitor we therefore highly over-expressed INCENP-ΔCEN to sequester endogenous Aurora B away from centromeres and central spindle [258], however labeling of cell extracts derived from INCENP-ΔCEN expressing cells did not yield kinetochore substrates. Instead, increasing the input concentration of recombinant INCENP-Aurora $B^{L154G/H250Y}$ kinase identified less abundant known kinetochore substrates such as HEC1 [82, 145], sororin [45, 192] and SGO2 [208] (data not shown). For now, the major challenge is to validate all potential novel substrates as Aurora B targets and to understand the physiological relevance of these phosphorylation events. Many of the identified substrates are highly abundant and described to fulfill functions outside of mitosis. This could mean that Aurora B also has non-canonical functions outside mitosis, or that the potential substrates fulfill non-canonical roles during mitosis. An siRNA-mediated knock-down screen in combination with live cell video microscopy would be an initial filter to discriminate which potential substrates are fulfilling functions during mitosis.

HMGN2 is a *bona fide* Aurora B substrate

To prove that we identified novel Aurora B substrates we validated the phosphorylation of HMGN2 *in vivo* (Chapter 3). HMGN2 binds to nucleosomes and reduces chromatin compaction and probably promotes gene expression [303, 395]. HMGN2 is phosphorylated during mitosis and this coincides with its release from nucleosomes [298]. HMGN2 re-associates with chromatin during anaphase, when the CPC translocate from the inner centromere to the central spindle. We confirmed that the *in vitro* phosphorylated residues (Ser-25 and Ser-29) in the nucleosomal binding domain of HMGN2 were also phosphorylated by Aurora B *in vivo*. Moreover, inhibition of Aurora

B prevented the release of HMGN2 from chromatin in mitosis, and artificial chromatin-tethering of Aurora B in anaphase by expression of an H2B-INCENP fusion protein perturbed the re-association of HMGN2 (Figure 3). Our work thus revealed that Aurora B is responsible for the dissociation of HMGN2 from nucleosomes during mitosis. HMGN2 is a member of the high mobility group chromosomal proteins, and thus far five HMGN (HMGN1-HMGN5) proteins have been identified that share a similar nucleosomal binding domain. In our combined published and unpublished screens we identified all five HMGN proteins as potential Aurora B substrates (Chapter 3 and data not shown). The physiological relevance of the Aurora B-dependent chromatin release of HMNG2 (and most likely also of the other HMGN family members) is currently unknown. Analysis of mitotic progression in cells that express non-phosphorylatable mutants of the HMNG proteins would provide insight in the possible mitotic defects induced by maintained binding of HMGN proteins to nucleosomes. Since HMNG proteins are described to open the chromatin structure [395], a likely hypothesis is that the release of HMGN 1-5 contributes to proper chromosome condensation during mitosis.

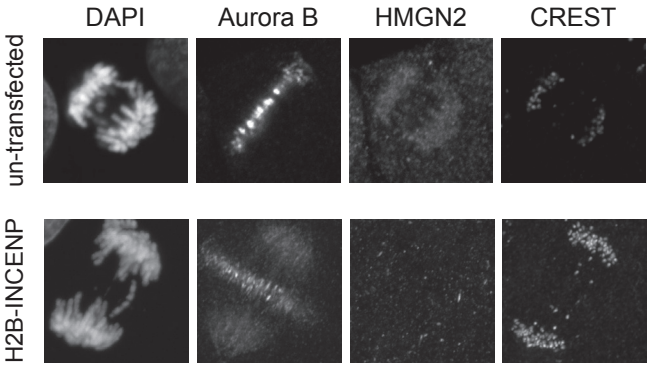

Figure 3l Chromatin-tethering of Aurora B perturb re-association of HMGN2 during anaphase
U2OS cells transfected with H2B-INCENP and subjected to immunofluorescence of HMGN2, Aurora B and CREST (to label kinetochores). DNA was visualized by DAPI staining.

Rif1, a novel Aurora B substrate?

In the screen that identified HMGN2 as an Aurora B substrate, we also identified Rif1 as a potential substrate (Chapter 3). Rif1 raised our interest because the phosphorylated residue appeared to be located in a (SILK-RVSF) protein phosphatase-binding motif. And we reasoned that similar to phosphorylation of the SILK-RVSF motif in KNL1 [147], phosphorylation of this binding motif in Rif1 would disturb the Rif1-PP1 interaction. Moreover, at that time Rif1 was described to localize to microtubules of the central spindle in anaphase in close proximity of Aurora B [355]. However, when we studied the anaphase localization of Rif1 in more detail we found that Rif1 was not recruited to microtubules but to UFBs (Chapter 5). This novel finding, combined with the fact that the *in vivo* validation of Aurora B-mediated Rif1 phosphorylation turned out to be not straightforward (discussed later), prompted us to focus on the role of Rif1 in the resolution UFBs during anaphase.

Rif1 is required for UFB resolution

Centromeric DNA catenanes form UFBs in early anaphase, which are actively resolved by the action of Topoisomerase IIα (TOPOIIα) and specialized UFB binding proteins

such as the DNA translocase PICH and the BTRR complex (Bloom's Syndrome RecQ-like DNA helicase (BLM), Topoisomerase IIIα and RecQ-Mediated Genome Instability 1 and 2 (RMI1 and RMI2)) [306, 311, 312, 316, 317, 319]. Additionally, when replication stress is induced, incompletely replicated DNA loci arise at Common Fragile Sites (CFSs), which are actively processed before anaphase onset [307, 331]. However, when processing in prometaphase fails, under-replicated DNA becomes visible in anaphase as CFS-derived UFBs (Chapter 4). We found that Rif1 was recruited to both centromeric and CFS-derived UFBs and that its localization to UFBs required PICH (Chapter 5). Unfortunately, we were unable to determine a specific region in PICH that was required for the recruitment of Rif1 to UFBs. In co-immunoprecipitation experiments we found that the N- and C-terminal TPR domains of PICH were required to interact with Rif1, yet these domains appeared dispensable for Rif1 recruitment to UFBs. Since PICH functions as a DNA translocase [315], it might remodel the DNA at UFBs and this could be the trigger to recruit Rif1 without direct binding to PICH. If true, knock-down of endogenous PICH and add-back of a translocase-dead (K128A, [306]) PICH mutant is expected to perturb Rif1 recruitment.

While catenane-derived UFBs predominantly contain double stranded (ds) DNA, UFBs derived from under-replicated CFS loci are mainly single stranded [311, 367]. This is corroborated by the fact that next to PICH, BLM and Rif1, these CFS-derived UFBs also recruit the single stranded DNA binding protein RPA70 [367]. Interestingly, we found that inhibition of TOPOIIα at anaphase onset promoted massive appearance of RPA70-positive UFBs, suggesting that formation of ssDNA containing UFBs can also be a consequence of impaired resolution of double stranded centromeric DNA catenanes (Chapter 5). Knock-down of Rif1 also led to an elevation of RPA70-positive UFBs, independent of replication stress, and this implied a role for Rif1 in the resolution of UFB resolution during anaphase. Defects associated with impaired UFB resolution, such as an increase in DNA bridges, micronuclei and 53BP1-positive nuclear bodies in G1 in the absence of Rif1 further supported this hypothesis. Possible mechanisms by which Rif1 might contribute to the resolution of UFBs are discussed below.

The formation of RPA-70-postive UFBs is BLM dependent

As mentioned above, RPA70-positive UFBs are formed upon TOPOIIα inhibition, Rif1 depletion or failed processing of under replicated CFSs [317, 367]. These UFBs therefore most likely contain single stranded DNA. RPA70-positive UFBs disappear in late anaphase or telophase, but it is currently unclear whether this is due to physical breakage of the RPA70-positive UFBs caused by the forces exerted by the segregating chromosomes, or due to active resolution. UFBs that either contain double or single stranded DNA possibly require different mechanisms for their resolution: UFBs containing dsDNA are known to require TOPOIIα for their resolution (Figure 4A) [311], however UFBs containing single stranded DNA might be resolved by Topoisomerase IIIα (TOPOIIIα) [312], an enzyme that catalyzes the transient breaking and joining of single stranded DNA (Figure 4B). In line with this, we found that TOPOIIIα was efficiently recruited to UFBs when TOPOIIα was inhibited (unpublished data). Because specific TOPOIIIα inhibitors are not yet available, it remains difficult to test whether TOPOIIIα is indeed required for the resolution of RPA70-positive UFBs. Interestingly, formation of RPA70-positive UFBs upon TOPOIIα inhibition is dependent on BLM (Chapter 5)

(Figure 4B), and Chan *et al.* [312] showed that TOPOIIIα recruitment to UFBs occurred downstream of BLM. This may infer that BLM could mediate a switch from double stranded to single stranded UFBs, and it would be informative to test whether BLM helicase activity is required for this possible conformation. If true, this could either mean that resolution of UFBs derived from dsDNA catenanes involves a transient step where dsDNA is converted to ssDNA, or that the formation and resolution of single stranded UFBs only serves as a back-up mechanism when double stranded (i.e. TOPOIIα-mediated) UFB resolution is impaired. Of note, since we observed that RPA70 was preferentially recruited to longer UFBs we cannot exclude the possibility that double stranded UFBs under high tension may adopt alternative DNA confirmations that allow an interaction with RPA70.

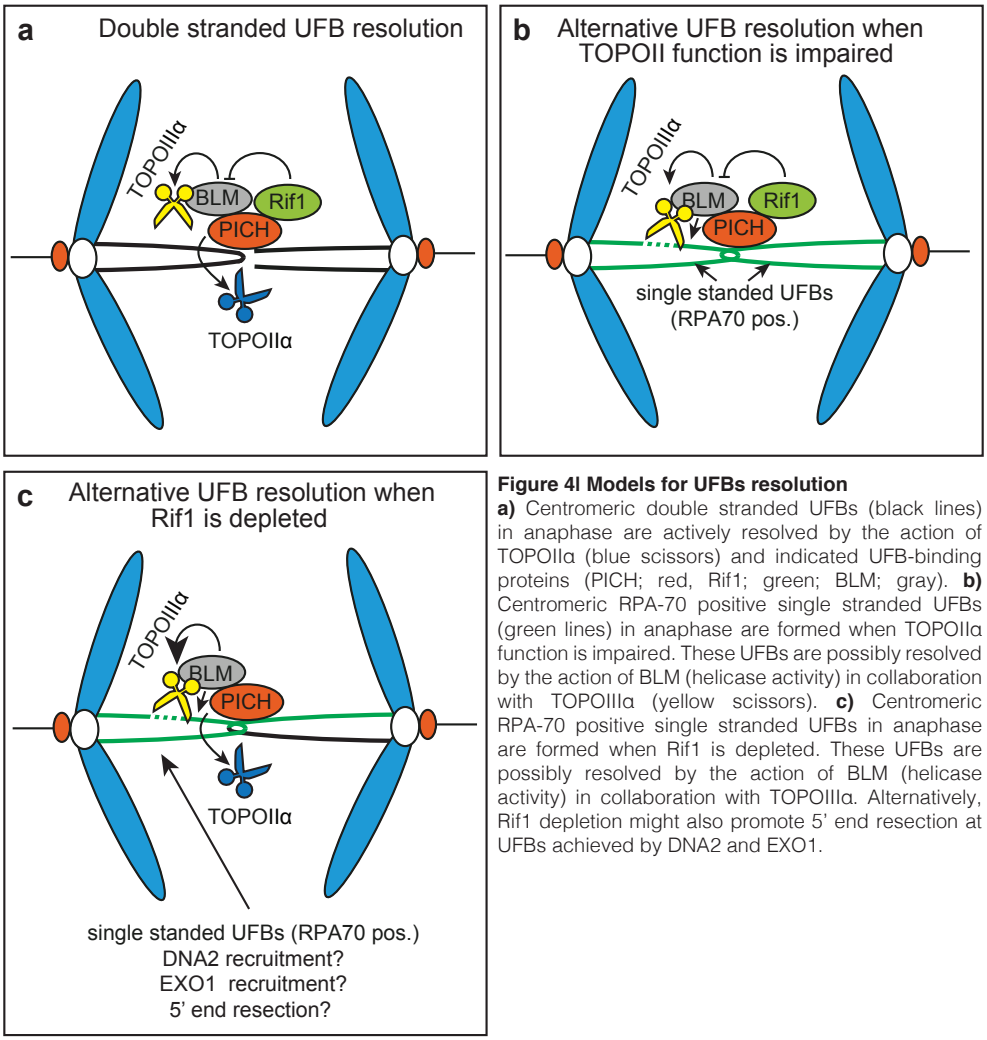

Figure 4l Models for UFBs resolution
a) Centromeric double stranded UFBs (black lines) in anaphase are actively resolved by the action of TOPOIIα (blue scissors) and indicated UFB-binding proteins (PICH; red, Rif1; green; BLM; gray). **b)** Centromeric RPA-70 positive single stranded UFBs (green lines) in anaphase are formed when TOPOIIα function is impaired. These UFBs are possibly resolved by the action of BLM (helicase activity) in collaboration with TOPOIIIα (yellow scissors). **c)** Centromeric RPA-70 positive single stranded UFBs in anaphase are formed when Rif1 is depleted. These UFBs are possibly resolved by the action of BLM (helicase activity) in collaboration with TOPOIIIα. Alternatively, Rif1 depletion might also promote 5' end resection at UFBs achieved by DNA2 and EXO1.

How Rif1 might contribute to the resolution of UFBs

How Rif1 contributes to the resolution of UFBs is unclear. Our initial and in part unpublished data showed that in Rif1-depleted cells the number of PICH-positive

UFBs during early anaphase was reduced, while the number of RPA70-positive UFBs in late anaphase increased. Together with the observed requirement for BLM in the formation of RPA70-positive UFBs, this could suggest that Rif1 regulates BLM function and indirectly controls the switch from PICH-positive, RPA70-negative double stranded UFBs to PICH-negative, RPA70-positive single stranded UFBs (Figure 4C). Although the physical interaction between Rif1 and the BTRR complex appears to be required for BLM localization to stalled replication forks during interphase [363], we found that Rif1 does not control the localization of BLM to UFBs. However, it might be that Rif1 interacts with BLM on UFBs and that this interaction inhibits BLM helicase activity to stall the formation of single stranded UFBs and promoting resolution via TOPOIIα.
Alternatively, the role of Rif1 at UFBs might be linked to its known function in DNA damage repair. Rif1 was shown to promote DNA damage repair in G1 via non-homologous end joining by preventing 5' end resection, a first step of homologous recombination [342-345]. Rif1 recruitment to DNA damage foci is dependent on ATM kinase and 53BP1. During DNA damage, 53BP1 binds directly to nucleosomes in which histone H2A at lysine 15 is ubiquitinated and histone H4 at lysine 20 is methylated [396]. This probably explains why 53BP1 is not recruited to histone-free UFBs [306, 311, 312]. At DNA damage loci, Rif1 inhibits the recruitment of BRCA1, a promoter of homologous recombination-directed repair [343-345]. BRCA1 in turn is localized to DNA damage foci during S/G2 phase and prevents the recruitment of Rif1. These proteins are thus required to ensure the choice between non-homologous end-joining and homologous recombination in G1 and S/G2 phase respectively. Homologous recombination requires BLM and the nuclease activities of DNA Replication Helicase/Nuclease 2 (DNA2) and Exonuclease 1 (EXO1) for 5' end resection [397]. 5' end resection results in the formation of ssDNA that is coated by RPA70. Exactly how Rif1 antagonizes 5' end resection is unclear. Since we found that RPA70 is recruited to unprocessed centromeric UFBs, i.e. upon TOPOIIα inhibition (Chapter 5), it would be interesting to test whether, similar to its function in DNA damage repair, Rif1 also protects UFBs from 5' end resection, independent of 53BP1 (Figure 4C). This could be demonstrated by co-depletion of Rif1 and factors involved in 5' end resection (DNA2 and EXO1), which should rescue the formation of Rif1 knock-down induced RPA70-positive UFBs in late anaphase. In addition, whether DNA2 and EXO1 localize to UFBs when UFB resolution is impaired will be interesting to investigate. Although PICH is not recruited to DNA damage sites during interphase, it might act as a unique platform for the recruitment of proteins involved in DNA processing (i.e. proteins that in interphase require modified histones for their recruitment to DNA damage foci) to histone free UFBs. The identification of additional PICH binding proteins via immunoprecipitations in combination with mass spectrometry might help to gain insight into the mechanism(s) of UFB resolution during anaphase.

Rif1 and Aurora B

As mentioned, we identified Rif1 as a potential Aurora B substrate in our *in vitro* substrate screen. The S2205 residue that we found phosphorylated lies in the RVSF motif, the phosphatase-binding domain of Rif1, and similar to phosphorylation of this motif in KNL1 we predict that it would also interfere with the Rif1-PP1γ interaction [147]. Until now we do not have data to support PP1γ recruitment to UFBs and whether Aurora B-dependent phosphorylation of the PP1γ-binding domain of Rif1 occurs *in vivo*. However, quantitative phosphoproteomics screens identified this site as phosphorylated

in vivo during mitosis [210, 398]. Inhibition of Aurora B kinase activity at anaphase onset affects the hypercondensation of chromosomal arms, impairs central spindle formation and completion of cytokinesis [374]. This made analysis of Rif1 and PP1γ localization on UFBs and measurements of UFB resolution efficiency in the absence of Aurora B kinase activity difficult. Furthermore, replacement assays in which endogenous Rif1 is replaced by a Rif1 mutant defective in PP1γ binding are needed to evaluate the contribution of the Rif1-PP1γ interaction in mitosis and at UFBs. If we consider the latter, why should Aurora B antagonize PP1γ recruitment at UFBs? During early anaphase many UFBs are in close proximity of the spindle midzone. PLK1 and Aurora B kinase activity is required to establish the spindle midzone and to promote cleavage furrow ingression [276]. A high concentration of PP1γ activity close to the spindle midzone might interfere with these PLK1 and Aurora B dependent phosphorylation events and should therefore be antagonized by Aurora B. Additionally, during late cytokinesis when the CPC is localized at the midbody, Aurora B imposes an abscission delay and prevents furrow regression, and thereby tetraploidization, when a lagging chromosome or chromosome bridge is still present in the midzone (referred to as the abscission checkpoint) [399]. Moreover, in cells without chromosome bridges chemical inhibition of Aurora B accelerates abscission, suggesting that Aurora B activity has to drop below a certain threshold to initiate abscission. Interestingly, UFBs can also delay abscission [319, 351, 400]. In PICH-/- HeLa cells bi-nucleated cells were observed which is indicative for abscission failure [319]. In budding yeast impaired UFB resolution due to a deletion of TopBP1/Dpb11, resulted in an abscission delay [351]. If Rif1 would recruit PP1γ to these late UFBs, PP1γ activity might inactivate the Aurora B-dependent abscission checkpoint. However, Aurora B-dependent release of PP1γ from Rif1 would prevent this from happening. Future research is needed to demonstrate how UFBs can activate the abscission checkpoint and whether Aurora B dependent phosphorylation of Rif1 is involved in this process.

Concluding remarks

The work presented in this thesis provides new insights into the regulation of chromosome bi-orientation, sister chromatid disjunction and faithful chromosome segregation during mitosis. We demonstrate that inner centromere localization of the CPC is required for centromeric cohesin protection and silencing of the mitotic checkpoint upon chromosome bi-orientation. Moreover, we generated a chemical genetic tool to specifically inhibit Aurora B and that identified novel CPC substrates. Lastly, we revealed a thus far unknown function of Rif1 in the resolution of UFBs during anaphase. Interestingly, Passerini *et al.* [401] recently published that mild aneuploidy, which can be caused by erroneous chromosome segregation, induces DNA replication defects, due to impaired expression of the replicative helicase MCM2-7 subunits. The mechanism behind the down regulation of this replication factor remains to be established. Remarkably however, one extra chromosome was sufficient to cause genomic instability by impairing DNA replication and by increasing the formation of UFBs, providing an explanation for how aneuploidy can cause structural chromosomal aberrations [11]. Our work contributes to the understanding of both chromosome segregation fidelity and UFB resolution and thereby on the maintenance of genomic integrity.

Addendum

References
Samenvatting in het Nederlands
Curriculum Vitae
List of publications
Dankwoord

References

1. Holland, A.J. and D.W. Cleveland, Boveri revisited: chromosomal instability, aneuploidy and tumorigenesis. Nat Rev Mol Cell Biol, 2009. 10(7): p. 478-87.
2. Lindqvist, A., V. Rodriguez-Bravo, and R.H. Medema, The decision to enter mitosis: feedback and redundancy in the mitotic entry network. J Cell Biol, 2009. 185(2): p. 193-202.
3. Tanenbaum, M.E. and R.H. Medema, Mechanisms of centrosome separation and bipolar spindle assembly. Dev Cell, 2010. 19(6): p. 797-806.
4. Tanaka, T.U., M.J. Stark, and K. Tanaka, Kinetochore capture and bi-orientation on the mitotic spindle. Nat Rev Mol Cell Biol, 2005. 6(12): p. 929-42.
5. Heald, R. and A. Khodjakov, Thirty years of search and capture: The complex simplicity of mitotic spindle assembly. J Cell Biol, 2015. 211(6): p. 1103-11.
6. Kops, G.J., B.A. Weaver, and D.W. Cleveland, On the road to cancer: aneuploidy and the mitotic checkpoint. Nat Rev Cancer, 2005. 5(10): p. 773-85.
7. Fededa, J.P. and D.W. Gerlich, Molecular control of animal cell cytokinesis. Nat Cell Biol, 2012. 14(5): p. 440-7.
8. Thompson, S.L., S.F. Bakhoum, and D.A. Compton, Mechanisms of chromosomal instability. Curr Biol, 2010. 20(6): p. R285-95.
9. Ricke, R.M., J.H. van Ree, and J.M. van Deursen, Whole chromosome instability and cancer: a complex relationship. Trends in genetics : TIG, 2008. 24(9): p. 457-66.
10. Janssen, A., et al., Chromosome segregation errors as a cause of DNA damage and structural chromosome aberrations. Science, 2011. 333(6051): p. 1895-8.
11. Sheltzer, J.M., et al., Aneuploidy drives genomic instability in yeast. Science, 2011. 333(6045): p. 1026-30.
12. Schvartzman, J.M., R. Sotillo, and R. Benezra, Mitotic chromosomal instability and cancer: mouse modelling of the human disease. Nat Rev Cancer, 2010. 10(2): p. 102-15.
13. Bornens, M., The centrosome in cells and organisms. Science, 2012. 335(6067): p. 422-6.
14. Ferenz, N.P., A. Gable, and P. Wadsworth, Mitotic functions of kinesin-5. Semin Cell Dev Biol, 2010. 21(3): p. 255-9.
15. Kapitein, L.C., et al., The bipolar mitotic kinesin Eg5 moves on both microtubules that it crosslinks. Nature, 2005. 435(7038): p. 114-8.
16. Tanenbaum, M.E., et al., Kif15 cooperates with eg5 to promote bipolar spindle assembly. Curr Biol, 2009. 19(20): p. 1703-11.
17. Vanneste, D., et al., The role of Hklp2 in the stabilization and maintenance of spindle bipolarity. Curr Biol, 2009. 19(20): p. 1712-7.
18. Raaijmakers, J.A., et al., Nuclear envelope-associated dynein drives prophase centrosome separation and enables Eg5-independent bipolar spindle formation. EMBO J, 2012. 31(21): p. 4179-90.
19. Sharp, D.J., et al., Functional coordination of three mitotic motors in Drosophila embryos. Mol Biol Cell, 2000. 11(1): p. 241-53.
20. Cytrynbaum, E.N., et al., Early spindle assembly in Drosophila embryos: role of a force balance involving cytoskeletal dynamics and nuclear mechanics. Mol Biol Cell, 2005. 16(10): p. 4967-81.
21. Ferenz, N.P., et al., Dynein antagonizes eg5 by crosslinking and sliding antiparallel microtubules. Curr Biol, 2009. 19(21): p. 1833-8.
22. Khodjakov, A., et al., Centrosome-independent mitotic spindle formation in vertebrates. Curr Biol, 2000. 10(2): p. 59-67.
23. Khodjakov, A. and C.L. Rieder, Centrosomes enhance the fidelity of cytokinesis in vertebrates and are required for cell cycle progression. J Cell Biol, 2001. 153(1): p. 237-42.
24. Sir, J.H., et al., Loss of centrioles causes chromosomal instability in vertebrate somatic cells. J Cell Biol, 2013. 203(5): p. 747-56.
25. Nasmyth, K., Cohesin: a catenase with separate entry and exit gates? Nat Cell Biol, 2011. 13(10): p. 1170-7.
26. Waizenegger, I.C., et al., Two distinct pathways remove mammalian cohesin from chromosome arms in prophase and from centromeres in anaphase. Cell, 2000. 103(3): p. 399-410.
27. Haarhuis, J.H., et al., WAPL-mediated removal of cohesin protects against segregation errors and aneuploidy. Curr Biol, 2013. 23(20): p. 2071-7.
28. Nasmyth, K. and C.H. Haering, The structure and function of SMC and kleisin complexes. Annu Rev Biochem, 2005. 74: p. 595-648.
29. Peters, J.M., A. Tedeschi, and J. Schmitz, The cohesin complex and its roles in chromosome biology. Genes Dev, 2008. 22(22): p. 3089-114.
30. Ciosk, R., et al., Cohesin's binding to chromosomes depends on a separate complex consisting of Scc2 and Scc4 proteins. Mol Cell, 2000. 5(2): p. 243-54.

31. Bernard, P., et al., A screen for cohesion mutants uncovers Ssl3, the fission yeast counterpart of the cohesin loading factor Scc4. Curr Biol, 2006. 16(9): p. 875-81.
32. Chao, W.C., et al., Structural Studies Reveal the Functional Modularity of the Scc2-Scc4 Cohesin Loader. Cell Rep, 2015. 12(5): p. 719-25.
33. Gruber, S., et al., Evidence that loading of cohesin onto chromosomes involves opening of its SMC hinge. Cell, 2006. 127(3): p. 523-37.
34. Buheitel, J. and O. Stemmann, Prophase pathway-dependent removal of cohesin from human chromosomes requires opening of the Smc3-Scc1 gate. EMBO J, 2013. 32(5): p. 666-76.
35. Murayama, Y. and F. Uhlmann, DNA Entry into and Exit out of the Cohesin Ring by an Interlocking Gate Mechanism. Cell, 2015. 163(7): p. 1628-40.
36. Kueng, S., et al., Wapl controls the dynamic association of cohesin with chromatin. Cell, 2006. 127(5): p. 955-67.
37. Gandhi, R., P.J. Gillespie, and T. Hirano, Human Wapl is a cohesin-binding protein that promotes sister-chromatid resolution in mitotic prophase. Curr Biol, 2006. 16(24): p. 2406-17.
38. Chan, Y.W., et al., Aurora B controls kinetochore-microtubule attachments by inhibiting Ska complex-KMN network interaction. The Journal of cell biology, 2012. 196(5): p. 563-71.
39. Ivanov, D., et al., Eco1 is a novel acetyltransferase that can acetylate proteins involved in cohesion. Curr Biol, 2002. 12(4): p. 323-8.
40. Rolef Ben-Shahar, T., et al., Eco1-dependent cohesin acetylation during establishment of sister chromatid cohesion. Science, 2008. 321(5888): p. 563-6.
41. Rowland, B.D., et al., Building sister chromatid cohesion: smc3 acetylation counteracts an antiestablishment activity. Mol Cell, 2009. 33(6): p. 763-74.
42. Unal, E., et al., A molecular determinant for the establishment of sister chromatid cohesion. Science, 2008. 321(5888): p. 566-9.
43. Nishiyama, T., et al., Sororin mediates sister chromatid cohesion by antagonizing Wapl. Cell, 2010. 143(5): p. 737-49.
44. Dreier, M.R., M.E. Bekier, 2nd, and W.R. Taylor, Regulation of sororin by Cdk1-mediated phosphorylation. J Cell Sci, 2011. 124(Pt 17): p. 2976-87.
45. Nishiyama, T., et al., Aurora B and Cdk1 mediate Wapl activation and release of acetylated cohesin from chromosomes by phosphorylating Sororin. Proc Natl Acad Sci U S A, 2013. 110(33): p. 13404-9 .
46. Hauf, S., et al., Dissociation of cohesin from chromosome arms and loss of arm cohesion during early mitosis depends on phosphorylation of SA2. PLoS Biol, 2005. 3(3): p. e69.
47. Sumara, I., et al., The dissociation of cohesin from chromosomes in prophase is regulated by Polo-like kinase. Mol Cell, 2002. 9(3): p. 515-25.
48. McGuinness, B.E., et al., Shugoshin prevents dissociation of cohesin from centromeres during mitosis in vertebrate cells. PLoS Biol, 2005. 3(3): p. e86.
49. Salic, A., J.C. Waters, and T.J. Mitchison, Vertebrate shugoshin links sister centromere cohesion and kinetochore microtubule stability in mitosis. Cell, 2004. 118(5): p. 567-78.
50. Kitajima, T.S., et al., Shugoshin collaborates with protein phosphatase 2A to protect cohesin. Nature, 2006. 441(7089): p. 46-52.
51. Riedel, C.G., et al., Protein phosphatase 2A protects centromeric sister chromatid cohesion during meiosis I. Nature, 2006. 441(7089): p. 53-61.
52. Tang, Z., et al., PP2A is required for centromeric localization of Sgo1 and proper chromosome segregation. Dev Cell, 2006. 10(5): p. 575-85.
53. Liu, H., S. Rankin, and H. Yu, Phosphorylation-enabled binding of SGO1-PP2A to cohesin protects sororin and centromeric cohesion during mitosis. Nat Cell Biol, 2013. 15(1): p. 40-9.
54. Hara, K., et al., Structure of cohesin subcomplex pinpoints direct shugoshin-Wapl antagonism in centromeric cohesion. Nat Struct Mol Biol, 2014. 21(10): p. 864-70.
55. Nicklas, R.B. and S.C. Ward, Elements of error correction in mitosis: microtubule capture, release, and tension. J Cell Biol, 1994. 126(5): p. 1241-53.
56. Solomon, D.A., et al., Mutational inactivation of STAG2 causes aneuploidy in human cancer. Science, 2011. 333(6045): p. 1039-43.
57. Taylor, C.F., et al., Frequent inactivating mutations of STAG2 in bladder cancer are associated with low tumour grade and stage and inversely related to chromosomal copy number changes. Hum Mol Genet, 2014. 23(8): p. 1964-74.
58. Guo, G., et al., Whole-genome and whole-exome sequencing of bladder cancer identifies frequent alterations in genes involved in sister chromatid cohesion and segregation. Nat Genet, 2013. 45(12): p. 1459-63.
59. Balbas-Martinez, C., et al., Recurrent inactivation of STAG2 in bladder cancer is not associated with aneuploidy. Nat Genet, 2013. 45(12): p. 1464-9.
60. Losada, A., Cohesin in cancer: chromosome segregation and beyond. Nat Rev Cancer, 2014. 14(6): p. 389-93.

61. Cheeseman, I.M., The kinetochore. Cold Spring Harb Perspect Biol, 2014. 6(7): p. a015826.
62. Cleveland, D.W., Y. Mao, and K.F. Sullivan, Centromeres and kinetochores: from epigenetics to mitotic checkpoint signaling. Cell, 2003. 112(4): p. 407-21.
63. Fachinetti, D., et al., DNA Sequence-Specific Binding of CENP-B Enhances the Fidelity of Human Centromere Function. Dev Cell, 2015. 33(3): p. 314-27.
64. Fujita, R., et al., Stable complex formation of CENP-B with the CENP-A nucleosome. Nucleic Acids Res, 2015. 43(10): p. 4909-22.
65. Kapoor, M., et al., The cenpB gene is not essential in mice. Chromosoma, 1998. 107(8): p. 570-6.
66. Burrack, L.S. and J. Berman, Flexibility of centromere and kinetochore structures. Trends Genet, 2012. 28(5): p. 204-12.
67. Hasson, D., et al., The octamer is the major form of CENP-A nucleosomes at human centromeres. Nat Struct Mol Biol, 2013. 20(6): p. 687-95.
68. Tachiwana, H., et al., Crystal structure of the human centromeric nucleosome containing CENP-A. Nature, 2011. 476(7359): p. 232-5.
69. Barnhart, M.C., et al., HJURP is a CENP-A chromatin assembly factor sufficient to form a functional de novo kinetochore. J Cell Biol, 2011. 194(2): p. 229-43.
70. Moree, B., et al., CENP-C recruits M18BP1 to centromeres to promote CENP-A chromatin assembly. J Cell Biol, 2011. 194(6): p. 855-71.
71. Wang, J., et al., Mitotic regulator Mis18beta interacts with and specifies the centromeric assembly of molecular chaperone holliday junction recognition protein (HJURP). J Biol Chem, 2014. 289(12): p. 8326-36.
72. McKinley, K.L. and I.M. Cheeseman, Polo-like kinase 1 licenses CENP-A deposition at centromeres. Cell, 2014. 158(2): p. 397-411.
73. Silva, M.C., et al., Cdk activity couples epigenetic centromere inheritance to cell cycle progression. Dev Cell, 2012. 22(1): p. 52-63.
74. McAinsh, A.D. and P. Meraldi, The CCAN complex: linking centromere specification to control of kinetochore-microtubule dynamics. Semin Cell Dev Biol, 2011. 22(9): p. 946-52.
75. Carroll, C.W., K.J. Milks, and A.F. Straight, Dual recognition of CENP-A nucleosomes is required for centromere assembly. J Cell Biol, 2010. 189(7): p. 1143-55.
76. Fachinetti, D., et al., A two-step mechanism for epigenetic specification of centromere identity and function. Nat Cell Biol, 2013. 15(9): p. 1056-66.
77. Kato, H., et al., A conserved mechanism for centromeric nucleosome recognition by centromere protein CENP-C. Science, 2013. 340(6136): p. 1110-3.
78. Screpanti, E., et al., Direct binding of Cenp-C to the Mis12 complex joins the inner and outer kinetochore. Curr Biol, 2011. 21(5): p. 391-8.
79. Gascoigne, K.E., et al., Induced ectopic kinetochore assembly bypasses the requirement for CENP-A nucleosomes. Cell, 2011. 145(3): p. 410-22.
80. Przewloka, M.R., et al., CENP-C is a structural platform for kinetochore assembly. Curr Biol, 2011. 21(5): p. 399-405.
81. Petrovic, A., et al., The MIS12 complex is a protein interaction hub for outer kinetochore assembly. J Cell Biol, 2010. 190(5): p. 835-52.
82. Cheeseman, I.M., et al., The conserved KMN network constitutes the core microtubule-binding site of the kinetochore. Cell, 2006. 127(5): p. 983-97.
83. Cheeseman, I.M., et al., A conserved protein network controls assembly of the outer kinetochore and its ability to sustain tension. Genes Dev, 2004. 18(18): p. 2255-68.
84. Wang, H., et al., Human Zwint-1 specifies localization of Zeste White 10 to kinetochores and is essential for mitotic checkpoint signaling. J Biol Chem, 2004. 279(52): p. 54590-8.
85. Kops, G.J., et al., ZW10 links mitotic checkpoint signaling to the structural kinetochore. J Cell Biol, 2005. 169(1): p. 49-60.
86. Nishino, T., et al., CENP-T-W-S-X forms a unique centromeric chromatin structure with a histone-like fold. Cell, 2012. 148(3): p. 487-501.
87. Nishino, T., et al., CENP-T provides a structural platform for outer kinetochore assembly. EMBO J, 2013. 32(3): p. 424-36.
88. Wan, X., et al., Protein architecture of the human kinetochore microtubule attachment site. Cell, 2009. 137(4): p. 672-84.
89. Rieder, C.L., The structure of the cold-stable kinetochore fiber in metaphase PtK1 cells. Chromosoma, 1981. 84(1): p. 145-58.
90. Kirschner, M. and T. Mitchison, Beyond self-assembly: from microtubules to morphogenesis. Cell, 1986. 45(3): p. 329-42.
91. Wollman, R., et al., Efficient chromosome capture requires a bias in the 'search-and-capture' process during mitotic-spindle assembly. Curr Biol, 2005. 15(9): p. 828-32.
92. Gruss, O.J., et al., Ran induces spindle assembly by reversing the inhibitory effect of importin alpha on TPX2 activity. Cell, 2001. 104(1): p. 83-93.

93. Koffa, M.D., et al., HURP is part of a Ran-dependent complex involved in spindle formation. Curr Biol, 2006. 16(8): p. 743-54.
94. Nachury, M.V., et al., Importin beta is a mitotic target of the small GTPase Ran in spindle assembly. Cell, 2001. 104(1): p. 95-106.
95. Groen, A.C., et al., XRHAMM functions in ran-dependent microtubule nucleation and pole formation during anastral spindle assembly. Curr Biol, 2004. 14(20): p. 1801-11.
96. Goshima, G., et al., Augmin: a protein complex required for centrosome-independent microtubule generation within the spindle. J Cell Biol, 2008. 181(3): p. 421-9.
97. Kapoor, T.M., et al., Chromosomes can congress to the metaphase plate before biorientation. Science, 2006. 311(5759): p. 388-91.
98. Cai, S., et al., Chromosome congression in the absence of kinetochore fibres. Nat Cell Biol, 2009. 11(7): p. 832-8.
99. Varma, D., et al., Direct role of dynein motor in stable kinetochore-microtubule attachment, orientation, and alignment. J Cell Biol, 2008. 182(6): p. 1045-54.
100. Yang, Z., et al., Kinetochore dynein is required for chromosome motion and congression independent of the spindle checkpoint. Curr Biol, 2007. 17(11): p. 973-80.
101. Wandke, C., et al., Human chromokinesins promote chromosome congression and spindle microtubule dynamics during mitosis. J Cell Biol, 2012. 198(5): p. 847-63.
102. Iemura, K. and K. Tanaka, Chromokinesin Kid and kinetochore kinesin CENP-E differentially support chromosome congression without end-on attachment to microtubules. Nat Commun, 2015. 6: p. 6447.
103. Brouhard, G.J. and A.J. Hunt, Microtubule movements on the arms of mitotic chromosomes: polar ejection forces quantified in vitro. Proc Natl Acad Sci U S A, 2005. 102(39): p. 13903-8.
104. Barisic, M., et al., Mitosis. Microtubule detyrosination guides chromosomes during mitosis. Science, 2015. 348(6236): p. 799-803.
105. Magidson, V., et al., Adaptive changes in the kinetochore architecture facilitate proper spindle assembly. Nat Cell Biol, 2015. 17(9): p. 1134-44.
106. Wynne, D.J. and H. Funabiki, Kinetochore function is controlled by a phospho-dependent coexpansion of inner and outer components. J Cell Biol, 2015. 210(6): p. 899-916.
107. Shrestha, R.L. and V.M. Draviam, Lateral to end-on conversion of chromosome-microtubule attachment requires kinesins CENP-E and MCAK. Curr Biol, 2013. 23(16): p. 1514-26.
108. Drpic, D., et al., Polar Ejection Forces Promote the Conversion from Lateral to End-on Kinetochore-Microtubule Attachments on Mono-oriented Chromosomes. Cell Rep, 2015. 13(3): p. 460-9.
109. Santaguida, S. and A. Musacchio, The life and miracles of kinetochores. EMBO J, 2009. 28(17): p. 2511-31.
110. Musacchio, A. and E.D. Salmon, The spindle-assembly checkpoint in space and time. Nat Rev Mol Cell Biol, 2007. 8(5): p. 379-93.
111. Lan, W. and D.W. Cleveland, A chemical tool box defines mitotic and interphase roles for Mps1 kinase. J Cell Biol, 2010. 190(1): p. 21-4.
112. Maciejowski, J., et al., Mps1 directs the assembly of Cdc20 inhibitory complexes during interphase and mitosis to control M phase timing and spindle checkpoint signaling. J Cell Biol, 2010. 190(1): p. 89-100.
113. Nijenhuis, W., et al., A TPR domain-containing N-terminal module of MPS1 is required for its kinetochore localization by Aurora B. J Cell Biol, 2013. 201(2): p. 217-31.
114. Santaguida, S., et al., Dissecting the role of MPS1 in chromosome biorientation and the spindle checkpoint through the small molecule inhibitor reversine. The Journal of cell biology, 2010. 190(1): p. 73-87.
115. Sliedrecht, T., et al., Chemical genetic inhibition of Mps1 in stable human cell lines reveals novel aspects of Mps1 function in mitosis. PloS one, 2010. 5(4): p. e10251.
116. London, N., et al., Phosphoregulation of Spc105 by Mps1 and PP1 regulates Bub1 localization to kinetochores. Curr Biol, 2012. 22(10): p. 900-6.
117. Shepperd, L.A., et al., Phosphodependent recruitment of Bub1 and Bub3 to Spc7/KNL1 by Mph1 kinase maintains the spindle checkpoint. Curr Biol, 2012. 22(10): p. 891-9.
118. Vleugel, M., et al., Evolution and function of the mitotic checkpoint. Dev Cell, 2012. 23(2): p. 239-50.
119. Vleugel, M., et al., Sequential multisite phospho-regulation of KNL1-BUB3 interfaces at mitotic kinetochores. Mol Cell, 2015. 57(5): p. 824-35.
120. Vleugel, M., et al., Arrayed BUB recruitment modules in the kinetochore scaffold KNL1 promote accurate chromosome segregation. J Cell Biol, 2013. 203(6): p. 943-55.
121. Karess, R., Rod-Zw10-Zwilch: a key player in the spindle checkpoint. Trends Cell Biol, 2005. 15(7): p. 386-92.
122. Kim, S., et al., Structure of human Mad1 C-terminal domain reveals its involvement in kinetochore targeting. Proc Natl Acad Sci U S A, 2012. 109(17): p. 6549-54.
123. Klebig, C., D. Korinth, and P. Meraldi, Bub1 regulates chromosome segregation in a kinetochore

independent manner. J Cell Biol, 2009. 185(5): p. 841-58.
124. Moyle, M.W., et al., A Bub1-Mad1 interaction targets the Mad1-Mad2 complex to unattached kinetochores to initiate the spindle checkpoint. J Cell Biol, 2014. 204(5): p. 647-57.
125. London, N. and S. Biggins, Mad1 kinetochore recruitment by Mps1-mediated phosphorylation of Bub1 signals the spindle checkpoint. Genes Dev, 2014. 28(2): p. 140-52.
126. Zhou, H., et al., Cep57 is a Mis12-interacting kinetochore protein involved in kinetochore targeting of Mad1-Mad2. Nat Commun, 2016. 7: p. 10151.
127. De Antoni, A., et al., The Mad1/Mad2 complex as a template for Mad2 activation in the spindle assembly checkpoint. Curr Biol, 2005. 15(3): p. 214-25.
128. Chung, E. and R.H. Chen, Spindle checkpoint requires Mad1-bound and Mad1-free Mad2. Mol Biol Cell, 2002. 13(5): p. 1501-11.
129. Sacristan, C. and G.J. Kops, Joined at the hip: kinetochores, microtubules, and spindle assembly checkpoint signaling. Trends Cell Biol, 2015. 25(1): p. 21-8.
130. Hiruma, Y., et al., CELL DIVISION CYCLE. Competition between MPS1 and microtubules at kinetochores regulates spindle checkpoint signaling. Science, 2015. 348(6240): p. 1264-7.
131. Ji, Z., H. Gao, and H. Yu, CELL DIVISION CYCLE. Kinetochore attachment sensed by competitive Mps1 and microtubule binding to Ndc80C. Science, 2015. 348(6240): p. 1260-4.
132. Kops, G.J. and J.V. Shah, Connecting up and clearing out: how kinetochore attachment silences the spindle assembly checkpoint. Chromosoma, 2012. 121(5): p. 509-25.
133. Nijenhuis, W., et al., Negative feedback at kinetochores underlies a responsive spindle checkpoint signal. Nat Cell Biol, 2014. 16(12): p. 1257-64.
134. Gao, Y.F., et al., Cdk1-phosphorylated CUEDC2 promotes spindle checkpoint inactivation and chromosomal instability. Nat Cell Biol, 2011. 13(8): p. 924-33.
135. Xia, G., et al., Conformation-specific binding of p31(comet) antagonizes the function of Mad2 in the spindle checkpoint. Embo J, 2004. 23(15): p. 3133-43.
136. Hagan, R.S., et al., p31(comet) acts to ensure timely spindle checkpoint silencing subsequent to kinetochore attachment. Mol Biol Cell, 2011. 22(22): p. 4236-46.
137. Jia, L., et al., Defining pathways of spindle checkpoint silencing: functional redundancy between Cdc20 ubiquitination and p31(comet). Mol Biol Cell, 2011. 22(22): p. 4227-35.
138. Westhorpe, F.G., et al., p31comet-mediated extraction of Mad2 from the MCC promotes efficient mitotic exit. J Cell Sci, 2011. 124(Pt 22): p. 3905-16.
139. Foster, S.A. and D.O. Morgan, The APC/C subunit Mnd2/Apc15 promotes Cdc20 autoubiquitination and spindle assembly checkpoint inactivation. Mol Cell, 2012. 47(6): p. 921-32.
140. Stegmeier, F., et al., Anaphase initiation is regulated by antagonistic ubiquitination and deubiquitination activities. Nature, 2007. 446(7138): p. 876-81.
141. Carmena, M., et al., The chromosomal passenger complex (CPC): from easy rider to the godfather of mitosis. Nat Rev Mol Cell Biol, 2012. 13(12): p. 789-803.
142. van der Horst, A. and S.M. Lens, Cell division: control of the chromosomal passenger complex in time and space. Chromosoma, 2014. 123(1-2): p. 25-42.
143. Kitagawa, M. and S.H. Lee, The chromosomal passenger complex (CPC) as a key orchestrator of orderly mitotic exit and cytokinesis. Front Cell Dev Biol, 2015. 3: p. 14.
144. Liu, D., et al., Sensing chromosome bi-orientation by spatial separation of aurora B kinase from kinetochore substrates. Science, 2009. 323(5919): p. 1350-3.
145. DeLuca, J.G., et al., Kinetochore microtubule dynamics and attachment stability are regulated by Hec1. Cell, 2006. 127(5): p. 969-82.
146. Welburn, J.P., et al., Aurora B phosphorylates spatially distinct targets to differentially regulate the kinetochore-microtubule interface. Mol Cell, 2010. 38(3): p. 383-92.
147. Liu, D., et al., Regulated targeting of protein phosphatase 1 to the outer kinetochore by KNL1 opposes Aurora B kinase. J Cell Biol, 2010. 188(6): p. 809-20.
148. Kim, Y., et al., Aurora kinases and protein phosphatase 1 mediate chromosome congression through regulation of CENP-E. Cell, 2010. 142(3): p. 444-55.
149. Lampson, M.A. and I.M. Cheeseman, Sensing centromere tension: Aurora B and the regulation of kinetochore function. Trends in cell biology, 2011. 21(3): p. 133-40.
150. Hanisch, A., H.H. Sillje, and E.A. Nigg, Timely anaphase onset requires a novel spindle and kinetochore complex comprising Ska1 and Ska2. The EMBO journal, 2006. 25(23): p. 5504-15.
151. Theis, M., et al., Comparative profiling identifies C13orf3 as a component of the Ska complex required for mammalian cell division. The EMBO journal, 2009. 28(10): p. 1453-65.
152. Gaitanos, T.N., et al., Stable kinetochore-microtubule interactions depend on the Ska complex and its new component Ska3/C13Orf3. The EMBO journal, 2009. 28(10): p. 1442-52.
153. Raaijmakers, J.A., et al., RAMA1 is a novel kinetochore protein involved in kinetochore-microtubule attachment. Journal of cell science, 2009. 122(Pt 14): p. 2436-45.
154. Welburn, J.P., et al., The human kinetochore Ska1 complex facilitates microtubule depolymerization-coupled motility. Developmental cell, 2009. 16(3): p. 374-85.

155. Daum, J.R., et al., Ska3 is required for spindle checkpoint silencing and the maintenance of chromosome cohesion in mitosis. Current biology : CB, 2009. 19(17): p. 1467-72.
156. Schmidt, J.C., et al., Aurora B kinase controls the targeting of the Astrin-SKAP complex to bioriented kinetochores. The Journal of cell biology, 2010. 191(2): p. 269-80.
157. Manning, A.L., et al., CLASP1, astrin and Kif2b form a molecular switch that regulates kinetochore-microtubule dynamics to promote mitotic progression and fidelity. The EMBO journal, 2010. 29(20): p. 3531-43.
158. Vader, G. and S.M. Lens, Chromosome segregation: taking the passenger seat. Current biology : CB, 2010. 20(20): p. R879-81.
159. Yamagishi, Y., et al., Two histone marks establish the inner centromere and chromosome bi-orientation. Science, 2010. 330(6001): p. 239-43.
160. Kelly, A.E., et al., Survivin Reads Phosphorylated Histone H3 Threonine 3 to Activate the Mitotic Kinase Aurora B. Science, 2010. 330(6001): p. 235-39.
161. Wang, F., et al., Histone H3 Thr-3 Phosphorylation by Haspin Positions Aurora B at Centromeres in Mitosis. Science, 2010. 303(6001): p. 231-35.
162. Kawashima, S.A., et al., Phosphorylation of H2A by Bub1 prevents chromosomal instability through localizing shugoshin. Science, 2010. 327(5962): p. 172-7.
163. Tsukahara, T., Y. Tanno, and Y. Watanabe, Phosphorylation of the CPC by Cdk1 promotes chromosome bi-orientation. Nature, 2010. 467: p. 719-23.
164. Hengeveld, R.C., et al., Development of a chemical genetic approach for human Aurora B kinase identifies novel substrates of the chromosomal passenger complex. Molecular & cellular proteomics : MCP, 2012.
165. Wang, F., et al., A positive feedback loop involving Haspin and Aurora B promotes CPC accumulation at centromeres in mitosis. Curr Biol, 2011. 21(12): p. 1061-9.
166. Qian, J., et al., Aurora B defines its own chromosomal targeting by opposing the recruitment of the phosphatase scaffold Repo-Man. Curr Biol, 2013. 23(12): p. 1136-43.
167. Ditchfield, C., et al., Aurora B couples chromosome alignment with anaphase by targeting BubR1, Mad2, and Cenp-E to kinetochores. J Cell Biol, 2003. 161(2): p. 267-80.
168. van der Waal, M.S., et al., Mps1 promotes rapid centromere accumulation of Aurora B. EMBO reports, 2012.
169. Vader, G., A.F. Maia, and S.M. Lens, The chromosomal passenger complex and the spindle assembly checkpoint: kinetochore-microtubule error correction and beyond. Cell Div, 2008. 3: p. 10.
170. Nezi, L. and A. Musacchio, Sister chromatid tension and the spindle assembly checkpoint. Curr Opin Cell Biol, 2009. 21(6): p. 785-95.
171. Vader, G., et al., The chromosomal passenger complex controls spindle checkpoint function independent from its role in correcting microtubule kinetochore interactions. Mol Biol Cell, 2007. 18(11): p. 4553-64.
172. Petersen, J. and I.M. Hagan, S. pombe aurora kinase/survivin is required for chromosome condensation and the spindle checkpoint attachment response. Curr Biol, 2003. 13(7): p. 590-7.
173. Kallio, M.J., et al., Inhibition of aurora B kinase blocks chromosome segregation, overrides the spindle checkpoint, and perturbs microtubule dynamics in mitosis. Curr Biol, 2002. 12(11): p. 900-5.
174. Vanoosthuyse, V. and K.G. Hardwick, A novel protein phosphatase 1-dependent spindle checkpoint silencing mechanism. Current biology : CB, 2009. 19(14): p. 1176-81.
175. Santaguida, S., et al., Evidence that Aurora B is implicated in spindle checkpoint signalling independently of error correction. The EMBO journal, 2011. 30(8): p. 1508-19.
176. Saurin, A.T., et al., Aurora B potentiates Mps1 activation to ensure rapid checkpoint establishment at the onset of mitosis. Nat Commun, 2011. 2: p. 316.
177. Yue, Z., et al., Deconstructing Survivin: comprehensive genetic analysis of Survivin function by conditional knockout in a vertebrate cell line. The Journal of cell biology, 2008. 183(2): p. 279-96.
178. Xu, Z., et al., INCENP-aurora B interactions modulate kinase activity and chromosome passenger complex localization. The Journal of cell biology, 2009. 187(5): p. 637-53.
179. Morrow, C.J., et al., Bub1 and aurora B cooperate to maintain BubR1-mediated inhibition of APC/CCdc20. Journal of cell science, 2005. 118(Pt 16): p. 3639-52.
180. Maldonado, M. and T.M. Kapoor, Constitutive Mad1 targeting to kinetochores uncouples checkpoint signalling from chromosome biorientation. Nature cell biology, 2011. 13(4): p. 475-82.
181. Lampson, M.A. and T.M. Kapoor, The human mitotic checkpoint protein BubR1 regulates chromosome-spindle attachments. Nat Cell Biol, 2005. 7(1): p. 93-8.
182. Hauf, S., et al., The small molecule Hesperadin reveals a role for Aurora B in correcting kinetochore-microtubule attachment and in maintaining the spindle assembly checkpoint. J Cell Biol, 2003. 161(2): p. 281-94.
183. Suijkerbuijk, S.J., et al., Integration of kinase and phosphatase activities by BUBR1 ensures formation of stable kinetochore-microtubule attachments. Dev Cell, 2012. 23(4): p. 745-55.
184. Kruse, T., et al., Direct binding between BubR1 and B56-PP2A phosphatase complexes regulate

mitotic progression. J Cell Sci, 2013. 126(Pt 5): p. 1086-92.
185. Xu, P., et al., BUBR1 recruits PP2A via the B56 family of targeting subunits to promote chromosome congression. Biol Open, 2013. 2(5): p. 479-86.
186. Tada, K., et al., Condensin association with histone H2A shapes mitotic chromosomes. Nature, 2011. 474(7352): p. 477-83.
187. Nakazawa, N., et al., Condensin phosphorylated by the Aurora-B-like kinase Ark1 is continuously required until telophase in a mode distinct from Top2. Journal of cell science, 2011. 124(Pt 11): p. 1795-807.
188. Hergeth, S.P., et al., Isoform-specific phosphorylation of human linker histone H1.4 in mitosis by the kinase Aurora B. Journal of cell science, 2011. 124(Pt 10): p. 1623-8.
189. Goto, H., et al., Aurora-B phosphorylates Histone H3 at serine28 with regard to the mitotic chromosome condensation. Genes Cells, 2002. 7(1): p. 11-7.
190. Perrera, C., et al., Identification of Myb-binding protein 1A (MYBBP1A) as a novel substrate for aurora B kinase. J Biol Chem, 2010. 285(16): p. 11775-85.
191. Rogers, E., et al., The aurora kinase AIR-2 functions in the release of chromosome cohesion in Caenorhabditis elegans meiosis. The Journal of cell biology, 2002. 157(2): p. 219-29.
192. Borton, M.T., et al., Multiple Levels of Regulation of Sororin by Cdk1 and Aurora B. J Cell Biochem, 2016. 117(2): p. 351-60.
193. Kassardjian, A., et al., The transcription factor YY1 is a novel substrate for Aurora B kinase at G2/M t ransition of the cell cycle. PLoS One, 2012. 7(11): p. e50645.
194. Yasui, Y., et al., Autophosphorylation of a newly identified site of Aurora-B is indispensable for cytokinesis. J Biol Chem, 2004. 279(13): p. 12997-3003.
195. Gassmann, R., et al., Borealin: a novel chromosomal passenger required for stability of the bipolar mitotic spindle. J Cell Biol, 2004. 166(2): p. 179-91.
196. Hayama, S., et al., Phosphorylation and activation of cell division cycle associated 8 by aurora kinase B plays a significant role in human lung carcinogenesis. Cancer research, 2007. 67(9): p. 4113-22.
197. Zeitlin, S.G., R.D. Shelby, and K.F. Sullivan, CENP-A is phosphorylated by Aurora B kinase and plays an unexpected role in completion of cytokinesis. J Cell Biol, 2001. 155(7): p. 1147-57.
198. Hua, S., et al., CENP-U cooperates with Hec1 to orchestrate kinetochore-microtubule attachment. The Journal of biological chemistry, 2011. 286(2): p. 1627-38.
199. Keating, P., et al., Ipl1-dependent phosphorylation of Dam1 is reduced by tension applied on kinetochores. Journal of cell science, 2009. 122(Pt 23): p. 4375-82.
200. Cheng, L., et al., Aurora B regulates formin mDia3 in achieving metaphase chromosome alignment. Developmental cell, 2011. 20(3): p. 342-52.
201. Yang, Y., et al., Phosphorylation of HsMis13 by Aurora B kinase is essential for assembly of functional kinetochore. The Journal of biological chemistry, 2008. 283(39): p. 26726-36.
202. Honda, R., R. Korner, and E.A. Nigg, Exploring the functional interactions between Aurora B, INCENP, and survivin in mitosis. Mol Biol Cell, 2003. 14(8): p. 3325-41.
203. Knowlton, A.L., et al., ICIS and Aurora B coregulate the microtubule depolymerase Kif2a. Current biology : CB, 2009. 19(9): p. 758-63.
204. Andrews, P.D., et al., Aurora B regulates MCAK at the mitotic centromere. Dev Cell, 2004. 6(2): p. 253-68.
205. Zhang, X., et al., Aurora B Phosphorylates Multiple Sites on MCAK to Spatially and Temporally Regulate Its Function. Mol Biol Cell, 2007.
206. Resnick, T.D., et al., INCENP and Aurora B promote meiotic sister chromatid cohesion through localization of the Shugoshin MEI-S332 in Drosophila. Dev Cell, 2006. 11(1): p. 57-68.
207. Carmena, M., et al., The Chromosomal Passenger Complex Activates Polo Kinase at Centromeres. Plos Biology, 2012. 10(1): p. e1001250.
208. Tanno, Y., et al., Phosphorylation of mammalian Sgo2 by Aurora B recruits PP2A and MCAK to centromeres. Genes Dev, 2010. 24(19): p. 2169-79.
209. Nousiainen, M., et al., Phosphoproteome analysis of the human mitotic spindle. Proc Natl Acad Sci U S A, 2006.
210. Olsen, J.V., et al., Quantitative phosphoproteomics reveals widespread full phosphorylation site occupancy during mitosis. Sci Signal, 2010. 3(104): p. ra3.
211. Kasuboski, J.M., et al., Zwint-1 is a novel Aurora B substrate required for the assembly of a dynein-binding platform on kinetochores. Molecular biology of the cell, 2011. 22(18): p. 3318-30.
212. Zimniak, T., et al., Phosphoregulation of the budding yeast EB1 homologue Bim1p by Aurora/Ipl1p. Journal of Cell Biology, 2009. 186(3): p. 379-91.
213. Kim, H.J., et al., Specific primary sequence requirements for Aurora B kinase-mediated phosphorylation and subcellular localization of TMAP during mitosis. Cell cycle, 2010. 9(10): p. 2027-36.
214. Uehara, R., et al., Aurora B and Kif2A control microtubule length for assembly of a functional central

spindle during anaphase. J Cell Biol, 2013. 202(4): p. 623-36.
215. Nunes Bastos, R., et al., Aurora B suppresses microtubule dynamics and limits central spindle size by locally activating KIF4A. J Cell Biol, 2013. 202(4): p. 605-21.
216. Neef, R., et al., Cooperation between mitotic kinesins controls the late stages of cytokinesis. Curr Biol, 2006. 16(3): p. 301-7.
217. Guse, A., M. Mishima, and M. Glotzer, Phosphorylation of ZEN-4/MKLP1 by aurora B regulates completion of cytokinesis. Curr Biol, 2005. 15(8): p. 778-86.
218. Douglas, M.E., et al., Aurora B and 14-3-3 coordinately regulate clustering of centralspindlin during cytokinesis. Curr Biol, 2010. 20(10): p. 927-33.
219. Wu, D., et al., Phosphorylation of myosin II-interacting guanine nucleotide exchange factor (MyoGEF) at threonine 544 by aurora B kinase promotes the binding of polo-like kinase 1 to MyoGEF. J Biol Chem, 2014. 289(10): p. 7142-50.
220. Gadea, B.B. and J.V. Ruderman, Aurora B is required for mitotic chromatin-induced phosphorylation of Op18/Stathmin. Proc Natl Acad Sci U S A, 2006. 103(12): p. 4493-8.
221. Asano, E., et al., The Aurora-B-mediated phosphorylation of SHCBP1 regulates cytokinetic furrow ingression. J Cell Sci, 2013. 126(Pt 15): p. 3263-70.
222. Tian, J., et al., Aurora B-dependent phosphorylation of Ataxin-10 promotes the interaction between Ataxin-10 and Plk1 in cytokinesis. Sci Rep, 2015. 5: p. 8360.
223. Carlton, G.C., et al., ESCRT-III governs the Aurora B-mediated abscission checkpoint through CHMP4C. Science, 2012. Published online DOI: 10.1126/science.1217180.
224. Kawajiri, A., et al., Functional significance of the specific sites phosphorylated in desmin at cleavage furrow: Aurora-B may phosphorylate and regulate type III intermediate filaments during cytokinesis coordinatedly with Rho-kinase. Mol Biol Cell, 2003. 14(4): p. 1489-500.
225. Ban, R., et al., Mitotic regulation of the stability of microtubule plus-end tracking protein EB3 by ubiquitin ligase SIAH-1 and Aurora mitotic kinases. The Journal of biological chemistry, 2009. 284(41): p. 28367-81.
226. Ferreira, J.G., et al., Aurora B spatially regulates EB3 phosphorylation to coordinate daughter cell adhesion with cytokinesis. J Cell Biol, 2013. 201(5): p. 709-24.
227. Guise, A.J., et al., Aurora B-dependent regulation of class IIa histone deacetylases by mitotic nuclear localization signal phosphorylation. Mol Cell Proteomics, 2012. 11(11): p. 1220-9.
228. Minoshima, Y., et al., Phosphorylation by aurora B converts MgcRacGAP to a RhoGAP during cytokinesis. Dev Cell, 2003. 4(4): p. 549-60.
229. Murata-Hori, M., et al., Myosin II regulatory light chain as a novel substrate for AIM-1, an aurora/Ipl1p-related kinase from rat. J Biochem (Tokyo), 2000. 128(6): p. 903-7.
230. Yokoyama, T., et al., Aurora-B and Rho-kinase/ROCK, the two cleavage furrow kinases, independently regulate the progression of cytokinesis: possible existence of a novel cleavage furrow kinase phosphorylates ezrin/radixin/moesin (ERM). Genes to cells : devoted to molecular & cellular mechanisms, 2005. 10(2): p. 127-37.
231. Yan, J., et al., Aurora B interaction of centrosomal Nlp regulates cytokinesis. The Journal of biological chemistry, 2010. 285(51): p. 40230-9.
232. Shandilya, J., et al., Phosphorylation of multifunctional nucleolar protein nucleophosmin (NPM1) by aurora kinase B is critical for mitotic progression. FEBS Lett, 2014. 588(14): p. 2198-205.
233. Song, S.J., et al., Aurora B-mediated phosphorylation of RASSF1A maintains proper cytokinesis by recruiting Syntaxin16 to the midzone and midbody. Cancer research, 2009. 69(22): p. 8540-4.
234. Chow, C., et al., Regulation of APC/C(Cdc20) activity by RASSF1A-APC/C(Cdc20) circuitry. Oncogene, 2011.
235. Qi, M., et al., Septin1, a new interaction partner for human serine/threonine kinase aurora-B. Biochemical and biophysical research communications, 2005. 336(3): p. 994-1000.
236. Wheatley, S.P., et al., Aurora-B Phosphorylation in Vitro Identifies a Residue of Survivin That Is Essential for Its Localization and Binding to Inner Centromere Protein (INCENP) in Vivo. J Biol Chem, 2004. 279(7): p. 5655-60.
237. Delacour-Larose, M., et al., Role of survivin phosphorylation by aurora B in mitosis. Cell cycle, 2007. 6(15): p. 1878-85.
238. Goto, H., et al., Aurora-B regulates the cleavage furrow-specific vimentin phosphorylation in the cytokinetic process. J Biol Chem, 2003. 278(10): p. 8526-30.
239. Loughlin, R., et al., Katanin contributes to interspecies spindle length scaling in Xenopus. Cell, 2011. 147(6): p. 1397-407.
240. Han, Z., et al., The C. elegans Tousled-like kinase contributes to chromosome segregation as a substrate and regulator of the Aurora B kinase. Curr Biol, 2005. 15(10): p. 894-904.
241. Yang, C., et al., Aurora-B mediated ATM serine 1403 phosphorylation is required for mitotic ATM activation and the spindle checkpoint. Molecular cell, 2011. 44(4): p. 597-608.
242. Floyd, S., et al., Spatiotemporal organization of Aurora-B by APC/CCdh1 after mitosis coordinates cell spreading through FHOD1. J Cell Sci, 2013. 126(Pt 13): p. 2845-56.

243. Xiao, L., et al., KIBRA protein phosphorylation is regulated by mitotic kinase aurora and protein phosphatase 1. The Journal of biological chemistry, 2011. 286(42): p. 36304-15.
244. Sakita-Suto, S., et al., Aurora-B regulates RNA methyltransferase NSUN2. Molecular biology of the cell, 2007. 18(3): p. 1107-17.
245. Wu, L., et al., Aurora B interacts with NIR-p53, leading to p53 phosphorylation in its DNA-binding domain and subsequent functional suppression. The Journal of biological chemistry, 2011. 286(3): p. 2236-44.
246. Nair, J.S., et al., Aurora B kinase regulates the postmitotic endoreduplication checkpoint via phosphorylation of the retinoblastoma protein at serine 780. Molecular biology of the cell, 2009. 20(8): p. 2218-28.
247. Kettenbach, A.N., et al., Quantitative phosphoproteomics identifies substrates and functional modules of aurora and polo-like kinase activities in mitotic cells. Sci Signal, 2011. 4(179): p. rs5.
248. Koch, A., et al., Mitotic substrates of the kinase aurora with roles in chromatin regulation identified through quantitative phosphoproteomics of fission yeast. Science signaling, 2011. 4(179): p. rs6.
249. Hegemann, B., et al., Systematic phosphorylation analysis of human mitotic protein complexes. Science signaling, 2011. 4(198): p. rs12.
250. Tanaka, T.U., et al., Evidence that the Ipl1-Sli15 (Aurora kinase-INCENP) complex promotes chromosome bi-orientation by altering kinetochore-spindle pole connections. Cell, 2002. 108(3): p. 317-29.
251. Krenn, V. and A. Musacchio, The Aurora B Kinase in Chromosome Bi-Orientation and Spindle Checkpoint Signaling. Front Oncol, 2015. 5: p. 225.
252. Zaytsev, A.V., et al., Bistability of a coupled Aurora B kinase-phosphatase system in cell division. Elife, 2016. 5.
253. DeLuca, K.F., S.M. Lens, and J.G. DeLuca, Temporal changes in Hec1 phosphorylation control kinetochore-microtubule attachment stability during mitosis. J Cell Sci, 2011. 124(Pt 4): p. 622-34.
254. Campbell, C.S. and A. Desai, Tension sensing by Aurora B kinase is independent of survivin-based centromere localization. Nature, 2013. 497(7447): p. 118-21.
255. Jeyaprakash, A.A., et al., Structure of a Survivin-Borealin-INCENP core complex reveals how chromosomal passengers travel together. Cell, 2007. 131(2): p. 271-85.
256. Eckley, D.M., et al., Chromosomal proteins and cytokinesis: patterns of cleavage furrow formation and inner centromere protein positioning in mitotic heterokaryons and mid-anaphase cells. J Cell Biol, 1997. 136(6): p. 1169-83.
257. Vader, G., et al., Survivin mediates targeting of the chromosomal passenger complex to the centromere and midbody. EMBO Rep, 2006. 7(1): p. 85-92.
258. Ainsztein, A.M., et al., INCENP centromere and spindle targeting: identification of essential conserved motifs and involvement of heterochromatin protein HP1. J Cell Biol, 1998. 143(7): p. 1763-74.
259. van der Lelij, P., et al., Warsaw breakage syndrome, a cohesinopathy associated with mutations in the XPD helicase family member DDX11/ChlR1. Am J Hum Genet, 2010. 86(2): p. 262-6.
260. Whelan, G., et al., Cohesin acetyltransferase Esco2 is a cell viability factor and is required for cohesion in pericentric heterochromatin. EMBO J, 2012. 31(1): p. 71-82.
261. Losada, A., M. Hirano, and T. Hirano, Cohesin release is required for sister chromatid resolution, but not for condensin-mediated compaction, at the onset of mitosis. Genes Dev, 2002. 16(23): p. 3004-16.
262. Dai, J., B.A. Sullivan, and J.M. Higgins, Regulation of mitotic chromosome cohesion by Haspin and Aurora B. Dev Cell, 2006. 11(5): p. 741-50.
263. Gimenez-Abian, J.F., et al., Regulation of sister chromatid cohesion between chromosome arms. Curr Biol, 2004. 14(13): p. 1187-93.
264. Lee, J., et al., Unified mode of centromeric protection by shugoshin in mammalian oocytes and somatic cells. Nat Cell Biol, 2008. 10(1): p. 42-52.
265. Liu, H., L. Jia, and H. Yu, Phospho-H2A and cohesin specify distinct tension-regulated Sgo1 pools at kinetochores and inner centromeres. Curr Biol, 2013. 23(19): p. 1927-33.
266. Tanno, Y., et al., The inner centromere-shugoshin network prevents chromosomal instability. Science, 2015. 349(6253): p. 1237-40.
267. Daum, J.R., et al., Cohesion fatigue induces chromatid separation in cells delayed at metaphase. Curr Biol, 2011. 21(12): p. 1018-24.
268. Etemad, B., T.E. Kuijt, and G.J. Kops, Kinetochore-microtubule attachment is sufficient to satisfy the human spindle assembly checkpoint. Nat Commun, 2015. 6: p. 8987.
269. Tauchman, E.C., F.J. Boehm, and J.G. DeLuca, Stable kinetochore-microtubule attachment is sufficient to silence the spindle assembly checkpoint in human cells. Nat Commun, 2015. 6: p. 10036.
270. Musacchio, A., The Molecular Biology of Spindle Assembly Checkpoint Signaling Dynamics. Curr Biol, 2015. 25(20): p. R1002-18.
271. Klein, U.R., E.A. Nigg, and U. Gruneberg, Centromere targeting of the chromosomal passenger

complex requires a ternary subcomplex of Borealin, Survivin, and the N-terminal domain of INCENP. Mol Biol Cell, 2006. 17(6): p. 2547-58.
272. Ruchaud, S., M. Carmena, and W.C. Earnshaw, Chromosomal passengers: conducting cell division. Nat Rev Mol Cell Biol, 2007. 8(10): p. 798-812.
273. Monaco, L., et al., Inhibition of Aurora-B kinase activity by poly(ADP-ribosyl)ation in response to DNA damage. Proc Natl Acad Sci U S A, 2005. 102(40): p. 14244-8.
274. Sabbattini, P., et al., A novel role for the Aurora B kinase in epigenetic marking of silent chromatin in differentiated postmitotic cells. EMBO J, 2007. 26(22): p. 4657-69.
275. Weiss, W.A., S.S. Taylor, and K.M. Shokat, Recognizing and exploiting differences between RNAi and small-molecule inhibitors. Nat Chem Biol, 2007. 3(12): p. 739-44.
276. Lens, S.M., E.E. Voest, and R.H. Medema, Shared and separate functions of polo-like kinases and aurora kinases in cancer. Nat Rev Cancer, 2010. 10(12): p. 825-41.
277. Shah, K., et al., Engineering unnatural nucleotide specificity for Rous sarcoma virus tyrosine kinase to uniquely label its direct substrates. Proc Natl Acad Sci U S A, 1997. 94(8): p. 3565-70.
278. Bishop, A.C., et al., A chemical switch for inhibitor-sensitive alleles of any protein kinase. Nature, 2000. 407(6802): p. 395-401.
279. Bishop, A., et al., Unnatural ligands for engineered proteins: new tools for chemical genetics. Annu Rev Biophys Biomol Struct, 2000. 29: p. 577-606.
280. Zhang, C., et al., A second-site suppressor strategy for chemical genetic analysis of diverse protein kinases. Nat Methods, 2005. 2(6): p. 435-41.
281. Blethrow, J.D., et al., Covalent capture of kinase-specific phosphopeptides reveals Cdk1-cyclin B substrates. Proc Natl Acad Sci U S A, 2008. 105(5): p. 1442-7.
282. Blethrow, J., et al., Design and use of analog-sensitive protein kinases. Curr Protoc Mol Biol, 2004. Chapter 18: p. Unit 18 11.
283. Bishop, J.D. and J.M. Schumacher, Phosphorylation of the carboxyl terminus of inner centromere protein (INCENP) by the Aurora B Kinase stimulates Aurora B kinase activity. J Biol Chem, 2002. 277(31): p. 27577-80.
284. Sessa, F., et al., Mechanism of Aurora B activation by INCENP and inhibition by hesperadin. Mol Cell, 2005. 18(3): p. 379-91.
285. Pinsky, B.A., et al., The Ipl1-Aurora protein kinase activates the spindle checkpoint by creating unattached kinetochores. Nat Cell Biol, 2006. 8(1): p. 78-83.
286. Hauf, S., et al., Aurora controls sister kinetochore mono-orientation and homolog bi-orientation in meiosis-I. EMBO J, 2007. 26(21): p. 4475-86.
287. Girdler, F., et al., Molecular basis of drug resistance in aurora kinases. Chem Biol, 2008. 15(6): p. 552-62.
288. Jordan, M.A. and L. Wilson, Microtubules as a target for anticancer drugs. Nat Rev Cancer, 2004. 4(4): p. 253-65.
289. Lens, S.M., et al., Survivin is required for a sustained spindle checkpoint arrest in response to lack of tension. Embo J, 2003. 22(12): p. 2934-47.
290. Murata-Hori, M. and Y.L. Wang, The kinase activity of aurora B is required for kinetochore-microtubule interactions during mitosis. Curr Biol, 2002. 12(11): p. 894-9.
291. Allen, J.J., et al., A semisynthetic epitope for kinase substrates. Nat Methods, 2007. 4(6): p. 511-6.
292. Hertz, T.N., et al., Chemical genetic approach for kinase-substrate mapping by covalent capture of thiophosphopeptides and analysis by Mass Spectrometry, in Current Protocols in Chemical Biology. 2010, John Wiley and Sons. p. 15 - 36.
293. Baker, P.R., J.C. Trinidad, and C. R.J., Modification site localization scoring integrated into a search engine. Mol Cell Proteomics, 2011. 10(7): p. M111.008078.
294. Cheeseman, I.M., et al., Phospho-regulation of kinetochore-microtubule attachments by the Aurora kinase Ipl1p. Cell, 2002. 111(2): p. 163-72.
295. Alexander, J., et al., Spatial exclusivity combined with positive and negative selection of phosphorylation motifs is the basis for context-dependent mitotic signaling. Sci Signal, 2011. 4(179): p. ra42.
296. Goto, H., et al., Complex formation of Plk1 and INCENP required for metaphase-anaphase transition. Nat Cell Biol, 2006. 8(2): p. 180-7.
297. Hummer, S. and T.U. Mayer, Cdk1 negatively regulates midzone localization of the mitotic kinesin Mklp2 and the chromosomal passenger complex. Curr Biol, 2009. 19(7): p. 607-12.
298. Cherukuri, S., et al., Cell cycle-dependent binding of HMGN proteins to chromatin. Mol Biol Cell, 2008. 19(5): p. 1816-24.
299. Ueda, T., et al., Delineation of the protein module that anchors HMGN proteins to nucleosomes in the chromatin of living cells. Mol Cell Biol, 2008. 28(9): p. 2872-83.
300. Johnson, E.O., et al., PHLDA1 is a crucial negative regulator and effector of Aurora A kinase in breast cancer. Journal of cell science, 2011. 124(Pt 16): p. 2711-22.
301. Girdler, F., et al., Validating Aurora B as an anti-cancer drug target. J Cell Sci, 2006. 119(Pt 17): p.

3664-75.
302. Hornbeck, P.V., et al., PhosphoSite: A bioinformatics resource dedicated to physiological protein phosphorylation. Proteomics, 2004. 4(6): p. 1551-61.
303. Postnikov, Y. and M. Bustin, Regulation of chromatin structure and function by HMGN proteins. Biochim Biophys Acta, 2010. 1799(1-2): p. 62-8.
304. Subramanian, M., et al., The nucleosome-binding protein HMGN2 modulates global genome repair. FEBS J, 2009. 276(22): p. 6646-57.
305. Rochman, M., et al., The interaction of NSBP1/HMGN5 with nucleosomes in euchromatin counteracts linker histone-mediated chromatin compaction and modulates transcription. Mol Cell, 2009. 35(5): p. 642-56.
306. Chan, K.L. and I.D. Hickson, New insights into the formation and resolution of ultra-fine anaphase bridges. Semin Cell Dev Biol, 2011. 22(8): p. 906-12.
307. Mankouri, H.W., D. Huttner, and I.D. Hickson, How unfinished business from S-phase affects mitosis and beyond. EMBO J, 2013. 32(20): p. 2661-71.
308. Wang, L.H., et al., Centromere DNA decatenation depends on cohesin removal and is required for mammalian cell division. J Cell Sci, 2010. 123(Pt 5): p. 806-13.
309. Wang, J.C., Cellular roles of DNA topoisomerases: a molecular perspective. Nat Rev Mol Cell Biol, 2002. 3(6): p. 430-40.
310. Spence, J.M., et al., Depletion of topoisomerase IIalpha leads to shortening of the metaphase interkinetochore distance and abnormal persistence of PICH-coated anaphase threads. J Cell Sci, 2007. 120(Pt 22): p. 3952-64.
311. Baumann, C., et al., PICH, a centromere-associated SNF2 family ATPase, is regulated by Plk1 and required for the spindle checkpoint. Cell, 2007. 128(1): p. 101-14.
312. Chan, K.L., P.S. North, and I.D. Hickson, BLM is required for faithful chromosome segregation and its localization defines a class of ultrafine anaphase bridges. EMBO J, 2007. 26(14): p. 3397-409.
313. Wang, L.H., et al., Persistence of DNA threads in human anaphase cells suggests late completion of sister chromatid decatenation. Chromosoma, 2008. 117(2): p. 123-35.
314. Hubner, N.C., et al., Re-examination of siRNA specificity questions role of PICH and Tao1 in the spindle checkpoint and identifies Mad2 as a sensitive target for small RNAs. Chromosoma, 2010. 119(2): p. 149-65.
315. Biebricher, A., et al., PICH: a DNA translocase specially adapted for processing anaphase bridge DNA. Mol Cell, 2013. 51(5): p. 691-701.
316. Ke, Y., et al., PICH and BLM limit histone association with anaphase centromeric DNA threads and promote their resolution. EMBO J, 2011. 30(16): p. 3309-21.
317. Hengeveld, R.C., et al., Rif1 Is Required for Resolution of Ultrafine DNA Bridges in Anaphase to Ensure Genomic Stability. Dev Cell, 2015. 34(4): p. 466-74.
318. Deans, A.J. and S.C. West, DNA interstrand crosslink repair and cancer. Nat Rev Cancer, 2011. 11(7): p. 467-80.
319. Nielsen, C.F., et al., PICH promotes sister chromatid disjunction and co-operates with topoisomerase II in mitosis. Nat Commun, 2015. 6: p. 8962.
320. Vinciguerra, P., et al., Cytokinesis failure occurs in Fanconi anemia pathway-deficient murine and human bone marrow hematopoietic cells. J Clin Invest, 2010. 120(11): p. 3834-42.
321. Chan, K.L., et al., Replication stress induces sister-chromatid bridging at fragile site loci in mitosis. Nat Cell Biol, 2009. 11(6): p. 753-60.
322. Gaillard, H., T. Garcia-Muse, and A. Aguilera, Replication stress and cancer. Nat Rev Cancer, 2015. 15(5): p. 276-89.
323. Helmrich, A., M. Ballarino, and L. Tora, Collisions between replication and transcription complexes cause common fragile site instability at the longest human genes. Mol Cell, 2011. 44(6): p. 966-77.
324. Thys, R.G., et al., DNA secondary structure at chromosomal fragile sites in human disease. Curr Genomics, 2015. 16(1): p. 60-70.
325. Palumbo, E., et al., Replication dynamics at common fragile site FRA6E. Chromosoma, 2010. 119(6): p. 575-87.
326. Letessier, A., et al., Cell-type-specific replication initiation programs set fragility of the FRA3B fragile site. Nature, 2011. 470(7332): p. 120-3.
327. Naim, V. and F. Rosselli, The FANC pathway and BLM collaborate during mitosis to prevent micro-nucleation and chromosome abnormalities. Nat Cell Biol, 2009. 11(6): p. 761-8.
328. Wang, W., Emergence of a DNA-damage response network consisting of Fanconi anaemia and BRCA proteins. Nat Rev Genet, 2007. 8(10): p. 735-48.
329. Naim, V., et al., ERCC1 and MUS81-EME1 promote sister chromatid separation by processing late replication intermediates at common fragile sites during mitosis. Nat Cell Biol, 2013. 15(8): p. 1008-15.
330. Ying, S., et al., MUS81 promotes common fragile site expression. Nat Cell Biol, 2013. 15(8): p. 1001-7.

331. Minocherhomji, S., et al., Replication stress activates DNA repair synthesis in mitosis. Nature, 2015. 528(7581): p. 286-90.
332. O'Sullivan, R.J. and J. Karlseder, Telomeres: protecting chromosomes against genome instability. Nat Rev Mol Cell Biol, 2010. 11(3): p. 171-81.
333. Barefield, C. and J. Karlseder, The BLM helicase contributes to telomere maintenance through processing of late-replicating intermediate structures. Nucleic Acids Res, 2012. 40(15): p. 7358-67.
334. d'Alcontres, M.S., et al., TopoIIalpha prevents telomere fragility and formation of ultra thin DNA bridges during mitosis through TRF1-dependent binding to telomeres. Cell Cycle, 2014. 13(9): p. 1463-81.
335. Nera, B., et al., Elevated levels of TRF2 induce telomeric ultrafine anaphase bridges and rapid telomere deletions. Nat Commun, 2015. 6: p. 10132.
336. Zhang, Y., et al., ZNF365 promotes stability of fragile sites and telomeres. Cancer Discov, 2013. 3(7): p. 798-811.
337. Sanz, M.M. and J. German, Bloom's Syndrome, in GeneReviews(R), R.A. Pagon, et al., Editors. 1993: Seattle (WA).
338. Alter, B.P. and G. Kupfer, Fanconi Anemia, in GeneReviews(R), R.A. Pagon, et al., Editors. 1993: Seattle (WA).
339. Zhang, C.Z., et al., Chromothripsis from DNA damage in micronuclei. Nature, 2015. 522(7555): p. 179-84.
340. Lukas, C., et al., 53BP1 nuclear bodies form around DNA lesions generated by mitotic transmission of chromosomes under replication stress. Nat Cell Biol, 2011. 13(3): p. 243-53.
341. Harrigan, J.A., et al., Replication stress induces 53BP1-containing OPT domains in G1 cells. J Cell Biol, 2011. 193(1): p. 97-108.
342. Di Virgilio, M., et al., Rif1 prevents resection of DNA breaks and promotes immunoglobulin class switching. Science, 2013. 339(6120): p. 711-5.
343. Zimmermann, M., et al., 53BP1 regulates DSB repair using Rif1 to control 5' end resection. Science, 2013. 339(6120): p. 700-4.
344. Chapman, J.R., et al., RIF1 is essential for 53BP1-dependent nonhomologous end joining and suppression of DNA double-strand break resection. Mol Cell, 2013. 49(5): p. 858-71.
345. Escribano-Diaz, C., et al., A cell cycle-dependent regulatory circuit composed of 53BP1-RIF1 and BRCA1-CtIP controls DNA repair pathway choice. Mol Cell, 2013. 49(5): p. 872-83.
346. Foley, E.A. and T.M. Kapoor, Microtubule attachment and spindle assembly checkpoint signalling at the kinetochore. Nat Rev Mol Cell Biol, 2013. 14(1): p. 25-37.
347. Sundin, O. and A. Varshavsky, Terminal stages of SV40 DNA replication proceed via multiply i ntertwined catenated dimers. Cell, 1980. 21(1): p. 103-14.
348. Holm, C., et al., DNA topoisomerase II is required at the time of mitosis in yeast. Cell, 1985. 41(2): p. 553-63.
349. Porter, A.C. and C.J. Farr, Topoisomerase II: untangling its contribution at the centromere. Chromosome Res, 2004. 12(6): p. 569-83.
350. Liu, Y., et al., The origins and processing of ultra fine anaphase DNA bridges. Curr Opin Genet Dev, 2014. 26: p. 1-5.
351. Germann, S.M., et al., TopBP1/Dpb11 binds DNA anaphase bridges to prevent genome instability. J Cell Biol, 2014. 204(1): p. 45-59.
352. Hardy, C.F., L. Sussel, and D. Shore, A RAP1-interacting protein involved in transcriptional silencing and telomere length regulation. Genes Dev, 1992. 6(5): p. 801-14.
353. Chapman, J.R., M.R. Taylor, and S.J. Boulton, Playing the end game: DNA double-strand break repair pathway choice. Mol Cell, 2012. 47(4): p. 497-510.
354. Silverman, J., et al., Human Rif1, ortholog of a yeast telomeric protein, is regulated by ATM and 53BP1 and functions in the S-phase checkpoint. Genes Dev, 2004. 18(17): p. 2108-19.
355. Xu, L. and E.H. Blackburn, Human Rif1 protein binds aberrant telomeres and aligns along anaphase midzone microtubules. J Cell Biol, 2004. 167(5): p. 819-30.
356. Cornacchia, D., et al., Mouse Rif1 is a key regulator of the replication-timing programme in mammalian cells. EMBO J, 2012. 31(18): p. 3678-90.
357. Hayano, M., et al., Rif1 is a global regulator of timing of replication origin firing in fission yeast. Genes Dev, 2012. 26(2): p. 137-50.
358. Peace, J.M., A. Ter-Zakarian, and O.M. Aparicio, Rif1 regulates initiation timing of late replication origins throughout the S. cerevisiae genome. PLoS One, 2014. 9(5): p. e98501.
359. Yamazaki, S., et al., Rif1 regulates the replication timing domains on the human genome. EMBO J, 2012. 31(18): p. 3667-77.
360. Heijink, A.M., M. Krajewska, and M.A. van Vugt, The DNA damage response during mitosis. Mutat Res, 2013. 750(1-2): p. 45-55.
361. Giunta, S., R. Belotserkovskaya, and S.P. Jackson, DNA damage signaling in response to double-strand breaks during mitosis. J Cell Biol, 2010. 190(2): p. 197-207.

362. Orthwein, A., et al., Mitosis inhibits DNA double-strand break repair to guard against telomere fusions. Science, 2014. 344(6180): p. 189-93.
363. Xu, D., et al., Rif1 provides a new DNA-binding interface for the Bloom syndrome complex to maintain normal replication. EMBO J, 2010. 29(18): p. 3140-55.
364. Gomez, R., et al., Cohesin removal precedes topoisomerase IIalpha-dependent decatenation at centromeres in male mammalian meiosis II. Chromosoma, 2014. 123(1-2): p. 129-46.
365. Stanvitch, G. and L.L. Moore, cin-4, a gene with homology to topoisomerase II, is required for centromere resolution by cohesin removal from sister kinetochores during mitosis. Genetics, 2008. 178(1): p. 83-97.
366. Toyoda, Y. and M. Yanagida, Coordinated requirements of human topo II and cohesin for metaphase centromere alignment under Mad2-dependent spindle checkpoint surveillance. Mol Biol Cell, 2006. 17(5): p. 2287-302.
367. Burrell, R.A., et al., Replication stress links structural and numerical cancer chromosomal instability. Nature, 2013. 494(7438): p. 492-6.
368. Burckstummer, T., et al., A reversible gene trap collection empowers haploid genetics in human cells. Nat Methods, 2013. 10(10): p. 965-71.
369. Feng, L., et al., RIF1 counteracts BRCA1-mediated end resection during DNA repair. J Biol Chem, 2013. 288(16): p. 11135-43.
370. Manthei, K.A. and J.L. Keck, The BLM dissolvasome in DNA replication and repair. Cell Mol Life Sci, 2013. 70(21): p. 4067-84.
371. Wold, M.S., Replication protein A: a heterotrimeric, single-stranded DNA-binding protein required for eukaryotic DNA metabolism. Annu Rev Biochem, 1997. 66: p. 61-92.
372. van Vugt, M.A., et al., A mitotic phosphorylation feedback network connects Cdk1, Plk1, 53BP1, and Chk2 to inactivate the G(2)/M DNA damage checkpoint. PLoS Biol, 2010. 8(1): p. e1000287.
373. Tanaka, T.U., Chromosome bi-orientation on the mitotic spindle. Philos Trans R Soc Lond B Biol Sci, 2005. 360(1455): p. 581-9.
374. van der Waal, M.S., et al., Cell division control by the Chromosomal Passenger Complex. Experimental cell research, 2012. 318(12): p. 1407-20.
375. Vader, G. and S.M. Lens, The Aurora kinase family in cell division and cancer. Biochim Biophys Acta, 2008. 1786(1): p. 60-72.
376. Vader, G., R.H. Medema, and S.M. Lens, The chromosomal passenger complex: guiding Aurora-B through mitosis. J Cell Biol, 2006. 173(6): p. 833-7.
377. Haarhuis, J.H., A.M. Elbatsh, and B.D. Rowland, Cohesin and its regulation: on the logic of X-shaped chromosomes. Dev Cell, 2014. 31(1): p. 7-18.
378. Liu, H., et al., Mitotic Transcription Installs Sgo1 at Centromeres to Coordinate Chromosome Segregation. Mol Cell, 2015. 59(3): p. 426-36.
379. Kang, J., et al., Mitotic centromeric targeting of HP1 and its binding to Sgo1 are dispensable for sister-chromatid cohesion in human cells. Mol Biol Cell, 2011. 22(8): p. 1181-90.
380. Hirota, T., et al., Histone H3 serine 10 phosphorylation by Aurora B causes HP1 dissociation from heterochromatin. Nature, 2005. 438(7071): p. 1176-80.
381. Fischle, W., et al., Regulation of HP1-chromatin binding by histone H3 methylation and phosphorylation. Nature, 2005. 438(7071): p. 1116-22.
382. Yamagishi, Y., et al., Heterochromatin links to centromeric protection by recruiting shugoshin. Nature, 2008. 455(7210): p. 251-5.
383. Watanabe, Y., Shugoshin: guardian spirit at the centromere. Curr Opin Cell Biol, 2005. 17(6): p. 590-5.
384. Ng, T.M., et al., Pericentromeric sister chromatid cohesion promotes kinetochore biorientation. Mol Biol Cell, 2009. 20(17): p. 3818-27.
385. Biggins, S., The composition, functions, and regulation of the budding yeast kinetochore. Genetics, 2013. 194(4): p. 817-46.
386. Akiyoshi, B., et al., Tension directly stabilizes reconstituted kinetochore-microtubule attachments. Nature, 2010. 468(7323): p. 576-9.
387. Sarangapani, K.K., et al., Phosphoregulation promotes release of kinetochores from dynamic microtubules via multiple mechanisms. Proc Natl Acad Sci U S A, 2013. 110(18): p. 7282-7.
388. Rivera, V.M., et al., A humanized system for pharmacologic control of gene expression. Nat Med, 1996. 2(9): p. 1028-32.
389. Rieder, C.L., et al., The checkpoint delaying anaphase in response to chromosome monoorientation is mediated by an inhibitory signal produced by unattached kinetochores. J Cell Biol, 1995. 130(4): p. 941-8.
390. Dick, A.E. and D.W. Gerlich, Kinetic framework of spindle assembly checkpoint signalling. Nat Cell Biol, 2013. 15(11): p. 1370-7.
391. Collin, P., et al., The spindle assembly checkpoint works like a rheostat rather than a toggle switch. Nat Cell Biol, 2013. 15(11): p. 1378-85.

392. de Groot, C.O., et al., A Cell Biologist's Field Guide to Aurora Kinase Inhibitors. Front Oncol, 2015. 5: p. 285.
393. Jinek, M., et al., A programmable dual-RNA-guided DNA endonuclease in adaptive bacterial immunity. Science, 2012. 337(6096): p. 816-21.
394. Banko, M.R., et al., Chemical genetic screen for AMPKalpha2 substrates uncovers a network of proteins involved in mitosis. Mol Cell, 2011. 44(6): p. 878-92.
395. Kato, H., et al., Architecture of the high mobility group nucleosomal protein 2-nucleosome complex as revealed by methyl-based NMR. Proc Natl Acad Sci U S A, 2011. 108(30): p. 12283-8.
396. Panier, S. and S.J. Boulton, Double-strand break repair: 53BP1 comes into focus. Nat Rev Mol Cell Biol, 2014. 15(1): p. 7-18.
397. Symington, L.S. and J. Gautier, Double-strand break end resection and repair pathway choice. Annu Rev Genet, 2011. 45: p. 247-71.
398. Dephoure, N., et al., A quantitative atlas of mitotic phosphorylation. Proc Natl Acad Sci U S A, 2008. 105(31): p. 10762-7.
399. Agromayor, M. and J. Martin-Serrano, Knowing when to cut and run: mechanisms that control cytokinetic abscission. Trends Cell Biol, 2013. 23(9): p. 433-41.
400. Mackay, D.R. and K.S. Ullman, ATR and a Chk1-Aurora B pathway coordinate postmitotic genome surveillance with cytokinetic abscission. Mol Biol Cell, 2015. 26(12): p. 2217-26.
401. Passerini, V., et al., The presence of extra chromosomes leads to genomic instability. Nat Commun, 2016. 7: p. 10754.

Samenvatting in het Nederlands voor niet ingewijden

Celdeling

Een mens bestaat uit biljoenen cellen die nodig zijn om biologische functies te vervullen om het lichaam optimaal te kunnen laten functioneren. Na de bevruchting gaat de eicel zich delen om een embryo te ontwikkelen en te laten groeien. Het delen van cellen is ook belangrijk om beschadigde cellen te vervangen. Celdeling, ook wel mitose genoemd, is dus essentieel voor de ontwikkeling en behoudt van het menselijk lichaam. Tijdens mitose splits een enkele moedercel zich op tot twee dochtercellen. De genetische samenstelling (het genoom) van elke cel, bestaat uit DNA dat is verpakt in 46 chromosomen. In een celcyclus worden deze chromosomen gedupliceerd en de kopieën blijven verbonden tot aan mitose. Tijdens mitose dienen deze chromosoomparen eerlijk verdeeld te worden (chromosoom segregatie) over de twee dochtercellen om het genoom te behouden in elke dochtercel (hoofdstuk 1, Figuur 1). Het is van groot belang dat dit proces nauwkeurig wordt gereguleerd, omdat het functioneren van een cel bepaald wordt door de genetische samenstelling. Een numerieke afwijking in het aantal chromosomen (aneuploidy) in een bevruchte eicel kan problemen veroorzaken in de ontwikkeling van een mens. Het meest bekende voorbeeld is een extra kopie van chromosoom 21 dat leidt tot het syndroom van Down. Ook de hoeveelheid chromosomen in kankercellen wijken vaak af van het correcte aantal van 46. Er zijn aanwijzingen dat dit bijdraagt aan het ontstaan van tumoren en de groei van tumoren kan versnellen. Wanneer er tijdens mitose chromosomen vaak oneerlijk worden verdeeld over twee dochtercellen (chromosoom missegregatie), dan wordt dit gerefereerd als chromosomale instabiliteit. Dit leidt tot constante veranderingen in de genetische samenstelling van de gevormde dochtercellen en kan de functionaliteit van een cel negatief beïnvloeden (kanker).

Om te kunnen begrijpen hoe chromosomale instabiliteit veroorzaakt wordt, is het bestuderen hoe een correcte celdeling in zijn werk gaat de eerste stap. Na de duplicatie van de chromosomen worden de chromosoomparen bij elkaar gehouden door specialiseerde eiwitringen, genaamd de cohesine complexen (hoofdstuk 1, Figuur 2). Tevens worden, tijdens de duplicatie van de chromosomen, de DNA strengen gedeeltelijk in elkaar verweven (DNA catenatie). Wanneer alle chromosomen zijn gedupliceerd zal een cel zich op een gegeven moment gaan delen. Het celdelingsproces, mitose, is onderverdeeld in verschillende fasen (hoofdstuk 1, Figuur 1). Tijdens de eerste fase, profase, worden de chromosoomparen (ook wel zuster-chromatiden genoemd) opgevouwen (gecondenseerd) tot korte stijve structuren, zodat deze vrij in de cel kunnen ‘zweven’. De cohesine complexen worden tijdens deze fase gedeeltelijk verwijderd (hoofdstuk 1, Figuur 2) en de DNA strengen gedeeltelijk ‘uit de knoop’ gehaald (DNA decatenatie). De twee zuster-chromatiden blijven echter verbonden op één specifieke plek, namelijk het centromeer (hoofdstuk 6, Figuur 1). Vanaf het centromeer, bevindt zich aan beide zuster-chromatiden een eiwit complex (het kinetochoor, hoofdstuk 6, Figuur 1) dat een verbindingspunt vormt voor ongeveer 20 kabels (microtubuli)(hoofdstuk 1, Figuur 3). Deze microtubuli worden gevormd vanuit twee centrosomen (spoellichamen) die afkomstig zijn van tegenovergestelde polen in de cel. Dit vormt een mitotische spoel van vele microtubuli die vervolgens de kinetochoren gaan ‘zoeken en vangen’ (prometafase, hoofdstuk 1, Figuur 1). Wanneer alle kinetochoren zijn aangesloten aan microtubuli, zullen de zuster-chromatiden uit elkaar worden getrokken. Dit proces is foutgevoelig en wordt daarom nauwkeurig gereguleerd. Voordat de zuster-chromatiden verdeeld worden over twee dochtercellen worden deze eerst netjes geordend in het

midden van de cel waarna de microtubuli correct moeten worden aangesloten aan de kinetochoren. Wanneer alle zuster-chromatiden het midden van de cel hebben bereikt en alle kinetochoren correct zijn aangesloten aan de microtubuli, dan bevindt de cel zich in metafase. Vervolgens worden de cohesine ringen rondom het centromeer geknipt en de trekkracht van de microtubuli aan de kinetochoren zullen de chromosomen laten bewegen richting tegenovergestelde centrosomen in de cel (anafase). Tevens worden de overige 'knopen' uit het centromeer geassocieerde DNA gehaald (DNA decatenatie) (hoofdstuk 4, Figuur 1). Tijdens telofase en cytokinese wordt de mitotische spoel afgebroken, de chromosomen ontvouwen en twee dochtercellen gevormd.

De onderzoeken beschreven in dit proefschrift
Voor het behoud van chromosomale stabiliteit mogen er geen fouten worden gemaakt tijdens mitose. De zuster-chromatiden moeten lang bij elkaar worden gehouden (door de cohesine complexen) en de kinetochoren moeten correct worden aangesloten aan microtubuli afkomstig vanuit tegenovergestelde centrosomen. Wanneer een kinetochoor aan een microtubuli bindt dat afkomstig is van het verkeerde centrosoom, dan zal deze weer los laten door de aanwezigheid van een correctie mechanisme (hoofdstuk 1, Figuur 6). Dit mechanisme is actief totdat alle kinetochoren zijn aangesloten aan microtubuli, afkomstig van het correcte centrosoom (chromosoom bi-oriëntatie). Een cel heeft tijd nodig om chromosoom bi-oriëntatie te kunnen bereiken en daarvoor meet het kinetochoor de status of het gebonden is aan microtubuli. Indien dit niet het geval is, dan wordt het mitotische checkpoint geactiveerd. Het ongebonden kinetochoor amplificeert een moleculair signaal om vroegtijdige anafase te voorkomen. Wanneer chromosoom bi-oriëntatie is bereikt dan zal dit signaal afzwakken, de cohesine ringen worden geknipt en chromosoom segregatie plaats vinden (anafase).

Het 'Chromosomal Passenger Complex' (CPC)(de eiwitten: Aurora B, Inner CENtromere Protein, survivin en borealin) is onmisbaar voor het bereiken van chromosoom bi-oriëntatie en het goed te kunnen laten functioneren van het mitotische checkpoint. De enzymatische component van het complex, Aurora B, kan negatief geladen fosfaatgroepen 'plakken' aan andere eiwitten (substraat fosforylatie) om de functie eigenschappen van deze substraten lokaal te veranderen. Veel Aurora B substraten bevinden zich in het kinetochoor en het CPC kan op deze manier kinetochoor-microtubuli interacties en het mitotische checkpoint reguleren. Aurora B heeft de andere CPC componenten nodig om volledig actief te kunnen zijn en om het naar de juiste locatie in de cel te lokaliseren. In prometafase en metafase lokaliseert het CPC in het midden van het centromeer (inner centromeer, de regio tussen de twee kinetochoren, hoofdstuk 6, Figuur 1). De functie van het CPC op deze specifieke locatie is beschreven als een vereiste om foutieve kinetochoor-microtubuli interacties te kunnen corrigeren. Eén van de doelen van de onderzoeken die zijn beschreven in dit proefschrift was het begrijpen hoe het CPC deze essentiële processen controleert vanaf het inner centromeer. In **hoofdstuk 2** wordt een onderzoek beschreven waarin wij de rol van het CPC op deze specifieke lokalisatie onder de loep hebben genomen. Wij vonden dat het CPC precies op het inner centromeer moet lokaliseren om daar de cohesine complexen te beschermen van verwijdering (en dus vroegtijdige zuster-chromatide separatie te voorkomen). Verder vonden wij dat het lokaliseren van het CPC op het inner centromeer belangrijk is voor het uitzetten van het mitotische checkpoint wanneer een cel chromosoom bi-oriëntatie heeft bereikt.

Omdat de functie van het CPC grotendeels bepaald wordt door Aurora B gemedieerde

substraat fosforylatie hebben wij een methode toegepast om onbekende Aurora B eiwitsubstraten te identificeren (**hoofdstuk 3**). In dit onderzoek hebben wij het eiwit Rif1 als een potentieel Aurora B substraat geïdentificeerd. Tijdens de validatie van deze bevinding, ontdekten wij dat Rif1 specifiek lokaliseert op DNA draden die tijdens anafase gedecateneerd worden. In **hoofdstuk 5** wordt het onderzoek beschreven hoe Rif1 naar deze DNA draden (UFBs) wordt gerekruteerd. Wij hebben ook aangetoond dat Rif1 bijdraagt aan het decatenatieproces van UFBs tijdens anafase om verlies van genomische integriteit te voorkomen. In **hoofdstuk 6** worden de bevinden die zijn beschreven in dit proefschrift samengevat en bediscussieerd ten opzichte van de huidige literatuur en er worden suggesties gedaan voor vervolgonderzoeken.

Curriculum Vitae

Rutger Cornelis Christiaan Hengeveld werd geboren op 19 juli 1987 te Zwolle. In 2005 behaalde hij het HAVO diploma met de profielen Natuur en Techniek & Natuur en Gezondheid aan het Thomas a Kempis College te Zwolle. In september van datzelfde jaar startte hij met de bacheloropleiding Biologie en Medisch Laboratorium onderzoek aan de Hogeschool Saxion te Deventer, die hij in 2009 cum laude heeft afgerond. Vervolgens begon hij aan de masteropleiding Cancer Genomics and Developmental Biology aan de Universiteit Utrecht, die hij in 2011 afrondde. Tijdens deze studies heeft hij gedurende negen maanden een onderzoeksstage gedaan in het Nederlands Kanker Instituut te Amsterdam in het laboratorium van Prof. dr. Jacques Neefjes op de afdeling immunologie. Onder begeleiding van Dr. Tineke van den Hoorn en Dr. Petra Paul heeft hij onderzoek gedaan naar genen die betrokken zijn bij de MHC klasse II afhankelijke antigen presentatie. Vervolgens bestudeerde hij de peroxisomale β-oxidatie van vetzuren in het Academisch Centrum Amsterdam in het laboratorium van Dr. Carlo van Roermund op de afdeling kindergeneeskunde en klinische chemie. Daarna heeft hij een derde onderzoeksstage gedaan in het laboratorium van Prof. dr. Susanne Lens in het Universitair Medisch Centrum Utrecht op de afdeling moleculair kanker onderzoek. Hier werkte hij aan rol van het Chromosomal Passenger Complex tijdens de celdeling. In september 2011 is Rutger gestart met zijn promotieonderzoek tevens in het laboratorium van Prof. dr. Susanne Lens. De resultaten van dit onderzoek zijn beschreven in dit proefschrift.

List of publications

Hengeveld R.C.C., Vromans M.J.M., Vleugel M., Kops G.J.P.L., Hadders M. and Lens S.M.A.
Inner centromere localization of the CPC is required for cohesion protection and mitotic checkpoint silencing.
Manuscript submitted

Hengeveld R.C.C., de Boer R., Lens S.M.A. and van Vugt M.A.T.M.
RIF1 localizes to ultrafine DNA bridges during anaphase to ensure genomic integrity.
Developmental Cell, August 2015; 34, 466-474

van der Waal M.S., **Hengeveld R.C.C.**, van der Horst A. and Lens S.M.A.
Cell division control by the Chromosomal Passenger Complex.
Experimental Cell Research, July 2012; 318, 1407-1420

Hengeveld R.C.C., Hertz N.T., Vromans M.J.M., Zhang C., Burlingame A.L., Shokat K.M. and Lens S.M.A.
Development of a chemical genetic approach for human Aurora B kinase identifies novel substrates of the chromosomal passenger complex.
Molecular & Cellular Proteomics, January 2012; 11:10.1074, 47-59

Paul P., van den Hoorn T., Jongsma M.L.M., Bakker M.J., **Hengeveld R.C.C.**, Janssen L., Cresswell P., Egan D.A., van Ham M., Ten Brinke A., Ovaa H., Beijersbergen R.L., Kuijl C. and Neefjes J.
A Genome-wide multidimensional RNAi screen reveals pathways controlling MHC class II antigen presentation.
Cell, April 2011,15;145(2):268-83.

Dankwoord

Het proefschrift is klaar! Wat is de tijd snel gegaan! Dit kwam vooral omdat ik veel fijne mensen om mij heen heb gehad die mij hebben geholpen, gesteund en afleiding hebben gegeven tijdens het leuke maar ook soms zware promotietraject. Ik wil deze mensen heel graag bedanken in dit deel van het proefschrift.

Allereerst wil ik natuurlijk mijn begeleider en promotor Prof. dr. Susanne Lens bedanken. Beste Susan, ik weet nog als de dag van gisteren dat ik voor een afstudeerplek bij jou op gesprek mocht komen. Ik kan mij vooral goed herinneren met hoeveel passie jij over de wetenschap praatte en hoeveel energie jij uitstraalde. Ik dacht meteen, in dit lab wil ik werken en kan ik veel gaan leren! Gelukkig mocht ik beginnen aan een uitdagend project en na het behalen van mijn diploma mocht ik in jouw lab met mijn promotraject beginnen. Daarvoor ben ik je nog steeds heel erg dankbaar. We kennen elkaar al een lange tijd en ik heb alle jaren als zeer prettig en leerzaam ervaren. De deur van jouw kantoor stond altijd open. Wanneer er goede lab-resultaten waren behaald wilde jij het meteen weten en reageerde jij altijd razend enthousiast. Dat gaf mij een boost om meteen vervolgproeven uit te gaan voeren. Ik ben trots dat ik in jouw lab heb mogen werken en dat we samen mooie onderzoeken hebben gepubliceerd. Nogmaals bedankt voor alles!

De leden van mijn beoordelingscommissie: Prof. dr. ir. B.M.T. Burgering, Prof. dr. A.S. Akhmanova, Prof. dr. J.J.C. Neefjes, Dr. M.M. Maurice en Prof. dr. G.J.P.L. Kops. Bedankt voor het doorlezen en het beoordelen van mijn proefschrift.

Iemand die zeker een apart kopje verdient in het dankwoord ben jij natuurlijk! Mijn paranimf, Martijn, volgens mij is er niemand zo vaardig in het laboratorium als jij. Het heeft mij enorm geholpen dat jij mij hebt bijgestaan met vele proeven. Ik heb veel van jou geleerd. Daarnaast bracht jij ook elke dag de ‘Brabantse gezelligheid’ met je mee (jammer dat ik de Bossche bollen heb gemist). Ik heb genoten van je (soms foute) grappen en je inzet tijdens het darten en borrels.

Beste labgenootjes, het was een eer om met jullie, zulke goede wetenschappers, samengewerkt te hebben. Ik wil jullie bedanken voor de gezellige sfeer die er heerste binnen de groep. Amanda, misses SGO1, ik wil je bedanken voor alle gezellige momenten. Maar vooral de zelfgemaakte culinaire creaties van jou of bakker Bas waren erg lekker. Jouw vrolijke persoonlijkheid is aanstekelijk en zorgde voor een goede sfeer binnen de groep. Succes met het afronden van je onderzoeken! Ingrid, ik vond het leuk dat je altijd aan mijn linkerzijde in kantoor hebt gezeten. Ik zal jouw passie voor het opzetten van dieren en broodjes Londen met bacon en extra mayo niet snel meer vergeten. Het ga je goed. Armando, je bent al een tijdje weg, maar ik mis je droge humor nog steeds. Succes met je nieuwe uitdaging als klinisch chemicus. Hadders, bedankt voor de vele wetenschappelijke discussies. Helaas weten we nog steeds niet precies hoe het CPC lokaliseert op het inner centromeer. Hopelijk kan jij het dynamic-dual-core-mechanical-force-quattropole-hang-over model bewijzen om meer duidelijkheid te bieden. Arne, ik kijk leuk terug dat wij aan dezelfde labbench hebben gewerkt. Sorry dat ik nooit de handschoenen, buizen, pipetten, eppen etc. etc. bijvulde. Sanne, natuurlijk ben ik jou niet vergeten. Je liet mij iedere dag wel weer eens verbazen over iets….Hoe jij bijvoorbeeld met het oog het volume bepaalde in een epje, buis of petrischaal vond

ik erg bijzonder. Ook jij succes met de eindsprint naar je promotie. Sippe, jij bent een aanwinst voor het Lens lab. Je weet veel en gaat er voor de volle 100% voor. Ik wens je heel veel succes met je promotietraject. Livio, ten eerste bedankt voor je hulp wanneer de microscoop, FACS of iets anders niet goed functioneerde. Maar ik wil je ook zeker bedanken voor je inzet tijdens de voetbal en de daarop volgende derde helft. Sibel (labmommy), jij bent een inspirerend persoon. Jij staat altijd voor iedereen klaar. Ik mis de toastyday op woensdag. Heel erg veel succes met je promotieonderzoek. Je kunt het!

Ik heb de eer gehad om tijdens mijn promotietraject drie studenten te mogen begeleiden. Ik heb veel van jullie geleerd (en ik hoop jullie ook van mij) en daarvoor wil ik jullie bedanken. Sander, je bent een slimme wetenschapper. Ik ben blij dat je je plek hebt gevonden in de wereld van de bio-informatica. Heel veel succes! Domie!!!!!! Jij was bij uitstek de meest vrolijke student die wij ooit hebben gehad. Je mag trots zijn op wat je tot nu toe al allemaal hebt bereikt. Ik kijk uit om voor jou te speechen tijdens jouw buluitreiking. Anne, je was een makkelijke student. En dat is een groot compliment. Jouw vaardigheden in het laboratorium zijn zo goed dat ik bijna geen omkijken naar je had. Succes met het afronden van je studie en ik weet zeker dat je ver gaat komen als wetenschapper.

De heren van de ICT, Wim nog sorry van onze botsing, hopelijk is de koffievlek uit je overhemd gekomen. Marc en Erik, bedankt voor jullie hulp wanneer mijn computer weer eens niet deed wat ik in gedachten had.

De leden van het Derksen lab, Patrick, ik vond het leuk om voor jou het 'Fer project' op te starten. Hopelijk pakt iemand anders het goed op om het af te maken. Robert, je bent een goede wetenschapper en je zal zeker een aanwinst voor Harvard zijn. Bedankt dat ik met jou op maandag het voetbalweekend door kon nemen. Milou, het was gezellig om al die tijd tegenover jou gezeten te hebben. Succes met het afronden van je proefschrift. Miranda, de vrouwelijke Martijn van het Derksen lab, bedankt voor de gezelligheid van al de algelopen jaren. Ron, je bent al een tijdje in Amerika, maar ik wil je alsnog bedanken voor de leuke tijd.

De artsen, Jennifer bedankt voor de vrolijkheid die je iedere dag weer meebracht naar het Stratenum. Ik ken weinig mensen die zoveel energie hebben dan jij. Ik vind het knap dat je jouw promotieonderzoek zo goed kan combineren met je inzet voor de marathon en vele andere bezigheden. Kari, ook jij bedankt voor de gezelligheid. Ik vond het altijd leuk om te horen hoe jij van het kitesurfen geniet. Beide, veel succes met het afronden van jullie onderzoeken. Niek, ook met jou kon ik het voetbalweekend rustig analyseren. Bedankt voor de leuke tijd. Graag wil ik ook bedanken: Jamila, Danielle, Benjamin, Ernst, Lutske, Joost, Laura, Julia, Sander en Marco.

Het Kops lab, Geert bedankt voor al de nuttige input die jij mij hebt gegeven. Ik vond het leerzaam om met jouw lab samengewerkt te hebben en ik wil sommige huidige en oud Kopsjes daarvoor bedanken. Wie zal er eerst komen? Verassend, Mattie, ik vond het altijd gezellig om samen met jou bakkies te doen in het HVB, de brug, balkon of in het gras. Je bent echt een goede wetenschapper en ik ben trots dat jij op één van mijn onderzoeken coauteur bent. Nu gaan we samen de geschiedenisboeken in. Richard, ik kijk uit naar je twee Nature paper. Het was een leuke tijd, alleen jammer dat ik nooit van je kon winnen met darten. Wilco, je was de kloneer en IF koning van het Stratenum,

bedankt voor al je wetenschappelijke discussies. Ik vond het leuk om samen met jou in het lab te werken. Natuurlijk Banafsheh, jij bent meelevend en staat voor iedereen klaar. Daar wil ik je voor bedanken. Je bent een creatieve wetenschapper met een enorme drive. Succes met de laatste loodjes. Ajit, jij bent een bijzonder goed persoon. Ik ga de disco-lab-Friday muziekmomenten erg missen. Nannette, mooi man! Verder wil ik nog Timo, Saskia, Adrian, Tale, Manja, Vincent, Ana, Antoinette, Bas, Carlos, Deborah, Eelco, Spiros en Wilma bedanken voor de mooie tijd in het lab!

De huidige en oud Medemaatjes, René ik wil je erg graag bedanken voor de input die jij mij hebt gegeven. De H250Y mutant en de tip dat Marcel ook aan Rif1 werkte heeft mij enorm geholpen. Ik wil graag Rob, Aniek, Indra, Wytse, Marvin, Lenno, Melinda, Monica, Arne, Libor, Belén, Roy, Jonne, Daniël, Femke, Anja, Jeroen, André en Mihoko bedanken voor de wetenschappelijke discussies en de gezellige momenten tijdens borrels en lab retreats. De Rowland groep, Benjamin, bedankt voor al de updates over het cohesin complex. Judith, de eerste weddenschap heb ik gewonnen! Jij hebt het cohesin virus van Benjamin volledig overgenomen. Succes met het laatste mooie onderzoek voor je promotie. Ahmed, thanks for the good times.

De mensen van de derde verdieping, de plek waar Marten niet is weg te denken. Ik heb genoten van jouw kritische kijk op de wetenschap en alles daarom heen. Succes met het (rustig) afronden van je proefschrift. Harmjan bedankt voor alle gezellige momenten bij de koffiemachine. Hugo, bedankt voor de leuke tijd, vooral tijdens de zaalvoetbal. Succes met het runnen van je eigen lab. Verder wil ik: Boudewijn, Tobias, Jasmin, Willem-Jan, Astrid, Andrée en Rick bedanken voor de mooie jaren.

Tevens wil ik mijn oud HLO-maatjes: Jasper, Ilona, Marjolein, Charlotte, Wilbert, Hendrik, Tom, Sanne, Sjors, Nina, Jeroen, Rosanne, Gerrit en Susanne bedanken voor de mooie, leerzame en gezellige studiejaren. De weekendjes in de rozenstraat voel ik nog steeds.

Vrienden en vriendinnen, vooral jullie hebben voor fijne afleiding gezorgd tijdens mijn promotietraject. Graag wil ik Robin en Linda, Martijn en Samantha, Tom en Rainne, Gerben en Vivianne, Mitchell en Maaike, Bram en Tamsin, Joram en Merel, Mathijs, Ilona, Lesley en in het bijzonder Jordy bedanken. Jordy, bedankt dat jij altijd voor mij klaar staat. Nadat ik een wetenschappelijke meeting in New York had bijgewoond, was jij ook overgevlogen en hebben we samen een week NYC bezocht. Het was een week om nooit meer te vergeten. Bedankt daarvoor en hopelijk kunnen we in de toekomst nog veel van dat soort mooie momenten gaan beleven. Glenn, ik kon jou op meerdere plekken plaatsen in dit dankwoord: je bent een oud klasgenoot, collega, mijn paranimf maar vooral een goede vriend. Ik wil je bedanken voor alles. Vooral voor de mooie tijd toen wij samen in de gansstraat woonden. Jij ook succes met het afronden van je promotietraject.

Natuurlijk wil ik ook graag mijn familie (Hengeveld en Meekers) bedanken. Vooral voor het aanhoren van mijn onbegrijpelijke wetenschappelijke verhalen tijdens verjaardagen. In het bijzonder wil ik Opa Meekers bedanken. Helaas ben je er al een aantal jaren niet meer, maar ik wil toch dat je een plekje krijgt in dit proefschrift. Je was een bijzondere man en jouw fijne visie op het leven zal ik de rest van mijn leven bij mij blijven dragen.

Mijn schoonfamilie. Coen, Jolanda en Raymond, net als bij mijn eigen familie kan ik bij jullie ook heerlijk mezelf zijn. Ik wil jullie bedanken omdat jullie altijd achter mij hebben

gestaan, vooral tijdens het schijven van dit proefschrift. Gelukkig kon ik alsnog mee op wintersport en hebben we een geweldige tijd gehad en heb ik de promotiestress even van mij af kunnen zetten. Daar wil ik ook de hele wintersport groep (Familie Drenth, Hersevoort en van Lottum) graag voor bedanken.

Pa en Ma, mede door jullie sturing tijdens mijn jonge jaren is het toch nog goed gekomen. Ik wil jullie bedanken voor een fijne thuisbasis en het vertrouwen in mij tijdens mijn studies en promotieonderzoek. Jullie tonen altijd interesse in wat Jos en ik doen en staan altijd voor ons klaar. Ik hoop dat we samen nog vele mooie momenten mogen meemaken.

Jos en Hester, mijn broer en kleine schoonzusje, bedankt voor jullie steun tijdens mijn studies en promotietraject. Ik vind het fijn dat we nu weer dicht bij elkaar wonen. Jullie zijn heel erg belangrijk voor mij.

Lieve Daphne, bedankt voor al je steun die jij mij hebt gegeven tijdens de laatste jaren van mijn promotietraject. Vooral de laatste maanden zijn erg zwaar geweest en ik vond het fijn dat je altijd achter mij stond. Vooral jouw positiviteit heeft mij geholpen tijdens het schrijven van dit proefschrift. Samen staan wij sterk en ik wil zeggen dat ik heel veel van je hou.

Rutger